



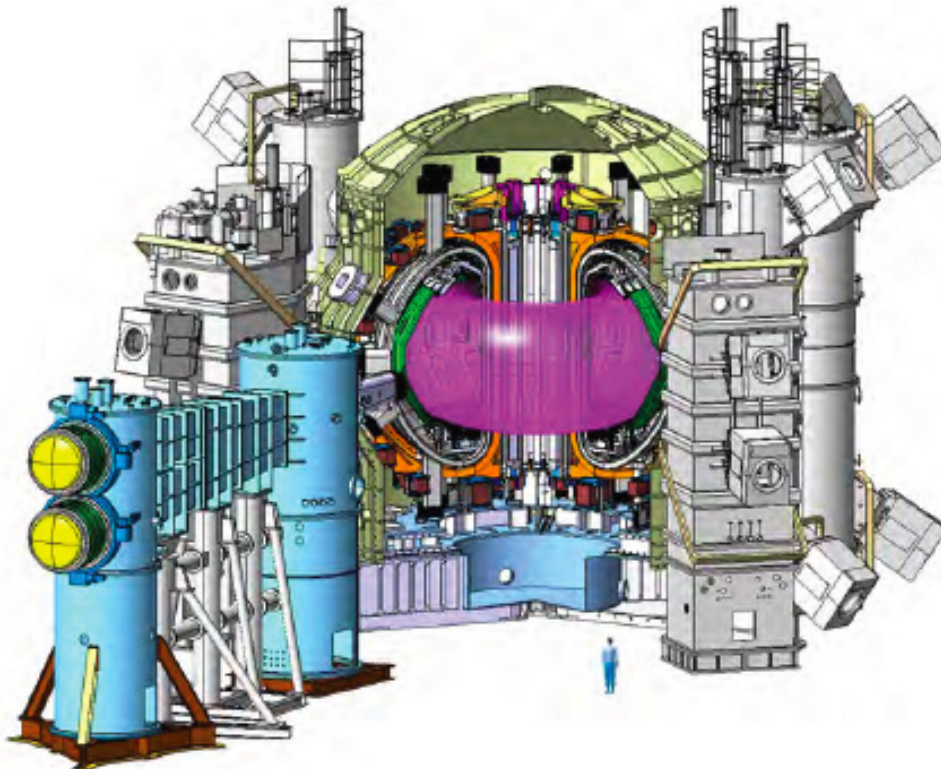
JT-60SA Research Plan

= Research Objectives and Strategy =

Version 4.0

2018, September

JT-60SA Research Unit



JT-60SA Research Unit

JA Home Team:

QST: Nobuyuki AIBA, Hiroyuki ARAKAWA, Nobuyuki ASAKURA, Takahiro BANDO, Andreas BIERWAGE, Mikio ENOEDA, Masakatsu FUKUMOTO, Kiyotaka HAMAMATSU, Masaya HANADA, Takaki HATAE, Nobuhiko HAYASHI, Takao HAYASHI, Satoru HIGASHIJIMA, Makoto HIROTA, Ryouji HIWATARI, Mitsuru HONDA, Katsumichi HOSHINO, Masahiro ICHIKAWA, Shunsuke IDE, Yoshitaka IKEDA, Ryota IMAZAWA, Shizuo INOUE, Akihiko ISAYAMA, Sinichi ISHIDA, Yasutomo ISHII, Kiyoshi ITAMI, Yutaka KAMADA, Kensaku KAMIYA, Koji KAMIYA, Yasunori KAWANO, Kaname KIZU, Yoshinori KAWAMURA, Takayuki KOBAYASHI, Yoshihiko KOIDE, Atsushi KOJIMA, Hirotaka KUBO, Kenichi KURIHARA, Genichi KURITA, Kei MASAKI, Makoto MATSUKAWA, Go MATSUNAGA, Akinobu MATSUYAMA, Kazuhiro MIKI, Naoyuki MIYA, Yoshiaki MIYATA, Naoaki MIYATO, Masahiro MORI, Shinichi MORIYAMA, Haruyuki MURAKAMI, Osamu NAITO, Makoto NAKAMURA, Tomohide NAKANO, Emi NARITA, Kyohei NATSUME, Kazumi OASA, Yoshiaki OHTANI, Makoto ONO, Naoyuki OYAMA, Takahisa OZEKI, Yoshiteru SAKAMOTO, Akira SAKASAI, Shinji SAKURAI, Ryuichi SANO, Hajime SASAO, Yusuke K. SHIBAMA, Kiyoshi SHIBANUMA, Katsuhiko SHIMIZU, Kouji SHINOHARA, Hiroshi SHIRAI, Junya SHIRAISHI, Yoji SOMEYA, Atsuhiko SUKEGAWA, Takahiro SUZUKI, Satoshi SUZUKI, Haruhiko TAKASE, Manabu TAKECHI, Hidenobu TAKENAGA, Hiroyasu TANIGAWA, Kenji TOBITA, Hiroshi TOJO, Mitsunori TOMA, Katsuhiko TSUCHIYA, Daigo TSURU, Hiroyasu UTOH, Hajime URANO, Takuma WAKATSUKI, Shohei YAMOTO, Masatoshi YAGI, Kiyoshi YOSHIDA, Maiko YOSHIDA,

JA Contributors

Fukui University of Technology: Hiroshi HORIIKE,

Hokkaido University: Yuji NOBUTA, Yuji YAMAUCHI,

Japan Atomic Energy Agency: Yasuhiro IDOMURA,

Keio University: Akiyoshi HATAYAMA, Kazuo HOSHINO, Kunihiko OKANO,

Kyoto Institute of Technology: Sadao MASAMUNE, Akio SANPEI,

Kyoto University: Atsushi FUKUYAMA, Shinichiro KADO, Shinji KOBAYASHI, Satoshi KONISHI, Tomoaki KUNUGI, Takashi MAEKAWA, Takashi MINAMI, Tohru MIZUUCHI, Sadayoshi MURAKAMI, Kazunobu NAGASAKI, Taiichi SHIKAMA, Fumitake WATANABE, Satoshi YAMAMOTO,

Kyushu University: Kazuaki HANADA, Hiroshi IDEI, Kazunari KATAYAMA, Masabumi NISHIKAWA, Shigeru INAGAKI,

Nagoya University: Takaaki FUJITA, Shin KAJITA, Shinya MAEYAMA, Noriyasu OHNO, Kozo YAMAZAKI, Tomohiko WATANABE,

National Institute for Fusion Science: Tsuyoshi AKIYAMA, Naoko ASHIKAWA, Mitsutaka ISOBE, Ryutaro KANNO, Masahiro KOBAYASHI, Suguru MASUZAKI, Junichi MIYAZAWA, Tomohiro MORISAKI, Noriyoshi NAKAJIMA, Yukio NAKAMURA, Motoki NAKATA, Yoshiro NARUSHIMA, Shin NISHIMURA, Satoshi OHDACHI, Tetsutarou OISHI, Masaki OSAKABE, Akio SAGARA, Satoru SAKAKIBARA, Shinsuke SATAKE, Yasuhiro SUZUKI, Yasuhiko TAKEIRI, Naoki TAMURA, Kenji TANAKA, Yasushi TODO, Kazuo TOI, Masayuki TOKITANI, Masayuki YOKOYAMA, Kiyomasa WATANABE,

National Institute of Technology, Gifu College: Yoshihide SHIBATA,

Osaka University: Takeshi FUKUDA, Tomonori TAKIZUKA, Yoshio UEDA,

Shizuoka University: Yasuhisa OYA,

The University of Tokyo: Akira EJIRI, Michiaki INOMOTO, Masaki NISHIURA, Yuichi OGAWA, Yuichi TAKASE,

Tohoku University: Sumio KITAJIMA,

Tokyo Institute of Technology: Shunji IIO, Shinzaburou MATSUDA,

Tottori University: Masaru FURUKAWA,

University of Tsukuba: Makoto ICHIMURA, Tsuyoshi IMAI, Yousuke NAKASHIMA, Mizuki SAKAMOTO, Shuhei SUMIDA,

EU Home Team

- Fusion for Energy/Garching (Germany), Naka (Japan), Barcelona (Spain):* Pietro BARABASCHI, Antonino CARDELLA, Susana CLEMENT-LORENZO, Alberto COLETTI, Sam DAVIS, Enrico DI PIETRO, Daniel DUGLUE, Jonathan FARTHING, Giampaolo FRELLO, Nandor HAJNAL, Helmut HURZLMEIER, Antti JOKINEN, Daiva KANAPIENYTE, Luca NOVELLO, Emanuele PERETTI, Guy PHILLIPS, Petra RANCSIK, Ettore SALPIETRO, Armin SCHERBER, Bill SPEARS, Bernhard TEUCHNER, Valerio TOMARCHIO, Mario VERRECCHIA, Manfred WANNER, Louis ZANI,
- CEA/Cadarache (France):* Oliver BAULAIGUE, Fabrice BENOIT, Daniel CIAZYNSKI, Patrick DECOOL, Hubert DOUGNAC, Jean-Luc DUCHATEAU, Nicolas DUMAS, Pascal FEJOZ, Jeronimo GARCIA, Alain GERAUD, Samir GHARAFI, Gerardo GIRUZZI, Romain GONCALVES, René GONDE, Gilles GROS, Patrick HERTOOUT, François JESTIN, Guillaume JIOLAT, Benoit LACROIX, Sébastien LAMY, Jean-Louis MARECHAL, Sylvie NICOLLET, Bertrand PELUSO, Andrea SANTAGIUSTINA, Beaufils STEPHNIE, Alexandre TORRE, Arnaud VAGLIANI, Jean-Claude VALLET, Jean-Marc VERGER,
- CEA/Grenoble (France):* François BONNE, Sylvain GIRARD, Christine HOA, Valerie LAMAISON, Frederic MICHEL, Jean-Marc PONCET, Pascal ROUSSEL,
- CEA/Saclay (France):* Walid ABDEL MAKSOUD, Florence ARDELLIER, Gael DISSET, André DONATI, Laurent GENINI, Christophe MAYRI, Frederic MOLINIE, Francois NUNIO, Patrick PONSOT, Bernard SALANON, Loris SCOLA, Laurence VIEILLARD,
- CIEMAT/Madrid (Spain):* Javier ALONSO, German BARRERA, Jose BOTIJA, Santiago CABRERA PEREZ, Pilar FERNANDEZ, Elena DE LA LUNA, Mercedes MEDRANO, Francisco Jose RAMOS, Esther RINCON, Alfonso SOLETO,
- Consorzio RFX/Padva (Italy):* Tommaso BOLZONELLA, Alberto FERRO, Elena GAIO, Ferdinando GASPARI, Alberto MAISTRELLO,
- ENEA/Frascati (Italy):* Giorgio BROLATTI, Giovanni COCCOLUTO, Valter COCILOVO, Valentina CORATO, Pietro COSTA, Carla CRISTOFANI, Antonio CUCCHIARO, Attilio DE VELLIS, Luigi DI PACE, Paolo FROSI, Grazia GINOULHIAC, Alessandro LAMPASI, Giuseppe MAFFIA, Aldo PIZZUTO, Gian Mario POLLI, Paolo ROSSI, Fabio STARACE, Chiarasole FIAMOZZI ZIGNANI, Pietro ZITO,
- IFP-CNR/Milano (Italy):* Carlo SOZZI,
- KIT/Karlsruhe (Germany):* Sandra DROTZIGER, Christian DAY, Walter FIETZ, Reinhard HELLER, Alberto MASSIMI, Ingebourg MEYER, Dirk RADLOFF, Giuseppe RAMOGIDA, Camillo RITA, Elisabeth URBACH,
- SKC.CEN/Mol (Belgium):* Bill COLLIN, Christophe DELREZ, Pierre JAMOTTON, Vincent MASSAUT,

EU Contributors

- Aalto University/Helsinki (Finland):* Taina KURKI-SUONIO, Antti SALMI, Konsta SÄRKIMÄKI, Jari VARJE,
- Aix-Marseille University (France):* Sadruddin BENKADDA,
- CCFE/Culham (UK):* Alexandru BOBOC, Clive CHALLIS, Ian CHAPMAN, Ian JENKINS, Vasili KIPTILY, Andrew KIRK, Costanza MAGGI, Joëlle MAILLOUX, Luca GARZOTTI, Yueqiang LIU, Michele ROMANELLI, Sandra ROMANELLI, Samuli SAARELMA, Sergei SHARAPOV,
- CEA, IRFM/Cadarache (France):* Jean-François ARTAUD, Marina BÉCOULET, Clarisse BOURDELLE, Jérôme BUCALOSSO, David DOUAI, Rémi DUMONT, Gloria FALCHETTO, Jeronimo GARCIA, Eric GAUTHIER, Christophe GIL, Gerardo GIRUZZI, Marc GONICHE, Tuong HOANG, Emmanuel JOFFRIN, Xavier LITAUDON, Philippe LOTTE, Patrick MAGET, Didier MAZON, Philippe MOREAU, Bernard PEGOURIE, Mireille SCHNEIDER, Jean-Marcel TRAVÈRE, Jean-Claude VALLET,
- CIEMAT/Madrid (Spain):* Emilia SOLANO, Elena De la LUNA, Jesus VEGA,
- Consorzio RFX/Padova (Italy):* Matteo BARUZZO, Paolo BETTINI, Tommaso BOLZONELLA, Alessandra CANTON, Alessandro FASSINA, Elena GAIO, Leonardo GIUDICOTTI, Shi Chong GUO, Paolo INNOCENTE, Giuseppe MARCHIORI, Roberto PASQUALOTTO, Leonardo PIGATTO, David TERRANOVA, Marco VALISA, Matteo VALLAR, Xinyang XU,
- EUROfusion /Garching (Germany):* Duarte BORBA, Fabio CISMONTI, Darren McDONALD, Irina VOITSEKHOVITCH,
- ENEA/Frascati (Italy):* Emilia BARBATO, Paolo BURATTI, Flavio CRISANTI, Vincenzo VITALE,

ENEA-CREATE/Napoli (Italy): Stefano MASTROSTEFANO, Francesco ORSITTO, Alfredo PIRONTI, Gianmaria De TOMMASI, Fabio VILLONE,
ERM/Brussels (Belgium): Jef ONGENA,
FOM/Nieuwegein (The Netherlands): Marco de BAAR,
Fusion for Energy/Barcelona (Spain): Roberta SARTORI,
FZ/Jülich (Germany): Yunfeng LIANG, Sven WIESEN,
ICIT (Romania): Sorin SOARE,
IFP-CNR/Milano (Italy): Alessandro BRUSCHI, Daniela FARINA, Lorenzo FIGINI, Gustavo GRANUCCI, Paola MANTICA, Alessandro MORO, Silvana NOWAK, Enrico PERELLI-CIPPO, Paola PLATANIA, Daria RICCI, Carlo SOZZI, Marco TARDOCCHI, Matteo ZUIN,
IPP/Garching (Germany): Clemente ANGIONI, Garrard CONWAY, Mathias DIBON, Mike DUNNE, Ursel FANTZ, Benedikt GEIGER, Tim HAPPEL, Philipp LAUBER, Karl LACKNER, Peter LANG, Rudolf NEU, Gabriella PAUTASSO, Philip SCHNEIDER, Marco WISCHMEIER,
IPP/Greifswald (Germany): Marc BEURSKENS, Georg KÜHNER, Alessandro ZOCCO
IPPLM/Warsaw (Poland): Krzysztof GALAZKA, Irena Ivanova STANIK, Roman STANKIEWICZ, Włodzimierz STĘPNIEWSKI, Roman ZAGÓRSKI,
ITER Organization (France): Peter De VRIES, Uron KRUEZI,
IST/Lisbon (Portugal): Ivo CARVALHO, Rui COELHO, Nuno CRUZ,
JET-EUROFusion/Culham (UK): Stefan JACHMICH, Isabel NUNES, George SIPS,
KIT/Karlsruhe (Germany): Christian DAY, Cristian GLEASON GONZÁLEZ, Xueli LUO, Matthieu SCANNAPIEGO, Stylianos VAROUTIS
National Technical University of Athens (Greece): Avrilios LAZAROS,
Politecnico di Torino (Italy): Roberto BONIFETTO
SFP/EPFL/Lausanne (Switzerland): Stefano CODA, Joan DECKER, Ambrogio FASOLI, Timothy GOODMAN, Yves MARTIN, Olivier SAUTER, Christian THEILER
University of Seville (Spain): Juan AYLLON-GUEROLA, Manuel GARCIA-MUNOZ, Eleonora VIEZZER,
University of Milano-Bicocca (Italy): Giuseppe GORINI, Massimo NOCENTE,
University of York (UK): Howard WILSON
Wigner RCP (Hungary): Dániel DUNAI, Ákos KOVÁCSIK, Tamás SZEPESI, Sándor ZOLETNIK

Satellite Tokamak Project Team

Hisato KAWASHIMA, Toshihide OGAWA, Akira SAKASAI, Masayasu SATO, Masami SEKI

***JA and EU Technical Responsible Officers
of the JT-60SA Research Unit, Satellite Tokamak Project
(contact persons of the JT-60SA Research Plan document), and JA university key persons.***

	<i>JA-TROs</i>	<i>EU-TROs</i>
	<i>JA-Univ. key persons</i>	
Ch.1 Research Strategy of JT-60SA:	Yutaka KAMADA, Yuichi TAKASE	Darren MCDONALD
Ch.2 Research Priority:	Maiko YOSHIDA,	Gerardo GIRUZZI
Ch.3 Operation Regime Development:	Takahiro SUZUKI, Kazunobu NAGASAKI	Emmanuel JOFFRIN
Ch.4 MHD Stability and Control:	Go MATSUNAGA, Masaru FURUKAWA	Tommaso BOLZONELLA
Ch.5 Transport and Confinement:	Maiko YOSHIDA, Kenji TANAKA	Michele ROMANELLI
Ch.6 High Energy Particle Behavior:	Kouji SHINOHARA, Masaki OSAKABE	Philipp LAUBER
Ch.7 Pedestal and Edge Physics:	Hajime URANO, Tomohiro MORISAKI	Elena de la LUNA
Ch.8 Divertor, SOL and PMI:	Tomohide NAKANO, Mizuki SAKAMOTO	Marco WISCHMEIER
Ch.9 Fusion Engineering:	Go MATSUNAGA Kazunari KATAYAMA	Christian DAY
Ch.10 Theoretical models and simulation codes:	Nobuhiko HAYASHI, Masayuki YOKOYAMA	Jeronimo GARCIA

Representative QST Authors of Appendix and EU responsible persons for specification

Appendix A:	Mieko KASHIWAGI (NB), Akihiko ISAYAMA (EC),	Carlo SOZZI
Appendix B:	Go MATSUNAGA, Tomohide NAKANO,	Marco WISCHMEIER
Appendix C:	Go MATSUNAGA, Manabu TAKECHI,	Tommaso BOLZONELLA
Appendix D:	Naoyuki OYAMA,	Carlo SOZZI
Appendix E:	Kouji SHINOHARA,	Philipp LAUBER
Appendix F:	Shunsuke IDE, Hajime URANO,	Emmanuel JOFFRIN
Appendix G:	Go MATSUNAGA,	Christian DAY

JT-60SA Research Plan organization and coordination

	<i>JA</i>	<i>EU</i>
JT-60SA Research Plan organization:	Yutaka KAMADA,	Gerardo GIRUZZI
JT-60SA Research Plan coordination:	Maiko YOSHIDA,	Gerardo GIRUZZI

Contents

Introduction.....	6
1. Research Strategy of JT-60SA	8
2. Research Priority	36
3. Operation Regime Development	44
4. MHD Stability and Control	64
5. Transport and Confinement	74
6. High Energy Particle Behavior	90
7. Pedestal and Edge Physics	99
8. Divertor, Scrape Off Layer and Plasma-Material Interaction	116
9. Fusion Engineering	126
10. Theoretical Models and Simulation Codes	139
Appendix A: Heating and Current Drive Systems	155
Appendix B: Divertor Power Handling and Particle Control Systems ...	164
Appendix C: Stability Control Systems	168
Appendix D: Plasma Diagnostics Systems	170
Appendix E: Magnetic field ripple	180
Appendix F: Operational scenarios	183
Appendix G: Design guide lines for additional components	186

Introduction

This document summarizes the JT-60SA Research Plan constructed by the JT-60SA Research Unit (Fig.I-1) collaborating with Japanese and European fusion research communities; Fusion Energy Forum of Japan and the European Consortium for the Development of Fusion Energy (EUROfusion). Based upon scientific achievements in Tokamak devices worldwide, we propose a consistent set of research objectives and strategy covering all major research fields of i) operation regime development, ii) MHD stability and control, iii) transport and confinement iv) high energy particle behavior, v) Pedestal and edge physics, vi) divertor, scrape off layer (SOL) and plasma material interaction (PMI), vii) fusion engineering, and viii) theoretical models and simulation codes.

The project mission of JT-60SA is to contribute to early realization of fusion energy by supporting the exploitation of ITER and by complementing ITER in resolving key physics and engineering issues for DEMO reactors. The JT-60SA device has been designed in order to satisfy all of the central research needs for ITER and DEMO. In other words, the JT-60SA research project complements ITER in all areas of fusion plasma development necessary to decide DEMO construction. In particular, the most important goal of JT-60SA is to decide the practically acceptable DEMO plasma design including practical and reliable plasma control schemes suitable for a power plant.

In order to establish the JT-60SA Research Plan, we have to consider the position of JT-60SA relative to ITER and DEMO in the time schedule of fusion energy development. The operation of JT-60SA will start earlier than ITER by 5 years. In addition, the tight experimental schedule of ITER towards $Q=10$ requires exploration of key physics and operational techniques in satellite devices. Therefore, the experiences and achievements in JT-60SA are indispensable for an efficient and reliable execution of ITER experiments. Once ITER operation starts, efficient collaborations between JT-60SA and ITER are required to mitigate the main ITER risks. In this period, the flexibility of JT-60SA will contribute to ITER in various research fields. It should be stressed that the integration of achievements in JT-60SA high- β steady-state plasmas and achievements in ITER burning plasmas is required to make DEMO designs more realistic and attractive. For early realization of a DEMO reactor, such parallel and integrated exploitation of JT-60SA and ITER is necessary.

Based on the background mentioned above, we propose a set of JT-60SA research objectives and strategy along the project mission and the research phases agreed between Japan and EU. The central DEMO design reference for JT-60SA is an ‘economically attractive (= compact) steady-state’ reactor. However, the JT-60SA Research Plan has to treat the ‘DEMO regime’ as a spectrum of options around the reference design. It should be pointed out that the final design of a DEMO reactor must be determined based on achievements in JT-60SA and ITER. This is precisely the role of JT-60SA.

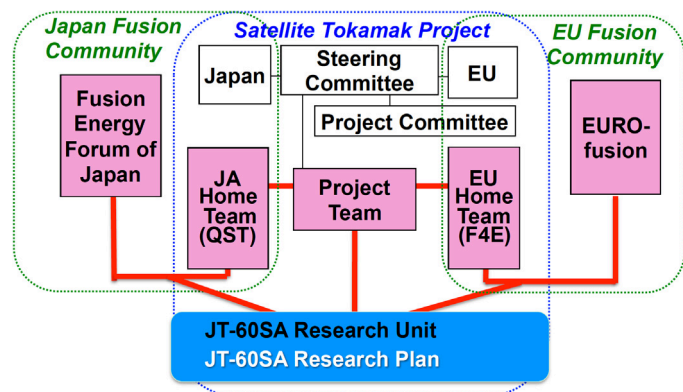


Fig.I-1 Organization structure of the JT-60SA Project and the JT-60SA Research Unit

Log of the JT-60SA Research Plan:

Version	Date
Ver.1	: 11 May, 2009
Ver.1.1	: 21 July, 2009
Ver.2.0	: 6 January, 2010
Ver.2.1	: 28 February, 2011
Ver.3.0	: 21 December, 2011
Ver.3.1	: 20 December, 2013
Ver.3.2	: 16 February, 2015
Ver.3.3	: 1 March, 2016
Ver.4.0	: 10 September, 2018

1. Research Strategy of JT-60SA

1.1. Mission and Plasma Regimes of JT-60SA

The project mission of JT-60SA [1, 2] is to contribute to early realization of fusion energy by supporting the exploitation of ITER and by complementing ITER in resolving key physics and engineering issues for DEMO reactors (Fig.1-1).

The JT-60SA device is capable of confining break-even-equivalent class high-temperature deuterium plasmas lasting for a duration (typically 100 s) longer than the time scales characterizing key plasma processes, such as

current diffusion and particle recycling, using superconducting toroidal and poloidal field coils. The maximum plasma current is 5.5 MA. The device should also pursue fully non-inductive steady-state operations with high values of the plasma pressure exceeding the no-wall ideal MHD stability limits. The target regimes of JT-60SA are shown in Fig.1-2. The JT-60SA experiments should explore ITER and DEMO-relevant plasma regimes in terms of non-dimensional plasma parameters at high densities in the range of $1 \times 10^{20} \text{ m}^{-3}$. JT-60SA operation starts with carbon wall and explores the ITER and DEMO plasma regimes as well as over a wide range of plasma parameters. The JT-60SA's main mission related to high- β steady-state operations has to be firstly achieved with the carbon wall. After maturing integrated plasma control systems, in the later phase of the project, the divertor target and the first wall will be fully replaced by tungsten-coated carbon. Under this 'metal-wall' environment, the JT-60SA's main missions 'supporting ITER' and 'complementing ITER to DEMO' will be ultimately investigated and achieved.

In order to satisfy these requirements, the JT-60SA device has been designed to realize a

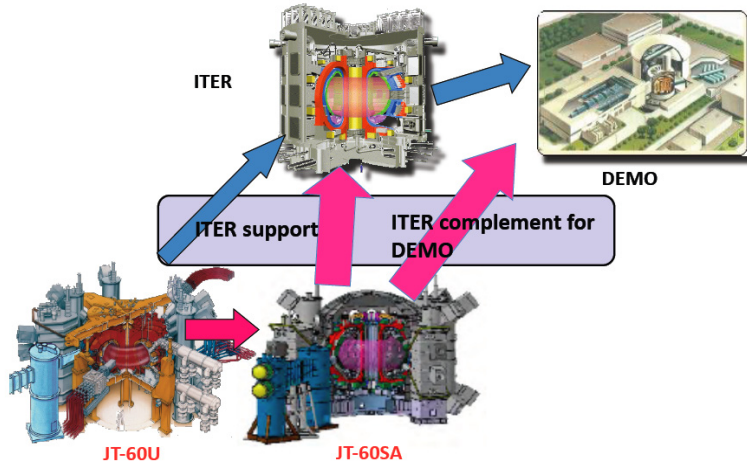


Fig.1-1 Roles of JT-60SA contributing to ITER and DEMO

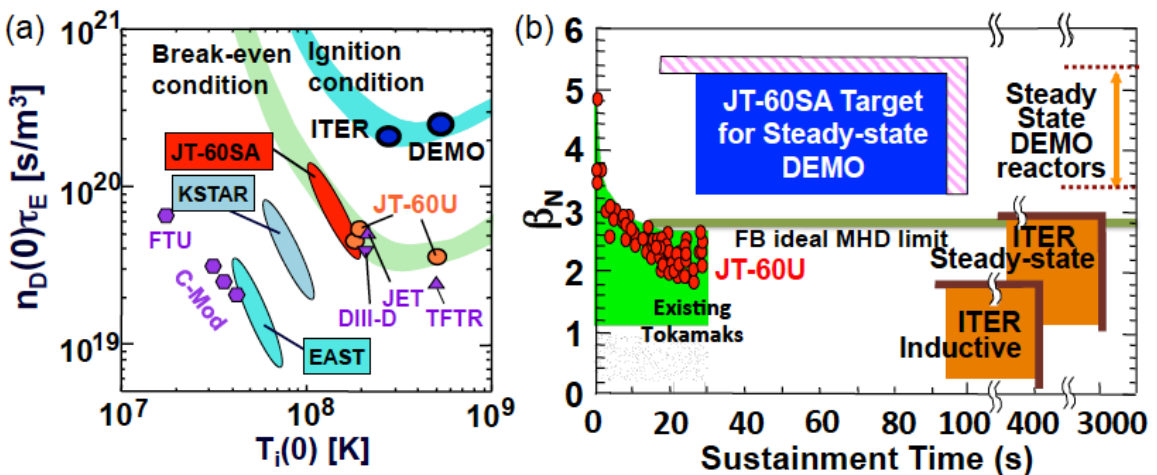


Fig.1-2 Target regimes of JT-60SA

wide range of diverted plasma equilibrium configurations covering a high plasma shaping factor ($S = q_{95} I_p / (a B_t) \sim 7$) and low aspect ratio ($A \sim 2.5$) with a sufficient inductive plasma current flat-top duration and additional heating power of up to 41 MW for 100 s. The plasma size and shape of JT-60SA are shown in Fig.1-3. Figure 1-3(a) shows the typical JT-60SA single null equilibrium at $I_p=5.5\text{MA}$. Compared with the JT-60U device, the plasma elongation is high ($\kappa_x \sim 1.9$) simultaneously with high plasma triangularities ($\delta_x = 0.4 - 0.5$) at high plasma currents (up to $I_p=5.5\text{ MA}$). As shown in Fig.1-3(b), the shape parameter of JT-60SA is equivalent to that of the Slim-CS DEMO [3] which has the highest shape parameter among the DEMO designs (Demo CREST[4], JA DEMO 2014 [5], EU DEMO 1 & 2 [6]). The major radius of JT-60SA is about half of ITER and the Slim CS DEMO. The plasma size of JT-60SA locates between ITER and other non-circular cross-section superconducting tokamaks (Fig.1-3(c), KSTAR [7], EAST [8], SST-1 [9] and WEST [10]). An integrated knowledge of these superconducting tokamaks, JT-60SA and ITER will establish a reliable nuclear fusion science and technology basis for DEMO.

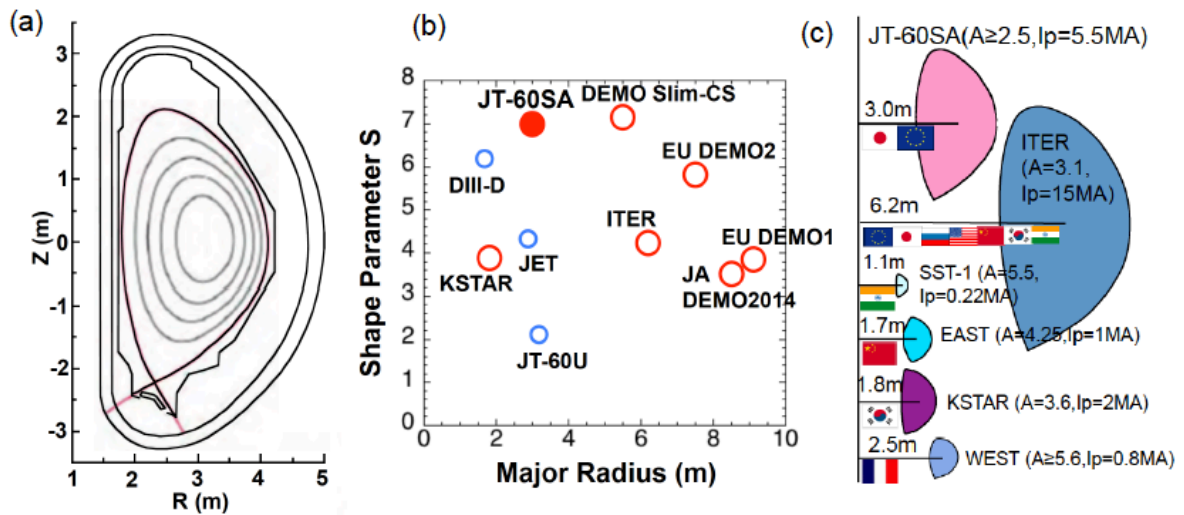


Fig.1-3 (a) JT-60SA single null equilibrium at $I_p=5.5\text{MA}$, (b) plasma major radius and the shape parameter (large circles: superconducting tokamaks), and (c) plasma cross section of world non-circular superconducting tokamaks.

Typical parameters of JT-60SA are shown in Table 1-1. (More detailed plasma parameters for various operation scenarios are described later in Table 1-3.) The maximum plasma currents are 5.5 MA in a low aspect ratio configuration ($R_p=2.96\text{ m}$, $A=2.5$, $\kappa_x=1.87$, $\delta_x=0.50$) and 4.6 MA in the ITER-shaped configuration ($R_p=2.93\text{ m}$, $A=2.6$, $\kappa_x=1.81$, $\delta_x=0.41$). Inductive operations at $I_p=5.5\text{ MA}$ with a flat top duration of up to 100s is possible with the available flux of $\sim 9\text{ Wb}$. The heating and current drive systems will provide neutral beam injection of 34 MW (10 MW, 500 keV N-NB + 24 MW, 85 keV P-NB) and ECRF of 7 MW with 110 GHz + 138GHz dual frequency. The divertor target is designed to be water-cooled in order to handle the expected heat flux up to 15 MW/m^2 for up to 100 s. With these capabilities, JT-60SA allows explorations in ITER- and DEMO-relevant plasma regimes in terms of non-dimensional parameters (such as the normalized poloidal gyro radius ρ_p^* , the normalized collisionality ν^* , and the normalized plasma pressure β_N) (Fig.1-4).

Table 1-1 Typical Parameters of JT-60SA

Parameters	#2 Full Ip Inductive 41MW	#4-1 ITER-like-Shape Inductive 34MW	#4-2 Advanced inductive (hybrid) 37MW	#5-1 High β_N Full CD 37MW	#5-2 High β_N Full CD 31MW
Plasma current, I_p (MA)	5.5	4.6	3.5	2.3	2.1
Toroidal magnetic field, B_T (T)	2.25	2.28	2.28	1.72	1.62
Major radius, R_p (m)	2.96	2.93	2.93	2.97	2.96
Minor radius, a (m)	1.18	1.14	1.14	1.11	1.12
Aspect ratio, A	2.5	2.6	2.6	2.7	2.6
Elongation, κ_X, κ_{95}	1.87, 1.72	1.81, 1.70	1.80, 1.72	1.90, 1.83	1.91, 1.84
Triangularity, δ_X, δ_{95}	0.50, 0.40	0.41, 0.33	0.41, 0.34	0.47, 0.42	0.45, 0.41
Safety factor, q_{95}	3.0	3.2	4.4	5.8	6.0
Shape Parameter ($=q_{95}I_p/(aB_T)$)	6.3	5.7	5.9	7.0	7.0
Plasma Volume (m ³)	131	122	122	124	124
Heating Power, P_{heat} (MW)	41	34	37	37	31
Temperature (Vol-ave.), $\langle T_i \rangle, \langle T_e \rangle$ (keV)	6.3, 6.3	3.7, 3.7	3.7, 3.7	3.4, 3.3	3.1, 2.9
Electron Density, Vol-ave. (E20/m ³)	0.56	0.81	0.62	0.42	0.43
Stored Energy (Thermal, Fast ion) (MJ)	22.2, 4.0	18.0, 1.5	13.4, 2.1	8.4, 2.7	8.1, 1.7
Thermal Energy Confinement Time τ_E (s)	0.54	0.52	0.36	0.23	0.25
Current Diffusion Time (s)	32.7	15.2	14.6	12.6	10.8
Assumed Confinement improvement, $HHy2$	1.3	1.1	1.2	1.3	1.38
Normalized beta, β_N	3.1	2.8	3.0	4.3	4.3
Bootstrap current fraction, f_{BS}	0.28	0.3	0.4	0.68	0.79
Non inductive CD fraction, f_{CD}	0.5	0.43	0.58	1	1
Normalized density, n_e/n_{GW}	0.5	0.8	0.8	0.85	1.0

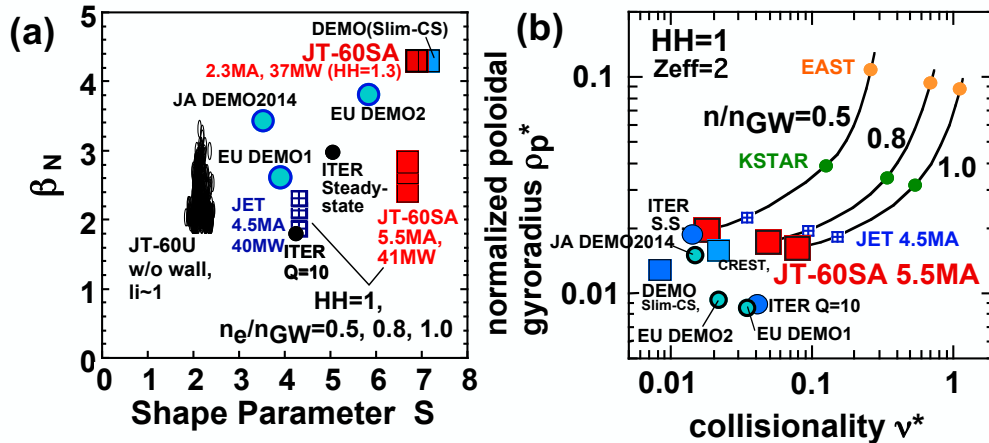


Fig. 1-4 Non-dimensional plasma parameter regimes of JT-60SA: (a) the normalized beta and the shape factor, (b) the normalized collisionality ν^* and the normalized poloidal gyro radius ρ_p^* . (Definitions of ν^* and ρ_p^* are given in Chap.5.)

In DEMO reactors, we need to sustain high values of the energy confinement improvement factor (the HH -factor), the normalized beta β_N , the bootstrap current fraction, the non-inductively driven current fraction, the plasma density normalized to the Greenwald density, the fuel purity, and the radiation power simultaneously in steady-state. However, such a high ‘integrated performance’ has never been achieved. The most important goal of JT-60SA for DEMO is to demonstrate and sustain such high integrated performance. JT-60SA allows exploitations of fully non-inductive steady-state operations with 10 MW/500 keV tangential N-

NBCD and 7 MW ECCD. The expected plasma current for a high β_N ($=4.3$) fully non-inductively current driven operation is 2.3 MA with $P_{in} = 37$ MW ($P_{N-NB} = 10$ MW and $P_{P-NB} = 20$ MW and $P_{EC} = 7$ MW) with the assumed $H_H = 1.3$ (the high β_N Scenario 5-1 in Table 1-3). (When we use the CDBM model for transport evaluation, the predicted H_H -factor is 1.5 which is higher than the assumed value.) When we assume $H_H = 1.38$, a full non-inductive operation with $f_{BS} = 0.79$ and $\beta_N = 4.3$ is expected at $I_p = 2.1$ MA and $f_{GW} = 1$ with $P_{N-NB} = 7$ MW, $P_{EC} = 7$ MW and $P_{P-NB} = 17$ MW (the high β_N Scenario 5-2 in Table 1-3). In this case, controllability of such a high β_N high f_{BS} plasma can be studied by utilizing the remaining power of the N-NB (3 MW) and P-NB (7 MW). These plasma regimes satisfy the research goal of the highly integrated performance as shown in Fig.1-5.

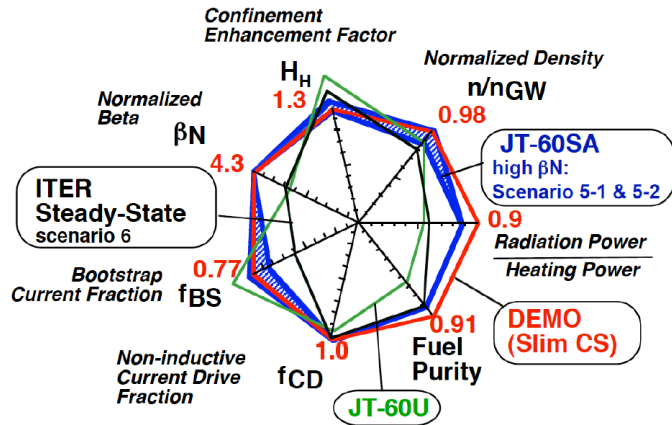


Fig.1-5 Integrated plasma performance in DEMO (Slim-CS), JT-60SA, ITER, and JT-60U [11]. In all cases, $q_{95} = 5.4-6.0$.

In order to perform all the research missions mentioned above, the plasma flat-top length, $\tau_{flat-top}$, has to be sufficiently longer than the resistive diffusion time of plasma current τ_R . For this purpose, $\tau_{flat-top}/\tau_R > 2-3$ is required. Figure 1-6 shows I_p and $\tau_{flat-top}/\tau_R$ for the representative JT-60SA operation scenarios listed in Table 1-3 ($\tau_R = 11 - 34$ s, $\tau_{flat-top} = 100$ s). All scenarios satisfy $\tau_{flat-top}/\tau_R > \sim 3$.

1.2. Research needs for ITER and DEMO plasma development

Towards economically attractive steady-state DEMO reactors, the nuclear fusion research should establish reliable control schemes of burning high β high bootstrap current fraction (f_{BS}) plasmas. Towards this goal, an integrated research program at high values of β_N and f_{BS} exceeding ITER is required. From the view point of burning plasma development, which is the main mission of ITER, satellite devices are required to support ITER by resolving its R&D issues [12, 13] with flexible exploration of fusion plasma experiments in the ITER-relevant plasma parameter (such as the non-dimensional parameters) regime. Tokamak devices in the world have been contributing to these ITER and DEMO related issues and constructing reliable physics basis; such as in JET [14], JT-60U [15], DIII-D [16], ASDEX-U [17] for high integrated plasma performance, EAST [8], KSTAR [7] and Tore Supra [18] for long pulse superconducting tokamak operation, Alcator C-Mod [19] and FTU [20] for high density physics, MAST [21],

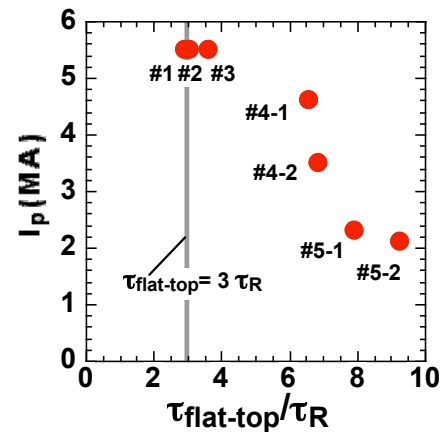


Fig.1-6 I_p and $\tau_{flat-top}/\tau_R$ for the representative JT-60SA operation scenarios.

NSTX [22] and TCV [23] for plasma shaping physics etc.

Based upon these experimental achievements and assessment of the key research issues for ITER and DEMO, Table 1-2 summarizes the central research needs for ITER and DEMO, and device capabilities required for a satellite tokamak. The JT-60SA device has been designed in order to satisfy all of these research needs, namely, a highly shaped large superconducting tokamak with variety of plasma actuators allowing integrated plasma research in the ITER- and DEMO-relevant plasma parameter regimes. The plasma parameters for typical operation scenarios of JT-60SA are given in Table 1-3 together with those for ITER and DEMO (Slim-CS [3] and Demo CREST [4]).

Table 1-2 Central research needs for ITER and DEMO, and device capabilities required for a satellite tokamak in order to satisfy these research needs

Main Issues		ITER	DEMO	Requirements for devices
Integration	Demonstration	Integrated Performance required for Q=10 in ITER	Integrated performance required for DEMO, high $n_e > n_{Greenwald}$	Integration of the followings and Off-axis NNBCD
	Identification of operational boundaries	stability limit, density limit etc. in high I_p ITER-like plasmas	stability limit, density limit etc. in high β_N & high bootstrap & radiative plasmas	
	Development of integrated control and study on plasma response	Test of controls for ITER at ITER-like regime & configurations	Development of Integrated Control for highly self-regulating high β_N & high bootstrap & radiative plasmas, non-inductive I_p ramp-up	
	current profile control $j(r)$	relaxed $j(r)$ with	relaxed $j(r)$ with	Long Pulse ~100s
		bootstrap fraction <50%	bootstrap fraction >50%	
	Particle Control	Particle Control under saturated wall condition and fuel retention		
Equilibrium Control	Fully superconducting operation		Super Conducting TF & PF coils	
MHD Stability and Disruption	high β operation boundary	Demonstrate long pulse high $\beta_N \sim 3$ and determine stability boundary	Demonstrate long pulse high $\beta_N = 3 - 5.5$. Determine stability boundary. Clarify shape effects	Low-A, strong shaping, NNB
	RWM	RWM Control with internal coils Compatibility with RMP	RWM stabilization with rotation RWM control-coil	Rotation Control and fast internal active coils
		Kinetic stabilization effect of energetic particles on RWM stability in burning plasmas		NNB
	NTM	Efficient real time control with ECCD, Compatibility with RMP	Simultaneous stabilization of NTM & RWM at high $\beta_N > 3$	ECCD, NNB, CO/CTR/Perp-NB
	Sawtooth	Sawtooth control by using ECCD under alpha particles		ECCD/NNB
	Disruption mitigation	Disruption mitigation system able to reduce thermal and electromagnetic loads within engineering limits		Disruption Mitigation Systems
	Disruption prediction / avoidance	Develop prediction and avoidance scheme	Disruption limits & behavior at high β_N & high radiation, prediction, and disruption-free operation	Active MHD diagnostics by applying external magnetic field

continued on the following page

Table 1-2 Central research needs for ITER and DEMO, and device capabilities required for a satellite tokamak in order to satisfy these research needs (cont'd)

Main Issues		ITER	DEMO	Requirements for devices
Confinement & Transport	confinement	Confirmation / extrapolation to ITER (mainly H-mode)	Confirmation / extrapolation to DEMO (advanced Operation)	High Ip and large plasmas
		Scaling with high triangularity and shaping (mainly H-mode)	Scaling with high triangularity and shaping (advanced Operation)	High triangularity and shaping
	heat, particle, momentum transport and confinement	Low collisionality & normalized gyro radius at high density		High Ip and large plasmas
		Dominant electron heating		NNB & ECH
		Low central fueling		
		Density control		CO/CTR/Perp-NB, NNB & ECH, puff, pellet
		Rotation effects including low external torque input		CO/CTR/Perp-NB, NNB & ECH
		Suppression of impurity accumulation at high confinement regimes		CO/CTR/Perp-NB, NNB & ECH, puff, pellet
		Turbulence transport at ITER and DEMO relevant regimes (in the presence of a large population of fast ions)		
		H-mode threshold power	High-density operations above the Greenwald density	
		Effect of test blanket modules to toroidal rotation	Test blanket modules	
			Double-null configuration	
	Response & Control of burning plasmas	Response & Control of transport in highly self-regulating plasmas		CO/CTR/Perp-NB, NNB & ECH, puff, pellet
High Energy particle	AE	Stabilization / Control of AE at high fast ion beta Application to MHD spectroscopy		High energy & high power NNB
	Transport	Study transport of high energy particles		
	Interaction with MHD modes	Clarify Interaction of high energy ions with various MHD modes, in particular impact of high energy particles on high β stability		
	NBCD	High energy NBCD	High energy off-axis NBCD	

continued on the following page

Table 1-2 Central research needs for ITER and DEMO, and device capabilities required for a satellite tokamak in order to satisfy these research needs (cont'd)

Main Issues		ITER	DEMO	Requirements for devices
Pedestal	L-H transition	low collisionality at high ne electron heating	highly shaped configuration	High Ip and large scale & highly shaped plasmas
		H-mode experiment with detached divertor for mitigation of ELM heat load		
	Pedestal structure	Pedestal characteristics and control at high current & high density	Pedestal characteristics and control with highly shaped configuration	
			Control of burning plasma by optimized pedestal condition	
ELM control	Behavior of type I ELMs Mitigation with RMP and pellet	small/no ELM regime development at high β_N	RMP, high shape, Rotation Control	
Divertor & SOL&PWI	Particle Control	Fuel and impurity particle (incl. He) control with high-confinement and high-purity core plasma		Strong Pumping, Pellet, puff,
	Power handling	High radiation fraction (low heat flux to the target) and detachment control		V-shaped corner
	compatibility of PFC materials with high performance plasmas	tungsten divertor material	advanced wall material and divertor geometry	Replaceable divertor structure Replacement of first walls

Table 1-3: Plasma Parameters for JT-60SA, DEMO and ITER

Parameters	JT-60SA										DEMO			ITER	
	#1 Full Ip Inductive DN 41MW	#2 Full Ip Inductive SN 41MW	#3 Full Ip Inductive SN 30MW High density	#4-1 ITER like Inductive SN 34MW	#4-2 Advanced inductive (hybrid) SN 37MW	#5-1 High β_N Full CD SN 37MW	#5-2 High β_N Full CD SN 31MW	Slim CS	JA DEMO2014	EU DEMO1	EU DEMO2	scenario 2, Inductive II	scenario 6, Non- inductive Steady- state		
Plasma current, I_p (MA)	5.5	5.5	5.5	4.6	3.5	2.3	2.1	16.7	12.3	19.6	21.63	15.0	9.0		
Toroidal magnetic field, B_t (T)	2.25	2.25	2.25	2.28	2.28	1.72	1.62	6	5.94	5.67	5.63	5.3	5.18		
Major radius, R_p (m)	2.96	2.96	2.96	2.93	2.93	2.97	2.96	5.5	8.5	9.1	7.5	6.2	6.35		
Minor radius, a (m)	1.18	1.18	1.18	1.14	1.14	1.11	1.12	2.1	2.4	2.9	2.9	2.0	1.85		
Aspect ratio, A	2.5	2.5	2.5	2.6	2.6	2.7	2.6	2.6	3.1	3.1	2.6	3.1	3.4		
Elongation, κ , κ_{95}	1.95, 1.77	1.87, 1.72	1.86, 1.73	1.81, 1.70	1.80, 1.72	1.90, 1.83	1.91, 1.84	*, 2.0	*, 1.65	*, 1.65	*, 1.75	1.85, 1.70	2.0, 1.86		
Triangularity, δ_v , δ_{95}	0.53, 0.42	0.50, 0.40	0.50, 0.40	0.41, 0.33	0.41, 0.34	0.47, 0.42	0.45, 0.41	*, ~0.4	*, 0.33	*, 0.33	*, 0.33	0.48, 0.33	0.5, 0.41		
Safety factor, q_{95}	3.2	3.0	3.0	3.2	4.4	5.8	6.0	5.4	4.1	3.25	4.4	3.0	5.4		
Shape Factor (=qsip/(aBt))	6.7	6.3	6.2	5.7	5.9	7.0	7.0	7.2	3.5	3.9	5.8	4.3	5.1		
Plasma Volume (m ³)	132	131	131	122	122	124	124	941	1647	2502	2217	831	730		
Fusion output, P_{fus} (MW)	-	-	-	-	-	-	-	3000	1462	2037	3255	400	340		
Fusion gain, Q (SA: QDT equivalent)	~0.6	~0.5	~0.4	~0.3	~0.23	~0.2	~0.2	52	17.5	41	24	10	5.7		
Heating Power (α + external), Pheat (MW)	41	41	30	34	37	37	31	678	377	457	784	120	128		
Current drive power, PCD (MW)	10	10	10	10	17	17	13	59	84	50	133	40	60		
N-NB, P-NB, ECH power (MW)	10, 24, 7	10, 24, 7	10, 20, 0	10, 24, 0	10, 20, 7	10, 20, 7	7, 17, 7	59	84	50	133				
Ion Temperature, Vol-ave., Central (keV)	6.3, 13.5	6.3, 13.5	3.7, 7.9	3.7, 8.0	3.7, 7.5	3.4, 7.1	3.1, 6.1	17, 28	16*	13.1, 27.5	18.1, 34.8	8.0, 19	12.1*		
Electron Temp., Vol-ave., Central (keV)	6.3, 13.5	6.3, 13.5	3.7, 7.9	3.7, 8.0	3.7, 7.5	3.3, 6.7	2.9, 5.8	17, 28	16*	13.1, 27.5	18.1, 34.8	8.8, 23	13.3*		
Electron Density, line-average, Vol-ave., Central (E20/m ³)	0.63, 0.77	0.63, 0.77	1.0, 1.23	0.91, 1.11	0.69, 0.84	0.5, 0.53	0.43, 0.79	1.01, 1.7	0.66*	0.80, 1.04	0.85, 1.19	1.01, 1.05	0.65*		
Stored Energy (Thermal, Fast Ion) (MJ)	22.4, 4.0	22.2, 4.0	21.1, 1.3	18.0, 1.5	13.4, 2.1	8.4, 2.7	8.1, 1.7	942, 299	786, 182			320, 32	287, 100		
Energy Confinement Time τ_E (s) thermal, total	0.54, 0.64	0.54, 0.64	0.68, 0.75	0.52, 0.57	0.36, 0.42	0.23, 0.31	0.25, 0.30	1.3, 1.8	2.7*	4.2*	4.0*	3.7	3.1		
Current Diffusion Time (s)	34.1	32.7	16.6	15.2	14.6	12.6	10.8	514.2				198.6	314.8		
Flattop Duration (s)	100	100	60	100	100	100	100	S.S.	S.S.	pulse	S.S.	400	3000		
Assumed Confinement improvement, H _H	1.3	1.3	1.1	1.1	1.2	1.3	1.38	1.3	1.31	1.1	1.4	1.0	1.61		
Normalized beta, β_N	3.1	3.1	2.6	2.8	3.0	4.3	4.3	4.3	3.4	2.6	3.8	1.8	2.9		
Bootstrap current fraction, fBS	0.29	0.28	0.25	0.3	0.4	0.68	0.79	0.77	0.61	0.35	0.61	0.15	0.46		
Non inductive CD fraction, fCD	0.51	0.5	0.36	0.43	0.58	1	1	1	1	0.44	1	0.21	1		
Normalized density, n_e/n_{GW}	0.5	0.5	0.8	0.8	0.8	0.85	1.0	0.98	1.2	1.2	1.2	0.85	0.78		
Radiation Power Fraction (Prad / Pheat)						0.77		0.9	0.8						
Fuel Purity, nDT/ne	0.8	0.8	0.8	0.8	0.8	0.8	0.8	0.91	fHe=0.07	fHe=0.1	fHe=0.1	0.82	0.77		
Toroidal beta, β_t (%)	6.5	6.5	5.4	5	4.1	5.1	5.0	5.7	2.9	1.1	1.4	2.5	2.8		
Pooidal beta, β_p	0.85	0.81	0.67	0.82	1.15	2.0	2.1	2.53	2.4	2.6	3.8	0.65	1.48		
fast ion beta, β_{fast} (%)	0.98	0.98	0.31	0.4	0.5	1.24	0.87	1.25	0.67	0.35	0.61	0.23			
Normalized Gyro radius, ρ^* (pooidal)	0.020	0.020	0.015	0.018	0.024	0.036	0.037	0.013	0.016	0.0086	0.0094	0.009	0.019		
Normalized Collisionality, ν^*	0.018	0.018	0.080	0.076	0.057	0.052	0.068	0.008	0.013	0.034	0.022	0.040	0.014		

* Definitions of ρ^* and ν^* are given in Chapt.5.

1.3. Roles of JT-60SA for DEMO

This section describes the main roles of JT-60SA for DEMO. As mentioned in the previous section, the JT-60SA device has been designed in order to satisfy all of the central research needs for ITER and DEMO. In other words, the JT-60SA research project complements ITER in all areas of fusion plasma development necessary to decide DEMO construction. For this purpose, the JT-60SA Research Plan has been organized to complete the main mission of JT-60SA before the end of DEMO construction design.

The most important goal of JT-60SA is, by collaborating with ITER, to decide the practically acceptable DEMO plasma design including practical and reliable plasma control schemes suitable for a power plant. The DEMO design reference for JT-60SA is an ‘economically attractive (= compact) steady-state’ reactor and the target values for the key plasma parameters have been set as shown in Fig.1-5. However, the JT-60SA research plan has to treat the ‘DEMO regime’ as a spectrum spreading around the reference. It should be also noted that DEMO needs to have realistic control margin. If JT-60SA cannot reach the reference values, we have to reduce the DEMO design parameters. In turn, if JT-60SA can demonstrate higher values, we can design a more compact DEMO reactor. However, if JT-60SA finds that the control margin is unrealistically small, we have to keep the present reference values. It should be emphasized that, for such decision making of DEMO plasma parameters, we have to consider ‘practicality, reliability and economy’. Evaluation of the DEMO plasma regime in terms of safety and availability as a power plant is also needed. The important role of JT-60SA is to provide sufficient data sets for these evaluations.

Such roles of JT-60SA are illustrated in Fig.1-7. The key research elements are a) extension of operation boundaries above ITER, b) demonstration of high integrated performance, c) development of an integrated plasma control system and then d) decision of DEMO design parameters. In exploring these subjects, collaborative studies with modeling / simulation, fusion engineering, and ITER are indispensable.

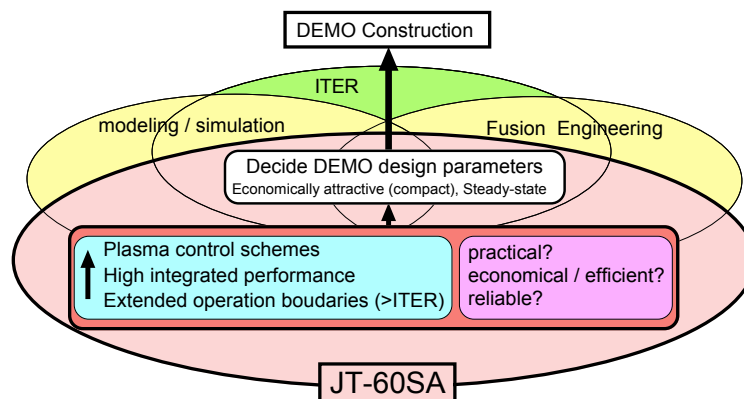


Fig.1-7 Roles of JT-60SA for DEMO

1) Characteristics of the self-regulating plasma system in DEMO

The fusion plasma is a self-regulating combined system. The most important role of JT-60SA research is to understand this plasma system and to establish a suitable control scheme and to demonstrate steady-state sustainment of the required integrated plasma performance (shown in Fig.1-5). Figure 1-8 shows a schematic feature of this fusion plasma system. The key points are as follows:

i) Fusion plasmas are governed by strong linkages among radial profiles of the plasma current

density, the plasma pressure and the plasma rotation both in the core plasma region and in the pedestal region. The degree of self-regulation (such as bootstrap current, intrinsic rotation) becomes stronger at higher β .

ii) Fusion plasmas have a global or semi-global nature encompassing the whole plasma regions from the core to the pedestal (Fig.1-9). This nature produces radial structures or resilience of plasma profiles. The pedestal plasma, giving the boundary condition for the core plasma, and SOL / divertor plasmas also have strong linkages involving plasma processes, neutral particle processes, and plasma-material interactions.

iii) Time scales of the processes determining such a fusion plasma system span (JT-60SA – ITER – DEMO regimes) from the growth time of ideal MHD instabilities / turbulence (\sim micro second), parallel and perpendicular transport time (\sim ms - second), plasma current profile evolution time (second \sim 10 second) to the wall saturation time (\sim 100 sec).

iv) The allowed fractions of external control (shown in violet in Fig.1-8) are small. In case of 70% bootstrap current fraction, for example, the fraction of externally driven current is 30%. The total current profile must be controlled with this small fraction. In case of Q (the fusion gain)=30 - 50, the fraction of external heating is 14% - 9% of the total heating power.

Related with iv) above, it should be noted that the most important issue for DEMO reactor design is integration of the achievements in JT-60SA and ITER for predictions of burning ($Q = 30-50$) high β high bootstrap fraction plasmas. In order to establish the plasma controllability for DEMO, both ‘burn control’ and ‘high β_N high f_{BS} plasma control’ have to be combined.

As shown in Fig.1-10(a), the fusion gain Q in DEMO is 30-50 and the external heating fraction (= external controllability) is 9-14%. In case of the ITER $Q=10$ operation, the external heating fraction is 33%. It is needless to say that demonstration of $Q=10$ in ITER is indispensable for development of burning plasma control. However, we need extrapolation / prediction from the ITER $Q=10$ plasmas to the DEMO $Q=30-50$ plasmas. In order to compensate this gap from ITER to DEMO, predictive studies with modeling / simulation are necessary.

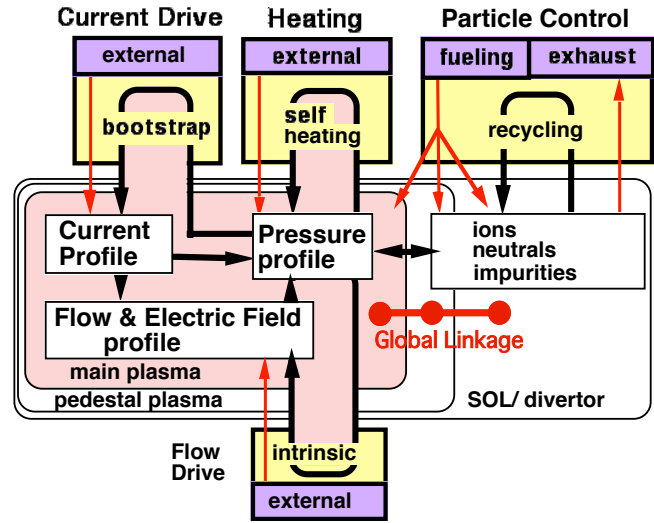


Fig.1-8 Parameter linkages in the fusion plasma system.

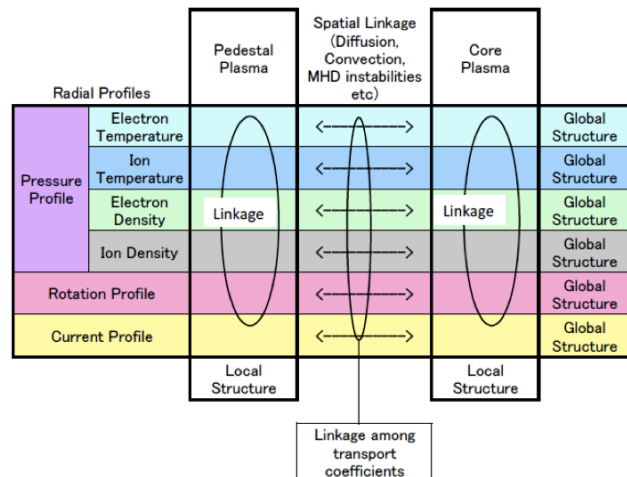


Fig.1-9 Global and local linkages of radial profiles of plasma parameters.

In addition, an attractive ‘burning plasma simulation’ can be carried out in JT-60SA. For example with the ‘high β_N Scenario 5-2’, when we inject P-NB (~ 17 MW) and ECH (~ 7 MW) power in proportion to the DD neutron production (or in proportion to $n_i^2 T_i^2$) by real time feedback, we can simulate a $Q \sim 20$ ($= 24 \times 5/6$; simulated α -power of 24 MW and external N-NBCD power of 6 MW) burn control in this high β_N high f_{BS} regime (triangle in Fig. 1-10(a)).

Figure 1-10(b) shows the bootstrap current fraction versus the external current drive fraction (= external controllability). The JT-60SA plasma regime is equivalent to that of DEMO. On the other hand, the ITER steady-state operation regime is insufficient to study the controllability at the small external current drive fraction required for DEMO. Figure 1-11 shows β_N and $f_{BS}/(1-f_{BS})$ = the ratio of the self-driven current to the externally driven current for the JT-60SA high β_N Scenarios 5-1 and 5-2, the ITER steady-state scenario, DEMOs (Slim CS, CREST, JA DEMO 2014 and EU DEMO2) and experimental results in JT-60U. When f_{BS} is 66 - 75 %, the ratio ‘self-driven: externally driven’ = 2 : 1 - 3 : 1. Only with this small fraction of the external drive, the ‘self regulating combined system’ should be controlled in DEMO. JT-60SA can explore such controllability at high values of β_N . However, JT-60SA cannot study real burning plasmas.

Therefore, ITER and JT-60SA needs to complement to each other. However, ‘ITER+JT-60SA’ is still not sufficient. When we predict DEMO plasmas based upon ITER and JT-60SA plasmas, we need a reliable set of modeling and simulation codes that can reproduce both ITER and JT-60SA and predict DEMO. In order to accomplish this integrated study of ‘ITER + JT-60SA + modeling/simulation = DEMO’, an integrated research for validation of theories and modeling / simulation codes is essential. Throughout the research areas treated in this document, JT-60SA Research Plan organizes such an activity in particular for validation of integrated modeling codes.

The central reference design of DEMO for JT-60SA is a compact steady-state DEMO. However, as mentioned above, the JT-60SA research project has to treat the ‘DEMO regime’

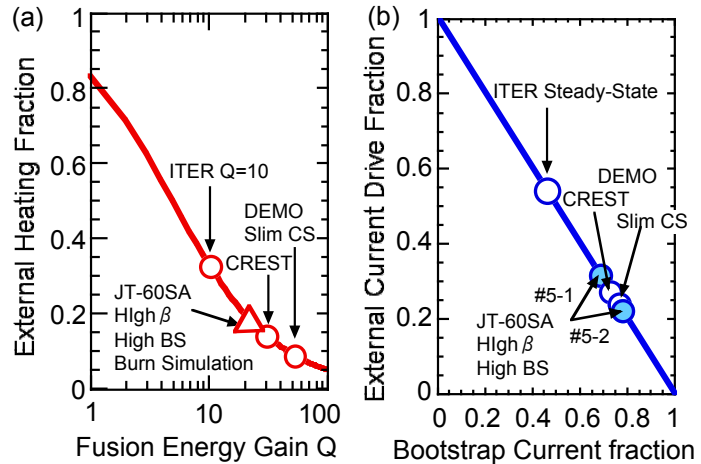


Fig.1-10 (a) The fusion energy gain Q for the ITER $Q=10$ scenario, DEMO (Slim CS and CREST), and the simulated Q by JT-60SA (high β_N Scenario 5-2 in Table.1-3). (b) The bootstrap current fraction and the external driven current fraction for the ITER steady-state scenario, DEMO (Slim CS and CREST) and JT-60SA (high β_N Scenarios 5-1 & 5-2 in Table.2-3).

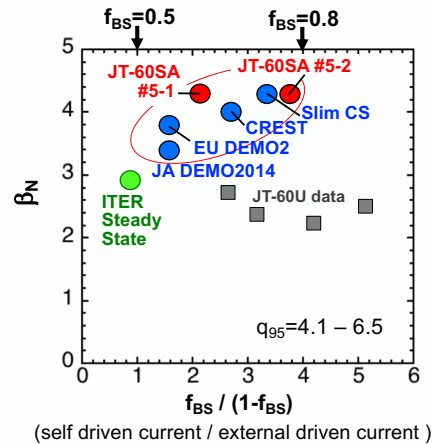


Fig.1-11 β_N and $f_{BS}/(1-f_{BS})$ = self driven current / external driven current for JT-60SA, ITER steady-state, DEMO (Slim CS and CREST) and JT-60U experimental achievements

broadly as a spectrum around the reference design, and has to assess reliable DEMO design

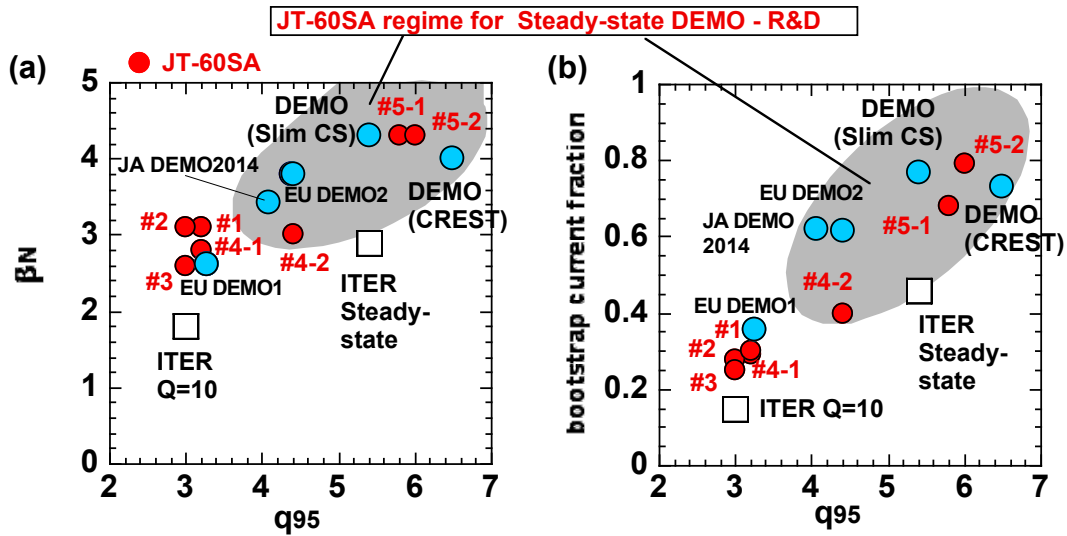


Fig.1-12 The JT-60SA research regime for assessment of DEMO designs.

targets. The JT-60SA research regime for such DEMO assessment is shown in Fig.1-12.

2) Extension of operation boundaries and demonstration of high integrated performance

As for contribution to DEMO, the first step is to extend the operational boundaries exceeding the requirements for ITER. In terms of the plasma pressure limit, the operation boundary have to be extended above the non-wall ideal MHD stability limit, such as $\beta_N=3-5.5$, for an economically attractive compact DEMO design. Identification of the acceptable bootstrap current fraction boundary in the fully non-inductive current drive condition is also fundamentally important to decide the steady-state DEMO design with a small circulating electric power inside the plant. Another operation boundary critical for DEMO design is the minimum required magnetic flux produced by the center solenoid (CS) coils for plasma current ramp-up. This is because the size of the CS coil determines size, shape and radial build-up of the DEMO reactor. For this study, sustainable bootstrap current fraction during the plasma current ramp-up phase and the applicability of external current drive from an early phase of the discharge are central research subjects. For these purposes related with high- β_N high bootstrap fraction with full non-inductive current drive, the JT-60SA device is given a capability to produce high-shape-parameter plasmas equivalent to Slim-CS DEMO and is equipped with various stability controllers and strong plasma current drivers.

As for the plasma density limit, possibility of operation above the Greenwald density limit, such as $n_e/n_{GW} = 1.1-1.3$, with keeping a sufficient H_H -factor is also a key factor for DEMO design in order to achieve high fusion power. At present, however, there is no reliable solution. One possibility is to optimize the plasma regime with both internal and edge transport barriers (ITB and ETB) with a centrally peaked density profile inside ITB. In this case, impurity accumulation inside ITB has to be avoided and degradation of energy confinement of ETB has to be minimized. Towards this optimization, JT-60SA prepares maximum possibilities such as the highly shaped plasma equilibrium for improving ETB confinement, central ECH for impurity reduction, off-axis N-NB for optimizing the flat / reversed current profile in order to control strength of ITB, variety of particle injection, and changeable divertor pumping.

Minimization of the divertor heat flux ($<5 \text{ MW/m}^2$), in other words, maximization of divertor radiation, is another critical issue in DEMO. In order to contribute to this issue, JT-60SA expands the required data set applicable directly to DEMO by utilizing the W-shaped

divertor with V-corner, changeable divertor pumping and the various particle fueling systems. The replaceable divertor structure system in JT-60SA enables easy modification of the divertor shape. The change of the first wall from carbon to tungsten will enable the validation of the divertor concept for DEMO in a metallic environment.

In DEMO reactors, we have to sustain the high integrated performance shown in Fig.1-5. Based on, or in parallel to, the extended operation boundaries mentioned above, JT-60SA proceeds exploration for demonstration and sustainment of this integrated performance towards DEMO. This study of the integrated performance includes applicability of naturally producible small ELMs (such as Grassy ELMs or no-ELM regime), controllability of fast ion transport, compatibility with metallic wall with high-Z impurity control, disruptivity, compatibility with DEMO components such as blanket, etc.

3) Development of an integrated plasma control system

In order to establish control schemes of burning high β plasmas, we have to decide plasma actuators, parameters to be controlled, and sets of control matrix by taking account of required integrated performance, fractions of external controls and control time scales. The required functions of plasma control are shown in Fig.1-13. For a plasma parameter to be controlled, there is an operation boundary (upper limit or lower limit). Within the operation boundary, a target value (a mean reference value) and a control window have to be decided. The control window has to be set within a control margin. The control margin and the control window are functions of plasma parameters and should be determined by plasma response characteristics. In addition, some decisions (such as soft-landing) have to be made according to ‘real time prediction’. Thus, proper functions of ‘measurement - prediction - control - decision’ should be applied for the steady-state phase and the transient phases such as increase / decrease of fusion output, plasma current ramp-up / down etc.

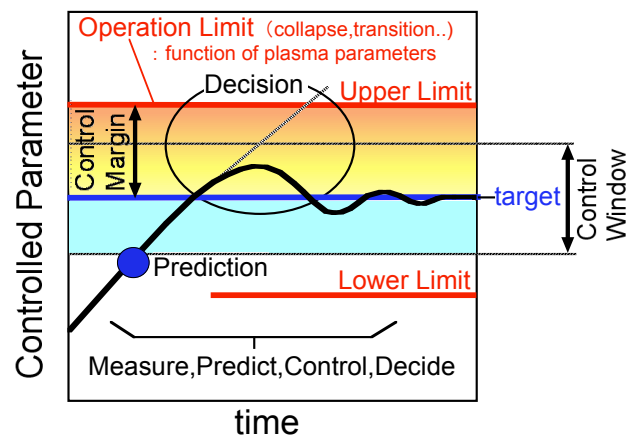


Fig.1-13 Required function of Plasma Control

From the view point of DEMO, minimization of electric power consumption required for plasma control and simplification of diagnostics and actuators are important. For example, in order to keep a required tritium breeding ratio (TBR), we have to minimize the area (space) occupied by diagnostics. Therefore, we need to determine a minimum set of measurement required for plasma control. As for plasma actuators, it may not be practical to install in-vessel coils such as RMP coils and RWM control coils in DEMO. Therefore, we need to utilize naturally produced small-ELMs, such as Grassy ELMs, and naturally produced (intrinsic) plasma rotation for RWM stabilization.

As for the plasma rotation, if the rotation control is required only for RWM stability and if the intrinsic rotation speed is above the threshold speed required for RWM suppression, we do not need real-time feedback of rotation. However, if a control method having the energy / particle confinement time scale is required in addition to the particle fueling control, we need real-time control of the plasma rotation. Such a situation appears when the burn-control cannot be covered only by particle fueling control. The required time scale for burn-control is the energy / particle confinement time scale. However the external heating power fraction is quite

small in DEMO and time scale of the plasma current profile control is much longer than the energy / particle confinement time. The important role of JT-60SA is to decide whether real-time control of rotation is needed in DEMO or not.

The above mentioned ‘simplification of diagnostics and actuators’ is a completely different approach compared with what we have been promoting in the present-day experiments. Towards DEMO, the final goal of JT-60SA is such simplification.

1.4. JT-60SA Fusion Plasma Research Areas for ITER and DEMO

JT-60SA supports the exploitation of ITER and complements ITER in resolving key physics and engineering issues for DEMO reactors. The JT-60SA device has been designed to satisfy all of the central research needs for DEMO and ITER (Table1-2). This section summarizes research areas of JT-60SA for ITER and DEMO. JT-60SA starts operation with carbon wall and explores the following ITER and DEMO plasma regimes in a wide range of plasma parameters. After maturing the integrated control system, the divertor target and the first wall will be fully changed to tungsten-coated carbon and all the research targets will be achieved under the metal wall.

1) Operation Regime Development

By utilizing the capabilities mentioned above, JT-60SA can promote the following studies for establishment of the integrated control schemes.

1-1) for ITER and DEMO

- (i) JT-60SA identifies operational boundaries, determines control margins, clarifies plasma responses, selects the optimum and minimum set of actuators and diagnostics, determines the suitable control logic (such as non-linear control gain matrix, real time prediction, etc.), and demonstrates the real-time control in long pulse discharges exceeding the longest time scale governing the plasma system.
- (ii) Controllability of plasma equilibrium including recovery after plasma events (such as disruption) has to be clarified considering engineering limitations of the super conducting poloidal field coil system. Particle control has to be demonstrated under saturated wall conditions. Current profile control has to be demonstrated in the vicinity of the relaxed current profile with high bootstrap current fraction ($<50\%$ for ITER and $>50\%$ for DEMO) in durations largely exceeding the resistive time.
- (iii) These studies of operational regime development are carried out at ITER- and DEMO-relevant parameter regions of low collisionality, small gyro radius, dominant electron heating, low external torque input, and low central fueling. One of the key element for achievement of a required integrated plasma performance is achievement of high confinement and stability together with radiative divertor and low impurity accumulation by optimizing fueling (pellet, gas) and pumping.

1-2) for ITER

- (i) In order to contribute to the $Q=10$ operation in ITER, JT-60SA demonstrates the required integrated performance of H-mode with the ITER-like plasma shape at high plasma current (4.6 MA, $q_{95}\sim 3$) and high density ($\sim 1 \times 10^{20} \text{ m}^{-3}$) by applying the plasma control techniques planned in ITER such as RMP, pellet injection, divertor pumping, etc.
- (ii) JT-60SA demonstrates advanced inductive operation in improved H-mode at plasma current $\sim 3.5 \text{ MA}$ ($q_{95}\sim 4$) in order to contribute to the so-called ITER hybrid operation and provide the $Q=10$ alternative scenario.

- (iii) JT-60SA studies operational boundaries (such as the stability limit and the density limit) and determines control margins for the plasmas described in (i) and (ii).

1-3) for DEMO

- (i) JT-60SA explores and demonstrates the required integrated performance in steady-state (shown in Fig.1-5) at high values of β_N exceeding the no-wall ideal MHD stability limit, the bootstrap current fraction, the confinement improvement factor, the normalized density, the fuel purity, and the radiation fraction (required for sufficiently small heat load on to the divertor plates). The high power (10MW) off-axis NNB current drive system is used for optimization of weak / negative magnetic shear plasmas.
- (ii) JT-60SA determines the operational boundaries and control margins, in particular at high β_N exceeding the no-wall stability limit, at high radiation fraction >90% relative to the heating power, and their composite state. JT-60SA also explores high-density operations above the Greenwald density, such as 1.1- 1.3 x n_{GW} .
- (iii) JT-60SA studies the ‘self-regulating combined system’ and develops a suitable integrated control system for the plasmas described in (i) with a minimum set of actuators and diagnostics applicable for DEMO. Towards DEMO, JT-60SA develops RWM stabilization without RWM control coils by plasma rotation, and demonstrates type-I ELM mitigation without RMP application by developing small ELM regimes (such as Grassy ELMs or no-ELM regimes).
- (iv) JT-60SA develops non-inductive current ramp-up schemes for minimization of required poloidal flux. Operation scenarios helpful for identifying of DEMO/reactor operation patterns and their commissioning procedures (such as recovery from thermal collapse and target plasma suitable for commissioning DEMO plant components) are investigated as well.
- (v) Based on the experiments described in (i) – (iii) and results in ITER burning plasmas, validation of integrated modeling codes is systematically conducted for predictions of burning ($Q>10$) high-beta high-bootstrap- fraction plasmas.

2) MHD Stability and Control Studies

2-1) for ITER and DEMO

- (i) JT-60SA explores the kinetic stabilization effect of energetic particles by using NNB with 500keV beam energy in order to investigate RWM stability for ITER and DEMO high- β_N plasmas.
- (ii) JT-60SA validates ECCD sawtooth control for ITER hybrid scenario and low-performance DEMO ($q_0\sim 1$). Alpha particle stabilization on sawtooth can be also investigated by NNB with 500keV beam energy.
- (iii) JT-60SA explores avoidance of VDE by the neutral point operation and runaway electron mitigation by applying massive matter injection and/or application of helical fields by in-vessel coils in high I_p large bore plasmas for ITER and DEMO.

2-2) for ITER

- (i) JT-60SA optimizes effective real-time stabilization schemes for $m/n=2/1$ and $3/2$ NTMs by ECCD using movable mirrors and high frequency Gyrotron modulation at >5kHz for the high I_p and low q_95 plasmas having the ITER-relevant non-dimensional parameters (ρ^* , v^* and β). Compatibility with RMP is also investigated.
- (ii) JT-60SA demonstrates long pulse high $\beta_N \sim 3$ plasmas and determines the MHD stability boundary by exploring RWM stabilization with RWM-control coils and high resolution magnetic diagnostics with the ITER-like plasma shape.
- (iii) For disruption avoidance, JT-60SA develops disruption prediction schemes (including the

use of neural network) and control logics for plasma recovery and landing in a sufficiently short time scale. JT-60SA also explores fast VDE controls using the vertical stabilization coils. In particular in order to contribute to ITER operation with the full tungsten divertor, the disruption mitigation systems (massive gas injection, impurity pellet injection and advanced system such as shattered pellet injection) will be strenuously developed and established on JT-60SA to avoid unacceptable heat loads with fast response.

2-3) for DEMO

- (i) Long sustainment of high β_N plasmas above the no-wall ideal MHD stability limit is the central research subject of JT-60SA. JT-60SA demonstrates long pulse high β_N (≈ 3.5 - 5.5) plasmas and determines the MHD stability boundary for DEMO-equivalent highly shaped plasmas (Fig.1-4(a)). At the same time, JT-60SA clarifies the minimum requirements for RWM stabilization by plasma rotation, rotation shear and other effects, and quantifies the stability boundary and operational margin. Interactions between RWMs and other MHD modes (such as EWM and ELMs) have to be investigated to evaluate the stability limit.
- (ii) JT-60SA demonstrates simultaneous stabilization of NTM and RWM at high $\beta_N > 3.5$. Since these plasmas have high $q_{\min} (> 1.5)$, $m/n=2/1$, $5/2$ and $3/1$ NTMs have to be stabilized.
- (iii) JT-60SA identifies disruption limits at high β_N and at high radiation with impurity seeding, and their combination, then clarifies disruption-free operational regimes and develops soft-landing schemes to avoid a hard thermal quench.

3) Confinement and Transport Studies

3-1) for ITER and DEMO

- (i) Confinement and transport (heat, particle, and momentum) characteristics including detailed physics processes such as plasma turbulence are clarified to understand the self-regulating combined system shown in Fig.1-7 and Fig.1-8 and to establish the integrated plasma control schemes at ITER- and DEMO- relevant non-dimensional parameters such as low values of the normalized collisionality and the normalized poloidal gyro radius as shown in Fig. 1-4(b). The non dimensional plasma parameters have a direct impact on small scale fluctuations and hence on turbulent transport.
- (ii) In addition, the studies of confinement and transport (heat, particle, and momentum) are conducted with ITER- and DEMO-relevant heating conditions; such as dominant electron heating, low central fueling enabled by NNB and ECH, in the presence of a large population of fast ions and low external torque input enabled by NNB, ECH, perpendicular PNBs and balanced injection of CO and CTR tangential PNBs. Effects of electron heating fraction and plasma rotation are also clarified by changing the combination of these heating systems.
- (iii) The origin and dependence of the intrinsic rotation are studied at high beta or high pressure region by taking advantage of various NB injection geometries and ECRF.
- (iv) Transport and confinement studies in JT-60SA will take advantage of its ability to operate highly shaped, long lasting discharges. The role of shaping on confinement of both the plasma core and the pedestal will be clarified.
- (v) Transport characteristics of light and heavy impurities is systematically studied under these ITER- and DEMO- relevant regimes in order to develop schemes of He-ash and impurity accumulation control.

3-2) for ITER

- (i) Confirmation and extrapolation of the energy and particle confinement times to ITER $Q=10$ plasmas are conducted using high- I_p high-density ITER-shape plasmas including hydrogen and helium discharges under ITER-relevant heating conditions described above with the

carbon wall and later with the metallic wall.

- (ii) JT-60SA promotes burning simulation experiments by using a variety of NBs, and clarifies plasma responses and controllability by applying the plasma control techniques planned in ITER, such as RMP, pellet injection, divertor pumping, etc. The key point is to clarify whether or not a reliable burn control can be accomplished by fuelling control.

3-3) for DEMO

- (i) As the most important research subject for DEMO, JT-60SA clarifies transport characteristics and plasma responses to external drives for highly self-regulating plasmas (Fig.1-7 and Fig.1-8) at high values of β_N and bootstrap current fraction.
- (ii) Confirmation and extrapolation of energy and particle confinement to DEMO plasmas are conducted using DEMO-equivalent highly shaped high β_N plasmas. Extension of high confinement regimes for higher densities, such as 1.1- 1.3 x n_{GW} , is explored. Particle confinement and exhaust, in particular for high Z impurities, in high energy confinement (H_H -1.3) plasmas should be clarified.

4) High Energy Particle Studies

4-1) for ITER and DEMO

- (i) Utilizing the high power (10 MW) and high energy (500 keV) NNB, JT-60SA clarifies the stability of Alfvén Eigenmodes (AEs) and the effects of AEs on fast ion transport at ITER- and DEMO-equivalent values of fast ion beta 0.2 – 1 % with $V_{fast-ion}/V_{alfven} = 1.5 - 2$ over a wide range of safety factor profiles from monotonic to reversed. In addition, an application of AEs to the control of α -particles and to the diagnostics, so-called MHD spectroscopy, for the bulk plasma characteristics, e.g. q_{min} , is investigated.
- (ii) In order to improve the predictability of α -particle behavior in ITER and DEMO, transport behaviors of tritons produced by DD reactions are studied.
- (iii) Interactions between high energy ions and MHD instabilities, such as sawtooth, NTM, EWM/RWM, are studied using NNB. In particular impact of high energy particles on high beta stability are studied.

4-2) for ITER

- (i) Current drive capability of high energy NBI is studied using the 500 keV 10 MW NNB.

4-3) for DEMO

- (i) Off-axis current drive and current profile controllability are evaluated with off-axis NNBCD.

5) Pedestal studies

5-1) for ITER

- (i) The L-H transition conditions, such as the threshold power, are quantified for hydrogen, helium and deuterium plasmas in the high I_p (4-5.5MA) and high density ($n_e/n_{GW}=0.5-1$, $n_e=0.5 - 1 \times 10^{20} \text{ m}^{-3}$) regime in particular with ITER-shape at $I_p=4.6\text{MA}$. In addition, the L-H transition threshold condition is confirmed for ITER with high power electron heating by ECH and NNB. JT-60SA is in a unique position to carry out L-H transition studies towards ITER at low v^* and high density under large fraction of electron heating using NNB. In addition the carbon wall allows easy access to carry out low density studies of the L-H transition. ITER will operate at relatively low input power above the L-H transition and at low plasma rotation and low plasma density. The capability of high current access, balanced beam operation and the tunable ratio of electron/ion heating places JT-60SA in an excellent

- position to carry out ITER relevant studies.
- (ii) The pedestal structure, the width and the height, and inter-ELM transport are clarified over wide ranges of I_p and density up to $I_p=5.5$ MA and $n_e=1 \times 10^{20}$ m⁻³ in order to predict the performance of Q=10 plasmas in ITER.
 - (iii) Reliable schemes of Type-I ELM mitigation are strongly required for ITER starting with full tungsten divertor. Type-I ELM energy loss is a function of the pedestal collisionality. JT-60SA pedestal plasmas can cover a wide range of collisionality from sufficiently lower to sufficiently higher than that of the ITER standard operation. JT-60SA clarifies the type-I ELM energy loss and the transient heat load to the divertor plates. At the same time, effects of RMP and pellet pace making (by both high-field-side and low-field-side injections) for ELM mitigation are clarified under ITER-relevant pedestal conditions.

5-2) for DEMO

- (i) Control of burning plasma by optimized pedestal condition which is easy to access utilizing the linkage between core and edge plasmas is very attractive as a control knob. Operational scenario of edge plasma control should be established under the condition of high beta plasma by both simulation and experiment for design and operation of DEMO reactor.
- (ii) For long pulse operation in DEMO reactor, studies on L/H transition and pedestal structure under detached divertor are an important issue in order to mitigate divertor heat load of type-I ELMs. The higher neutral flux at the detached divertor may affect the threshold power of H-mode transition so that this issue is studied as well.
- (iii) The high triangularity of JT-60SA plasmas is well inside the region suitable for the appearance of small ELMs (Grassy ELMs). JT-60SA expands the Grassy ELM regime and demonstrates ELM mitigation without RMP application. JT-60SA's aim is to support High β operation in DEMO. It is therefore important that scenario development should be linked to passive and active type I ELM control under the operation with a radiative divertor.

6) SOL, Divertor and Plasma-Material Interaction Studies

One of the most important missions of JT-60SA is to demonstrate divertor power and particle handling by a divertor under high heat and particle flux conditions from high performance core plasmas at a high heating power of 41 MW for a long pulse of 100 s. The edge plasma parameter range of high-density plasmas at high plasma current in JT-60SA is relevant to that of ITER and DEMO. In equilibria of all the plasmas shown in Table 1-3, '2cm SOL' connects with the vertical divertor target of the ITER-like divertor structure of JT-60SA.

In terms of selection of materials for the divertor and the first wall, the basic strategy of JT-60SA is to utilize carbon until achievement of the high β_N high bootstrap fraction steady-state plasmas (Fig.1-5).

6-1) for ITER and DEMO

- (i) JT-60SA pursues, at required levels in ITER and DEMO, compatibility of highly radiative divertor plasmas and high pressure pedestal plasmas in a wide parameter range of divertor plasmas by utilizing a variety of fuelling and pumping systems: gas-puffing into main and divertor plasmas, pellet injection, and divertor pumping.

6-2) for ITER

- (i) In order to support ITER divertor operation, a full tungsten divertor will be installed after Integrated Research Phase I. Stability and controllability of detached divertor plasmas are studied in long and high power heated discharges with the ITER-like divertor geometry, *i.e.*,

the vertical target and the ‘V-shaped corner’.

6-3) for DEMO

- (i) With the full metallic divertor and first wall installed after the Integrated Research Phase I, the high β_N high bootstrap fraction steady-state operation will be demonstrated.
- (ii) In order to optimize the power and particle handling capability, a full metallic divertor with an advanced geometry will be installed in Extended Research Phase. JT-60SA attempts to reduce the heat flux onto the divertor target down to the required level in DEMO, for example 5 MW/m^2 , for up to 100 s. This will be achieved with the high confinement core plasma required for DEMO together with sufficient He pumping efficiency.

1.5. Fusion Engineering Research in JT-60SA for ITER and DEMO

In the fusion engineering research, the most important loads which should be considered, are, particle load, heat load, electro-magnetic load and neutron load. Therefore, similar loading conditions to the development target are envisaged as experimental environments. Since above mentioned loadings will be loaded simultaneously to the materials and components in the real fusion engineering environment, research activities need complex testing environment. JT-60SA is a large Tokamak experimental machine, which handles significant particle loading, significant magnetic field and heat load. If it is used as test bed for fusion engineering research, its contribution to the fusion engineering research will be enormous.

In the component development, ITER is one of the most important milestones, by which fusion engineering components can be tested in the real fusion environment. On the other hand, the opportunity of component testing in ITER, however, will be limited. JT-60SA offers the important opportunity to test components in the equivalent magnetic fusion environment to complement the data and to enhance the reliability of testing. Especially, in the blanket development program, test blanket module testing in ITER is one of the most important missions, however all test blanket modules are made of ferritic steels, which are the selected structural materials for DEMO blanket. Therefore, prior to the ITER TBM testing, ferro-magnetic effect of the test blanket modules on ITER plasma needs to be carefully evaluated so that the ITER mission $Q=10$ shall not be deteriorated. JT-60SA is one of the most important experimental machines for this matter. This ferro-magnetic testing is not only the testing of component but also the influence to the plasma.

Toward DEMO, fusion engineering research needs to enhance the performance and reliability under the real magnetic fusion environment, including innovative research for highly advanced DEMO reactors. JT-60SA can also offer testing opportunities to such research areas. Such testing will be more and more important toward the realization of DEMO reactor.

The major R&D items of component development are mainly categorized into the following areas,

- Tests of Measurement Equipments
- Ferro-magnetic Influence Test
- Blanket Structure Test
- Blanket Mockup Neutronics Measurement
- Divertor Mockup Test

The content, test mockup scale and objectives of each research area are summarized in Table 1-4.1. As mentioned above, some items are objected to specification decisions of ITER related components, test schedule of such area is relatively early.

Further investigations are necessary to specify quantitative and effective test plans of the fusion engineering component development using JT-60SA.

Because of high erosion and tritium retention rates of carbon, plasma facing material will be metal in DEMO, and tungsten is a candidate for the material. Therefore studies of plasma-material interactions on metallic walls are crucial issues toward DEMO. For these studies, JT-60SA can be a good test bed (summarized in Table 1-4.2), and collaboration studies with other fusion devices, laboratory experiments, and modelings are important.

The major issues are categorized into the following areas;

- Hydrogen isotopes retention in all-metal device
- Erosion and damage of metallic plasma facing components
- Safety and maintenance issues of all-metal device
- Development of new materials.

Reliable operation and improvement of technical systems at JT-60SA is essential to ensure the success of the experiment. JT-60SA can also provide valuable return of experience with the operation of these systems, if the technology used at JT-60SA is similar or related to the one foreseen at ITER and DEMO.

- Development and improvement of remote handling systems
- Integration of CODAC system for large fusion device
- Reliable operation of large cryogenic systems
- Demonstration of ITER relevant pumping and fuelling systems
- Return of experience in pumping, fuelling, cryogenic, magnets, power supply, NBI and ECRH heating systems.

Table 1-4.1 Research Areas of Component Development in Fusion Engineering Research in JT-60SA

Research Area	Content	Test Scale	Objective
Tests of Instrumentation Equipment	To test performance of various measurement equipment for component development, such as thermo couples, strain gauge etc. for component test module.	Small mockups attached in diagnostic port	ITER Test Blanket, DEMO, DEMO Test components
Ferro-magnetic Influence Test	To test performance of the plasma by ferritic test components and the damage of ferritic test components as well as blanket structure tests	Small to full test port size, multiple test ports	Several years before start of DD in ITER
Blanket Structure Test	To test high heat flux and electro-magnetic force	Small mockup of diagnostic port size to large full port size	DEMO Test components
Blanket Mockup Neutronics Measurement	To obtain neutronics performance data by DD neutrons , validate blanket module neutronics performance and testing neutronic instrumentation	Small mockup of diagnostic port size to large full port size	ITER Test Blanket
Divertor Mockup Test	To test performance of high heat flux components in real plasma environment	Divertor outer target size	Before decision of future W divertor decision for ITER and DEMO

Table 1-4.2 Research issues of plasma-material interactions in JT-60SA

Research area	content	Test scale	objective
Hydrogen isotopes retention in all-metal device	To investigate hydrogen isotope retention in metallic bulk and deposition layer. To develop and test hydrogen isotope removal method.	Particle balance study and postmortem analysis of plasma facing components in JT-60SA with all-metal wall. Laboratory experiments and modeling are also necessary.	DEMO
Erosion, migration and damage of metallic plasma facing components	To investigate mechanisms of erosion caused by sputtering and by high heat flux. To investigate mechanisms and effects of damages caused by neutron irradiation.	Material probes in JT-60SA. Laboratory experiments and modeling are also necessary.	DEMO, ITER
Safety and maintenance issues	To investigate mechanisms of metallic dust formation and deposition profile of them. To develop dust monitor and removal method.	Dust collection after experimental campaign and test the monitor and removal method in JT-60SA. Laboratory experiments and modeling are also necessary.	DEMO, ITER
Development of new materials	To develop new materials, such as tungsten alloy, and test them in JT-60SA.	Material probes in JT-60SA. Laboratory experiments are also necessary.	DEMO

1.6 Development and improvement of theoretical models and integrated simulation codes in JT-60SA for ITER and DEMO

The theoretical models and simulation codes play an indispensable role to understand various linked phenomena expected to appear in burning plasmas with high-beta and high-bootstrap-fraction, and to predict the behavior of such plasmas in ITER and DEMO. The theoretical models and simulation codes can predict plasma behaviors which are not yet found in the experiment and thus play a key role to plan the experiment in order to confirm the prediction. The prediction confirmation by the JT-60SA experiment leads to the validation of theoretical models and simulation codes in high-beta high-bootstrap-fraction plasmas. The validated theoretical models and simulation codes will be applicable to the prediction of burning plasmas in ITER and they will be validated again with the experimental observations of burning plasmas in the ITER experiment. The validation of the theoretical models and simulation codes by both the JT-60SA and ITER experiments is required to reliably predict the behavior of burning plasmas in DEMO. Thus, the validation of theoretical models and simulation codes with the aim of establishing a solid basis for the design of ITER and DEMO scenarios is one of the main objectives of the JT-60SA scientific programme.

The theoretical models and simulation codes should cover issues in the central research needs for ITER and DEMO (see Table 1-2) and include both physics and engineering issues. First, codes which can describe each of issues need to be developed and improved in order to understand the mechanisms and predict them. We should make the strategy to develop codes/models towards DEMO by knowing existing/developing codes/models and then finding missing codes/models to be developed in future. Then, an integrated code including the modules which describe physics and engineering issues is necessary for understanding the physics mechanisms linked with each other, predicting complicated behavior of self-regulating plasmas, developing operation scenarios and establishing the integrated control system. In addition, owing to the limitation of available measurements in DEMO, it is necessary to develop a tokamak simulator which provides reliable and precise prediction of the dynamic behavior of burning plasmas. Modeling and simulation studies based on the JT-60SA experiments should

aim to develop the burning plasma simulator applicable to ITER and DEMO.

In order to efficiently carry out the verification (including code-to-code benchmark tests) and the validation (code-to-experiment comparison) of available codes, it is required to establish a common framework which defines the interface for data exchange among the codes and comparison with experimental data. This framework is helpful not only for direct comparison between the codes and the experiments, but also for smooth integration of various codes. The framework to be developed in JT-60SA research should aim to be extended as a standard framework for DEMO.

Before the start of JT-60SA experiment, theoretical models and simulation codes are developed, improved and validated by using the experimental data in JT-60U and other machines. In particular, an integrated modelling set of prescriptions should be prepared and validated in order to have a sound basis for the JT-60SA simulations. It appears that simulations of JT-60SA scenarios should be based at least on experimental results of the two machines that are the most similar, for size and configuration: JT-60U and JET. The validation of models and codes against JT-60U and JET plasmas serves to improve the predictive capability towards scenario development for JT-60SA. The validated models and codes will be used for the plasma design, for clarifying the operation boundary, defining target plasmas and planning operation scenarios to realize the target plasma and so on.

After the start of JT-60SA experiment, validation of the theoretical models and simulation codes using the experimental data becomes available. Emphasis should be made on the model validation for the phenomena specific to high-beta and high-bootstrap-current physics in the JT-60SA experiment. In the Initial Research Phase of JT-60SA, simulation codes will be validated and improved individually. In the Integrated Research Phase and the Extended Research Phase, the integrated code will be developed and validated. The validation will be also carried out for ITER experiments, especially on burning physics. The theoretical models and simulation codes validated by both JT-60SA and ITER experiments help to reliably predict the behavior of burning high-beta high-bootstrap-fraction plasmas and to develop operation scenarios in DEMO. All these efforts will contribute to the development of comprehensive tokamak simulators available for ITER and DEMO.

1.7. Main features of the JT-60SA device

The main features of the JT-60SA device are summarized as follows:

a. Fully Superconducting Large Tokamak

JT-60SA is a fully superconducting tokamak capable of confining break-even equivalent class high-temperature deuterium plasmas (the maximum plasma current of 5.5 MA) lasting for a duration up to 100 s, longer than the timescales characterizing key plasma processes. In case of reduced plasma current and heating power, discharge duration longer than 100 s (for example 300 s) is possible.

b. Highly Shaped Plasma Configuration

JT-60SA allows exploration of plasma configuration optimization for ITER and DEMO with a wide range of plasma shape (plasma elongation κ_x up to ~ 1.9 , triangularity δ_x up to ~ 0.5 , shape factor $S=q_0 I_p / (a B_t)$ up to ~ 7 , and aspect ratio A down to ~ 2.5 including the shapes of ITER and DEMO, with a capability to produce both single- and double-null configurations.

c. Strong Heating and Current Drive Power with Various Mix [see Appendix A]

The JT-60SA heating and current drive systems allow 41 MW plasma injection for 100 s, which consist of 34 MW of neutral beam injection (10 MW of N-NB + 24 MW of P-NB) and 7 MW of ECRF.

The negative ion source based neutral beam (N-NB) system provides 10 MW/500 keV co-tangential injection. The positive ion source based neutral beams (P-NBs) at 85 keV consist of 2 units of co-tangential beams (4 MW), 2 units of counter-tangential beams (4 MW), and 8 units of near perpendicular beams (16 MW). The N-NB system consists of two beams (5MW maximum for each beam) with different injection trajectory; one is relatively on-axis and the other is pretty off-axis. This N-NB injection trajectory has been optimized to sustain the weak / negative magnetic shear plasmas in steady-state. The N-NB driven current profile and the resultant q-profile can be controlled by changing combination of these two beams. This NB system allows a variety of heating/current-drive/momentum-input combinations.

The ECRF system with 9 Gyrotrons allows the injection power of 7MW x100s. The Gyrotrons will be dual-frequency at the first frequency of 110GHz and the second frequency of 138GHz in order to cover a wide experimental regime of the toroidal field, electron density and resonant locations. The ECRF system allows a real time control of the deposition location by steerable mirrors and high frequency (>5 kHz) modulation of the injection power.

d. Large Capability of Divertor Power Handling and Particle Control [see Appendix B]

JT-60SA allows studies of power and particle handling at the full injection power of 41 MW for 100 s using the lower and upper water-cooled divertors compatible with the maximum heat flux of 15 MW/m² for both carbon mono-block divertor and tungsten-coated carbon mono-block divertor. The W-shaped configuration and the vertical target with a V-corner (at the outer target) enhance radiation from the divertor area. Material of the plasma facing components (divertor and first wall) is initially Carbon. Metallic divertor targets and first wall together with an advanced shape divertor will be installed in a later phase of the JT-60SA project in order to demonstrate the high integrated performance with metallic wall. The divertor pumping speed up to 100 m³/s can be changed in 8 steps for the lower divertor. The fuelling system consists of the main- and divertor-gas puffing for multiple gas species and high- and low-field-side pellet injection.

e. Large Capability of Stability Control [see Appendix C]

JT-60SA allows exploitations of high beta regimes with stabilizing shell matched to the highly shaped configurations, the first position control coils (FPCs: two independently controllable coils) for equilibrium control, the resistive wall mode (RWM) stabilization coils (RWMCs: 3-poloidal x 6-toroidal), the error field correction (generation) coils (EFCCs: 3-poloidal x 6-toroidal) and the high power heating, current drive, and momentum-input systems. The error field correction coils allow resonant magnetic perturbation (RMP, n=3) for ELM suppression for various plasma regimes.

f. Variety of High Resolution Diagnostics [see Appendix D]

At present, 26 systems are in preparation for plasma diagnostics with high spatial and temporal resolutions sufficient for conducting the physics research and plasma real-time controls proposed in this document. In particular, by combining these diagnostics systems and the plasma actuators listed above, advanced real-time control schemes for the highly self-regulating plasmas will be developed.

1.8. Research Phases of JT-60SA

The research phases of JT-60SA consist of 1) the initial research phase (hydrogen phase and deuterium phase), 2) the integrated research phase, and 3) the extended research phase as shown in table 1-5. The machine capability, such as heating, divertor, remote handling etc. will be enhanced step by step.

Table 1-5 Research phases and status of the key components

	Phase	Expected operation schedule	Annual Neutron Limit	Remote Handling	Divertor	P-NB Perp.	P-NB Tang.	N-NB	NB Energy Limit	ECRF 110 GHz & 138 GHz	Max Power	
Initial Research Phase	phase I	2020–2021 (5M)	H	–	R&D	Upper Carbon	0	0	0	0	1.5MWx5s 2Gyrotrons	1.5MW
		2023 (2M)				Lower Carbon Div. Pumping	3MW 4units	3MW 4units	20MW x 100s 30MW x 60s duty = 1/30	1.5MWx100s 2Gyrotrons + 1.5MWx5s 2Gyrotrons	19MW	
	2023 (6M)	6.5MW 4units	7MW 4units	10MW 2units			26.5MW					
	2024–2025 (8M)	D				3.2E19	Lower monoblock-Carbon Div. Pumping	13MW 8units		7MW 4units	10MW 2units	7MW x 100s 9Gyrotrons
Integrated Research Phase	phase I	2026– 2028	D	4E20	Lower monoblock-Tungsten-coated Carbon Div. Pumping	16MW 8units	8MW 4units	34MW x 100s				
Extended Research Phase	phase II	2030 –	D	1E21	SN/DN monoblock-Tungsten-Coated Carbon Advanced Structure				>5y	D	1.5E21	41MW

Upper Divertor (open divertor, inertia cooling) is always ready

1) Initial Research Phase

1-1) Phase I (Hydrogen Phase)

The main aim of this phase is the integrated commissioning of the entire system.

The first part of this phase includes the first plasma (Sep. 2020) and subsequent 5 months of integrated commissioning with plasmas. In this period, JT-60SA is equipped with the upper divertor plates (Carbon, inertial cooling), two Gyrotrons (1.5 MW x 5 s) with waveguide launchers, the power supply system for the full-operation of the superconducting coil system, and the set of plasma diagnostics needed in this phase. The maximum plasma current is 2.5 MA and the nominal toroidal field of 2.25T is ready. The main target of the plasma operation is ‘demonstration of equilibrium control with MA-class diverted plasmas’.

Physics experiments start from the second part of the Initial Research Phase I after installation of the lower divertor, in-vessel coils (FPCC, EFCC, RWMCC), stabilizing plates, active cooling of in-vessel components and vacuum vessel, divertor pumping, 8 units of P-NB, 2 units of N-NB and additional 2 Gyrotrons, pellet injectors, massive gas injectors, plasma diagnostics satisfying the physics research in the Initial Research Phases I and II. The material of the divertor target and the first wall is fully carbon. The first objective of the Initial Research Phase I is ‘Stable operation at high current in large superconducting machine’ with the maximum plasma current up to 5.5 MA and high power heating of 19 MW with lower divertor configurations. Another main objective is ‘ITER risk mitigation for non-activated phase’ such as basic disruption studies (see Chap.2).

1-2) Phase II (Deuterium)

The remaining commissioning related to neutron production, nuclear heating and radiation

safety will be carried out with deuterium operation up to the full technical performance allowable under the limitation of the annual neutron production of 3.2×10^{19} before high activation operations during the integrated research phase. After characterization of operational boundaries and experimental flexibilities, all experimental target regimes in JT-60SA will be studied using relatively short pulse discharges. The allowable heat flux onto the divertor plate is $10 \text{ MW/m}^2 \times 5 \text{ s}$, $3 \text{ MW/m}^2 \times 20 \text{ s}$ and $1 \text{ MW/m}^2 \times 100 \text{ s}$ for the lower divertor and $0.45 \text{ MW/m}^2 \times 100 \text{ s}$ for the upper divertor. The number of long pulse discharges will be decided considering the annual neutron production limit. The heating power will be 20 MW for P-NBs, 10MW for N-NBs and 3 MW for ECRF at 110 GHz and 138 GHz. The main research targets are ‘ITER scenario development’, ‘Steady-state high beta scenario development’ and ‘ITER risk mitigation’ (Chap.2).

2) Integrated Research Phase

2-1) Phase I

The main mission of JT-60SA will be investigated and demonstrated utilizing high-power long-pulse discharges with the full carbon mono-block lower single-null divertor target which allows heat loads up to $15 \text{ MW/m}^2 \times 100\text{s}$. The NB injection performance will be $20 \text{ MW} \times 100\text{s}$ or $30 \text{ MW} \times 60\text{s}$ with a duty cycle of 1/30. The heating capability of ECRF will be increased up to $7 \text{ MW} \times 100 \text{ s}$. The annual neutron production is limited to 4×10^{20} in order to allow human access inside the vacuum vessel (after a cool down period of 1 year). Commissioning of the remote handling system must be completed during this phase. Before entering Phase II, the JT-60SA’s main mission related to high- β steady-state operations has to be achieved utilizing the wider range of operation regimes allowed by the carbon wall. In addition, dedicated machine time will be necessary to prepare the scenario for the tungsten wall transition.

2-2) Phase II

The divertor target and the first wall will be fully changed to tungsten-coated carbon. Under this ‘metal-wall’ environment, the compatibility of high density, high beta, high confinement and a radiative divertor will be explored using the upgraded power and divertor performance. In particular, the direct and quick contribution to ITER experiments will be the highest priority in this phase (see Sec.1.9). The annual neutron production limit will be increased to 1×10^{21} , which requires remote maintenance of in-vessel components.

3) Extended Research Phase

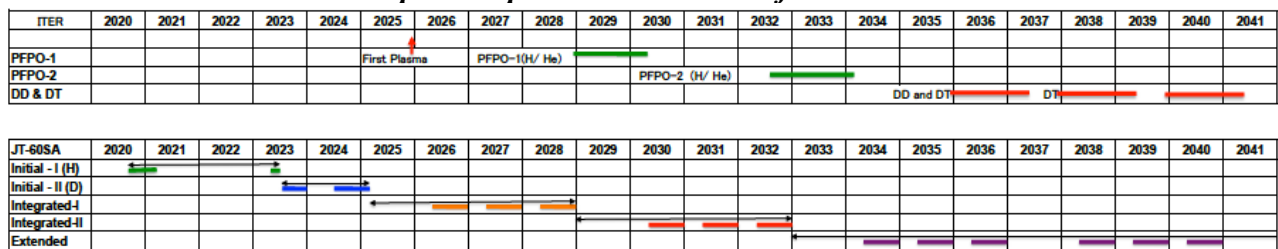
In this phase, the capability of JT-60SA is envisaged to extend to a higher heating power of $41 \text{ MW} \times 100 \text{ s}$ with single-null or double-null configurations with full mono-block divertors. The annual neutron production will be increased to 1.5×10^{21} . Taking advantage of JT-60SA’s flexibility of replaceable divertor cassette, metallic divertor targets with an advanced divertor shape will be installed in the extended research phase based on the progress of tokamak research worldwide including ITER.

1.9. Time schedule of JT-60SA experiments in the long-term fusion development

Toward DEMO construction, success of ITER is the most important mission in the fusion research, and JT-60SA is strongly expected to take the role of the main contributor to ITER. The tight experimental schedule of ITER up to the Q=10 long pulse DT operation requires sufficient explorations of the key physics issues and operational techniques in satellite devices. Therefore, experiences and achievements in JT-60SA are indispensable for an efficient and

reliable start-up of ITER operation and for optimizations of discharge scenarios in H/He, DD and DT phases of ITER. Therefore an adequate time schedule of JT-60SA experiments relative to those for ITER is essentially important for the JT-60SA project. Table 1-6 shows expected time schedule of ITER and JT-60SA. The first plasmas of JT-60SA and ITER are expected in 2020 and 2025, respectively.. As for the heating experiments, the operation of JT-60SA will start (2023) earlier than ITER’s first hydrogen / helium plasma operation (PFPO-1: 2028) by more than 5 years. The integrated research phase-II of JT-60SA with full metal first wall will start earlier than ITER PFPO-2 by 3 years. Therefore, JT-60SA precedes ITER by 3 – 5 years for each milestone. Once ITER operation starts, efficient collaborations between JT-60SA and ITER are required. During this period, the flexibility of JT-60SA will contribute to ITER in various research fields. Such combination of JT-60SA and ITER is fundamentally important for achieving the main missions of ITER.

Table 1-6 Expected operation schedules of ITER and JT-60SA



After 2026: Details are to be updated

As for construction of a DEMO reactor, integration of achievements in JT-60SA high-β steady-state plasmas and ITER burning plasmas is required to make DEMO designs more realistic and attractive. For early realization of the DEMO reactor, such parallel and integrated exploitation of JT-60SA and ITER is necessary. Since the concept of the key components of the DEMO reactor has to be narrowed down well before start of its construction, an early exploitation of the JT-60SA experiments is needed. The critical issue for DEMO reactor design is integration of the achievements in JT-60SA and ITER, for example predictions of burning ($Q>10$) high-beta high-bootstrap-fraction plasmas. In order to accomplish this study, an integrated research for validation of theories and modeling / simulation codes using data of JT-60SA and ITER is essentially important. In parallel to the DEMO construction, JT-60SA has to develop the optimized control / operation schemes for the DEMO reactor.

The ‘Japan’s Policy to promote R&D for a fusion DEMO reactor’ [24] defines that the decision to transition to the DEMO phase will be taken in the 2030s when fusion operation (DT) of ITER is expected. It is also requested that the economic feasibility of a commercial reactor is foreseeable when transitioning to the DEMO phase. Towards the decision to transition to DEMO, the intermediate Check & Review will be implemented in two periods: (i) when JT-60SA is expected to begin operations in around 2020, (ii) within a few years of 2025 when ITER’s first plasma is scheduled. The Check & Review items for the decision to transition to DEMO includes 1) validation of burn control in the self-heating area by ITER and 2) establishment of an operational technique for stationary high-beta plasma for operation of the DEMO reactor, 3) establishment of integrated technologies by ITER, 4) material development for the DEMO reactor etc. In the area of ‘ 2) stationary high-beta plasma’, the main subjects are as follows and JT-60SA has critical responsibilities.

C&R-1)

- Proceed with ITER collaborative research and preparatory studies on stationary high-beta

plasma and start JT-60SA research.

C&R-2)

- JT-60SA achieves a high-beta non-inductive current drive.
- Have integrated simulations including the divertor verified by JT-60SA and other projects.
- Create a plan for JT-60SA divertor research compatible with the DEMO reactor's plasma-facing walls.

The decision to transition to DEMO)

- Gain prospects for non-inductive steady operation by ITER's achievement of non-inductive current drive plasma and integrated simulations based on ITER's knowledge of burn control.
- JT-60SA validates the stationary operation of a high-beta ($\beta_N = 3.5$ or higher) collisionless plasma regime compatible with the DEMO reactor's plasma-facing walls.

References

- [1] Shirai H. *et al* 2017 *Nucl. Fusion* **57** 102002
- [2] Kamada Y. *et al* 2013 *Nucl. Fusion* **53** 104010
- [3] Tobita K. *et al* 2009 *Nucl. Fusion* **49** 075029
- [4] Hiwatari R. *et al* 2005 *Nucl. Fusion* **45** 96
- [5] Sakamoto Y. *et al* 25th IAEA Int. Conf. on Fusion Energy (St. Petersburg, Russia, 2014) FIP/3-4Rb
- [6] Federici G. *et al* 2016 *Fusion Eng. Des* **109-111** 1464
- [7] Kwak Jong-Gu. *et al* 2013 *Nucl. Fusion* **53** 104005
- [8] Wan B. N. *et al* 2017 *Nucl. Fusion* **57** 102019
- [9] Pradhan S. *et al* 2015 *Nucl. Fusion* **55** 104009
- [10] Bucalossi J. *et al* 2014 *Fusion Eng. Des.* **89** 907
- [11] Sakamoto Y. *et al* 2009 *Nucl. Fusion* **49** 095017
- [12] 'Progress in the ITER Physics Basis', 2007 *Nucl. Fusion* **47** S1
- [13] Hawryluk R.J. *et al* 2009 *Nucl. Fusion* **49** 065012
- [14] Litaudon X. *et al* 2017 *Nucl. Fusion* **57** 102001
- [15] Isayama A. and the JT-60 Team 2011 *Nucl. Fusion* **51** 094010
- [16] W.M. Solomon for The DIII-D Team, 2017 *Nucl. Fusion* **57** 102018
- [17] Kallenbach A. for the ASDEX Upgrade Team and the EUROfusion MST1 Team, 2017 *Nucl. Fusion* **57** 102015
- [18] Saoutic B. *et al* 2011 *Nucl. Fusion* **53** 104003
- [19] Marmor E.S. *et al* 2015 *Nucl. Fusion* **55** 104020
- [20] Pucella G. *et al* 2017 *Nucl. Fusion* **57** 102004
- [21] Kirk A. *et al* 2017 *Nucl. Fusion* **57** 102007
- [22] Kaye S. M. *et al* 2015 *Nucl. Fusion* **55** 104002
- [23] Coda S. *et al* 2017 *Nucl. Fusion* **53** 102011
- [24] 'Japan's Policy to promote R&D for a fusion DEMO reactor' the Science and Technology Committee on Fusion Energy of MEXT, 2017

2. Research Priority

2.1. Introduction

The JT-60SA Research Plan (SARP) has been formulated to address major issues in ITER and DEMO. Chapter 1 defines the general research goals and long-term research strategy for the JT-60SA project, whereas research items, experimental regimes and approaches in specific research areas are described in Chapters 3-10. As discussed in Chapter 1, the JT-60SA programme will be carried out following a logical sequence organized in different Research Phases supporting ITER and DEMO. Support to ITER and mitigation of the ITER project risks are expected to be the main focus of the JT-60SA programme, particularly during the first phases of operation. In line with the revised ITER schedule (Table 1-6) and ITER Research Plan, the high priority research items in the Initial Research Phases I and II of JT-60SA are presented in Chapter 2.

In order to prioritize the research items, the major objectives in Initial Research Phases I and II are defined as the main Headlines. The Headlines reflect general and comprehensive goals of the research phases and, thus, they include operational scenario R&D which are further described in Chapter 3. ITER risk mitigation and operational scenario development are the main targets of the Initial Research Phases. Research items which will make large contributions to the Headlines are described in this chapter, especially the research items which can be tested in JT-60SA capitalizing on its most distinctive features.

2.2. Initial Research Phase I

JT-60SA is a large superconducting machine with high plasma current and sufficiently high heating power. As the only such device scheduled to come into operation prior to ITER, the commissioning and establishing of high plasma current operation on JT-60SA will provide vital information for ITER. The highest priority of the Initial Research Phase I is to establish plasma operation at high plasma current, up to 5.5 MA, in hydrogen/helium plasmas, in order to prepare deuterium plasma operations. JT-60SA should also contribute to operation and risk mitigation for the ITER non-activated phases as well as for the activated phases as the Initial Research Phase I will start much earlier than ITER operation with auxiliary heating. Accordingly, the Headlines of the Initial Research Phase I are defined as

“H.I.1. Stable operation at high current in large superconducting machine” and
“H.I.2. ITER risk mitigation for non-activated phase”.

The first part of this phase is limited in plasma current, heating power, in-vessel components and diagnostics. In the latter part of this phase, the heating power of 19 MW (N-NB of 10 MW, P-NB of 6 MW, ECRF of 3 MW) will be available with a lower single null CFC divertor (Table 1-5). Also main and impurity gas puffing and in-vessel coils (FPCC, RWMC, EFCC) will be used. These tools enable the high priority R&D issues for ITER to be addressed. Thus, the major objectives, i.e. H.I.1 and H.I.2 will be addressed in the latter part of the Initial Research Phase I. The key research items under the Headlines are listed below, in the order in which they should be addressed. For each item, the relevant chapter of the Research Plan is indicated. The research items, especially in H.I.2 are selected considering the period of the Initial Research Phase I. Other important research items in hydrogen/helium plasmas will be conducted in the Initial Research Phases II and/or further phases, although these phases will be mostly deuterium plasma operations.

H.I.1. Stable operation at high current in large superconducting machine

- Current ramp-up scenario development up to full-current operation [Chap. 3]
- Plasma shape and equilibrium control avoiding vertical instability [Chap. 3, 4]
- Locked mode and kink mode avoidance during current ramp-up [Chap. 4]
- EC Wall conditioning [Chap. 8]
 - Light and heavier impurity control in the core [Chap. 5]
 - H-mode plasma operation [Chaps. 5, 7]

For the preparation of deuterium plasma operations, the first four research items in H.I.1 are essential in the Initial Research Phase I. An inter-shot wall-conditioning method by ECRH (ECWC) is required for the plasma operational start-up and recovery from disruptions. The optimal parameters for ECWC operation - such as pulse width, duty cycle, He pressure - in order to obtain the highest H outgassing will be established. The experiment will provide a wall conditioning scheme to start-up plasmas in a reliable way. Plasma current ramp-up scenario will be developed avoiding locked modes by EFCC / density / rotation as well as kink-modes, by optimizing the current ramp-up rate. During the current ramp-up, flat-top and ramp-down phases, controllability of plasma position and shape avoiding vertical instability, will be assessed. Fast position control coils (FPCC) will be used first, and then the position and shape controls will be attempted without FPCC to mimic ITER and DEMO operation. Intrinsic impurity in the core might be significant in the early phase. Excessive impurity accumulation would result in a low temperature plasma which is unfavourable for poloidal magnetic flux consumption.

The last two items are desirable as they can be addressed in the later phases with hydrogen/helium plasmas according to the research needs. Light and high-Z impurity accumulation will be minimized by optimizing density, ECH power and position, plasma shape and strike points. Long-pulse discharges with full-current and full-power conditions will be attempted up to the flat-top of 100 sec by optimizing the above-mentioned issues. Real-time control logic and systems such as density, stored energy and β_N will be validated in the Initial Research Phase I as a preparation for the Initial Research Phase II. Type-I ELMy H-modes in hydrogen/helium plasmas will be tried to check plasma controllability of transient events and estimate the machine performance, although the NB power of 16 MW may restrict operation regimes of density, plasma current and toroidal magnetic field to access to H-mode. Investigation of type-I ELMy H-modes at various plasma currents should be carried out in the latter phase with adequate power. Time-dependent integrated codes: MHD stability, plasma transport, energetic particles, SOL/DIV will be validated and improved using these plasmas.

The series of the H.I.1 experiments will give essential results to prepare the next phase “Initial Research Phase II”. They will also provide ITER with useful contributions on the plasma operation commissioning in the start-up campaign.

H.I.2. ITER risk mitigation for non-activated phase

- Basic disruption studies [Chap. 4]
- L-H transition studies in hydrogen / helium plasmas [Chaps. 5, 7]

JT-60SA will play an important role in reducing the risks in ITER operation through taking advantage of its characteristics, including high plasma current, high heat and particle flux, low collisionality, and carbon wall having enough robustness to transient events. The risks that will be dealt with during the Initial Research Phase I will depend on the priority and urgency of the risks for ITER. Risks that are not dealt with during Phase I could be addressed during a possible

H campaign in the Integrated Research Phase II. At present, it is foreseen that the first two points in the list above will be the priorities for H.I.2.

Vertical displacement events (VDEs) often cause or accompany disruptions. Asymmetric and rotating VDEs might lead to large uncertainties in the forces on the ITER vacuum vessel and blanket. JT-60SA is well-suited to perform VDE studies for ITER owing to the similarity of the vacuum vessel. Controllability of VDEs in JT-60SA will be assessed by neutral point monitoring and vertical stabilization coils. Halo currents and their toroidal peaking factor, associated heat load and runaway electrons at high plasma current will be estimated, and simulation codes will be validated using the data. Using the research items of H-mode plasma operation in H.I.1, L-H transition physics and threshold power will be investigated. The experiment will be conducted at low density of about $0.4n_{GW}$, in order to achieve L-H transition in the ITER like scenario with high plasma current ($I_p/B_T=4.6$ MA/2.28 T, $q_{95}=3.2$), ITER-like shape, low v^* , small ρ^* and low rotation conditions, to predict H-mode threshold power in hydrogen, helium and mixed plasmas. Systematic studies of L-H transition, ELM control and H-mode quality will be made in the Initial Research Phase II.

2.3. Initial Research Phase II

Deuterium operation starts from the Initial Research Phase II with heating power of 33 MW (N-NB of 10 MW, P-NB of 20 MW, ECRF of 3 MW). The high heating power and high plasma current enable access to the ITER and DEMO regimes of β_N , f_{BS} , ρ^* , v^* and electron heating ratio (Fig. 5-4), meaning that scenario development for ITER and DEMO can be launched in this phase. Accomplishment of steady-state operation in JT-60SA is considered an important milestone for deciding DEMO design and its operation regimes. Tackling the scenario development for DEMO from the Initial Research Phase is a high priority as well as that for ITER. Accordingly, the major objectives of the Initial Research Phase II are to work on

- “H.II.1. ITER scenario development”,
- “H.II.2. Steady-state high beta scenario development” and
- “H.II.3. ITER risk mitigation”.

Both NB and ECRF will be ready to be injected in long pulses (up to 100 s). On the other hand, the pulse duration with high power heating will be limited by the allowable heat flux onto the inertially cooled CFC divertor plate (10 MW/m² \times 5 s). The full-monoblock divertors will be ready in the Integrated Research Phase I. Thus, the main objective of this phase is to access stable steady-state regime of operation at high β_N and β_p . Current ramp-up scenarios will be developed by avoiding critical MHD modes and collapse, in order to obtain a q profile with target plasma parameters (β_N $H_{98y,2}$, etc.) of each scenario. Then, the achieved plasmas will be extended to a stationary phase limited by the allowable heat flux. The pulse duration and plasma parameters will be expanded in the Integrated Research Phase I. Long pulse operation will be attempted as a preparation for the Integrated Research Phase. A radiative divertor is a key ingredient for the high-power longer-pulse heating.

H.II.1. ITER scenario development

To prepare the ITER relevant plasma scenarios

- Sawtooth period real-time control by ECCD [Chap. 4]
- NTM real-time control by ECCD [Chap. 4]
- High density H-mode operation [Chap. 5, 7]
- Light and heavier impurity transport and control in the core [Chap. 5]

In the ITER relevant plasma scenarios

- Dominant electron heating in H-mode plasmas [Chaps. 5, 7]
- Intrinsic torque and intrinsic rotation studies [Chap. 5]
- Isotope studies by comparison of H and D plasmas [Chap. 5, 7]
- L-H transition, pedestal physics and scalings [Chap. 7]
- Energetic particle driven mode studies [Chaps. 4, 6]
- Energetic particle effects on transport and confinement [Chap. 5]
- Detachment physics and code validation [Chap. 8]

The ITER standard scenario will be developed at high plasma current of ≈ 4.6 MA, $B_T \approx 2.28$ T and $q_{95} \approx 3.2$ with an ITER-like shape configuration ($\delta_x \approx 0.41$, $\kappa_x \approx 1.81$). The first four items will be required to achieve the operational regime. First, the ITER scenario will be produced to satisfy the target confinement of $H_{98y,2} \approx 1$ and $\beta_N \approx 1.8$ at a moderate density. Then, density will be increased by gas-puff and pellets up to $\langle n_e \rangle \approx 0.81 \times 10^{20} \text{ m}^{-3}$ ($f_{GW} \approx 0.8$) keeping $H_{98y,2} \approx 1$ and $\beta_N \approx 1.8$. A heating power of about 33 MW will be required to achieve this plasma performance in such high-density plasma (Fig. 3-4, Table 3-5). In the ITER scenario discharge, the sawtooth period will be controlled by varying the ECCD injection angle and modulation frequency in real-time to avoid a large sawtooth crash and NTM. Detachment physics will be studied with a focus on protecting the divertor plates from the transient and continuous heat loads. The radiative volume and density will be expanded by optimizing the impurity seeding mixture. The low-density detached regime will be explored by impurity compression. Simulation codes will be validated with the detached divertor observations to understand the physics and improve the predictive basis for ITER and DEMO. The physics and controllability of the seeded impurity transport to the core will be studied from both the neoclassical and turbulence viewpoints. The dependences of the light and heavier impurity accumulation on density, density gradient, electron heating by ECH and NNBI will be assessed in order to optimize the control technique for ITER. The enhancement of the impurity transport and the impact of MHD on the impurity exhaust (sawtooth and ELMs) will be studied. The ITER standard scenario development and the steady-state scenario development (see H.II.2) are high priority. The ITER hybrid scenario will be explored at high plasma current of ≈ 2.6 - 3.5 MA, $B_T \approx 1.72$ - 2.28 T and $q_{95} \approx 4$ with an ITER-like shape configuration. Current drive will be optimized to achieve higher confinement of $H_{98y,2} > 1$ and higher beta of $\beta_N \approx 2.4$ - 3.0 . NTM stabilization will be required in the hybrid scenario with internal transport barriers. H-mode regimes with small ELMs at low ν^* will be developed using RMP, pellets and tuning of plasma shape, to find regimes which are compatible with favourable confinement and internal transport barriers.

The last seven items will be studied in the ITER relevant regime to understand the plasma and validate models to predict ITER plasma. Plasma confinement and transport in the core will be characterized for the ITER relevant regimes, i.e. low ν^* , small ρ^* , dominant electron heating and low rotation conditions with the ITER-like shape configuration. The intrinsic torque and intrinsic rotation will be studied using a combination of the tangential neutral beams, perpendicular beams, negative ion based neutral beam, ECH and RMP (EFCC). Turbulence and neoclassical transport models will be validated by means of experiments in an ITER-like regime whose parameters are not accessed by the present tokamaks simultaneously. H-mode pedestal characteristics and ELM behavior will be explored with an I_p scan at constant q_{95} around ITER relevant δ , ν^* , β , rotation and electron heating ratio. These data will expand the scalings of H-mode confinement, ELM size on ν^* , and ELM divertor heat flux width into the high plasma current regime. Isotope effects on the L-H threshold power and plasma confinement will be identified by comparison between H and D plasmas for extrapolation to ITER DT plasmas. The power and the H/He ratio required to achieve a good H-mode confinement will be examined to

extrapolate to the power in the ITER non-activated phases, where the available power will be close to the H-mode threshold power. The physics and mitigation of the energetic particle driven modes will be examined by using the powerful energetic ion source, i.e. the negative ion based neutral beam. The effects of the energetic particles on the MHD modes and transport will also be investigated to give a consistent understanding of burning plasma characteristics.

H.II.2. Steady-state high beta scenario development

To prepare the high beta plasma scenarios

- Current drive optimization [Chap. 3]
- Simultaneous stabilization of RWM and NTM [Chap. 4]
- Real-time kinetic profile control development [Chap. 5]
- Impurity transport with peaked density profiles [Chap. 5]
- Fuelling and pumping for density control [Chaps. 8, 9]
- Protecting target plates by detached divertor [Chaps. 8, 9]

In the high beta plasma scenarios

- Self-organization studies of current, pressure and rotation profiles [Chaps. 5, 6]
- ITB and intrinsic rotation studies [Chap. 5]
- Fast ion effects on turbulence and transport [Chap. 5]
- Anomalous heating by MHD modes damping [Chap. 6]
- Fast particle driven modes instability [Chap. 6]
- Compatibility of small/no ELM and high β [Chap. 7]

The steady-state scenario will be developed at medium plasma current of ≈ 2.3 MA, $B_T \approx 1.72$ T and $q_{95} \approx 5.8$ with a DEMO-like shape configuration ($A \approx 2.7$, $\delta_x \approx 0.47$, $\kappa_x \approx 1.91$, shape factor ≈ 7.0). The first six items will be required to achieve the operational regime. The target of this phase is to achieve a high beta fully non-inductively driven plasma with $\beta_N \geq 3$ ($\geq \beta_N^{\text{no-wall}}$), $f_{BS} > 0.5$ and $H_{98y,2} \approx 1.3$. Heating power of about 33 MW will be injected into a medium or high-density plasma to access high beta and high confinement regimes (Fig. 3-4, Table 3-5). These parameters and pulse duration will be extended in the Integrated Research Phase with the monoblock divertors and higher heating power. Reversed magnetic shear will be produced by optimizing the heating power and injection timing of NBs and ECH during the current ramp-up. The contribution of various current drive sources, BSCD, NBCD and ECCD, will be explored, in order to achieve the high beta non-inductive plasma and other applications of heating systems, such as NTM and impurity controls. Profiles of the plasma current, pressure and toroidal rotation velocity should also be optimized in real-time to avoid critical MHD modes and collapse. The core MHD modes will also be actively controlled in real-time using external actuators and plasma parameters. RWM will be controlled by the stabilizing plates, RWM coils and plasma rotation. ECCD will be applied to stabilize NTM as in the H.II.1 ITER scenario development. The seeded impurity mixture ratio and density will be controlled by fuelling and pumping in order to optimise the compatibility of high beta and high radiation at high plasma current. Impurity transport in the steady-state scenario with increased peakedness of the density profiles will be investigated to seek a possible impurity control for DEMO.

In the high beta plasmas, the last six research items will be studied to understand the high beta plasma behaviours in order to improve the operational regime. In high beta plasmas, self-organization of plasma current, pressure and rotation will be studied by changing the bootstrap current fraction to assess the controllability of burning and self-regulating DEMO plasmas. Understanding internal transport barriers and intrinsic rotation is essential for handling the self-organizing plasma. These properties will be investigated in DEMO-relevant regimes, i.e. high

β_N , small ρ^* , low ν^* , small torque input and electron heating conditions. Coupling among energetic particles, MHD modes and kinetic profiles will be stronger in DEMO than in ITER. Fast particle driven modes instability in elevated q profiles, impact of energetic fast ions on the bulk plasma transport and anomalous heating due to kinetic damping of resonant and nonresonant MHD modes will be studied at high β_{EP} , small ρ_{EP}^* and large ν_{EP}/ν_a by taking advantage of negative ion based neutral beam injection and high plasma current. Access to a small ELM regime without in-vessel components needs to be developed at high beta. Operational windows of QH-mode and grassy ELM mode will be explored by scanning the toroidal rotation velocity and plasma shape at high β_N and low ν_{ped}^* . Simulation codes and models will be validated using the data in DEMO-relevant plasmas and phenomena: turbulence transport models, RWM models with kinetic effects, nonlinear dynamics of energetic particles and MHD models, detached divertor models, etc. Model based real-time plasma control will be applied by taking advantage of simplified transport and MHD models. This will enable the production of high performance plasmas and the avoidance of critical MHD modes and disruption even though the operational window may be narrow.

H.II.3. ITER risk mitigation

- Disruption avoidance [Chap. 4]
- Runaway electron study at high current [Chap. 4]
- $H_{98y,2}=1$ operational boundaries [Chaps. 5, 7]
- ELM mitigation/suppression [Chap. 7]
- Compatibility of RMP with fast ion confinement [Chap. 6]
- SOL width scaling [Chap. 8]
 - Burning plasma simulation experiment [Chap. 5]
 - H/D ratio control by gas-puff and pellet [Chap. 8]
 - He pumping [Chap. 8, Chap. 9]

The above-mentioned research items will be studied in ITER like scenarios (e.g. $I_p/B_T=4.6$ MA/2.28 T, $q_{95}=3.2$, low ν_{ped}^*) in order to reduce the risks for ITER. Studies for machine protection from transient events are high priority ones. Most of the research items also relate to issues in DEMO. The risks in DEMO will be reduced through the ITER risk mitigation studies. As noted for the Integrated Research Phase I, some of the ITER risk mitigation for non-activated phase could be addressed during a possible H campaign in the Integrated Research Phase II.

The first six items in the list above will be the priorities for H.II.3. Disruption avoidance techniques which will not depend on the wall material significantly will be developed in the Initial Research Phase II. Disruption prediction will be attempted by detecting the response of marginally stable modes to a magnetic field perturbation by EFCCs or RWMCCs. Then, a real-time disruption avoidance method will be developed by monitoring the data from active MHD spectroscopy and real-time MHD stability analysis to prepare the fundamental algorithm for ITER. Runaway electron mitigation will be studied and modelled by using RMPs and MGI at different plasma current, toroidal field and plasma shape. MGI system will be needed for machine safety purposes in JT-60SA during the runaway electron experiments at high current. The data will be used to validate the models, which will then be used to predict how much impurity gas or magnetic perturbation will be required to mitigate the runaway electron generation in ITER. The disruption mitigation system will be required for the JT-60SA metal-wall experiment, which is planned for the Integrated Research Phase II. Active type-I ELM control will be developed by RMPs (EFCCs), pellets and plasma shape at the low ν^* condition

covering the ITER regime (Fig. 7-3). EFCCs current as RMP and q_{95} will be scanned to find the best operational window for ELM suppression and/or mitigation, whilst minimizing the impact on plasma confinement. The ELM control will also be studied in hydrogen and helium plasmas to contribute to the development of reliable ELM control in the ITER non-activated phases. The synergetic effects of the RMPs and the 3D magnetic field due to toroidal ripple will be studied in the ITER-like scenario, in order to address their compatibility with ITER conditions. In the RMP applied plasmas, heat load by fast ion losses, which can be a critical risk in ITER, will be measured and compared with codes. The effect of the RMPs on pedestal and rotation as well as ELMs and heat flux will be validated at low v^* regimes to improve these predictions for ITER. To reduce the transient and continuous heat loads, detached divertor physics will be studied at high neutral compression using the V-shaped corner. The impact on detachment physics and control of the V-shaped corner and Lyman absorption, which can be studied by VUV spectrometry, will be evaluated. SOL/DIV modelling will be validated by the data to develop a heat load handling technique for ITER. SOL width scaling beyond the parameter range of existing devices will be validated using high plasma current operation of ≈ 5.5 MA.

Burning plasma control studies are also important as well as machine protection studies. Burning plasma simulation experiment will be conducted to investigate plasma controllability under low auxiliary heating condition. Negative ion based NB and some perpendicular positive ion based NBs will be used to mimic the alpha particle heating. Calculated alpha particle heating power and heat load will be controlled by tangential beams and ECH/ECCD whilst monitoring the neutron production. Control of the H/D ratio will be examined by using gas-puffing and pellet as a mimic of D/T control in ITER. He exhaust after the DT reactions will be an issue in ITER. In JT-60SA, the best operation for He pumping compatible with detachment/divertor geometry will be explored at high neutral compression in the V-shaped corner. The impact on detachment physics and control of the V-shaped corner and Lyman absorption, which can be studied by VUV diagnosis, will be evaluated. SOL/DIV modelling will be also validated by this data to develop a heat load handling technique for ITER.

2.4. Summary of research priorities

In conclusion, ITER and DEMO relevant scenarios will be developed in the Initial Research Phases I and II. Research items using these scenarios in order to reduce risks for ITER operations and provide guidance to DEMO design will be investigated as high priority topics, by taking advantage of the characteristics of JT-60SA. The physics and controllability of ITER and DEMO relevant high confinement and/or high beta plasmas will be assessed to provide reliable theoretical models and control schemes for ITER and DEMO.

The pulse duration and plasma parameters in both scenarios will be expanded taking advantage of the monoblock divertors and higher heating power in the Integrated Research Phase I. The compatibility of high density, high beta, high confinement and a radiative divertor will be explored using the upgraded power and divertor performance. The physics and controllability of self-regulating and self-organizing plasmas will be addressed with long-pulse operations. By organizing and integrating the observations, fully non-inductive steady-state operation above the no-wall ideal MHD stability limits will be accomplished. In the late phase of Integrated Research Phase I, scenarios compatible with the future metal wall configuration will be investigated and prepared. Metal wall experiments will begin after the mission goal and major objectives are achieved. This is planned for the Integrated Research Phase II (≈ 2030) to support the ITER full power phase in 2031. Major objectives in the Integrated Research Phase II will be integrated power/particle exhaust studies and real-time control of radiative divertor

which is compatible with high beta plasmas. These experimental observations and theoretical models will contribute to develop reliable ITER operations and the basis for DEMO design.

3. Operation Regime Development

The two main objectives of the JT-60SA experimental program are (1) contributions to ITER as a large super-conducting (SC) tokamak device having similar shape to ITER, and (2) contributions to DEMO by developing long pulse operation and advanced tokamak (AT) scenarios. Both of them are closely linked with each other. For example, the AT scenario development in JT-60SA directly contributes to steady-state (SS) operations in ITER, and the operation scenarios developed in ITER contributes to DEMO. It should be noted here that the experiments in JT-60SA must precede similar experiments in ITER sufficiently in advance, and these JT-60SA experiments must provide applicable and optimized solutions to ITER.

In order to develop SS operation scenarios, the powerful 10 MW off-axis neutral beam current drive (NBCD) capability with negative ion source based neutral beams (N-NBs) at the beam energy up to 500 keV contributes to tailoring the current profile suitable for the high-beta AT scenarios under full non-inductive current drive (full-CD) conditions. Figure 3-1 shows the NBCD capability in JT-60SA aiming at a higher-energy (500 keV), larger-power (10 MW), and longer-duration (100 s) regime towards ITER and DEMO. In order to develop the high-beta AT scenarios, a conducting wall closely placed to the plasma and stabilization coils are available in JT-60SA so that stabilization of RWM not only by the plasma rotation but also by magnetic perturbation becomes possible, this is an advantage in scenario development in JT-60SA. Since the divertor target is water-cooled and the heating period is more than doubled (60-100 s) compared with JT-60U (30 s), experiments under steady particle recycling conditions can be extremely expanded to higher heat and particle flux regime. In the development of such high performance plasmas, the attainable plasma pressure, confinement and sustainment period are limited not only by physics issues (e.g. MHD instability) but also by available capability of auxiliary heating, current drive, divertor, and licensed annual neutron limit etc. Table 1-5 shows available capability of the key components along the phased upgrade schedule of JT-60SA. According to the upgrade of the key components, the phased experimental program is constructed. In the Initial Research Phase, main emphasis is placed on issues specific to the superconducting device operations. Developments for AT scenarios start in the deuterium phase. Since most of the studies on scenario development with hydrogen plasmas can be executed also with deuterium plasmas, an early transition to the deuterium experiment phase would be preferable. Looking at the Table 1-5, heating power increases and divertor upgrades until Integrated Research Phase I so that improvement of plasma performance is expected in these phases. Integrated Research Phase II, the transition to the tungsten wall and the annual neutron limit increase will ensure the development towards long pulse operation of the high performance plasma in a DEMO-like first wall environment on the basis of the scenario developed in carbon in the Initial Research Phase II and Integrated Research Phase I.

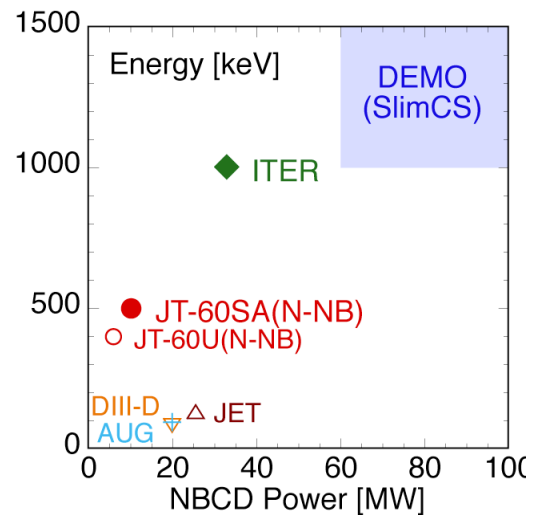


Fig. 3-1 NBCD power and the beam energy in various tokamaks toward ITER and DEMO.

Experimental Program

The following sections describe experimental programs broken down in the five operation phases of JT-60SA given in Table 1-5. The main plasma target parameters or the typical JT-60SA operation scenarios are listed in Table 3-1.

Table 3-1 Main target parameters for the typical operation scenarios with full device-capability (the order of scenario number is neither the priority nor the order of execution)

	#1	#2	#3	#4-1	#4-2	#5-1	#5-2	#6 ⁽¹⁾
	Full Current Inductive DN, 41MW	Full Current Inductive SN, 41MW	Full Current Inductive High density	ITER-like Inductive	Advanced Inductive (hybrid)	High β_N Full-CD	High β_N High f_{GW} Full-CD	High β_N 300s
Plasma Current (MA)	5.5	5.5	5.5	4.6	3.5	2.3	2.1	2.0
Toroidal field BT (T)	2.25	2.25	2.25	2.28	2.28	1.72	1.62	1.41
q_{95}	~3	~3	~3	~3	~4.4	~5.8	6.0	~4
R/a (m/m)	2.96/1.18	2.96/1.18	2.96/1.18	2.93/1.14	2.93/1.14	2.97/1.11	2.96/1.12	2.97/1.11
Aspect ratio A	2.5	2.5	2.5	2.6	2.6	2.7	2.6	2.7
Elongation κ_x	1.95	1.87	1.86	1.81	1.80	1.90	1.91	1.91
Triangularity δ_x	0.53	0.50	0.50	0.41	0.41	0.47	0.45	0.51
Shape factor S	6.7	6.3	6.2	5.7	5.9	7.0	7.0	6.4
Volume (m ³)	132	131	131	122	122	124	124	124
Cross-section (m ²)	7.4	7.3	7.3	6.9	6.9	6.9	6.9	6.9
Normalised beta β_N	3.1	3.1	2.6	2.8	3.0	4.3	4.3	3.0
Electron density (10 ¹⁹ m ⁻³) Line-average/volume-average	6.3/5.6	6.3/5.6	10.9	9.1/8.1	6.9/6.2	5.0/4.2	5.3/4.3	2.0/
Greenwald density, n_{GW} (10 ¹⁹ m ⁻³) / f_{GW}	13/0.5	13/0.5	13/0.8	11/0.8	8.6/0.8	5.9/0.85	5.3/1.0	5.2/0.39
Plasma thermal energy, W_{TH} (MJ)	22	22	21	18	13.4	8.4	8.1	3.8
P_{add} (MW)	41	41	30	34	37	37	30	13.2
$P_{NNB}/P_{PNB}/P_{PEC}$ (MW)	10/24/7	10/24/7	10/20/-	10/24/-	10/20/7	10/20/7	6/17/7	3.2/6/4
Thermal confinement time, τ_{Eth} (s)	0.54	0.54	0.68	0.52	0.36	0.23	0.25	0.3
$H_{98(y,2)}$	1.3	1.3	1.1	1.1	1.2	1.3	1.38	1.3
V(V)	0.06	0.06	0.15	0.12	0.07	0	0	0.02
Resistive time (s)	34.1	32.7	16.6	15.2	14.6	12.6	10.8	12.9
Neutron production rate, S_n (n/s)	1.3×10^{17}	1.3×10^{17}	7.0×10^{16}	6.7×10^{16}	5.4×10^{16}	4.5×10^{16}	2.9×10^{16}	1.2×10^{16}
Nominal repetition time for 60s flattop	1800	1800	1800	1800	1800	1800	1800	3000
Nominal repetition time for 100s flattop	3000	3000	3000	3000	3000	3000	3000	3000
Nominal repetition time after disruption	4000	4000	4000	4000	4000	4000	4000	4000

¹ Scenario 6 is, for the time being, to be considered a “to be assessed” scenario whereby the verification that it can be executed, within the limits set by the requirements from scenarios 1-5, is performed and that no extra requirements to the initial facility installation are required. Note that it is assumed that H_{98y2} can be as high as 1.3. This assumption is justified at this level of normalized pressure (β_N) by the results achieved in other devices (see T Luce et al Proc IAEA 2010 ITR/1-5 and X. Litaudon et al PPCF 46 (2004) A19). Resistive time is calculated using Mikkelsen et al., Phys. Fluids B 1 (1989) 333.

3.1. Initial Research Phase I

JT-60SA experimental program starts with the Initial Research Phase I. Commissioning of all the basic components must be completed using hydrogen plasmas in this phase. Since radio activation of the device is negligible in this phase, not only the commissioning but also the reliability examination of in vessel components should be done. The objective of operation scenario development in this phase is mainly on the definition of operation domain in various parameter spaces in relevance to the magnetic equilibrium. Since such operation domain can be sometimes extended by application of appropriate plasma control techniques, examination of applicability and effectiveness of controllers should be carried out. In addition, intensive works should be done in order to resolve scientific and technical issues specific to the superconducting (SC) divertor devices in this phase, and to maximize site availability and physics study in preparation for the deuterium phase. However, the period of this phase (Initial Research Phase I) should be as short as possible for commissioning of the facilities, and transition to the deuterium experiment in the next phase should be as early as possible. The following technical and operational issues (the order of items is neither priority nor the order of execution) should be studied for JT-60SA.

3.1-1. Controllability of plasma position and shape up to full current operation

It is preferable to demonstrate 5.5 MA full-current operations in this phase for commissioning of various facilities. Using a shot-by-shot increase of I_p toward 5.5 MA, the operation regime as well as the equilibrium control system should be examined and documented. Figure 3-2 shows an example of operation regime in the l_i - β_p space at different phases of poloidal magnetic flux swing Ψ_{extra} , for a 5.5-MA lower null (LN) plasma. The operation regime

drawn is bounded by limit of SC coil currents. However, note that this operation regime can also be limited by MHD instabilities. The coil currents of the SC coils (CS and EF) required fixing the plasma position and shape change as a function of Ψ_{extra} . This operation regime envelope shrinks with an increase of I_p and Ψ_{extra} . Since an operation outside this regime can lead to loss of shape control, this regime should be experimentally examined and documented. It is necessary to appropriately control β_p and l_i in all phases of the discharge. In addition, performance of position and shape control capability (including recovery capability) in terms of power supply voltage should be assessed, especially during vertical instabilities or during sudden changes in plasma β_p and l_i . The changes in β_p and l_i happen not only at the start/end of heating but also at some MHD activities (sawteeth, locked modes, large ELMs) and resulting collapses,

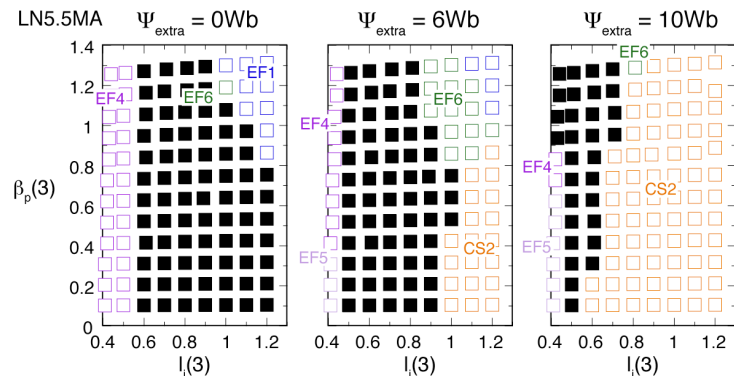


Fig. 3-2 An example of the operation regime (filled squares) of the LN 5.5-MA plasma in terms of β_p and l_i at various poloidal magnetic flux swings. (a) 0 Wb (start of the I_p flattop), (b) 6 Wb and (c) 10 Wb. If current in an external coil (CS and EF) exceeds its limit under fixing shape in equilibrium calculation, it is indicated by open squares. Thus, regime shown by filled squares is free from the limit in coil current. However, note that this operation regime can also be limited by MHD instabilities. Locations of the CS and EF coils are shown in Fig. 3-6.

during ramp up and down of I_p , at sudden L/H or H/L transitions, at an ITB formation and so on. Especially during the I_p ramp down, vertical stability maintained by the conducting shell can become insufficient, since l_i tends to increase and surface current tends to decrease. Controllability of plasma position using the fast plasma position-control system with ordinary-conducting in-vessel coils should be investigated, and the limit of I_p ramp down rate should be clarified in the first JT-60SA experiment. Prior to the experiment 3D modelling including the full vessel structure as well as 2D modelling should be performed aiming at identifying stable operation regime. Concerning the rapid change in plasma position and shape, an integrated control method using both the in-vessel coils (ordinary conductor) and the equilibrium field (EF) coils (super conductor) is necessary. The best achievable performance of the plasma position and shape control system should be evaluated against the most demanding disturbances by considering the limit on coil power supplies and diagnostics systems. This is particularly important, since JT-60SA plasmas are placed close to the stabilizing wall for higher stability, therefore, an accurate position control is necessary to prevent the plasma from touching the wall. Plasma clearance control from the wall will be also essential with the tungsten wall in the Integrated Research Phase II. Clarifying a criterion where operation shifts to shutdown procedure is an important topic as well.

3.1-2. Safe shut down at heavy collapse, disruption and quench of SC magnets

Safe shut down of plasmas after heavy collapses and disruptions must be established. Some techniques to mitigate quench of the plasma current may be necessary, e.g. automatic application of EC heating, etc. In the soft-landing phase (ramp-down of I_p to zero) after a heavy collapse, appropriate control methods should be developed avoiding vertical instability using fast plasma position-control by the in-vessel coils. It is essential to consider eddy currents in the passive structures induced by fast change in plasma parameters and external coil currents. The ramp-down rate of I_p must be sufficiently slow within the ramp-down rate limit of the EF coils. In addition, it is important for safer operation to develop a system predicting disruption and heavy collapse well in advance of those events and identify appropriate response. Applicability of safe shut down scheme developed here is to be reviewed and improved in high beta plasmas in later research phases and in particular with the tungsten wall in the Integrated Research Phase II.

3.1-3. Reliable plasma startup

Because of the available one-turn voltage is limited in JT-60SA (due to the SC center solenoid (CS)), the break down condition in JT-60SA (toroidal electric field < 0.5 V/m) is more severe than in JT-60U. Although a break down assist by ECRF is planned, optimizations of ECRF (power, injection angle, polarization) and gas pressure must be done in a wide range of magnetic field with EC resonance. A realistic calculation of the absorbed EC power has been carried out in order to maximize the X2 absorption for both 110 and 138 GHz (Electron Cyclotron resonance in HFS, injection angles: poloidal $\alpha=21^\circ$, toroidal $\beta=0^\circ$) at $B_T=2.25$ T. Although there are demonstrations of breakdown assist by second harmonic X-mode (X2) ECRF under low loop voltage (< 0.5 V/m) in some tokamaks including JT-60U, effectiveness of the ECRF assist after an air vent or after disruption of plasma having large stored energy is still to be investigated. Simulation works on X2 ECRF assisted startup conditions in a transport model showed that ECRF power of about 1 MW is required for the startup at ~ 0.5 V/m, stray field of 1 mT and hydrogen atom density of $3 \times 10^{18} \text{ m}^{-3}$ [1]. The results from this model are to be tested in JT-60SA experiment. Examination and demonstration of the break down condition without EC assist must also be done at the toroidal field where EC resonance is outside of the vacuum vessel (VV). In both cases (with/without EC assist), optimizations of the initial PF coil

currents must be done. Modeling of the plasma breakdown poloidal flux and kinetic dynamics prior to the experiment play an essential role in providing guidelines for the optimization of the start-up in particular with respect to the poloidal field coil misalignment and uncertainties or for compensating biases induced by eddy-currents. The coupling between 0D model and magnetic model in case of full (20 kA) and half (10 kA) charged CS at different breakdown time is also essential for exploring breakdown scenarios. Validity of the modeling works has to be confirmed in the initial JT-60SA experiments and prediction made for JT-60SA with the tungsten wall and ITER.

3.1-4. Volt-second consumption

In our design work, volt-second consumption has been calculated using $C_{Ejima}=0.45$. During the low I_p operations (less than about 2 MA), this assumption should be examined. Since this Ejima coefficient is also assumed in ITER ($C_{Ejima}=0.5$), this examination is an urgent task. Using this validated Ejima coefficient and magnetic energy stored in plasma $L_p I_p$, where L_p is proportional to I_i , volt-second consumption to reach 5.5 MA should be estimated in terms of I_i . For example, the high- I_i limit in Fig. 3-2 is given by the coil current in CS2 in case of $\Psi_{extra}=6$ Wb and 10 Wb. This experimental examination of the value of the Ejima coefficient may extend or shrink the operation regime in Fig. 3-2 in terms of the high- I_i boundary. Simulations also show possible reduction of volt-second consumption of about 3 Vs with a tungsten first wall due to reduction of Z_{eff} from 2 to 1, mainly due to resistive flux consumption (Ejima coefficient decreasing from 0.45 to 0.32) with no change in internal inductance and poloidal β time evolution as predicted by the METIS code [2].

3.1-5. Wall conditioning in SC devices

Since the Taylor discharge cleaning method is not available in JT-60SA, the wall-conditioning method using plasma produced by ECRF must be established and has been tested in TCV using an ECRH configuration close to that of JT-60SA. The ECRF wall conditioning [3] will be performed in the starting phase of each experimental campaign (and in particular before first plasma), after disruptions and wall saturation etc. In the starting phase of experimental campaign after an air vent, criteria of the wall condition allowing tokamak experiments should be clarified and documented. In addition, the assessment of conventional method efficiency (such as baking, glow discharge cleaning and boronization) to reduce oxygen content in JT-60SA plasma will be valuable information. The established knowledge should be extrapolated to ITER. This research item appears again in Chapter 8 “Divertor, SOL and PWI”.

3.1-6. Integrated real time control development

To achieve the JT-60SA goal of high beta long pulse operation a range of real time control schemes will be required. These requirements will increase throughout the various research phases and differ from scenario to scenario. In the first part of Initial Research Phase I, only the standard controls, plasma current, position, shape and density, will be required. As more heating power becomes available together with other actuators (P-NB, N-NB, EC, pellet injection, gas puff, etc) further control schemes should be implemented with the aim of achieving closed loop controls in the Initial Research Phase II as illustrated in figure 3-3. Table 3-6 shows a non-

exhaustive, list of required controllers for JT-60SA. For each controller, the specific plasma scenarios where this control is likely to be used are given together with the research phase where the controller should first be used. The table also shows the actuators, observers and diagnostics which could be used for each control scheme. The observers produce physical parameters from one or more diagnostic measurements in real time. The output from the observers will be used as inputs to the various controllers to produce request for the actuators.

To reach the point where closed loop real time controllers can be activated the following steps have to be undertaken; preferably in the research phase prior to the one where the closed loop control is needed:

Diagnostic data should be crosschecked against each other to ensure that reliable real time data are provided. Then the implementation of real-time data transfer to the data acquisition systems and the real-time data processing of diagnostic measurements should be implemented to produce ‘observed’ physics quantities ready for use by the controllers.

The response of the observer outputs to variations of the actuators (P-NB, N-NB, EC, pellet injection, gas puff, etc) should be quantified in open loop experiments. This should give information about time constants in individual control loops and the coupling between different control schemes. Note that real-time power control of N-NB has not been tried yet in JT-60U and hence fast on/off capability of N-NB power for control of the effective injection power in a time scale longer than the slowing down time should be demonstrated. Note that a 50-ms delay in the control system of P-NB may be too large for control of the pressure gradient near the stability boundary. In this case an upgrade of the control system may be required.

Based on the open loop tests, very simplified ‘control oriented’ models containing only the dominant dependencies should be developed and established. This design of the controllers can take advantage of these reduced models to assure that the controllers are reasonably well tuned before testing them in closed loop plasma operation. Each control scheme should preferably be tested on its own, without activation of any of the other control schemes (except the basic plasma position and current control).

Once controllers are operated together some decoupling is likely to be required. Whether decoupling is required should be seen from the open loop tests. Decoupling shall be implemented in cases with strong coupling, where the time constants of the various control loops are not very different. Decoupling is likely to be required between control loops using gas and/or impurity injection as their actuators.

3.1-7. Hydrogen phase

In the early phase of the Initial Research Phase I, JT-60SA has to demonstrate stable operation at high current (5.5 MA in H-mode in hydrogen). This objective will extend the machine

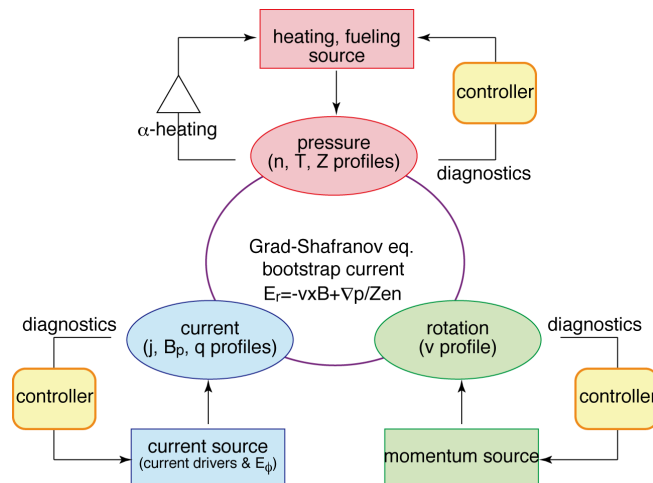


Fig. 3-3 A schematic diagram of the linkage among plasma parameters and actuators including controllers. Issues on controllers, plasma response to actuators and experimental simulations of α -heating are described in 2-6, 2-7 and 2-8, respectively, in this Chapter 3.

capabilities and prepare the operation in deuterium in the Initial Research Phase II. The divertor capability at this moment would limit the pulse length to about 5s which is sufficient to qualify the various sub-systems. Table 3-2 shows an example of H-mode operation scenario parameters in hydrogen as simulated by the METIS code. Please note that this scenario would have an L-H power threshold in hydrogen of typically 11 MW at $B_T=2.25$ T. Therefore, achieving H-mode in hydrogen looks feasible in this phase at maximum plasma current.

Once the objective of 5.5MA achieved, the JT-60SA hydrogen phase can contribute significantly to the ITER research plan in the PFPO non-activated phase. In this phase the headlines H.I.1 (stable operation at high current) and H.I.2 ITER risk mitigation for the non-activated phase) as summarized in chapter 2 can be addressed.

In particular, stable operation at high current can be strengthened by determining the impact of static error field of JT-60SA and testing the locked mode or kink mode boundaries.

The H-mode threshold power has to be investigated in JT-60SA and confirm whether the L-H transitions can occur at full power (probably possible at a lower B_T) and whether the understanding of the H-mode threshold power for hydrogen (or helium) plasmas is still insufficient for ITER.

The ELMy H-mode in the type-I ELM regime can be obtained in this hydrogen phase. ELM mitigation using magnetic perturbation should therefore be examined. The H-mode in hydrogen will be also essential for providing to ITER the plasma behavior just above the L-H threshold and the information about the isotope scaling of the core and pedestal confinement and SOL width.

In addition, the operating space of the machine can be expanded to different I_p/B_T using the ECRH resonance at different magnetic field such as 1.7T (see figure 3.4). This can also be used to study disruptions, vertical displacement events (VDEs) and run-aways build up the disruption management system (DMS) for JT-60SA from low to high plasma current and at the same time, thus providing to ITER with a template about how to integrate disruption prediction and mitigation in the control system during the non-activated phase. Broadening the operating space also offers to the scientific program a wider range of scenarios for developing the scenario building blocks (current ramp-up, flattop and termination) and the initial control schemes.

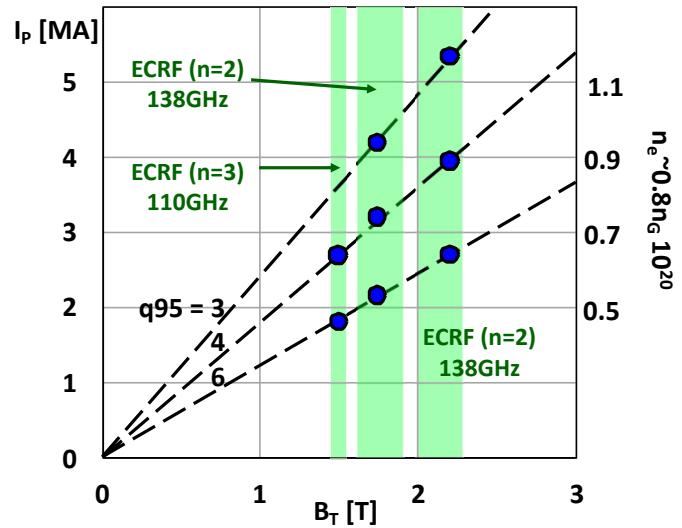


Fig 3-4 Range of possible scenarios with ECRH in the initial research phase I & II for expanding the operation of JT-60SA and studying the ITER risks.

Table 3-2 A scenario example for initial phase I (computed by METIS)

Scenario	I_p [MA], B_T [T] q_{95}	nI [10^{19} m^{-3}] f_{GW}	R [m], a [m] κ , δ	W_{TH} [MJ], H_{98}	P_{NNB} , P_{PNB} P_{EC} , P_{OH} [MW]
5.5 MA hydrogen	5.5, 2.25, 2.8	6.3 0.5	2.96, 1.18 1.95, 0.53	4.7, 1	0, 9.6 0, 4.1

3.2. Initial Research Phase II

The major objective of this first deuterium phase is to establish the deuterium scenario basis for JT-60SA compatible with ITER and DEMO scenario needs and prepare the grounds for controlled long-pulse operation. With respect to the DEMO physics issues (which will surely include ITER physics issues), the development of scenarios in JT-60SA would follow three lines of research:

- 1- High density operation (scenario 2, 4 and 5): this is aimed at exploring the accessibility to densities above the Greenwald density, investigating the power exhaust in prevision to a metallic-wall and developing the radiation layers in scenarios.
- 2- High β_N scenario (scenario 5.1 and 5.2): This type of scenario will specifically identify the MHD stability boundary domain for DEMO and optimize the burn phase and its active control.
- 3- High β_p scenarios: fully non-inductive operation is the main goal of these scenarios. They would use strong electron heating and be the workhorse of the development of efficient profile control schemes.

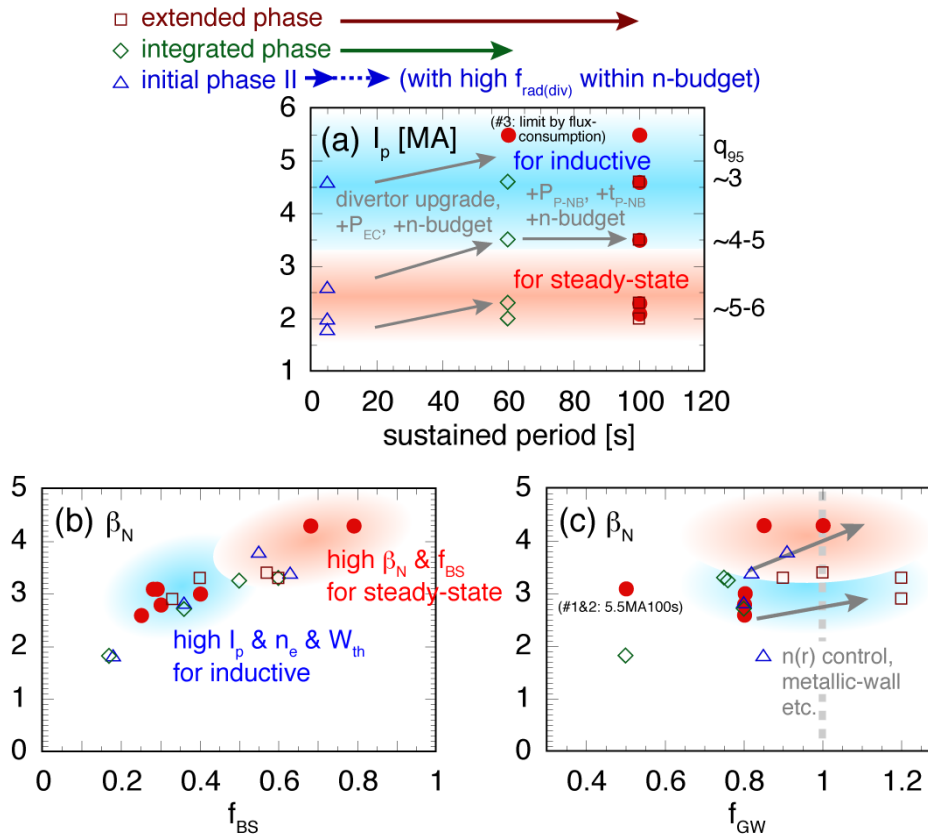


Fig. 3-5 Overview figures on the progress of main operation regimes along the research phases. Red circles show the typical operation scenarios with full machine capability shown in Table 3-3. Triangles, diamonds and squares show the scenarios shown in Table 3-5 as examples of possible scenarios within the machine capability in initial research phase II, integrated research phase and extended research phase, respectively. (a) Progress of operation regime development in plasma current and sustained period. Gray arrows show machine capability upgrades. (b) and (c) Operation regime in the β_N - f_{BS} (b) and β_N - f_{GW} (c) normalized parameter space. From the beginning of deuterium experiment in the initial research phase II, attractive experiments exploring broad spectrum of DEMO concept are possible at high values of the normalized-parameters.

Figure 3-5 illustrates the progress of the main operation regimes along the research phases. Fig. 3-5 (a) shows progress of sustained period of operation scenarios exploring broad spectrum of DEMO concept having different q_{95} . With upgrades of heat-handling capability in divertor, heating capability and neutron budget, long-pulse experiments exceeding the current diffusion time (see Table 3-1) become possible. Figure 3-5 (b) Regarding the Initial Research Phase II, radiative divertor study could mitigate the divertor heat load and contribute to early realization of scenario/physics study in a time scale of current diffusion time (validation of scenarios with respect to tearing stability and current profile control) in this research phase. On the normalized parameter regime, JT-60SA explores broad DEMO concept regimes (steady-state as well as inductive) toward feasible and attractive DEMO from the Initial Research Phase II. Since parameters β_N and bootstrap current fraction f_{BS} (Fig. 3-5 (b)) regarding the high β_N and high β_p scenarios, respectively, in the Initial Research Phase II overlap with those in the later phases, this Initial Research Phase is a good starting point of high beta scenario development (although it might start from a shorter period than the current relaxation time). High normalized-density (f_{GW}) scenario at high β_N would also be possible from the Initial Research Phase II (Fig. 3-5 (c)). Accessibility above the Greenwald density would be explored with development of density profile control, metallic wall etc.

3.2.1. Demonstration of ITER standard operation scenario ($q_{95}\sim 3$)

In order to directly contribute to ITER as the largest SC tokamak device in ITER shape, the ITER standard operation scenario should be demonstrated from the startup to the shutdown in deuterium plasmas as early as possible well in advance to ITER. Ultimately, this scenario could be run at currents from 4.6 MA (like scenario #4-1 with ITER-like shape as shown in Fig. 3-6) to 5.5 MA (like scenario #1, #2 and #3). The high confinement at high current will also provide an appropriate workhorse scenario for the operation at low collisionality and investigate plasmas close to the ITER collisionality. Also, helium exhaust can be experimentally simulated using helium NB injection. The suitable configuration should be at lower $\beta_N\sim 2$ and heating power. Since the neutron production rate of scenario #4-1 is 6.7×10^{16} n/s for 4.6 MA, the neutron production in one 30-s shot produces 2×10^{18} neutrons, then the annual neutron limit (4×10^{19} n/s, ~ 20 shots) would become a constraint on the long-sustainment experiment in high current in this phase.

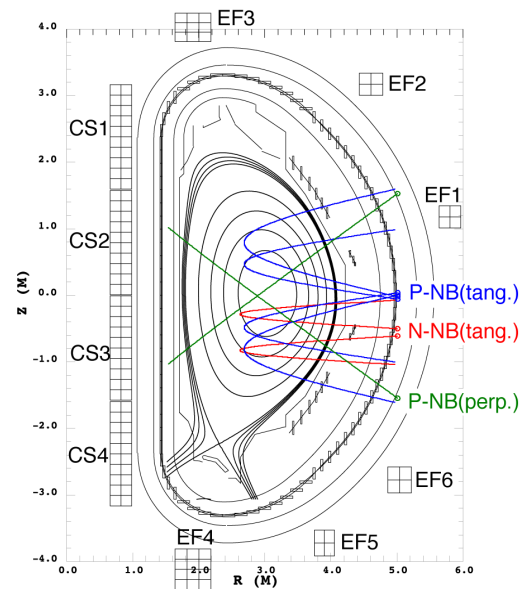


Fig. 3-6 Typical ITER-like plasma configuration and trajectories of NBs with respect to magnetic surfaces. Beam lines of tangential P-NBs and N-NBs are off-axis. Beam lines of perpendicular P-NBs are on-axis, but deposition can become off-axis at high density.

3.2.2. ITER advanced inductive (hybrid) operation scenario study ($q_{95}\sim 4$)

Based on the scenarios #4-1 and #4-2 shown in Table 3-1, the ITER advanced inductive (so-called hybrid) operation scenarios should be developed. These scenarios have an ITER-like plasma-boundary shape as illustrated in Fig. 3-5 and explore the q_{95} domain around 4 at reduced

plasma current (typically between 4.6 and 3.5MA). The normalized beta β_N can be as high as 3 when the injection power is 34-37 MW and the confinement enhancement factor over the H98(y,2) scaling H_H is assumed to be 1.1 to 1.2 in line with the results achieved in other devices [4] including JT-60U. Since the total heating power (NB+EC) is 33 MW (within 5 s) in this Initial Research Phase II, scenario #4-1 and 4-2 can be a target in this phase and started even at lower field if necessary to explore the high β_N domain. Achievement in a short period is aimed in this phase at this I_p for ITER relevant ρ^* and v^* condition. Since 30 MW of NB injection is possible for as long as 60 s in this phase (as far as heat load to divertor is maintained to be acceptable owing to radiative divertor study described in 2-5), steady sustainment of scenario #4-1 can be tried at lower I_p and B_t (or at higher H_H) while keeping $\beta_N \sim 2.8$. A higher q_{95} scenario at lower I_p and B_t than the scenario #4-1 will be investigated for performance optimization within the limits of volt-sec consumption and neutron flux. Using helium NB injection, helium transport and exhaust are investigated for development of ash control schemes. This scenario development should be sufficiently in advance to the advanced inductive scenario development in ITER, and the results obtained in JT-60SA should be extrapolated using modeling and optimized experiments have to be proposed to ITER. Since the neutron production rate of scenario #4-2 is 5.4×10^{16} n/s for 3.5 MA, the neutron production in one 30-s shot produces 1.6×10^{18} neutrons, then the annual neutron limit (4×10^{19} n/s, ~ 25 shots) would become a constraint on the long-sustainment experiment in high current in this phase.

This scenario and the $q_{95}=3$ scenario (section 3.2.1) will directly contribute to headline H.II.1 of Initial Research Phase II (ITER scenario development). For example, they will be the workhorse scenario for studying sawtooth and NTM control, high density operation, light and heavy impurity transport, H-mode physics and detachment.

3.2.3. Steady-state (SS) operation scenario study ($q_{95} \sim 6$)

The basis for the high β_N high non-inductive current drive fraction scenarios should be also established in this phase. Such scenarios should be referred to the scenario #5 and #6 in Table 3-1. The scenario #5 aims at high $\beta_N=4.3$ with 37 MW heating and $H_H=1.3$ at $I_p=2.3$ MA, $B_t=1.7$ T ($q_{95} \sim 5.7$) under full-CD. The ACCOME calculation predicts the scenario #5 has reversed magnetic-shear (RS). Since adjustment of target RS q profile is essential to obtain good confinement, off-axis N-NBCD is utilized in the adjustment. The real-time current profile control under development in 2-1 is expected to contribute to the adjustment and reproduction of the q profile. At slightly lower field and current within available power of 33MW, operation regimes would be explored in terms of q profile and hence the β_N and bootstrap current fraction f_{BS} (or β_p). The former (high β_N) scenario has the aim to study the MHD limit (RWM and NTM) for various q and pressure profiles and the latter (High f_{BS}) scenario the non-inductive current drive and current profile alignment to reach steady-state. While $f_{GW}=0.85$ in scenario #5, higher density regime above the Greenwald density, $f_{GW} \sim 1.1-1.3$ is explored in scenario #5.2 for attractive DEMO design. There is an estimate that higher electron density can allow smaller T/D injection ratio < 1 for fixed fusion power and hence contributes to reduction of T quantity in a plant. In this high confinement plasma, helium transport and exhaust are also investigated for ITER and DEMO. Density profile will be optimized using the pellet injection and divertor exhaust for the higher density and the effective helium exhaust. In order to reduce heat load to divertor, higher density in divertor and SOL is intended. It should be noted here that I_p build up scenario using mostly the non-inductively driven current (including bootstrap current) is required during the startup phase of the SS scenario for SlimCS DEMO concept due to its small capability of poloidal magnetic flux supply. For that purpose, the following studies should be conducted and the I_p build up scenario that matches to the SS operation scenario must be

developed; 1) to raise current by overdriving plasma current non-inductively or 2) to save mostly the consumption of poloidal flux at high non-inductive current fraction with small inductive current throughout the buildup phase. From the beginning of the SS operation scenario study, the I_p build up scheme using non-inductively driven current should be investigated for the SlimCS DEMO. The above-mentioned non-inductive current overdrive scenario was investigated in TOPICS transport simulation with CDBM thermal transport model with prescribed density profile, where current ramp-up from 0.5 to 2.1MA was demonstrated within JT-60SA heating capability but in a long ramp-up period (~ 150 s) [5]. A part of this scenario would be explored in JT-60SA experiment. The scenario #6 aims at steady sustainment for as long as 300 s (*if NB injection is allowed*) at a lower $\beta_N=3.0$ for 13.2 MW heating and $H_H=1.3$ at $I_p=2.0$ MA, $B_t=1.4$ T ($q_{95}\sim 4$) with small OH consumption. This scenario #6 is also a candidate of the advanced inductive scenario as described above. For the scenario #6 (the neutron production in a 300~s shot: 1.2×10^{16} n/s \times 300 s = 3.6×10^{18} neutrons), the annual neutron limit (4×10^{19} n/s, ~ 11 shots) may become a constraint on the experiment in this phase. Since allowable heat load on upper and lower divertors are almost the same in this phase, upper single null (USN) plasma can be a candidate for SS operation scenario for a short period of heating. The USN configuration has an advantage in getting further off-axis N-NBCD than LSN; see trajectory of N-NB in Fig. 3-5. Thus, this USN can be an option for broadening current profile rather than LSN (assessment to be done). However, long pulse operation of such LSN scenario must wait for the full-monoblock upper divertor in extended research phase.

This SS operation scenario development also contributes to the ITER SS operations. Therefore, the development should be sufficiently in advance to the SS scenario development in ITER, and the result obtained in JT-60SA should be extrapolated using modeling and optimized experiments have to be proposed to ITER.

The development of the non-inductive scenario at high β_N or high β_p is part of headline H.II.2 of the Initial Research Phase II (see chapter II). It will address issues such as current drive optimization, real time control development (see below), fast particle instabilities and self-organisation of current, pressure and rotation profiles.

3.2-4. Scenario integration in support of ITER and DEMO

The achievement of the scenario described above will require an intense activity on scenario integration, which are all essential for both ITER and DEMO long pulse scenario. The main items are:

- Achieving scenarios with dominant electron heating and low rotation.
- Radiative divertor
- Integrated plasma control
- Burn control

All these items will be also essential tools after the change to the metallic wall.

3.2.4-1 Dominant electron heating scenarios

The development of scenarios with dominant electron heating would contribute to the validation of the DEMO scenarios in JT-60SA. The main items that would benefit from dominant electron heating:

- The study in the low v_e^* domain (density peaking, scaling towards ITER, etc)
- Optimisation of non-inductive current drive efficiency in steady-state and advanced inductive scenario
- Burn control
- Impurity control (extrinsic and intrinsic impurities)

- Transport and confinement studies with $T_e > T_i$.

In this phase, JT-60SA is equipped with 3MW of ECRF and 10 MW of N-NB. However, depending on the scenario of Table 3-1, typically 1/3 to 1/2 of the power of the N-NB is deposited on the ions (by METIS computation for on-axis N-NB). In addition, ECRF has also other uses such as MHD control, q profile control or plasma start-up assist. This suggests that the increase of the installed ECRF power as an option would be beneficial to JT-60SA in exploring the electron heating scenarios in support of the DEMO. In addition, dominant electron heating can provide an important tool for high Z impurity control in preparation of the metallic wall.

3.2.4-2. Radiative divertor study

Study on steady and stable sustainment of highly radiative detached divertor at as high heating power as possible should be started in this phase with heating capability up to 30MW for 60s. Although the divertor target situation in this phase is a LSN partial monoblock divertor (see Table B-1 for the specifications), heat load mitigation using appropriate radiation control by impurity seeding is necessary, since this radiative divertor is a key for high-power long-pulse heating in this research phase. Assuming inertial components with 10MW/m² for 10s heat flux capabilities, λ_q from Fundamenski et al, (2011), the requirements for radiation fraction for the temperature not to exceed 2000°C on the divertor targets can be evaluated for the four scenarios of this phase (Table 3-5) as shown in Table 3-3. Therefore, high radiation with impurity seeding is necessary for long-pulse operation of these scenarios. The radiative divertor developed here should be applied to the scenarios in Sec. 3.2-1 – 3.2-3 in order to examine its compatibility to various scenarios and sustain the plasma for as long as possible above the divertor capability (within the neutron budget).

To be noted in this study is that appropriate interlock on heating systems based on divertor tile heat load measurement in real-time must be established. For contribution to ITER and DEMO, H-mode transition under detached divertor is an important issue in order to mitigate divertor heat load. This sequence of H-mode transition after divertor detach has not been studied well in currently operating tokamaks. The higher neutral flux at the detached divertor may affect the threshold power of H-mode transition so that this issue is studied as well.

Also, the radiative scenario study in the carbon-wall will be strongly dependent on the intrinsic impurity (carbon). Therefore, their development may not be directly transferable to a metallic-wall where the radiation will be provided by tungsten and extrinsic impurities such as nitrogen, neon or argon. However, the radiative divertor studies should provide an essential base for the preparation of long pulses with the metallic wall where detached divertor will be mandatory.

Table 3-3 An estimate of required radiative fraction for 30 s sustainment of scenarios (see Table 3-5) assuming inertial cooling of divertor

Scenarios	Loss power	Radiative fraction
ITER standard scenario	14.2 MW	90% (~85% if sweeping)
Advanced inductive scenario	21.3 MW	84% (~75% if sweeping)
High β_N Scenario	28 MW	84% (~75% if sweeping)
High β_P Scenario	29 MW	80% ~70% if sweeping)

3.2.4-3. Development of the advanced integrated control system for scenarios

Advanced real-time control schemes must be introduced and partially demonstrated in this phase. They include (1) real-time control of the current profile using control of the off-axis N-NB power, (2) real-time control of the plasma toroidal rotation using control of the tangential P-NB power, (3) real-time control of the pressure profile using control of the perpendicular P-NB power. Combination of the above 3 control schemes is also expected. Figure 3-3 shows schematic image of this real-time control system. Control cycle of heating and current drive systems would be 10ms which is enough shorter than the energy confinement time and current diffusion time. The real-time control system should work at the same cycle as the heating and current drive systems. In addition, to be demonstrated are the real-time control techniques of RWM stabilization using the in-vessel stabilization coils, NTM suppression and stabilization using real-time mirror-steering and synchronized modulation of ECCD, ELM control using the magnetic perturbation coils, fueling (or density gradient) control using pellet injection, divertor and SOL density control using gas-puff (see Table 3-6). A real-time MHD stability analysis (or prediction) using MARG2D should be tried in open-loop using the real-time data. Basic plasma response to various actuators must be quantitatively studied in deuterium plasmas, such as response of the pressure to heating, response of the current profile to current drive and response of the rotation profile to momentum input (external torque input and ripple losses). These data are used in development of the real-time control schemes described above. It is expected that functions of actuators can be more separated in JT-60SA compared with JT-60U. Since fast-ion losses due to the toroidal field ripple ($<0.5\%/0.9\%$ with/without ferritic inserts, respectively) decrease in JT-60SA than JT-60U, effects of perpendicular P-NB injection to the toroidal rotation become smaller than those in JT-60U. Since the beam energy of N-NB increases up to 500 keV, effects of the N-NB on the toroidal rotation are smaller than those of the tangential P-NBs. Thus, functions of the perpendicular P-NBs, N-NBs and tangential P-NBs will concentrate more on heating, current drive and momentum input, respectively. Therefore, the controllers for the pressure, current and rotation profiles in Fig. 3-3 are more decoupled compared to JT-60U. In addition, since the beam penetration (especially P-NBs) is a strong function of density, the heating and momentum input profiles depend strongly on density, and tend to be more off-axis than in JT-60U. This is because the expected operation density in JT-60SA will be higher than that in JT-60U. Therefore, understanding of characteristics of the actuators as a function of density becomes more important and to be examined and quantified.

3.2.4-4. Experimental simulation of burn control for ITER DT experiments and DEMO

Thermal stability of burning plasmas is a great interest in ITER DT experiments and DEMO. Although real burning plasma cannot be obtained until ITER, controllability of thermally self-regulated plasma should be studied before DT experiments in ITER in order to conduct the ITER experiments efficiently. Experimental simulation that was developed in JT-60U should be conducted at a higher beta and a highly self-regulated condition than JT-60U. The developed scheme utilizes two groups of heating systems (mainly NBs). One group simulating the α -heating positively feedbacks the heating power in proportion to the measured quantity, e.g. the neutron production rate or $n^2\langle\sigma v\rangle$ (see Fig. 3-3). The other group simulating the external heating controls this system in real-time. Since the available P-NB heating power increases up to 20 MW in this Initial Research Phase II, this phase is a good timing to start this study in advance to ITER DT experiments. In JT-60U, the α -heating was simulated by ion-heating dominant P-NB, while 17 MW of electron-heating dominant N-NB and ECRF in JT-60SA. It is necessary not only to study the thermal characteristics of the simulated burning plasmas, but also to start development of appropriate control schemes applicable to ITER. One of such controls would be control of fuel profile. Ion density profile can be evaluated through real-time

electron density profile by Thomson scattering and effective charge profile measurement, taking into account of fast ions. In controlling the fuel profile, pellet injector, divertor pumping and RMP can be used.

3.3. Integrated Research Phase I

The Integrated Research Phase I has the goal to:

- Develop the scenarios to higher power (37MW) and longer duration (60s)
- Establish the physics and operational basis for the DEMO scenarios
- Prepare the transition from the carbon wall to the metallic wall.

3.3.1 Achievement of the mission goal with the carbon wall

In this research phase, extensive studies for achieving the main mission goals of JT-60SA start by utilizing the heating capability of 37 MW \times 60 s (P-NB 20 MW, N-NB 10 MW, ECRF 7 MW) and the full-monoblock lower divertor target. The ECRF power is increased to 7 MW for 100 s. With this high power and the NTM control technique established in the Initial Research Phase, NTMs will be stabilized in various operations. Note that research items started in the Initial Research Phase II for advanced tokamak operation continue and are improved as shown later in the Table 3-4.

The high β_N full non-inductive current drive operation (the scenario #5), the full current inductive operation at high density (the scenario #3), and the ITER-like inductive operation (the scenario #4-1) and the ITER advanced inductive operation (the scenario #4-2) have to be demonstrated for a certain period. The period will be extended up to 60s (the heating capability) within the annual neutron production limit of 4×10^{20} n/s. Based on the developed high β_N full non-inductive current drive operation (the scenario #5) but at a lower I_p than 2.3 MA, development of non-inductive I_p ramp up is done in this research phase.

For extending the ITER advanced inductive scenario operation, realization of the scenario #2 should be tried in a short period. Since the available heating power in this phase is still 4 MW lower than the scenario #2 design, experimental condition at lower I_p and lower B_t could be possible.

Under these scenario development studies, the real-time control schemes developed in the Initial Research Phase would be improved and matured. In particular, the heat and particle control schemes under the high heating power with long pulse utilizing the completed lower single-null divertor (full-monoblock divertor target, V-shaped corner at the outer hit point, active divertor pumping) and particle fueling (pellet injection, gas-puff, impurity-puff) have to be established. At the same time, in particular for the SS and advanced inductive operations, the steady-state current profiles with external current drive have to be investigated and optimized. In development of the high β_N SS operation scenario, the RWM control system that is developed in the Initial Research Phase is applied and utilized. Finally, all the required active control methods have to be integrated in order to sustain the required integrated performance of the target plasmas. The Integrated Research Phase I is the time when the controllers allowing operation at high beta and high bootstrap fraction are required (beta control, NTM control/avoidance, RWM control, current profile control, pressure profile control). Once tungsten is introduced as a first wall material, in Integrated Research Phase II, another series of controls, some of which are desirable for long pulse operation already in Integrated Research Phase I, become essential. These are the control schemes required to prevent overheating of the divertor and to avoid impurity accumulation in the plasma centre. In addition to the schemes developed to achieve the desired JT-60SA plasma performance, other control schemes should be demonstrated in specific experiment such as isotope control and burn control simulation.

3.3.2 Establish the physics and operational basis for the DEMO scenarios

The development of the SS operation scenario should be directed to DEMO scenario development. Control scheme and diagnostics should be applicable to DEMO environment so that the use of in-vessel coils (e.g. for control of RWM and ELM as well as vertical position) should be minimum. Cost and efficiency of the (real-time) control schemes for DEMO should be considered in this phase in order to clarify parameters to be actively controlled and to remain uncontrolled (self-regulated). Margin of the controlled parameter for stable operation concerns the evaluation of the cost and efficiency, and hence the margin should be clearly defined. In comparison of the cost and efficiency of the developed control systems, data should be examined for proposals to ITER upgrade (e.g. momentum injection NB in ITER). In addition, if a specific real-time control system is unavoidable for achievement of the ITER advanced inductive and SS scenarios, it should be proposed to ITER.

3.3.3. Preparation of the transition to the tungsten wall

The transition to the tungsten wall will imply a large number of additional technical and operational requirements for the main scenarios of JT-60SA. As drawn from the experience in JET and AUG, the following prerequisite should be examined prior to the transition to the tungsten wall:

- High density/large gas puff will be required in the W-wall to avoid W influx and accumulation. This needs to be tested well in non-inductive scenarios in particular.
- Some of the ECRH power will be dedicated to W control and this needs to be tested in advance in relevant scenarios by injecting W or high Z species.
- Shine-through with the available NB power needs to be re-assessed for scenarios.
- Integrated disruption control and mitigation system will be required systematically to avoid or mitigate electro-magnetic and heat loads in high performance scenarios. This will need to be prepared in advance of the transition to W.
- New wall protection system and associated set of diagnostics (IR camera, thermocouple, Langmuir probes, pyrometers, spectroscopy, etc) will need to be installed and commissioned.
- ELM energy impact assessment, ELM mitigation and control or small ELM regime should be established before the installation of the new wall.
- Tungsten sputtering and erosion in the main chamber need to be minimized by careful plasma control clearance.
- Physics of low collisionality will be more difficult to access with the metallic-wall, therefore this part of the program should be done before the transition.

Many of these points are also related to ITER and DEMO research issues and therefore should strongly contribute to the development of DEMO scenario design.

3.4. Integrated Research Phase II with the W wall

DEMO is planned to have a metallic-wall, therefore, there are important DEMO physics issues that should be addressed with a metallic-wall in JT-60SA, such as high-density operation above the Greenwald limit and the reliable radiative detached divertor techniques which are strongly dependent on the wall material. In the following areas JT-60SA long pulse operation can benefit from transition to the W plasma facing components:

- High power scenario will produce less erosion and less deposition
- Z_{eff} will go down from typically 2 to 1, thus lowering dilution and current diffusion.
- More stable operation at high densities is expected: no more MARFE activities.
- Less surface conditioning necessary and easier plasma breakdown.

- More operational freedom to use radiative species (since there is no intrinsic carbon radiation)

With these new elements, JT-60SA can strongly support the integration of long duration scenarios compatible with metallic-wall for ITER and provide significant input to the conceptual studies of DEMO. Scenario integration (high-beta high-density control, non-inductive current drive, radiation control, etc) should become compatible with the metallic-wall. The following scientific items should be considered in the Integrated Research Phase II:

- High confinement operation above the Greenwald density has proved difficult in carbon machine. Therefore, the exploration of high-density scenario is a high priority for the metallic-wall phase and should confirm the ITER operating point.
- Feasibility of safe long-pulse high β_N non-inductive operation of plasma scenarios in a metallic-wall for DEMO should be explored.
- In scenarios, ECRH should take on the tasks of impurity control with the metallic-wall in addition to the other tasks (NTM control, plasma start-up, off-axis current drive, etc).
- Establishing radiative/detached in high performance scenario can directly benefit to DEMO conceptual design.
- In long pulses, the evolution of W erosion under high flux/power load can be investigated.

On this basis, right from the beginning of this phase, large emphasis is placed on establishing long pulse experiments with the metallic wall, since the annual neutron limit increases (1×10^{21} n/s) near the final specification and remote handling is enabled. Based on the development in the Integrated Research Phase I in the carbon wall, the main goals of JT-60SA plasma performances have to be achieved and sustained for 60 s, for the DEMO-equivalent high β_N and high β_p full non-inductive current drive operation (the scenarios #5) combined with non-inductive I_p ramp up prelude, the full-current inductive operation at high density (the scenario #3), and the ITER-like inductive (scenario #4-1) / advanced inductive (the scenario #4-2) operations. At the time of the Integrated Research Phase II, the development of the non-inductive scenario can also contribute directly to the ITER long pulse scenario beyond 400s so that the physics basis for DEMO scenarios needs to be established on two devices of different size i.e. JT-60SA and ITER.

Other operation scenarios helpful for identifying DEMO/reactor operation specific features and their commissioning procedures will be investigated in this phase. One issue is recovery from a thermal collapse to the high performance plasma in order to improve availability of reactor, because it is considered that shutting down the operation after the collapse and restarting the operation takes long time and drastically reduces plant availability. Another issue concerns steady-state plasma required for commissioning of reactor. It is considered that steady-state heat load to various plant components (coolant systems, turbines, etc) is required in a reasonably low power during initial commissioning phase. Thus, operation scenario of such target plasma suitable for steady-state low-power output and applicable to reactor is to be studied well in advance to the DEMO operation. This scenario integration work with the full W wall together with ELM mitigation, low disruptivity and improved core confinement and radiative layer should directly be transferred to DEMO future operation.

Requirements for DEMO should be documented, based on knowledge obtained in JT-60SA.

3.5. Extended Research Phase

The main objectives of the extended research phase are:

- Demonstrate DEMO scenario options at full power and for 100s duration.
- Establish fully integrated operation with the W wall in support of DEMO design.

This will be achieved using the full capability of JT-60SA, especially the heating system, the integrated control system and the double-null divertor. The heating power for ~100 s period largely increases in this phase to 41 MW from 27 MW. Note that heating power for 100 s is 27 MW (NB 20 MW + EC 7 MW) in the Integrated Research Phases, while 37 MW for 60 s (NB 30 MW + EC 7 MW) as shown in a column (“Power × Time”) in Table 1-5. Of course, accomplishment of the following missions in the Integrated Research Phase is preferable within 27 MW heating and higher confinement. In addition, operation scenarios in the Integrated Research Phase would be extended toward higher density reaching or exceeding the Greenwald density limit as in Table 3-5.

3.5.1. Accomplishment of the main mission goal

Utilizing the increased heating power to 41 MW (increase by 4 MW NBI), 5.5 MA full-current plasma is sustained for 100 s. The first target is the scenario #1. This plasma has $\beta_N=3.1$ using 41 MW heating and $H_H=1.3$ at $I_p=5.5$ MA, $B_t=2.3$ T ($q_{95}=3$). Since the estimated loop voltage in this scenario is 0.06 V and the available volt-second during flattop phase is 9 Wb as shown in Table 3-1, sustainment of this scenario #1 for ~100 s is possible (within the limit of heating capability). This scenario should be developed based on the scenario #4 that has been developed from the Initial Research Phase II toward higher I_p , higher β_N , higher confinement.

3.5.2. Demonstration of DEMO scenario (another main mission goal)

DEMO scenarios in the relevant normalized parameter space should be demonstrated, where the target plasma has $\beta_N=5$ under steady-state full CD at f_{BS} , H_H , f_{GW} , f_{rad} as high as possible at reasonably low q_{95} less than about 5. Optimization of the SS operation scenario is conducted in order to approach and exceed the normalized parameters for DEMO shown in Fig. 1-5. In addition, as long prelude of non-inductive I_p ramp up should be tried within the limit of annual neutron limit.

3.6. Summary

The summary of the experimental program is shown in Table 3-4.

References

- [1] Hada K. *et al* 2015 *Fusion Sci. Tech.* **67** 693; Hada K. *et al* 2012 *Plasma Fusion Res.* **7** 2403104.
- [2] Artaud J.F. *et al*, 2018 *Nucl. Fusion* **58** 105001.
- [3] Douai D. *et al*, 2018 *Nucl. Fusion* **58** 026018.
- [4] Luce T.C. *et al* 2014 *Nucl. Fusion* **54** 013015.
- [5] Wakatsuki T. *et al* 2015 *Plasma Phys. Control. Fusion* **57** 065005.

Table 3-4 Experimental program for operation scenario development

research issues	initial phase I	initial phase II	integ. phase I	integ. phase II	extended phase
controllability of plasma position and shape up to full current operation	■	■			
safe shut down at heavy collapse, disruption and quench of SC magnets	■	■	■		
reliable plasma startup	■	■			
volt-second consumption	■	■			
wall conditioning in SC device	■	■			
real-time function of actuators in open-loop	■	■			
validation of diagnostic data	■	■			
introduction of real-time diagnostics	■	■	■		
H-mode threshold power in hydrogen plasma	■	■			
ELM mitigation using magnetic perturbation	■	■	■		
advanced real-time control		■	■	■	■
demonstration of ITER standard operation scenario		■			
ITER hybrid operation scenario		■	■	■	■
ITER steady-state operation scenario		■	■	■	■
quantification of plasma response to actuators		■	■		
experimental simulation of burn control for ITER DT experiment and DEMO		■	■	■	
radiated divertor study		■	■	■	
accomplishment of a main mission goal				■	■
demonstration of DEMO scenario				■	■

Table 3-5 Summary of scenario examples for the initial research phase II, integrated research phases and extended research phase (computed by METIS)

For the initial research phase (section 2)

Scenario	I_p [MA], B_T [T] q_{95}	nl [e19m-3] n/ng	R[m], a[m] κ, δ	W_{TH} [MJ], H_{98} $\beta_{Nth} / \beta_{TOT} / \beta_{Pth}$	P_{NNB}, P_{PNB} P_{EC}, P_{OH} [MW]	P_{LOSS} [MW] P_{DIV} [MW]	I_{NI} [MA] I_{BOOT} [MA]
ITER-like Inductive	4.6, 2.28, 3.1	9.6, 0.85	2.93, 1.14, 1.81, 0.41	11.6, 1 1.75 / 1.83 / 0.57	0, 19 3, 1.0	14.2 9.3	1.25 0.82
Advanced Inductive	2.6, 1.72, 4	5.4 0.8	2.97, 1.11, 1.83, 0.47	7.2, 1.23 2.44/2.83 / 1.37	5, 18.5 1.0, 0.2	21.3 17.3	1.68 0.94
High β_N	2.0, 1.4, 5.0	4.7 0.91	2.97, 1.11, 1.90, 0.47	6.1, 1.25 3.2 / 3.8 / 2.35	10, 19 3.0, 0	28.5 24.3	1.9 1.1
High β_p	1.8, 1.6, 6.5	4.0 0.82	2.97, 1.11, 1.90, 0.47	5.1, 1.25 2.58 / 3.4 / 2.71	10, 19 3.0, 0	29.5 26.5	2.05 1.13

The ITER-like inductive (scenario #4-1 like) is designed to study the H-mode in support of ITER and provide the workhorse for the lowest possible collisionality with strong electron heating. The advanced inductive is a $q_{95}=4$ scenario with $q_0 > 1$ (#4-2 like). The high β_p and β_N (#5-1 and #5-2 like) are aimed at the study of the non-inductive current drive and MHD limit respectively (RWM and NTM at high β) for various q and pressure profiles.

For the integrated research phase (section 3)

Scenario	I_p [MA], B_T [T] q_{95}	nl [e19m-3] n/ng	R[m], a[m] κ, δ	W_{TH} [MJ], H_{98} $\beta_{Nth} / \beta_{TOT} / \beta_{Pth}$	P_{NNB}, P_{PNB} P_{EC}, P_{OH} [MW]	P_{LOSS} [MW] P_{DIV} [MW]	I_{NI} [MA] I_{BOOT} [MA]
ITER-like Inductive	4.6, 2.28, 3.1	5.6, 0.50	2.93, 1.14, 1.81, 0.41	11.5, 1 1.73, 1.82, 0.57	10, 10 7, 0.8	25.4 23.6	1.45 0.8
Advanced Inductive	3.5, 2.28, 4.0	6.34 0.8	2.97, 1.11, 1.83, 0.47	13.2, 1.3 2.52, 2.71, 1.22	10, 19.6, 7, 0.35	28.1 17.1	1.83 1.25
High β_N	2.3, 1.72 5.0	4.5 0.76	2.97, 1.11, 1.90, 0.47	7.1, 1.23 2.65, 3.25, 2.05	10, 19 7.0, 0	33 30	2.1 1.15
60s Full-CD	2.0, 2.25 6	4.0 0.75	2.97, 1.11, 1.90, 0.47	6.0, 1.23 2.53, 3.3, 2.45	10, 19 7.0, 0	33.5 31.1	2.2 1.2

The set of scenarios above has the objective to qualify the operational q profile for DEMO (in q_{95}/q_0) and validate profile control in different I_{NI}/I_p conditions. The ITER-like inductive could be extended to 5.5MA to reach ITER relevant v^* (scenario #2 in Table 3-1).

For the extended research phase (section 4)

Scenario	I_p [MA], B_T [T] q_{95}	nl [e19m-3] n/ng	R[m], a[m] κ, δ	W_{TH} [MJ], H_{98} $\beta_{Nth}, \beta_{TOT}, \beta_P$	P_{NNB}, P_{PNB} P_{EC}, P_{OH} [MW]	P_{LOSS} [MW] P_{DIV} [MW]	I_{NI} [MA] I_{BOOT} [MA]
High ne DEMO	4.6, 2.28 3.2	13.6 1.2	2.93, 1.14, 1.81, 0.41	19.5, 1.2 2.8, 2.9, 1.04	10, 24 7.0, 0.5	23.5 14	2.15 1.54
	3.5, 2.28, 4.0	9.4 1.2	2.97, 1.11, 1.83, 0.47	12.4, 1.3 3.1, 3.3, 1.6	10, 21, 7, 0.25	26.8 12.3	1.9 1.4
High β_N DEMO	2.3, 1.72 5.0	6.0 1.0	2.97, 1.11, 1.90, 0.47	8.1, 1.23 2.95, 3.4, 2.22	10, 24 7.0, 0	34.5 29.5	2.1 1.32
100s Full-CD DEMO	2.0, 2.25 6	5.0 0.90	2.97, 1.11, 1.90, 0.47	6.0, 1.23 2.53, 3.3, 2.45	10, 24 7.0, 0	33.5 31.1	2.2 1.2

In this table, the ‘‘High ne DEMO’’ could be based on the 4.6 MA ITER-like inductive or on the 3.5MA advanced inductive scenarios extending the density above the Greenwald density with the metallic-wall. The ‘‘100s Full-CD DEMO’’ and ‘‘High β_N DEMO’’ scenarios (see scenario #5-1) are derived from the ‘‘High β_N ’’ and the ‘‘60s Full-CD’’ scenarios developed in the integrated research phase.

Table 3-6: Overview of the control scheme for each research phase and scenario type.

Controller	Observer	Diagnostic	Actuators	Needed From	Scenarios
Plasma Position, Shape and Current	Boundary Reconstruction	Magnetics	Poloidal Field	Initial Research Phase I	All
Density	Average Density	Interferometer	Gas; Pellets	Initial Research Phase I	All
Disruption prediction	Stability boundaries (e.g. li q95), average density, total radiation, RT codes	Magnetics, Interferometry; bolometry, ECE	Poloidal field, ECRH, DMV, NBI	Initial research Phase I	All
ELMs	ELM frequency	Spectroscopy; Bolometry	Gas; Pellets; FPCs; EFCCs	Initial Research Phase II	All
Plasma Pressure	Beta; Stored Energy	Magnetics +?	ECRH; NBI; Gas	Initial Research Phase II	#5 #6
Sawteeth	Sawtooth Frequency	Soft X-ray; ECE	ECRH power and injection angle; NBI	Initial Research Phase II	#1 #2
NTMs	NTM location and amplitude	Magnetics + ECE	ECRH power and injection angle	Initial Research Phase II	#1, #2 #4, #5 #6
RWMs	RWM amplitude	Magnetics	RWMCs, EFCCs, NBI	Initial Research Phase II	#5 #6
Profiles	Equilibrium reconstruction; Current, Density, Pressure, Rotation Profiles	Magnetics+ MSE; ECE; Thompson Scattering; Charge Exchange	ECRH power and injection angle; NBI; Pellets; Gas	Initial Research Phase II	#4.2 #5 #6
Isotope	Isotope Mix	Spectroscopy	Gas; Pellets	Integrated Research Phase I	tbd
Burn Control Simulation	Fusion power – scaled	Neutron Rate	H and D gas injection; Heating power	Integrated Research Phase I	tbd
Divertor Heat Load	Divertor Temperature; Radiated Fraction; Detachment; ELM frequency	Infrared cameras; Bolometry; Langmuir Probes; Spectroscopy	Impurity injection; Gas Injection; Heating power	Integrated Research Phase II	All
Impurity Accumulation	Impurity Peaking; ELM frequency	Spectroscopy; Bolometry	ECRH power; Gas; Pellets; FPCs; EFCCs	Integrated Research phase II	All

4. MHD Stability and Control

Toward DEMO reactor with optimal reactor operations, high- β_N operations near or above the ideal β_N -limit without a conducting wall ($\beta_N^{\text{no-wall}}$) are set to be one of the main objectives on JT-60SA. These high- β_N operations depend on controllability of disruptive and influential MHD instabilities such as resistive wall modes (RWMs), neoclassical tearing modes (NTMs) and so on. Therefore, stability control techniques for these MHD modes should be established in order to achieve the JT-60SA mission. The MHD stability control in high- β_N plasmas is also important and rather indispensable for ITER and DEMO. Some solutions against these instabilities have been developed in the present devices. For NTM stabilization, effects of ECCD and the current and pressure profile control have been well-investigated and demonstrated. Feedback control by using coils is well-studied and is effective for RWM in current tokamaks. However, in-vessel coils covering large toroidal angles for low- n RWM are difficult to install and maintain inside vacuum vessel under higher neutron irradiation and radio-activation level in DEMO. For these reasons, another way without these coils should be established. A rotational stabilization has been demonstrated and it is to be one of the promising candidates. However, some aspects of those MHD instabilities are still unclear. Therefore, physics studies on these modes are also required to ensure the controllability of the MHD instabilities. For example, plasma rotation effect can be investigated with suppressing RWM by feedback control using coils. The plasma rotation flexibility is one of advantages in JT-60SA compared with ITER experiment. Thus, this can be realized by various combinations of NBI (see in Appendix A). In particular, for the relevance of ITER and DEMO, MHD studies with almost zero plasma rotation by the balanced NB injection is one of vital issues on JT-60SA.

Another important research aspect of JT-60SA is operation with high energy ions injected by the negative ion source-based neutral beams (NNBs) with the beam energy of 500 keV. The NNBs also make it possible to simulate burning plasmas in ITER and DEMO where MHD instabilities are predicted to interact with the high energy particles. Namely, energetic particles can affect the MHD stability and mode characteristics. On the other hand, MHD instabilities can change the fast ion confinement, transport and finally can cause energetic particle losses. Therefore, we should also pay attention to the interaction between MHD modes and high energy particles. Details of these issues are addressed in Chapter 6. Disruption control such as prediction, avoidance and mitigation is also a critical issue for ITER and fusion reactors.

The JT-60SA tokamak is designed to produce high performance plasmas suitable for MHD stability in high- β_N region with high values of the plasma elongation ($\kappa_x=1.8-1.9$) and the plasma triangularity ($\delta_x=0.4-0.5$), and small aspect ratio $A\sim 2.5-2.6$ (see Tables 1-1 and 3-1). Figure 4-1 shows shape parameter versus β_N in present

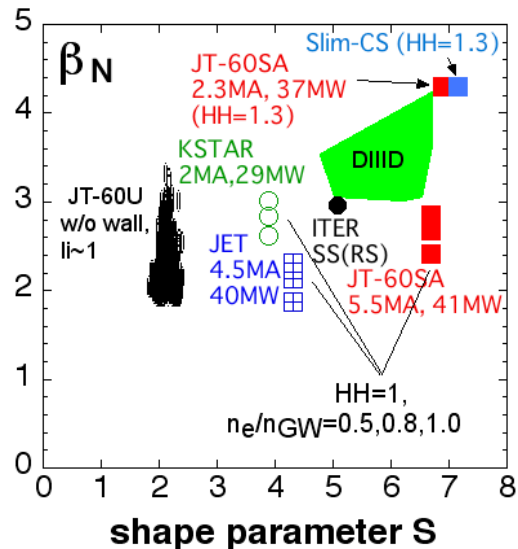


Fig. 4-1: Shape parameter versus achievable- β_N . The operation region of JT-60SA is possible to be DEMO relevant region due to improvement of MHD stability by strong shaping and feedback control.

tokamaks, ITER, DEMO (Slim-CS) and JT-60SA. Strong shaping makes it possible to access the high- β_N region predicted in DEMO. In addition to the strong shaping, JT-60SA has Stabilizing Plates (SP), Fast Plasma Position Control Coils (FPCC), Resistive Wall Mode Control Coils (RWMC: 3 poloidal x 6 toroidal), and Error Field Correction Coils (EFCC: 3 poloidal x 6 toroidal) inside the vacuum vessel as shown in Fig.4-2. The RWMC is also utilized for the study of disruption control, for example, application of helical fields with fast response time for runaway electron avoidance. The EFCC is also utilized for the resonant magnetic perturbation (RMP) technique for type-I ELM suppression (see in Chapter 7). A more detailed description of these systems can be found in Appendix C. On JT-60SA, advanced control utilizing these tools is developed and will be established. Based on knowledge that will be obtained on JT-60SA, steady-state scenarios for high- β_N with suppressing and controlling these MHD instabilities will be established. High- β_N steady-state operations with controlling MHD instabilities without any in-vessel coils are preferable and final target as one of JT-60SA missions.

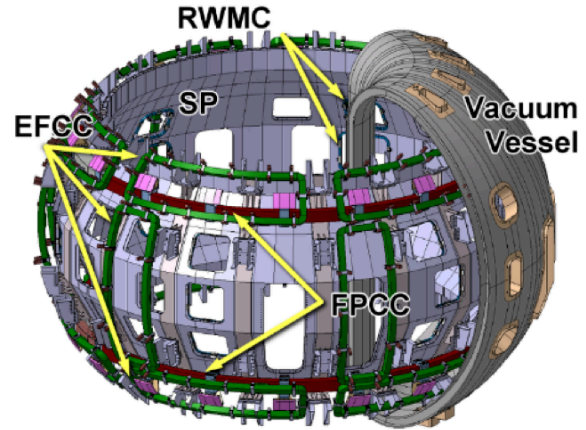


Fig. 4-2: In-vessel tools for MHD stabilization in JT-60SA. There are Stabilizing Plates (SPs) close to plasma, FPCC, EFCC and RWMC.

4.1. Resistive wall mode (RWM)

4.1.1. RWM Physics

(1) Rotational stabilization

Stability of resistive wall modes should be experimentally clarified for operations with high- β_N above $\beta_N^{\text{no-wall}}$. The RWM stability is theoretically well discussed; however, experimental validation is still inadequate. In JT-60SA, the RWM physics is positioned as one of the central and urgent issues to be solved. In particular, correlations between the plasma rotation and the RWM stability have to be focused on. The plasma rotation shear and profile effects will be investigated as well as the plasma rotation speed with the slowly rotating high- β_N plasmas produced by balanced-NB injection simulating DEMO relevant reactors. Also, the linear theory on the RWM predicts that the stability window by the wall position depends on the beta value, dissipative effects, toroidal mode number and equilibrium profiles. These parameter dependences of RWM will be surveyed in detail on JT-60SA.

(2) RWM in reversed shear plasmas

For steady-state high- β_N plasmas with optimum current drive associated with high bootstrap current fraction f_{BS} , reversed shear plasma with robust MHD stability properties is required. In particular, RWM in reversed shear plasmas should be controlled. Usually, the reversed shear plasma is self-organized, thus, plasma current, pressure and rotation profiles are mutually dependent suggesting that the flexibility of profile control is limited. Under this limitation, RWM controllability by profiles such as plasma rotation should be investigated for RWM stability control in reversed shear plasmas.

(3) Magnetic perturbation effects

Effect of RMP and non-RMP fields on RWM stability should be investigated because usually tokamaks have finite error fields from misalignment of toroidal and poloidal coils. On JT-60SA, these effects can be studied by superimposition of magnetic fields produced by EFCC. The system allows studying the effect of not only RMP but small magnetic field inhomogeneities on RWM destabilization. The flexibility of the feedback control system on JT-60SA allows the creation of static and rotating error fields with different amplitude and phase, the characterization of stable, and unstable and marginally stable modes for different plasma equilibria. The obtained results in JT-60SA will be compared with calculation results by numerical codes for extrapolation to ITER and DEMO.

(4) Other physics

In JT-60U, instabilities that could interact with RWM and finally destabilize RWM were observed in high- β_N plasma above $\beta_N^{\text{no-wall}}$. These mechanisms are still unclear, however, these observations suggest that kinetic effects of both bulk plasma and energetic ions are important to determine RWM stability. The kinetic effects are to be validated by changing a fraction of bulk and fast pressures. In particular, kinetic effect of energetic ions becomes important for RWM stability in burning plasmas with a number of alpha and energetic particles. JT-60SA will have unique possibilities in tailoring fast ions distribution and hence in studying its impact on RWM stability under different conditions. Moreover, the relevance of thermal ions on RWM damping will be assessed and compared to the energetic particles one.

4.1.2. RWM control

A promising candidate for RWM stabilization is an active feedback control by using coils. JT-60SA has eighteen saddle coils (toroidally 6 x poloidally 3) inside the vacuum vessel. The numerical estimation by VALEN shows that the feedback control can suppress the RWM up to β_N around the ideal β_N -limit with an ideal wall as shown in Fig.4-3.

Development of optimal RWM feedback control strategies in JT-60SA will start already during the Initial Research Phase having as target current driven RWMs. In fact, rotational stabilization has little effect on this branch of RWMs and for this reason they represent a severe test bed for feedback stabilization with active coils. Several steps of development can be envisaged: as a first step, when a magnetic flux leak detected with the pick-up coils exceeds a certain threshold, a control system applies current to the correction coils to suppress the flux leak. Second, we attempt to apply the mode suppression by applying the Fourier transform to the signals from the toroidal arrays; different mode identification strategies will be compared in this phase. Then, according to above results, optimum feedback logic for RWM control is identified. Finally, the RWM control will be applied for the slowly rotating high- β_N plasmas produced by balanced-NB injection in order to simulate ITER and fusion reactors where the external torque input is expected to be small.

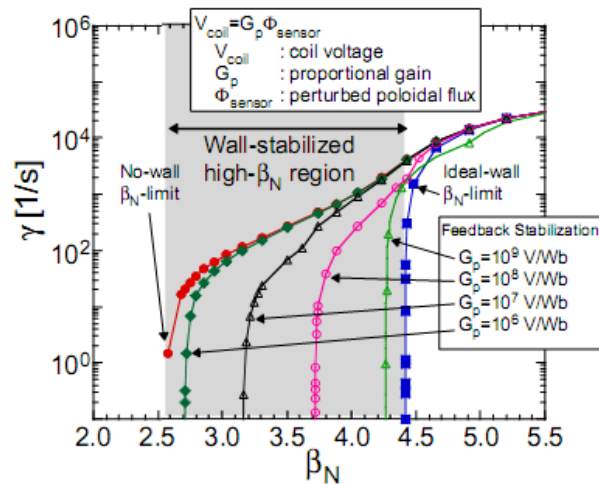


Fig.4-3: RWM growth rates versus achievable- β_N calculated by VALEN. The curves show no-wall, ideal wall β_N -limits and feedback with proportional gains 10^6 , 10^7 , 10^8 and 10^9 .

Controllability of the feedback system will be estimated with various parameters such as β_N and plasma rotation to assess realistic operation regimes with a safety margin for DEMO.

4.2. Neoclassical tearing mode (NTM)

4.2.1 NTM control

(1) Active stabilization by ECCD

Neoclassical tearing modes can appear in high-beta plasmas with positive magnetic shear. As well as in the present devices, control of NTMs is essentially important in JT-60SA in order to sustain high-beta plasmas. In particular, the $m/n = 2/1$ NTM should be suppressed because it causes mode locking and finally induces disruption. Although the $m/n = 3/2$ NTM also causes confinement degradation, the degree is moderate, and thus the $m/n = 3/2$ NTM may be utilized to control β_N and/or q_0 by changing pressure and/or q -profile at the $q=3/2$ surface. In order to actively control these NTMs, electron cyclotron current drive (ECCD) is the most promising candidate. In JT-60SA, dual-frequency gyrotron(s) with the frequency of 110 GHz and 138 GHz will be installed. Since the available ECH power will follow a staged development during JT-60SA operations, different control strategies should be implemented in time. In particular the injection power of ~ 3 MW from 4 gyrotrons, planned in the Initial Research Phase, could be used to develop NTM control tools, but might be insufficient for full NTM stabilization in all relevant scenarios (the most critical being probably plasmas close to scenario 2). Preliminary simulations by means of GREF code show however that, for advanced scenario, 3 MW seem to be sufficient to control the 2/1 mode and the results suggest testing this stabilization already in the Initial Research Phase II. This can be seen in Figs. 4-4 (a) and (b) showing a beam tracing simulation for a typical scenario 5 equilibrium and required EC power for the 2/1 mode stabilization.

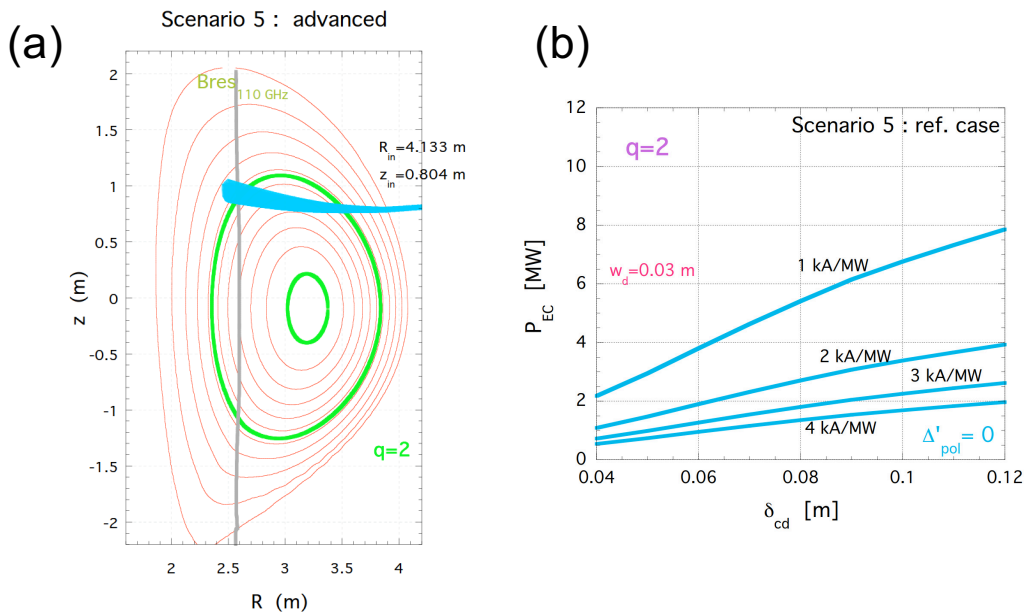


Fig.4-4 (a) equilibrium of advanced scenario 5: green contours correspond to $q=2$ surfaces and blue traces to beam tracing. (b) EC power needed to stabilize the 2/1 mode for 4 values of driven EC current and typical island threshold width, due to the perpendicular transport, $w_d=0.03$ m versus the full e^2 beam width δ_{cd} ; in this case I_{cd} down to a minimum of ~ 2 kA/MW and $\delta_{cd} \sim 0.08$ m can guarantee the 2/1 stabilization with less than 3 MW evaluated by GREF code

In order to enhance the stabilization effect, modulated ECCD will be effective. At present, modulation up to 10 kHz at 1 MW for 1 s has been achieved using the existing gyrotron. Further extension of the pulse duration will be performed during the construction phase of JT-60SA. Finally, pulse modulation will be independently available for every gyrotron. Details of ECRF system are addressed in Appendix A.2.

In order to drive localized EC driven current at the magnetic island center with high accuracy, real-time control of the injection angle of electron cyclotron (EC) wave with steerable mirrors will be adopted based on demonstration in JT-60U. Real-time equilibrium reconstruction using the motional Stark effect diagnostic and/or real-time measurement of the island structure using the electron cyclotron emission diagnostic will be the candidates for the input of the real-time control system. Simultaneous control of NTMs with different mode numbers, e.g. $m/n=2/1$ and $3/2$, will be possible in the Integrated Research Phase using 7 MW EC waves.

RMPs could assist in the suppression of NTMs by locking the NTM, either to a static RMP and then conducting continuous-work ECCD at the stationary O-point, or to a rotating RMP and then conducting modulated ECCD for power deposition at the rotating (in phase with the RMP) O-point.

(2) Avoidance by profile control

In addition to the active stabilization with ECCD, scenarios to avoid of NTM onset should be developed through optimization of the current and pressure profiles. The pressure gradient at the $q=1.5$ and 2 should be optimized to avoid the NTM onset. The effectiveness of this profile optimization was demonstrated in JT-60U, and high-beta weak-shear plasmas were sustained for several times longer than the current diffusion time. Moreover, control of rational surfaces position is also possible to avoid NTM onset. This can be performed based on full-CD scenario with $I_p=2.3$ MA and $q_{95}\sim 5.6$. On this scenario q_{\min} maintains above 1.5 and $q=2$ surface is fixed at edge region $\rho\sim 0.7$ where pressure gradient is weak. Control of both current and pressure profiles is tried adjusting NBCD. Although these schemes have the advantage of not using ECCD, their applicability is limited within the availability of neutral beams, i.e. limited within possible combinations of pressure and current profiles. Fully exploiting the unique capabilities of off-axis current drive by NNBI in JT-60SA, scenarios with $q_{\min}>2$ could be also attempted, where both $3/2$ and $2/1$ NTMs should be intrinsically stable. Development of operational scenario is an important issue for this scheme. This scheme is also beneficial to reduce the EC wave power required for NTM stabilization.

Moreover, ECCD could also be used for profile control in some suitable experimental conditions, where NBI for global profile control and ECCD for local profile control may lead to optimized control.

4.2.2. NTM physics

(1) Magnetic perturbation effects

A seed island of NTM is produced by error fields as well as MHD instabilities such as sawtooth and ELM. Since RMP is planned to be used in high-beta discharges, it is necessary to investigate the effect of RMP on NTM onset. From the viewpoint of MHD stability physics, theory suggests that NTM can be stabilized by externally applied magnetic fields. Experimental study to verify this theory may be possible using the RMP and non-RMP from RWMC and/or EFCC. By changing external field by EFCC, rotation braking by NTM and its effect on beta can be studied. Toward ITER and DEMO, these studies should be conducted with almost zero rotation where NTM will be easily locked.

(2) Rotation effect

It is recently reported that the plasma rotation affects the NTM onset: The beta value at the mode onset decreases with decreasing toroidal rotation velocity. Experimental study can be done by using the JT-60SA neutral beam system by which a variety of the toroidal rotation velocity and rotation profile can be produced. Also, RMP and non-RMP can be useful for plasma rotation control via magnetic acceleration and braking.

(3) Island transport

Transport in magnetic island is important for understanding of current drive mechanism for NTM suppression by ECCD. On JT-60SA, detailed measurements inside island will be done by several diagnostics with fast and high spatial resolutions (See in Appendix D).

3. Sawtooth oscillations

Whilst sawteeth are not expected in either advanced tokamak designs for DEMO, or indeed, even in less aggressive lower-beta higher-beam power designs, they certainly are an issue for ITER baseline scenario and could be an issue in a lower-risk pulsed inductively-driven DEMO design. JT-60SA has significant flexibility to study the control of sawtooth oscillations. It is worth noting that sawtooth control and, in particular real-time control, of naturally occurring sawteeth can be used efficiently in the Initial Research Phase to test the EC system and its alignment. Indeed, the tools needed for this purpose are essentially the same as the ones for NTM control and pre-emption.

The stabilizing effects of fusion-born α particles are likely to lead to long sawtooth periods in burning plasmas. However, sawteeth with long quiescent periods have been observed to result in the triggering of neo-classical tearing modes at low plasma pressure, which can, in turn, significantly degrade confinement. Consequently, recent experiments have identified various methods to deliberately control sawtooth oscillations in an attempt to avoid seeding NTMs whilst retaining the benefits of small, frequent sawteeth, such as the prevention of core impurity accumulation. The primary sawtooth control actuator planned for ITER is on-axis co-current electron cyclotron current drive. This deliberately destabilizes the internal kink mode thought to result in sawteeth by locally increasing the magnetic shear at $q=1$.

JT-60SA can test whether sawtooth control through co-ECCD with a resonance inside $q=1$ can result in NTM avoidance at high plasma pressure. This has been demonstrated in H-mode plasmas in present-day devices, but not extended to plasmas with a very large fast ion beta. With the flexible positive and negative NBI heating at high power levels, a demonstration of the effectiveness of ECCD in the presence of a significant population of core energetic ions should be attempted. This could determine whether deliberate destabilization with ECCD is likely to work in ITER, whether it should be supplemented by ICRH control, or whether stabilization techniques coupled with pre-emptive NTM control should be considered more appropriate. It should be noted that such a demonstration experiment will require a modest level of ECRH power and thus is probably precluded in the Initial Research Phase.

The other major development required for sawtooth control is in the field of real-time control. Developing robust control algorithms which can pace the sawtooth frequency (be it above or below the natural sawtooth frequency in the presence of energetic particles) is essential for reliable NTM avoidance in burning plasmas. The steerable mirror capability of JT-60SA, coupled with the large fast ion fraction and high plasma pressure, makes this an ideal test-bed for such control algorithms.

4.4. Disruption

Control of disruption should be established for safe operations in ITER and fusion reactors. In particular, disruption prediction and subsequent avoidance are urgent issues because any disruptions are unacceptable for DEMO. High beta operation toward DEMO is one of unique missions on JT-60SA compared with the present large tokamaks and ITER. Therefore disruption prediction and avoidance in high beta operation are important subjects in JT-60SA.

Disruptions are caused by vertical displacement event (VDE), MHD mode locking during I_p ramp, NTM, RWM, high density above the Greenwald density limit, machine troubles etc. Against the disruptions, JT-60SA has a passive stabilizing plate and FPPC inside the vacuum vessel as shown in Fig.4-2. In addition, massive gas injection (MGI), ECRF, RWMC and EFCC are also useful tools for disruption control. For a direct contribution to ITER, advanced disruption mitigation system such as shattered pellet injection is needed. Moreover, heat load at disruption will be monitored by IR camera for the health of the device. Utilizing these tools, advanced control of disruptions will be developed and established in terms of applicability to DEMO.

For a contribution to ITER, the plasma facing components on JT-60SA are planned to be changed from carbon to tungsten after the Integrated Research Phase I, thus, tungsten (W) coated full monoblock CFC divertor and full W first wall will be introduced. Basically, disruption study until the Integrated Research Phase I with carbon wall is not restricted because the JT-60SA components such as vacuum vessel, in-vessel components and so on are designed so as to withstand electromagnetic forces and heat loads of the disruption with $I_p = 5.5$ MA. However, disruption study and establishment of disruption control should be done before the replacement by the tungsten divertor and wall. In particular, disruption mitigation system will be strenuously developed and established to avoid unacceptable EM forces and heat loads to tungsten divertor and wall. The obtained findings are expected to contribute to ITER tungsten wall experiments. Also, the establishment of disruption control should be done before the radioactivation level in vacuum vessel becomes so high, thus, before the later phase of Integrated Research Phase and Extended Research Phase. Otherwise, maintenances of in-vessel components will be hard when these are damaged. These control methods will be validated in a wide variety of I_p , B_t and β_N as well as high performance plasmas. In these later phases, the established control methods will be applied as usual operations.

(1) Disruption database

Research activity of the disruption database is continued on JT-60SA. High I_p scenario with 5.5 MA on JT-60SA is expected to be useful in order to validate the extrapolability of the ITPA disruption database (IDDB) for ITER. Current quench (CQ) and thermal quench (TQ) times of JT-60SA can be validated compared with IDDB. New data of current quench time (dI_p/dt) obtained in JT-60SA could suggest the DEMO design concept. Since the maximum value of current quench time determines the device design, it is necessary to probe the current quench waveforms and the max value of current quench time in high I_p scenario with 5.5 MA in JT-60SA.

(2) Halo current

Halo current on JT-60SA is predicted to be totally 1.5 MA at a major disruption with full- I_p 5.5 MA and $\tau_{CQ}=10$ ms. The halo current can be measured by Rogowski coils installed under the CFC targets at some divertor cassettes, which are 36 divertor cassettes distributed at the bottom of the vacuum vessel (See in Appendix D). The Rogowski coils for halo current

measurement are to be distributed in the divertor cassette at interval of 60 degrees toroidally. They will be useful to estimate toroidal peaking factor (TPF). On two of the divertor cassettes, six Rogowski coils will be installed poloidally to measure halo current width. The total 1.5 MA halo current corresponds to about 10 kA in each Rogowski coils in divertor cassettes. Measured halo current and its electromagnetic force will be compared with simulation results.

(3) Runaway electrons (REs):

At a major disruption with $I_p = 5.5$ MA and $\tau_{CQ}=10$ ms, toroidal electric field inside a plasma is predicted to be higher than 100 V/m that exceeds the Dreicer electric field. Moreover, since JT-60SA operation will be done with $B_T > 2$ T, the REs could be generated. The REs can be unconditionally avoided by massive Ne and/or Ar injection with 5 kPam³ at least. Additionally, RE generation can be mitigated by application of RMP by using EFCC and RWMC. As for RE control, generated REs can be confined in divertor configuration with isolating first walls by FPPC and stabilizing plate, and then, confined REs (RE beam) will be mitigated with time by MGI.

(4) Prediction, avoidance and mitigation

As for disruption prediction, active MHD spectroscopy can be useful, since the marginally stable mode can respond to the magnetic field perturbation that has similar mode spectra. To diagnose the MHD stability limit, the magnetic field perturbation can be applied using EFCC or RWMC. When the magnetic response becomes larger, that is called resonant field amplification (RFA), heating power will be reduced or discharge sequence will be changed to soft-landing. Both prediction and termination schemes will also be developed and established on JT-60SA. For inescapable disruption, MGI will be kept on standby for quick injection. The mitigation system will be developed by using real time disruption detection. Toward an optional choice of metal wall such as tungsten, a heat load to divertor should be reduced at TQ. If the plasma thermal energy $W_{th} \sim 20$ MJ is fully rereleased to the divertor targets (~ 10 m²) during TQ, the heat load exceeds 1 MJ/m² that is unacceptable for the metal wall. Therefore, a mitigation of the heat load to divertor is necessary for the metal wall. To reduce the thermal energy of plasma in advance of TQ to half or less quickly, a large amount of impurity gas such as Ne needs to be injected; it is estimated to be 1×10^{23} atoms corresponding to ~ 1 kPam³. A disruption mitigation system with quick response and action must be developed for the metal wall experiments.

4.5. Error field related issues

Error fields, thus non-axisymmetric magnetic fields, can crucially affect MHD stability through resonance with dynamics of or structure in the plasma. In particular, these error fields can cause locked mode in low density plasma in a startup-phase and generate seed islands for NTM even with relatively small field of a few gauss. On JT-60SA, magnetic error fields from manufacturing errors, misalignments of superconducting coils and magnetic field cancellation coils in NB systems are evaluated to be several gauss in total at worst. Thus, EFCC is planned to be installed inside vacuum vessel to reduce these error fields. By using EFCC, locked mode onset with respect to residual error fields can be systematically studied. Moreover, various combinations of NBs enable us to clarify the shielding effect of plasma rotation against external fields. Error field correction in high- β_N is important to feedback control of RWM because plasma can respond to amplify the residual error fields. This amplification, that is so-called ‘Resonant Field Amplification (RFA),’ is a response of marginally stable RWM near/above $\beta_N^{no-wall}$. In contrast, RFA to applied fields by EFCC is useful to experimentally probe $\beta_N^{no-wall}$.

as active MHD spectroscopy.

4.6. Scenario development with advanced MHD controls

After developing MHD control methods against various MHD instabilities such as RWM and NTM independently on JT-60SA, those methods should be properly integrated to demonstrate a simultaneous control of the MHD modes. The control methods for not only RWMs, NTMs, and sawteeth but also ELMs are technically validated for long-pulse discharges up to 300 s much longer than current diffusion time. In other words, long duration scenarios are developed for this integration and demonstration.

On JT-60SA, RWM feedback control by RWMC is necessary to achieve the high- β_N plasma above $\beta_N^{\text{no-wall}}$. This is planned in reversed shear discharge plasmas with full non-inductive current drive for steady state. Usually, in reversed shear plasmas, infernal mode, resistive interchange mode, double tearing mode instabilities are also concerned as well as RWM and NTM. These modes will also be focused on if these are observed and found to limit plasma performance.

4.7. Hardware of feedback control system for MHD

Real time detection of the MHD activities is required for the MHD control. While the understanding of the MHD activities is improving, algorithm and needed data for detection will be also tuned. Therefore, a flexible and intelligent detection system is required having ability to respond to the distributed data acquisition system. Then a combined system, detection of the MHD activities and making demands to the control systems such as ECCD and/or gas puffing should be developed. Development using present fusion devices might be effective to achieve required accuracy in JT-60SA experiments.

4.6. Summary

In summary, the strategy of the MHD stability studies in each research phase of JT-60SA is given in Table 4-1.

Table 4-1: MHD Stability Research Items

Phase	Gas/ Heating	RWM	NTM	Sawtooth	Disruption
Initial Research I	H PNB 6MW NNB 10MW ECRF 3MW <hr/> Total 19MW	<ul style="list-style-type: none"> • Test / Application of FB on CD-RWM • RMP effect on CD-RWM 	<ul style="list-style-type: none"> • Development of real-time ECCD by using ECE and MSE • Real-time ECCD application to externally driven islands by RMP and non-RMP 	<ul style="list-style-type: none"> • ECCD effect • Development of real-time ECCD • Impurity exhaust 	<ul style="list-style-type: none"> • VDE study • Prediction; Active MHD diagnostic
Initial Research II	D PNB 20MW NNB 10MW ECRF 3MW <hr/> Total 33MW	<ul style="list-style-type: none"> • High-β_N RWM • RWM on reversed shear • Rotational shear/profile effects • Test / Application of FB on high-β_N RWM • Energetic particle effect 	<ul style="list-style-type: none"> • Minimum power for full stabilization • Mod-ECCD • Real-time ECCD • Real-time profile control • RMP effect on NTM onset/growth/saturation/stabilization • Rotation effect on NTM onset 	<ul style="list-style-type: none"> • ECCD effect on high-β_N • Seed island effect on NTM onset/growth • Energetic particle effect 	<ul style="list-style-type: none"> • Mitigation; massive gas injection, RMP, etc
Integrated Research I	D PNB 20MW NNB 10MW ECRF 7MW	<ul style="list-style-type: none"> • High-β_N operation with RWM rotation/ FB controls • RMP effect on high-β_N RWM 	<ul style="list-style-type: none"> • Real-time ECCD to high-β_N NTM • Simultaneous ECCD to m/n=2/1 and 3/2 NTMs 	<ul style="list-style-type: none"> • Simultaneous control of NTM and sawtooth 	<ul style="list-style-type: none"> • Real-time control
Integrated Research II	Total 37MW	<ul style="list-style-type: none"> • Real-time control 	<ul style="list-style-type: none"> • Real-time control 	<ul style="list-style-type: none"> • Real-time control 	<ul style="list-style-type: none"> • Real-time control
Extended Research	D PNB 24MW NNB 10MW ECRF 7MW <hr/> Total 41MW	<ul style="list-style-type: none"> • Real-time control 	<ul style="list-style-type: none"> • Real-time control 	<ul style="list-style-type: none"> • Real-time control 	<ul style="list-style-type: none"> • Real-time control

5. Transport and Confinement

5.1. Introduction

Transport and confinement studies in JT-60SA will take advantage of its ability to operate highly shaped, long lasting discharges while heating both ions and electrons through a flexible NBI (PNB, NNB) and ECRF systems. The JT-60SA transport and confinement studies will be focused on answering those critical questions and tackle those open issues attaining to experimental regimes of ITER and DEMO that can be directly simulated in a Super Advanced Tokamak:

- mutual interaction amongst plasma pressure, rotation and current profiles in highly self-regulating plasmas will be investigated taking advantage of the high beta and the high bootstrap current fraction. This will be done with plasmas lasting for time comparable to the resistive time (Fig. 5-1);
- the intrinsic rotation at high beta or high pressure region taking advantage of various NB injection geometries and ECRF,
- high confinement regimes at high-density, above the Greenwald density, will be possible through the control of the plasma profiles, plasma shape and particle fueling (Figs. 5-2 and 5-3),
- scaling of energy confinement time with high triangularity and shaping (hybrid scenarios, high beta scenarios),
- confinement time and transport of heat, momentum and particles in dominant electron heating plasmas (roles of heating ratio, T_e/T_i , collisionality and ExB shearing on density peaking and turbulence, role of electron-scale instabilities and multi-scale interactions, role of isotope mass),
- confinement time in the presence of a large population of fast ions (stabilization of turbulence through alpha optimization via NBI control, non-linear electromagnetic stabilization),
- fuelling and impurity control of long pulse discharges in ITER, DEMO-relevant conditions (pellet injection, core and edge particle pinch, density evolution with hollow density profiles, neutral penetration at high edge opacity, electron heating, rotation, particle transport in fully non-inductive discharges).

Furthermore, by virtue of its auxiliary heating systems JT-60SA allows to carry out transport experiments covering a wide region of the dimensionless plasma parameters space and will access, although not simultaneously, the ITER- and DEMO-relevant values of the normalized collisionality (ν^*), Larmor radius (ρ^*) and plasma pressure (β) with ITER- and DEMO-like plasma shapes (Figs. 5-1 and 5-4) (Ref. DEMO in [1]).

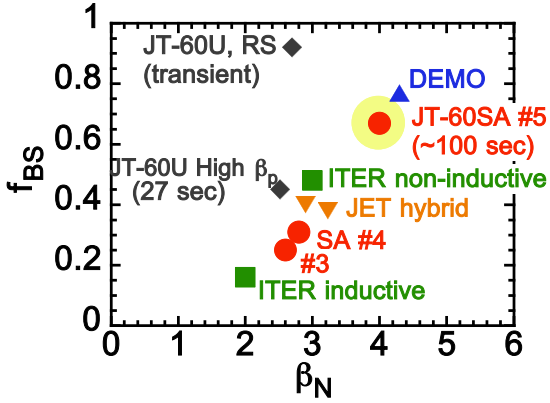


Fig. 5-1 The bootstrap current fraction (f_{BS}) against the normalized beta (β_N). Linkage between plasma pressure, rotation and current profiles in highly self-organized plasmas is clarified taking advantage of high β_N and high f_{BS} . (DEMO [1], JT-60U [2, 3], JET [5]).

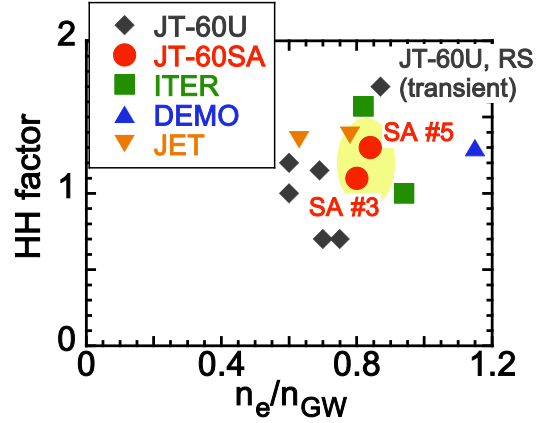


Fig. 5-2 Target regime in HH factor and the Greenwald Density fraction (n_e/n_{GW}). (DEMO [1], JT-60U [4], JET [5]).

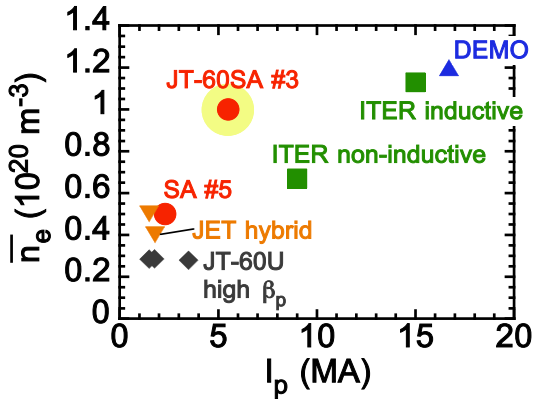


Fig. 5-3 Parameter regimes for the line averaged density (\bar{n}_e) and the plasma current (I_p). (DEMO [1], JT-60U [4], JET [5]).

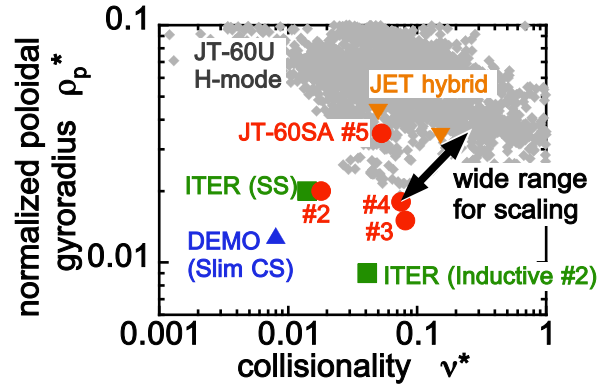


Fig. 5-4 Non-dimensional plasma parameter regimes. Transport experiment can be performed at ITER-relevant normalized collisionality (ν^*), poloidal larmor radius (ρ_p^*). JT-60U (Cloud) and JET hybrid plasmas (inverted triangles) are also shown.

The definitions of the normalized ion poloidal larmor radius (ρ_p^*) and the normalized effective electron collision frequency (ν^*) are, respectively, $\rho_p^* = 0.46 \times 10^{-2} (A_i)^{1/2} \langle T_i \rangle^{1/2} / B_p / a$ at $A_i=2$ and $\nu^* = 0.8 \times 10^{-2} q R A^{3/2} Z_{eff} \langle T_e \rangle^{-2} \langle n_e \rangle$. Here $\langle T_i \rangle$ and $\langle T_e \rangle$ are the volume averaged ion and electron temperature in keV and $\langle n_e \rangle$ is the volume averaged electron density in 10^{20} m^{-3} . B_p (T), a (m), q , R (m), A and A_i (AMU) are the poloidal magnetic field, minor radius, safety factor, major radius at the middle of plasma, aspect ratio and ion mass number. $Z_{eff}=2$ for JT-60SA, $Z_{eff}=1.7$ for ITER and $Z_{eff}=1.8$ for DEMO (Slim-CS) are used. The ion mass number is assumed as $A_i=2.5$ in ITER and DEMO. The safety factor of $q=2$ for JT-60SA, ITER, DEMO and JET is used.

5.2. Transport studies on JT-60SA relevant for both DEMO and ITER

5.2.1 Confinement studies in the DEMO and ITER relevant regimes

Various tokamaks have found a strong dependence of confinement on triangularity and shaping, particularly in hybrid scenarios, due to the high beta achieved which enhances the pedestal top pressure, where large values of the H factor have been achieved. The IPB98y2 scaling law used for ITER scenario modelling does not account for the dependence on shaping. JT-60SA has the necessary flexibility to undertake a detailed study on the role of shaping on confinement of both the plasma core and the pedestal. This might uncover important dependencies that can impact on both ITER scenarios and the design of DEMO (see Chapter 3 of this research plan).

In parallel with the detailed studies of the impact of shaping on confinement, JT-60SA offers the opportunity to investigate transport in dominant electron heating conditions. Electron heating by alpha particles will be dominant in ITER and DEMO burning plasmas. Also a strong external electron heating is expected in the ITER Pre-Fusion Power Operation-I (20 MW ECH, 10 MW ICRH). The core electron temperature and ion temperature can decouple at low plasma current and density. The properties of plasma transport in the dominant electron heating condition, however have not been investigated in details because of the lack of electron heating power in high power regime scenarios of present tokamaks. In JT-60SA, transport properties under dominant electron heating conditions can indeed be investigated. The ratio of the electron heating power to the total input power can be varied from ~20% to ~70% with low external fuelling and torque input by NNBI and ECRF as shown in Fig. 5-5(a). Transport dependence on T_e/T_i ratio will be investigated by varying the ratio of electron heating power. Figure 5-5(b) shows T_e/T_i averaged in $r/a=0-0.5$ as a function of the ratio of electron heating at high density (scenario 2) and low density (half the density of scenario 2). The electron heating ratios 60-70% and 80% are the available values at the initial research phase and the integrated research phase, respectively. The ratio T_e/T_i will vary from 1.0 to 1.2 in the scenario 2 plasma. At the half density operation, T_e/T_i can be scanned from 0.7 to 1.4. The point is the dominant electron heating conditions can be realized at low collisionality and small Larmor radius. In addition to the role of T_e/T_i , the role of heating ratio/method on transport can be separately evaluated from the role of T_e/T_i by using NNBI and ECRF and varying EC deposition profile. Recently, an important role of electron-scale modes (ETG) and

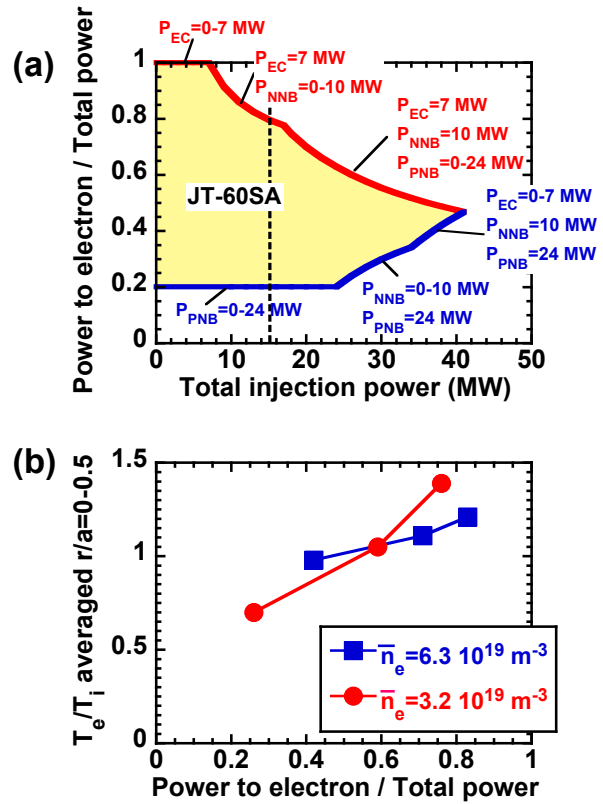


Fig. 5-5 (a) Ratio of electron heating power to total input power versus total injection power. (b) T_e/T_i averaged in $r/a=0-0.5$ as a function of the ratio of electron heating calculated by the transport code TOPICS and CDBM model without $E \times B$ rotation effect. Injection power of 18 MW and profiles of n_e , q and temperature pedestal are fixed.

of multi-scale interactions was pointed out in some experimental conditions in JET and Alcator C-Mod, and in multi-scale gyro-kinetic simulations. JT-60SA with its range of variation of T_e/T_i and its high electron heating will allow to further explore this physics and will provide new data for validation of models accounting for ETGs and multi-scale interactions.

Along with the ratio T_e/T_i the flexible heating systems allow also exploring a large region of dimensionless parameters space (Fig. 5.6-5.8). Characteristics of plasma transport and confinement vary with varying dimensionless plasma parameters, such as the normalized collisionality (ν^*), poloidal gyro radius (ρ_p^*) and pressure (β_N). New data will be provided by JT-60SA for transport scalings over a wide range of plasma parameters including ITER and DEMO-relevant values. The new data will increase the confidence in the prediction of plasma performances in ITER and DEMO. As already noted in the introduction JT-60SA allows us to carry out plasma transport experiments at DEMO- and ITER-relevant values of ν^* , ρ_p^* and plasma pressure β_N with DEMO- and ITER-like plasma shapes (Figs. 5-4, 5-6-5-8). Figure 5-6 shows accessible values of ν^* and β_N at constant ρ_p^* and q . Within one line at $B_T=2.25$ T and $I_p=5.5$ MA, the density is scanned between $0.5n_{GW}$ to $1n_{GW}$ and the heating power is properly varied to keep constant ρ_p^* . Figures 5-7 and 5-8 illustrate the accessible values of ρ_p^* and β_N at constant ν^* and the accessible values of ρ_p^* and ν^* at constant β_N , respectively. Here the density and heating power are varying within one line (B_T constant).

The non dimensional plasma parameters mentioned above have a direct impact on small scale fluctuations and hence on turbulent transport. The transport of fuel particles, impurity, heat, and momentum in advanced tokamaks are found to be dominated by turbulence-driven anomalous transport. The transport of impurities is provided by a combination of neoclassical and turbulent processes and an important element of the research will be to assess how relatively strong are the neoclassical and turbulent impurity transport components for light and heavy impurities depending on the different operation regimes. Decay time of zonal flow relates to ion-ion collision frequency and the radial scale of zonal flow relates to ion Larmor radius. Thus, it is absolutely essential to understand and clarify the driving and stabilizing mechanisms of turbulence also in the absence of transient collisional effects and in ITER- and DEMO-relevant regimes (low ν^* , ρ_p^* and β_N). The knowledge of turbulence driven transport is required to design steady state operation scenarios in both ITER and DEMO. Table 5-2 shows

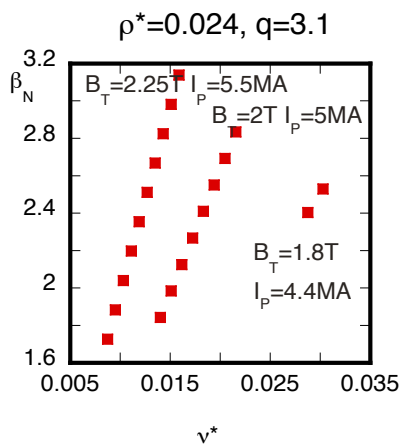


Fig.5-6 Accessible values of ν^* and β_N at fixed ρ_p^* . Auxiliary power is varied between ~ 10 and 41 MW.

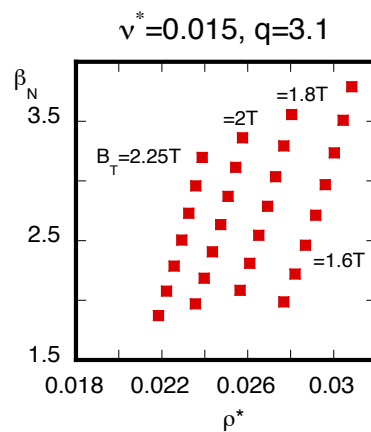


Fig.5-7 Accessible values of ρ_p^* and β_N at fixed ν^* . Auxiliary power is varied between ~ 10 and 41 MW. $\langle n_e \rangle \sim 0.5-1.3 \times 10^{20} \text{ m}^{-3}$.

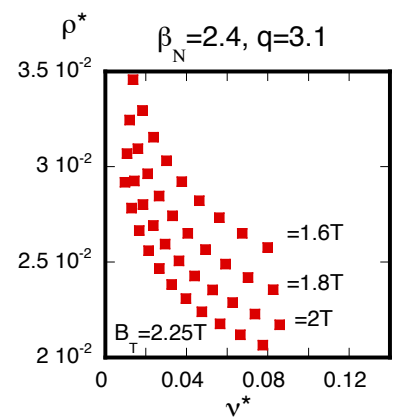


Fig.5-8 Accessible values of ρ_p^* and ν^* at fixed β_N . Auxiliary power is varied between ~ 10 and 41 MW. $\langle n_e \rangle \sim 0.5-1.3 \times 10^{20} \text{ m}^{-3}$.

a list of the expected core turbulence modes. It is noted that each turbulence mechanism plays a role on different aspects of the transport process. Detailed turbulence measurements by using the diagnostic listed in Table 5-3 will be investigated with focus on both the core and the pedestal and a comparison with theoretical predictions will be carried out. In a long pulse and high beta discharge, turbulence noise can stochastically excite a critical instability even in the absence of global trigger. Such stochastic excitation will determine lifetime of plasma. Experiment in JT-60SA will provide a new insight of transport physics, which does not appear in the short pulse experiments. Probabilistic approach will be introduced through the plasma parameter (e.g. β_N) dependence for understanding of sustainment of high beta plasmas.

In future burning plasma experiments, the external momentum input from the auxiliary heating is expected to be small and the toroidal rotation velocity driven by the external momentum input may not dominate that generated by the plasma itself. It is essential to understand the physical mechanisms determining the toroidal rotation profile including the intrinsic rotation. Study on the intrinsic rotation, heat and particle transport will be made at high pressure and in a small or no torque input using a combination of NBs and ECRF.

Using the flexible NBI system of JT-60SA it will be possible to modify locally the plasma pressure gradient (α) and optimize the heating to operate in regime of α close to α -critical where ITG turbulence is strongly stabilized and kinetic ballooning modes are not unstable.

Last, a still outstanding question is the change in transport when changing the main ion species, which is seen in present devices to scale opposite to basic theory-based gyro-Bohm scaling. Several effects are being pointed out in ongoing experiments in JET and ASDEX Upgrade. It is expected that JT-60SA by comparing operation in D, H and He plasmas, will be able to contribute to improved understanding both of core and edge transport changes with isotope mass.

5.2.2 Fuelling and impurity control

Another important issue for both ITER and DEMO is that of fuelling and impurity control. A strong radiation at the plasma edge and divertor with seeded impurities, such as Ne, Ar, Kr, would be a desirable means of distributing plasma power loss for heat load mitigation. On the other hand, in long lasting discharges as well as in burning plasmas it is crucial to avoid impurity accumulation which would lead to plasma dilution and increase of radiation losses in the core region. Moreover high fuel purity, which would lead to an increase in fusion gain, is necessary for high performance in both ITER and DEMO. Transport of light (Ne, Ar, Kr,) and heavier impurities along with transport of fuel particles will be investigated in H-mode and full non inductive plasmas using impurity diagnostics such as Z_{eff} monitor, VUV spectrometers, bolometer, SXR and so on (see Appendix D). Perturbation methods such as impurity seeding, laser blow-off, TESPEL, modulated gas puff injection from fast valves, divertor strike-points sweeping, SMBI are required as well as these diagnostics. Dependence of the particle flux on q profile, toroidal rotation, plasma gradients, collisionality, fast ions pressure and plasma composition will be assessed.

Metal impurity accumulation is found to be the main cause of early termination of recent JET-ILW (the beryllium first wall and tungsten divertor) high- β hybrid scenario plasmas showing the importance of developing good control techniques. In JT-60SA, Tungsten wall is planned in the Integrated Research Phase II. Understanding and suppression schemes of impurity accumulation will be developed using higher power of ECRF and NNBI (10 MW N-NB, 7 MW ECH) and/or controlling density profile in the core region. An appropriate method of impurity injection, which can control the total impurity amount and a local source profile of injected impurities, should be used to estimate impurity transport accurately.

Regarding the density control, pellet fuelling experiments in ITER relevant conditions will be carried out to demonstrate effective density control capability. The issue of the time scale of density profile relaxation in presence of hollow density profiles due to pellet injection will be investigated with dynamical experiments that will be able to discriminate amongst existing different models. Also, the possible presence of an inward particle pinch in the pedestal, which would greatly help the gas puff fuelling in plasmas with opaque edge and small neutral penetration, could be investigated in JT-60SA using the experimental techniques presently under development on various devices.

5.2.3 Plasma controllability study for burning plasma control

The control of plasma parameters is also crucial for the operability of ITER and DEMO. A significant plasma self-heating by alpha particles raises the issue of controllability with auxiliary heating in ITER and DEMO. Controllability of burning plasma will be investigated using burning plasma simulation experiments and modeling/simulation. For example, simulating alpha heating, as central electron heating, will be done with the combination of ECRH and N-NB. Since profile measurements become difficult in DEMO, a control scheme without profile data should be established. A control scheme with a model-based control will be explored in order to contribute to the development of control schemes in ITER and DEMO.

5.3. Specific Contributions of JT-60SA to ITER

A critical issue for ITER is the achievement of the H-mode operation with the available auxiliary heating power. Predictions of the H-mode threshold power in H, He and their mixed plasmas are therefore a key issue for ITER H and He operations. JT-60SA will investigate the parameter dependences of H-mode threshold power in H and He plasmas well in advance of ITER operations. Transport physics and scaling of the pedestal will be studied in support for the prediction of the H-mode threshold power for ITER and to allow designing operation scenarios in ITER which achieve the H-mode phase efficiently. Physics of the H-mode threshold power and confinement scaling will be explored in the high current and low collisionality plasma with carbon wall. Using the metal wall in the Integrated Research Phase II, the ITER prediction will be improved. JT-60SA has large heating power sufficiently above the L-H transition threshold already from the beginning of the Initial Research Phase II as shown in Fig. 5-9. The heating power at the Initial Research Phase II (33 MW) is up to 200% of the L-H transition threshold power even at high $I_p \sim 5.5$ MA and 100% Greenwald density. H-mode studies at high values of the thermal energy confinement time around $\tau_E \sim 1$ s (Fig. 5-9), and high plasma current and density (Fig. 5-3) will contribute to the ELMy H-mode thermal confinement scalings of ITER.

Another important issue for ITER is the effect of ripple on plasma confinement. Magnetic perturbations from the RMP coils and the insertion of test blanket modules (TBMs) will increase the field ripple in ITER. The increase of the field ripple in turn might have some influences on the alpha particle loss, plasma profiles, especially rotation profile. In JT-60SA, the impact of RMPs and TBMs on plasma profiles (density, temperature and rotation), will be clarified before RMPs and TBM experiments in ITER.

5.4. Specific contributions of JT-60SA to DEMO

In the strong self-regulating DEMO plasmas (high beta and high bootstrap), plasma pressure, rotation and current profiles are strongly linked to each other. JT-60SA should answer the questions how the strong self-regulating plasmas are sustained and controlled with small auxiliary heating and torque and what is the best operation regime in DEMO.

In JT-60SA, the mutual linkage among the plasma pressure, rotation and current profiles in highly self-regulating plasmas lasting several resistive times will be clarified taking advantage of the high beta and the high bootstrap current fraction (Fig. 5-1). Temporal and radial response and controllability of strong self-organized plasmas will be investigated with small momentum input (by combination of NBs), ECRF and pellet injection. Correlations between the rotation and current profiles, and the current and pressure profiles are observed by changing the timing, location and power of heating. After evaluating the controllability, the suitable operation regimes in DEMO will be proposed.

DEMO is currently designed to operate close to the Grenwald density, plasma density normalized to the Greenwald density (n_e/n_{GW}) is estimated to be 0.98 in DEMO. Higher density regimes will have an impact on the fusion energy gain (Q). JT-60SA will explore high-density operations above the Greenwald density ($\sim 1.1-1.3 \times n_{GW}$) for different designs of DEMO (Fig. 5-2).

Also construction of the database of density dependence on plasma confinement is important to predict the confinement performance of DEMO plasma. On what concerns the heat load of the divertor, sufficiently small heat-load onto the divertor plates is required in DEMO. On the other hand, divertor plates can reduce the breeding zone of the blanket and the tritium breeding ratio (TBR). In JT-60SA, double-null configuration can be realized with full mono-block lower and upper divertors. The advantage and issue of double-null configuration will be clarified in order to contribute to DEMO design.

5.5. Measurements, Analysis, Modeling and Real-time control

The following measurements, analysis, modeling and real-time control are needed to conduct transport and confinement studies.

5.5.1 Profile measurements

Measurements with good spatial and temporal resolutions are essential for understanding transport physics and evaluation of plasma performance accurately. The diagnostics for the

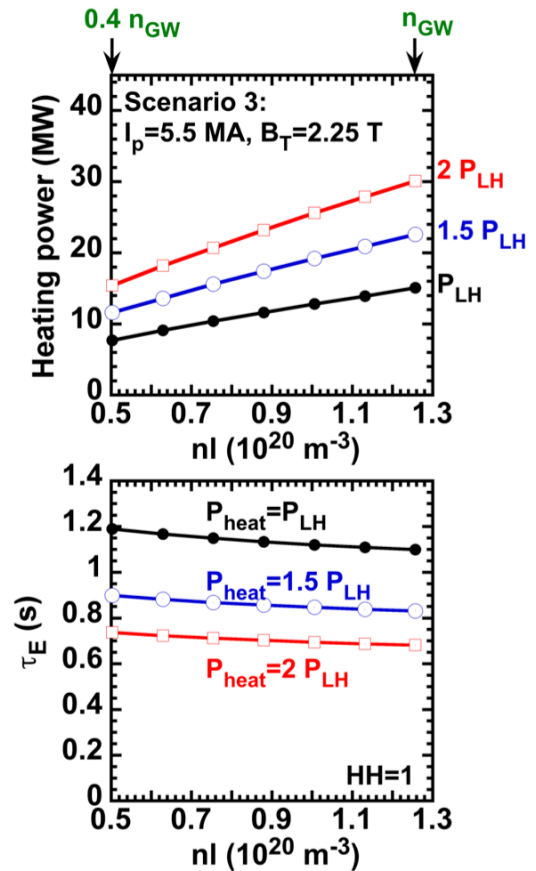


Fig. 5-9 Upper: L-H threshold power (P_{LH}) as a function of line averaged electron density (nl) for the Scenario 3. Lower: Thermal energy confinement time (τ_E) at P_{LH} , $1.5 P_{LH}$ and $2 P_{LH}$.

transport study are listed in Appendix D. Profiles of electron density, ion temperature, electron temperature and toroidal rotation will be measured by Thomson scattering systems (TS), electron cyclotron emission diagnostics (ECE) and charge exchange recombination spectroscopy (CXRS) systems. High spatial resolution, which is about one order of magnitude smaller than their scale length ($<1/10L_{ne}$, L_{Ti} , L_{Te} , L_{Vt}), is required to identify small structures including ITB regions. High temporal resolution of the density and temperature profiles (on a time scale about one or two orders of magnitude smaller than the transport time scale) is needed to resolve the plasma response and perform transient transport analysis. The poloidal rotation profile by CXRS systems with the same spatial and temporal resolution will be used for the evaluation of the radial electric field. In particular, there are needs to have good measurements of instantaneous radial electric field, with sufficiently large radial coverage, in order to measure at both edge and internal transport barrier locations. Impurity density profile with the spatial resolution of $1/10L_{n\ imp}$ and impurity species will be measured by Z_{eff} monitor, VUV spectrometers and visible spectrometers in both the core and the edge region for the studies of impurity transport. In order to measure the neutral density inside the plasma and their contribution to the particle source it is necessary to measure with time resolution of the order of 1 ms or better the D_{α} emission from the plasma edge and the neutral pressure in the vessel.

5.5.2 Fluctuation measurements

In JT-60SA, transport will be dominantly driven by turbulence. It is therefore essential to understand transport characteristics from both experimental and theoretical side. While simulations can predict transport mechanisms without turbulence measurements, the comparison between measured turbulence characteristics and simulations will help to progress in the understanding of transport physics. Also, fluctuation measurements will provide important information about the limitation of the simulation, e.g. whether or not the existing wave numbers (k) match with simulation or if the fluctuation level is small enough for the ordering in the simulation. In the development of the scenarios envisaged in JT-60SA, critical aspects involving turbulence and transport at both the edge and the core have to be investigated. To this end, a set of fluctuation diagnostics has to be operational covering a large spectral range for both edge and internal transport barrier locations as listed in Table 5-2. This is of interest considering the goal of developing advanced scenarios, potentially with transport barriers with strong rotational shear and flat or reversed magnetic shear.

Required turbulence diagnostics are listed in Table 5-3. For physical applications dedicated to the scenarios, the set of measurements over extended radial intervals, covering both edge and core, as well as extended spectral ranges is important. These would be technically feasible in JT-60SA and could measure the expected turbulence, although further detailed design studies are necessary. Each diagnostic covers particular k ranges and spatial locations. This coverage corresponds to the targeted turbulence mechanism. Detailed turbulence studies can be done through some density fluctuation measurements covering both ion scales (ion temperature gradient and trapped electron modes, as well as micro-tearing modes) and electron scales (electron temperature gradient modes). Possibilities of diagnosing both small poloidal wave numbers k_{θ} and large radial wave numbers k_r (micro-tearing), as well as large k_{θ} , with smaller k_r (electron temperature gradient modes) has to be considered of interest along with internal magnetic field fluctuation measurements in the context of high beta plasmas. In addition, Correlation ECE is a possible temperature fluctuation measurement and the results will be extremely useful for physical studies. The local poloidal velocity fluctuation will provide coherent E_r or potential fluctuation assuming that measured turbulence phase velocity is dominated by $E_r \times B_T$ poloidal rotation. This allows studies on the physics of zonal flows and geodesic acoustic modes, and on their role on the development of transport barriers using

microwave reflectometry and beam emission spectroscopy.

Measurements of quantities such as spatial distributions, wave number and frequency spectrum and absolute value of fluctuation level will be compared with theoretical calculations of gyrokinetic or gyrofluid simulations (see 7. Modeling). Appropriate synthetic diagnostics will be implemented enabling direct comparisons between the theoretical predictions and the measured signals. Firstly, the measured turbulence characteristics are compared with a linear stability analysis, in order to identify the type of the turbulence. Then the fluctuation level and fluctuation spectrum are compared with a non-linear simulation. Simulation results converted in the real space can be measured by using diagnostics listed in Table 5-3. For this comparison, the instrumental function of each diagnostic should be taken into account. These measurements will also be used for causality study by comparing the time scale or onset of the changes in turbulence and transport properties.

5.6. Analysis

Regarding methods of transport analysis, the steady state power balance equation will be solved using the transport codes: TOPICS, CRONOS, ETS and JINTRAC in order to calculate electron and ion heat diffusivities and global energy confinement time. It is essential to know the edge particle source provided by ionisation of neutrals to perform particle transport analysis in steady-state. The first piece of information will be provided by one-dimensional arrays of D_α light detectors (linear cameras, possibly distributed poloidally around the plasma separatrix), whereas the second piece of information will be provided by fast ion gauges. An inversion algorithm will be developed to translate line integrated D_α emission profiles into local emissivity profiles. A further level of analysis will be implemented and will deploy either one-dimensional (e. g. FRANTIC, KN1D) or two-dimensional (e. g. EDGE2D, SOLPS) codes to fit the neutral density to the spectroscopic and pressure measurements. Regarding the evaluation of momentum source, the intrinsic torque could be essential to solve the steady-state momentum balance equation. The intrinsic source (intrinsic rotation) will be studied with the force balance and transient transport analyses.

The transient transport analysis for particle, heat and momentum are also planned in order to evaluate diffusive and non-diffusive terms of transport matrix separately. Particle diffusivity and the convection velocity will be calculated through the transient transport analysis using a gas-puff modulation technique and/or pellet injections. Relative shape of source profiles, which can be obtained from three dimensional neutral particle simulation is required. Non-linearity of the ion and electron heat transport will be observed from cold/heat pulse propagations using pellet or EC injections. Momentum source modulations will be applied using $j \times B$ torque with perpendicular-NBs or the resonant magnetic perturbation (RMP). Especially, these transient transport analyses are essential for impurity, particle and momentum transport since the off-diagonal terms are not negligible. Then, these experimental results will be compared to theoretical models so as to understand the physical process of plasma transport.

5.7. Modeling

Transport and turbulence properties will be compared with numerical simulations from gyrokinetic and fluid codes and with theoretical models over the wide range of normalized plasma parameters including ITER- and DEMO-relevant regimes. The modeling activity is a necessary complement to the experimental investigations, in order to gain a theoretically

founded understanding of the fluctuation measurements, and place them in the broader context of the understanding of turbulence and transport properties of JT-60SA plasmas.

Qualitative identification of turbulence can be done from comparison between turbulence measurements and gyrokinetic linear calculations. Growth rates and propagation directions of the turbulence mode listed in Table 5-2 are obtained by a flux tube gyrokinetic code. After the qualitative identification of the turbulence, turbulence characteristics such as spectrum, spatial profile and fluctuation level are compared with non-linear results quantitatively using a synthetic method. Non-linear calculation will be done by GKV, GT5D, ORB5 and other codes. Finally profiles and transport coefficients are quantitatively compared with non-linear results in order to account for plasma profiles and its temporal behavior. Reduced gyrokinetic models and/or time-dependent predictive simulators with gyrokinetic codes will be developed

The knowledge gained from these investigations will be used to construct predictive transport codes for ITER and DEMO predictions. Integrated code (e.g. TOPICS) will be used to understand the transport mechanism and to control self-regulating plasmas along with the codes made available by the EU integrated modelling activities. The integrated models/codes will be extended by further integration of physics models such as transport codes of the plasma flow (e.g. TASK/TX), plasma turbulence codes, divertor codes (e.g. SONIC) and so on. The validation of transport models by transport simulations can be performed using the data from the present tokamaks and JT-60SA in the various experimental regimes including ITER- and DEMO-relevant parameters. These models/codes will be applied to the prediction of plasma performances in ITER and DEMO.

In the initial Research Phase, transport models including core, edge and SOL regions and turbulence codes will be improved individually and the integrated model will be validated with the JT-60SA experiments. In the Integrated Research Phase and the Extended Research Phase, integrated simulation codes including turbulence models for transport analysis will be developed and confirmed.

5.8. Real-time control

Controllability of plasma profile will be studied and real-time control systems will be developed in JT-60SA, in order to predict the controllability of ITER and DEMO plasmas. The results of plasma control studies in JT-60SA will contribute to propose a control scheme and suitable operation regimes for DEMO. First, integrated real-time control systems will be developed. Plasma response and controllability over the wide range of plasma parameters will be investigated in order to understand the transport physics and to optimize control logic. Model based control will be used in this control system in order to contribute to the development of control schemes in ITER and DEMO. An integrated non-linear real-time control system with real-time stability analysis will be constructed for achievement of high plasma performances with high beta and high bootstrap current fraction in steady-state. Burning plasma simulation experiments and isotope ratio (H/D) control will be demonstrated for the tritium density ratio control in DEMO.

For the plasma control studies, various heating systems (co-NB, ctr-NB, perp-NB, on-axis P-NB, of-axis P-NB, N-NB and ECRF), fuelling systems (gas puff, pellet injection), RWM stabilizing coils, error field correction coils and plasma shape control systems will be used. Diagnostics with high time and high spatial resolution covering the whole radius will be used in the control systems. Electron density control will be performed with pellet injection and gas-puffing. Ion temperature control will be carried out with perpendicular P-NBs. Plasma rotation control will be performed with tangential P-NBs. The active current profile control will be

demonstrated with off-axis tangential P-NBs and N-NB. Radiation control will be done by bolometer systems with impurity seeding. Ion pressure profile will be estimated in real-time from profiles of electron density by TMS, ion temperature by CXRS and Z_{eff} by Z_{eff} monitor. Current profile is evaluated by the motional Stark effect (MSE) diagnostic. Using these profile data, a real-time MHD stability analysis (or prediction) will be calculated by MARG2D.

5.9. Research items of transport and confinement studies

The main research items for transport and confinement studies in JT-60SA are listed below, grouped by topic. The asterisk indicates the high priority research items in the Initial Research Phase I and II defined in Chapter 2. Operational/parameter regimes will be progressively expanded following the upgrade of the heating systems, plasma control systems, fueling systems and so on. Each research item should be scheduled in the suitable research phases in order to contribute to ITER operation and DEMO design. The suitable phase for each item is also indicated below, and in addition Table 5-1 summarizes the possible time schedule of the various research items.

- Properties of transport and confinement
 - * **L-H transition threshold condition in hydrogen and helium mixed plasmas [Initial Research Phase I]**
 - * **Type-I H-mode and $H_{98y,2}=1$ at low power above threshold in hydrogen/helium plasmas [Initial Research Phase I]**
 - Transport properties in H-mode plasmas over a wide range of parameters and plasma shapes (elongation, triangularity, aspect ratio) [Initial Research Phase II -]
 - Transport properties in Hybrid H-mode plasmas with $q(0)>1$ [Initial Research Phase II -]
 - Transport properties in high β regime [Integrated Research Phase II -]
 - * **Transport properties in ITER-relevant normalized parameters [Initial Research Phase II]**
 - * **Transport properties in ITB and H-mode plasmas under dominant electron heating conditions [Initial Research Phase II -]**
 - * **Energetic particle effects on transport and confinement [Initial Research Phase II -]**
 - Turbulence transport studies [Initial Research Phase II -]
 - * **Establishment of an H-mode thermal confinement scaling [Initial Research Phase II -]**
 - Transport properties in long pulse discharges comparable to the wall saturation time (~60 s) with the forced water cooled divertor [Integrated Research Phase II]
 - Transport properties in double null discharges [Extended Research Phase]
 - Linkage among plasma pressure, rotation and current profiles [Integrated Research Phase I -]
 - Boundary condition for density, temperature and rotation [Integrated Research Phase I]
- Particle transport and fuelling study at high density and high confinement
 - * **Achievement of high density and high confinement regimes ($f_{\text{gw}}\sim 0.8$, $HH\sim 1.1$) [Initial Research Phase II -]**
 - * **Transport and control of low and higher Z impurities [Initial Research Phase II -]**

- * **Impurity transport with strong electron heating and peaked density profile [Initial Research Phase II -]**
- * **Isotope effects on plasma confinement [Initial Research Phase I, II]**
 - Tungsten transport and control in the core [Integrated Research Phase II]
- Momentum transport and rotation study
 - Effect of RWM stabilizing coils on rotation [Initial Research Phase I]
 - Effect of RMP on rotation in ITER-relevant normalized parameters [Initial Research Phase II]
 - * **Intrinsic torque and rotation in ITER- and DEMO-relevant regimes [Initial Research Phase II -]**
 - Momentum transport ITER- and DEMO-relevant regimes [Initial Research Phase II -]
 - Boundary condition [Integrated Research Phase I]
- Development of transport models
 - * **Transport models including core, edge and SOL regions [Initial Research Phase II]**
 - Integrated simulation code including turbulence models for transport analysis [Integrated Research Phase I]
 - Prediction of plasma performances in self-regulating and burning plasmas [Integrated Research Phase I]
- Real-time plasma control
 - * **Development of a feedback logic to sustain the high beta plasmas similar to scenario #5 [Initial Research Phase II -]**
 - Demonstration of steady-state operations with high beta like scenario #5 using real-time stability analysis [Integrated Research Phase II]
 - Experimental simulation of self heating plasma in H-mode plasmas and high beta and high bootstrap current plasmas [Integrated Research Phase II]
 - Investigation of controllability of highly self-regulating and high performance plasmas [Integrated Research Phase II]
 - Burn control study in ITER- and DEMO-relevant normalized parameters [Integrated Research Phase II -]
 - Exploration of operation regime and control method in DEMO [Integrated Research Phase II -]

In the Initial Research Phase, transport and confinement study in H-mode plasmas over a wide range of plasma parameters will be focused on combining high I_p -5 MA and high density ($n_e \sim 1 \times 10^{20} \text{ m}^{-3}$, $f_{GW}=85\%$) with high confinement ($HH \sim 1.1-1.3$) as shown in Figs. 5-7 and 5-8. In the Integrated Research Phase and the Extended Research Phase, transport and confinement in long pulse discharges will be investigated at ITER and DEMO-relevant normalized parameters (low $\nu^* \sim 0.02-0.05$, small $\rho_p^* \sim 0.02$ and high $\beta_N \sim 3-4$) with high density ($f_{GW}=80\%$) using higher heating power of 37- 41 MW (60 - 100 s). Here, ν^* is the effective electron collision frequency normalized to the bounce frequency, ρ_p^* is the ion poloidal Larmor radius normalized to the minor radius, and β_N is the normalized plasma pressure.

5.10. Summary

In summary, the strategy of the transport and confinement studies in each research phase of

JT-60SA is given in Table 5-1. Experimental data, theoretical models, and real-time control techniques in each phase contribute the plasma operation scenarios in ITER and DEMO.

References

- [1] Tobita K. *et al* 2009 *Nucl. Fusion* **49** 075029
- [2] Sakamoto Y. *et al* 2009 *Nucl. Fusion* **49** 095017
- [3] Oyama N. and the JT-60 Team 2009 *Nucl. Fusion* **49** 104007
- [4] Kamada Y. *et al* 2002 *Fusion Sci. Technol.* **42** 185
- [5] Beurskens M. *et al* 2011 proceedings of the 13th International Workshop on H-mode Physics and Transport Barriers, Oxford, UK

Table 5-1 Schedule of Research Items for Transport and Confinement Study

Phase	Gas/ Divertor	Power/ Neutron Limit	Research items
Initial Research Phase I	H, He USN/ LSN, Carbon, Inertial cooling	19 MW (6 MW P-NB, 10 MW N- NB, 3 MW ECH)	Measurements of transport and confinement properties (heat, particle, momentum) in L- and H-mode plasmas by parameter scans such as the heating power, density, plasma current, etc. Comparison with predictions and previous results, in particular check of improvements with respect to JT-60U.
			H-mode studies, such as H-mode quality, L-H threshold power, in He plasmas through scans of heating power, collisionality, toroidal rotation at the edge region, plasma shape (in advance of ITER He phase). Study mass effect from H to He and extrapolate performance in D.
			Impact of RWM stabilizing coils and RMP coils on particle, heat and momentum transport.
			Commissioning of plasma control and diagnostic systems.
Initial Research Phase II	D LSN, Carbon, Inertial cooling	33 MW (20 MW P- NB, 10 MW N- NB, 3 MW ECH) 3.2×10^{19} n/s	Particle transport study to achieve high density ($f_{GW} \sim 0.8$) and high confinement (HH-1.1) ELMy H-mode using various fueling techniques.
			Study of impurity transport and impurity control techniques for higher Z impurities (Ne, Ar, Kr) in high density and high confinement regimes.
			Development of edge radiating belt, with control of impurity accumulation by ECH and NNB. Power hysteresis for impurity accumulation.
			He exhaust with Ar frosted cryopumps at high density.
			Transport studies in H-mode plasmas with positive or weakly negative magnetic shear over a wide range of parameters ($I_p \sim 5.5$ MA, $n_e \sim 1 \times 10^{20}$ m ⁻³) using both steady state and transient analyses. Impact of density and shape and consistency with IPB98(y,2).
			Transport and confinement studies in ITER-like hybrid discharges in the ITER-relevant normalized parameters and/or $T_e/T_i > -1$.
			ITB and H-mode studies under dominant electron heating and low external fuelling. Transport dependences (threshold power, ITB structure and strength) on T_e/T_i . Role of rotation and magnetic shears on ITBs in high beta, high bootstrap current and high density plasmas.
			Properties of turbulence such as zonal flow generation in ITER- and DEMO-relevant regimes. Non-linear coupling between micro-scale fluctuations ($k_{\perp} \rho_i \sim 1$) and meso- and macro-scale structures ($(\rho_i)^{1/2}$, R/L_T). Influence of turbulence on transport and H-mode transition.
			Transport studies in ITER-relevant normalized parameters (low ν^* , small ρ^* and high β) and ITER-like configurations.
			Rotation study in ITER- and DEMO-relevant normalized parameters, with/without NB torque, in particular parameter dependences and properties of the intrinsic rotation. Rotation control with different actuators (NB, ECRF, RMP).
			Studies of the isotope effects on plasma confinement and controllability of isotope ratio. Controlling the amount of each species (full ratio) with pellets and gas puffing.
			Development of transport models including core, edge and SOL regions for the understanding of transport mechanism and the prediction of plasma performance in ITER and DEMO.
			Development of turbulence codes to understand ITB formation and L/H transition.
			Developments of integrated real-time control systems including plasma pressure, rotation, current profiles, radiation and RWM stabilizing coils.
			Demonstration of integrated real-time control in high beta plasma. Optimization of time and space response, both without and with MHD, in particular for high beta scenario #5.

Phase	Gas/ Divertor	Power/ Neutron Limit	Research items
Integrated Research Phase I	D LSN, Carbon, Full Mono- block	37 MW (20 MW P- NB, 10 MW N-NB, 7 MW ECH) 4×10^{20} n/s	Effects of electron heating on impurity transport at various Z in high density and high confinement regimes, with positive shear or weakly negative shear and ITBs. Conditions of suppression of accumulation through parameter scans (ECH power, v^* , q etc.).
			Studies of link between plasma pressure, rotation and current profiles in strongly self-organized plasmas by f_{BS} scan ($f_{BS} \sim 0.4-0.7$) for the development of real-time control systems to sustain high performance plasmas.
			Studies of edge or SOL rotation measured by VUV spectrometers and of the relation between boundary rotation and core rotation and plasma performances.
			Turbulence driven transport under strong electron heating. Relevance of ETGs and micro-tearings for electron transport.
			Development of integrated simulation code including turbulence models for transport analysis and prediction of plasma performance in self-regulating and burning plasmas.
			Developments of real-time control with model based control scheme, in particular for scenario #5.
Integrated Research Phase II	D LSN, Tungsten-coated carbon full Mono-block	37 MW (20 MW P- NB, 10 MW N-NB, 7 MW ECH) 1×10^{21} n/s	Transport study in long time discharges (~ 60 s) focusing on effects of recycling on confinement and on achieving particle control to sustain high values of beta, bootstrap current, plasma density, H-factor ($\beta_N \sim 4.3$, $f_{BS} \sim 0.7$, $f_{GW} \sim 0.85$, $HH \sim 1.3$) and radiation power simultaneously. Use of forced water-cooled divertor.
			Metal impurity transport and control studies in high density and high confinement regimes through ECH and density peakedness scans
			Specific features linked with the duration in long pulse high beta discharges, such as stochastic trigger of NTM.
			Correlation among different turbulence quantities such as density, electron temperature and magnetic fields. Noise reduction using longer integration times.
			Burning plasma simulation experiments in high beta, high density and high bootstrap current plasma with dominant electron heating, low torque input and low fuelling, first in H-mode and then in higher beta and higher bootstrap current plasmas.
			Developments of integrated real-time control systems with a real-time stability analysis for steady-state operations.
			Demonstration of steady-state operations with high beta using the integrated real-time control systems. Exploration into burn control schemes for DEMO.
Extended Research Phase	D DN/SN, Tungsten-coated carbon full Mono-block	41 MW (24 MW P- NB, 10 MW N-NB, 7 MW ECH) 1.5×10^{21} n/s	Transport study and particle and radiation controls in double null H-mode plasmas. Behaviors of particle transport and density and impacts of double null configuration on radiation and confinement.
			Transport scaling over the wide range of normalized plasma parameters including ITER- and DEMO-relevant regimes.
			Identification of zonal flow and investigation in ITER- and DEMO- relevant regimes. Impact of double null divertor on edge transport and link with core transport via meso-scale structures.
			Burning plasma simulation experiments in ITER- and DEMO- relevant normalized parameters (low v^* , small ρ^* and high β).
			Controllability of highly self-regulating and high performance plasmas at ITER- and DEMO-relevant density ($f_{GW} \sim 0.85$), confinement ($HH \sim 1.3$) and beta ($\beta_N \sim 4.3$).
			Development of integrated real-time control systems based on experimental data and developed modeling/simulation for demonstrations of long pulse operation (~ 100 s) of high performance plasmas ($\beta_N \sim 3-4$, full CD, $f_{GW} \sim 0.5$, $HH \sim 1.3$).

Table 5-2 List of predicted turbulence

Turbulence scale	Turbulence mechanism	Ruling transport
$k\rho_s=0.1-0.5$	ITG	ion energy, particle impurity, momentum
$k\rho_s=0.5 - 1.0$	TEM	particle, impurity
$k\rho_s>5 - 10$	ETG	electron energy
$k\rho_s<0.1-0.5$	Micro Tearing	electron energy

Table 5-3 List of required turbulence diagnostics

Measurement	Diagnostic	System	k range	Coverage	Spatial resolution	Issues
density fluctuation	Phase contrast imaging	Use the beam of tangential viewing CO ₂ laser interferometer	$k\rho_s=0.1-1$ (ITG, TEM, Micro tearing)	Core - Edge	The simplest version is line integrated. Modest local measurements ($\delta\rho=0.1-0.5$) may be possible using a magnetic shear	Effect of mechanical vibration, interpretation of spatially integrated data
density fluctuation	Microwave scattering	Use a heating gyrotron	$k\rho_s=5-10$ (ETG)	Core	Local measurements ($\delta\rho\sim 0.1$) are possible using a tangentially injected microwave	ECE back ground noise, stray radiation
density fluctuation and coherent Er fluctuation from poloidal velocity fluctuation	Microwave reflectometry	Use a diagnostic microwave sources	$k\rho_s=0.1-1$ (ITG, TEM, Micro tearing)	Core - Edge (mainly)	<1cm depending on the density and magnetic field scale length	Requirements of several sources to get spatial distributions
density fluctuation and coherent Er fluctuation from poloidal velocity fluctuation	Beam emission Spectroscopy	Use a heating neutral beam	$k\rho_s\leq 0.1-0.5$ (ITG, Micro tearing)	Core - Edge	~ 1 cm	SNR for turbulence measurements
density fluctuation	Lithium beam probe	Use a diagnostic beam	$k\rho_s<0.1$ (ITG, Micro tearing)	Edge	Several cm	SNR for turbulence measurements
electron temperature fluctuation	Correlation ECE	Use a heterodyne radiometer	$k\rho_s<0.5$ (ITG, Micro tearing)	core	~ 1 cm	SNR for turbulence measurements

6. High Energy Particle Behavior

In ITER, experiments with deuterium and deuterium-tritium are planned to start from 2035 and 2036, respectively. Although the energetic ions in JT-60SA are mainly beam ions produced by NNB, and not alpha particles produced by a D-T fusion reactions, JT-60SA operation will contribute substantially to the physics basis of high energy particles (EPs) in ITER and DEMO. Several aspects of EP physics will be unique in JT-60SA. For example, we can investigate instabilities in DEMO-relevant high beta plasmas which can enhance the interaction of Alfvén modes with low-frequency MHD; high plasma current operation in JT-60SA makes the normalised magnetic drift orbit widths of MeV-class ions (generated via NNB) comparable to alpha particle orbits at ITER and DEMO; thus, important aspects of MeV-class EP physics in ITER and DEMO can be directly investigated in experiments in JT-60SA.

We plan to focus particularly on three major areas:

- 1)The development of ITER and DEMO-relevant scenarios through understanding and predicting the role of energetic particles in them;
- 2)The feasibility check of the off-axis current drive using NNB;
- 3)The development of reactor-relevant monitoring methods using energetic particle phenomena, such as MHD spectroscopy.

In all three areas, it is essential to monitor the interaction between energetic particles and collective instabilities, such as Alfvén eigenmodes (AE), fishbone instabilities, and higher-frequency Compressional Alfvén Eigenmodes (CAE) and Global Alfvén Eigenmodes (GAE). The results from the first and second areas have to be obtained as early as possible because they may affect the detailed operation scenarios in ITER. As for the third area, the availability for the diagnostics will be strongly limited in the DEMO or reactors where a large area for the tritium-breeder blanket is required to ensure sufficient tritium breeding. In other words, less diagnostic area will be available in DEMO or in reactors. Thus we need to investigate the least set of measurements for energetic particles and the bulk plasma.

The details of each major area for the contributions are described below;

6.1. ITER and DEMO relevant scenarios

Based on the past work of fast-ion confinement studies, it was believed that the fast-ion confinement is subject to the classical collisional and orbital effects with the absence of MHD activities. Recently, it was proposed that the anomalous transport of fast ions could be induced by the micro turbulence. The ratio E_f/T_e is one of the key parameters in the theories that propose anomalous transport by the micro turbulence, where E_f is the energy of fast-ions and T_e is the electron temperature of plasmas. The pitch-angles of fast-ions also affect the E_f/T_e -dependence of the diffusion coefficients. Since several injection angles and different injection energies of NB will be available at JT-60SA together with additional electron heating by microwaves, this machine is expected to be one of the best machines to validate these theories. In the evaluation of the diffusion coefficients, a neutron profile monitor and a Fast-Ion D-Alpha (FIDA) measurement will have an important role: the former will provide us the behavior of fast-deuterium ions around the NNB-injection energy, and the latter the behavior of slowed-down fast-ions of around the PNB-injection energy. Verification & validation (V&V) activities of theory-based transport codes for energetic ions through experimental results are an important topic to predict the energetic ion transport in ITER and DEMO. In the previous study, a simple diffusion process was assumed, however, the radial broadening process by electromagnetic fluctuations is expected to be more complex, requiring more detailed modeling. Also the synergy effect of this type of transport with 3D static and dynamic magnetic fields such as the

toroidal ripple, the ELM controlling coils, etc. have to be investigated.

At the end of JT-60U campaign, we had developed a neutron profile measurement system, which can measure neutrons not only originating from D-D reactions, DD neutrons, but also, from D-T reactions, DT neutrons. Measuring DT neutrons, we can investigate the behavior of the transport of 1 MeV tritons, which are produced by D-D reactions. The Larmor radius of 1 MeV triton is similar to that of 3.5 MeV alphas. The research of 1 MeV triton transport supports the DT experiments in ITER from the viewpoint of alpha particle physics. At the end of JT-60U campaign, the high I_p operation was limited. In JT-60SA we can expect high I_p operation with $I_p \sim 5$ MA. Triton transport can be investigated in JT-60SA in conditions closer to ITER than in JT-60U.

The NNB is a powerful energetic ion source, which can be well-controlled for the study of energetic-particle-driven AE. The NNBs will be injected as off-axis beams, allowing us to investigate also reversed shear scenarios. In JT-60U, AEs were rarely induced when the upper NNB as an off-axis beam was injected alone with the power of about 2 MW, while AEs were induced when the lower NNB as an on-axis beam was injected alone with similar power. This confirms the common understanding that a high pressure in the central region leading to a high pressure gradient of energetic particles is important.

Based on this experience, the excitation of AEs might be difficult in JT-60SA at first glance because the NNB in JT-60SA will be injected off-axis, as shown in Fig. 6-1. However, the NNB is expected to have higher power and higher energy. Also, the steepest NNB ion gradient will be in a region with lower background temperature and thus AEs in that region are subject to lower ion Landau damping. In addition, the inverted EP gradient close to the plasma center might under certain conditions drive AEs propagating in the electron diamagnetic direction, as recently observed at AUG and NSTX-U, giving important information about the plasma rotation. In Table 6-1, the parameters of energetic ions induced by the NNB in JT-60SA for the five proposed scenarios (#1-#5) are compared with ITER, JT-60U and other conventional tokamaks. The region of the volume averaged energetic ion beta versus v_i/v_A is also depicted in Fig. 6-2, where v_i is energetic (fast) ion velocity and v_A is Alfvén velocity. Because of the high energy, a large population of energetic ions with $v_i/v_A > 1$ will be present in JT-60SA. Thus we

Table 6-1 Fast-ion parameters in contemporary experiments compared with projected JT-60SA and ITER values. Data in 2nd to 5th columns data is cited from “Progress in the ITER Physics Basis, Chapter 5: Physics of energetic ions”, Nucl. Fusion 47, S264 (2007)

Tokamak	TFTR	JET	JET	JT-60U	ITER	Slim CS	JT-60SA Scen#1-#5-1
Fast ion	Alpha	Alpha	Alpha	Deuterium	Alpha	Alpha	Deuterium
Source	Fusion	Fusion	ICRF tail	Co NBI	Fusion	Fusion	Co NBI
τ_s [s]	0.5	1.0	0.4	0.085	0.8	~2	0.5 - 1.6
n_i _max / $n_e(0)$ [%] ^(a)	0.3	0.44	1.5	2	0.85		0.35 - 2.2
β _max [%] ^(a)	0.26	0.7	3	0.6	1.2		0.54 - 2.3
$\langle \beta \rangle$ [%]	0.03	0.12	0.3	0.15	0.3	~1.2	0.2 - 0.9
β _max / $\langle \beta \rangle$	8.7	5.8	10	4	4		2.5 - 3.2
max $R \nabla \beta_i$ [%]	2.0	3.5	5	6	3.8		5.2 - 65
v_i _max / v_A	1.6	1.6	1.3	1.9	1.9	~2	1.0 - 1.26

^(a)Except for JT-60SA, “max” means the value at the plasma center.

can expect the excitation of AEs, such as RSAEs, TAEs, and EAEs, as well as higher frequency CAEs and GAEs. Since one of three major areas for the contributions to ITER and DEMO is the investigation of NNBI current drive, it is important to understand instabilities driven by energy gradients or temperature anisotropy of NNB-produced ions. Possible excitation of CAE and GAE via anomalous Doppler resonance could severely affect the current drive efficiency of the beam above V_A since the parallel beam energy will be transformed into perpendicular energy as a result of the interaction with CAEs and GAEs. Using the conventional formulae for drift orbit width and mode width, the toroidal mode numbers of TAEs are estimated to be $n < 5$, which is comparable to JT-60U. Energetic ions produced by tangential NBI may also excite waves with mixed acoustic and Alfvénic polarization in JT-60SA plasmas. The beta-induced Alfvén eigenmode (BAE) and beta-induced acoustic-Alfvén eigenmode (BAAE), whose frequency is lower than that of TAEs, can exist close to the gap formed by the geodesic curvature induced up-shift of shear Alfvén continuum and the coupling between the shear Alfvén continuum and the acoustic continuum, respectively. In particular, BAEs (finite n) and so called energetic ion driven GAMs (EGAMs) ($n=0$) emerging from the GAM continuum may be excited by energetic ions. Since the EGAM couples with the background turbulence and AEs, the excited EGAM may affect the anomalous transport caused by the turbulence and the saturated AE spectrum. We should investigate EGAMs in order to clarify their characteristics and their possible potential to increase the performance of JT-60SA plasmas.

The comparison of the modes' stability boundaries, spatial structure, and interaction with energetic ions between experiments and theory-based codes is important. Both, linear [1] and non-linear [2] codes can be validated with experimental measurements: the research subjects will be the investigation of mode behaviors and energetic-particle transport induced by Alfvén eigenmodes (RSAE, TAE, and so on), energetic-particle modes (EPMs), EGAMs and BAEs, fishbone modes and EWMs (see next paragraph), as well as MHD instabilities such as sawtooth events. Detailed comparisons of spatial mode profiles, amplitudes, and energetic-particle transport between experiment and simulation should be carried out.

Actively controlling the AE spectrum will be an integral part of the research that is needed to establish reliable scenarios with a large fraction of EPs. One can aim to eliminate AEs in some scenarios, or one can utilize the AEs to tailor an appropriate distribution function or to

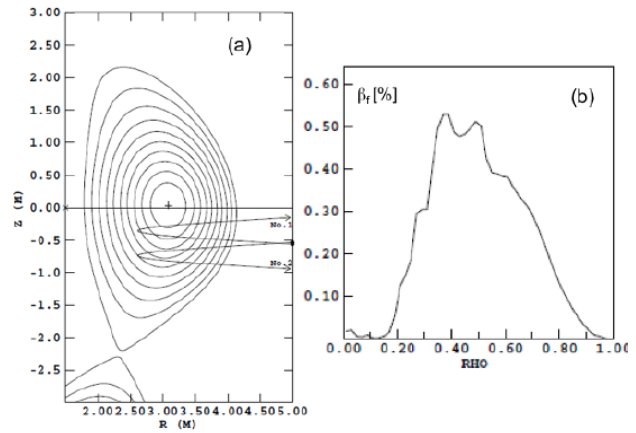


Fig.6-1 (a) Trajectory of the N-NB beam lines in poloidal cross section. (b) Profile of energetic ion beta, β_f , for the scenario #3 calculated by OFMC. Here, normalized Larmor radius is about 0.02.

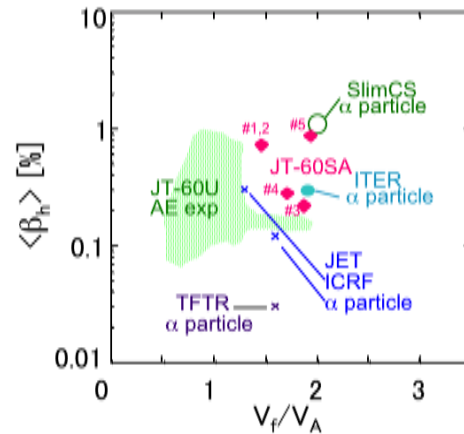


Fig.6-2 Volume averaged energetic ion beta versus v_f/v_A .

channel fast ion energy into bulk ions efficiently. We will investigate potential methods that can be applicable to DEMO.

During a high beta operation in JT-60U we have observed a new type of energetic particle mode. This mode was called energetic particle-driven wall mode, EWM. The EWM might be dangerous because this mode triggers the RWM and cannot be suppressed by a plasma rotation velocity of around $\sim 10\%$ of Alfvén velocity. On the other hand, the EWM might be a useful tool for the ELM pacing/control in DEMO where ELM coils will not be available: on JT-60U it was shown that the ELM frequency is much increased and the drop of the stored energy is reduced during the occurrence of the ELMs induced by the EWM. The EWM seems to be induced by a resonant mechanism with the precession motion of energetic ions injected by the perpendicular PNB. At present, the method to control this mode is to reduce the power of perpendicular NBs. This method cannot be effective in the environment of alpha heating. We should investigate the suppression/control method of the EWM as well as its physics mechanism, expecting the application of the EWM to the ELM control.

As can be seen in the case of this EWM, the impact of fast particles on MHD stability in high beta plasmas is an open question. During the occurrence of the EWM, the RWM and the ELMs are affected by fast ions. In the cases of the EWM, the contribution of the fast particle can be just a “trigger” for the dominant MHD stability. But the MHD stability might be affected when the fast particle beta cannot be neglected compared with the bulk plasma beta.

One of the targets in the JT-60SA project is the development of high beta plasma, that are crucial on the way to economical fusion reactors. In this development, we will actively research the impact of fast particles on MHD stability in high beta plasmas. EGAMs and BAEs in high beta plasmas might be attractive research objectives because they might transfer the energetic-particle energy to the bulk plasma through Landau damping, i.e. this can be seen as some kind of alpha channeling scheme.

Another crucial topic which has arisen recently is the effect of the ELM control field on the fast ion confinement. ELM control via such externally applied 3D magnetic perturbations is one of the important methods to prevent excessive heat load on the divertor by Type-I ELMs in ITER. ELM control field configurations which can be compatible with both proper fast ion confinement and tolerable heat load on the divertor, need to be identified and studied for ITER-relevant plasma parameters in JT-60SA. In order to apply the knowledge on the optimal ELM control field obtained in JT-60SA to ITER, it is necessary to develop and validate models of the perturbed magnetic field with plasma responses included, working closely together with the contributors for Chapter 4 and 7.

Obviously, the most effective contribution to ITER and DEMO is the development of theoretical/numerical models and their validation for the predictive simulation of plasma scenarios. The time scale that needs to be covered by a prediction code of this kind [3] is the characteristic time of bulk plasma transport, which is in the order of a second. On the other hand, the characteristic time for phenomena caused by AE instabilities is in the order of a millisecond. Due to this separation of time scales, the integration of anomalous transport caused by AE instabilities in a transport code may be accomplished in an efficient way by making use of reduced models. Simplified models, e.g. based on the Fokker-Planck equation with a radial transport term like the FP-RAT code in TOPICS or a critical gradient model, can be improved on the basis of knowledge obtained from JT-60SA experiments.

6.2. Off-axis N-NBCD

The physics basis of off-axis beam driven current should be clarified, especially for ITER. The fast ion transport in the off-axis region might be different than in the on-axis region. The

deviation from neoclassical transport might not be ignored in the off-axis region. The fast ions might be vulnerable to off-axis micro-turbulence since the micro-turbulence is typically larger in the off-axis region than in the on-axis region. RSAE type modes might affect the transport since the purpose of the off-axis current drive aims at the establishment of a low-shear plasma for a steady-state scenario, but such low-shear can create an extended continuum gap structure that facilitate the existence of global gap modes. The fast ions in the off-axis region could also be more vulnerable to 3D magnetic perturbations. These mechanisms which could affect the fast ion transport depend obviously on the conditions of the bulk plasma. Thus, the physics basis of off-axis beam driven current should be investigated in ITER and DEMO-relevant plasmas, e.g. with low-collisionality, electron-dominant-heating scheme, high-plasma current and high beta. These plasmas are the main scope of the JT-60SA mission.

In JT-60SA, off-axis NNB with energy of 500 keV will be available for current drive. Due to their high energy, the beams mainly transfer their energy to electrons. In this sense, this current drive is more similar to that in ITER than beam current drive by PNBs in other devices. The behavior of fast-ions during their slowing-down processes is also a key issue to understand the physics of off-axis NBCD since the current drive is dominated by these fast-ions. To evaluate this behavior and to compare with numerical simulations [4], the simultaneous measurements of fast-ions which are close to their birth energies and somewhat lower energies are important. The former can be done by the neutron-diagnostics and the latter can be done by FIDA measurements.

6.3. Development of reactor-relevant monitoring methods

To develop the diagnostics which satisfy the needs and limitations in the DEMO is an important research area. Monitoring the amount of alpha particles is important for controlling fusion power in the DEMO. The measurement of 14 MeV neutron is one of candidates. The measurement of the inner q profile is important to obtain steady state equilibria. However, the MSE measurement will not be available at the plasma center in DEMO because of its high density as well as the spatial limitation. One of possible approaches is MHD spectroscopy, where q_{\min} can be estimated by measuring reversed-shear AEs (RSAE) or core-localized TAEs. In the case where co- and counter propagating AEs are driven due to an off-axis peaked EP profile, their frequency difference can be used to constrain the local toroidal plasma rotation. We are planning to further investigate this method in order to increase its reliability. Namely, we will carefully compare the q_{\min} measured by MSE, the measured mode frequency, the measured rotation and the mode frequency estimated by linear codes. We will also investigate and extend the capability of MHD spectroscopy to other AEs and energetic-ion-driven modes, such as EGAMs, since RSAEs might not exist in high beta plasmas.

In order to investigate the above mentioned topics, the following diagnostics will be required to work effectively [5]. The magnetic sensors (magnetic pick-up coils) are essential to identify the above-mentioned modes. The sensors should have high sampling rate, higher than 500 kHz and the spacing for a high-n (~ 20) measurement. The confined energetic ion behavior can be investigated by using a neutron profile measurement, a FIDA measurement, a gamma ray profile measurement, a collective Thomson scattering (CTS), and a CX-NPA measurement. The lost energetic ion can be investigated using an infrared camera, a fast ion loss detector (FILD). The main characteristics of these diagnostics are the following. The neutron profile measurement will utilize organic scintillator detectors. The CX-NPA is planned to be a system viewing from a tangential port and a vertical port, using natural diamond detector. The diagnostic beam of FIDA is a P-NB of ~ 85 keV, thus the target of this diagnostics is NNB-produced energetic ions, which are somewhat slowed down, or PNB produced energetic ions.

The FIDA diagnostics can reveal the amount of slowing-down ions originated from MeV-class beam ions, which is one of important physics quantities from the viewpoint of confinement of energetic ions. Nevertheless, it has been found that up to ~ 200 keV ions can be detected by the FIDA system in JT-60SA from the detailed study at LHD, since the relation between the highest energy of injected NBs and the energy of a diagnostic beam for FIDA is similar at LHD. The CTS diagnostic can track the MeV fast ions originating from NNBs. The millimeter wave of ECRF (110 GHz) can be used for the probing beam. The infrared camera can preferably monitor localized energetic ion losses through heat load measurement on the first wall. The FILD can measure energy and pitch-angle of lost energetic ions, simultaneously. The combined use of FILD and profile diagnostics for confined energetic ions, can provide comprehensive understanding of energetic-ion transport and loss caused by energetic-ion-driven modes. The mode structure of MHD perturbations can be investigated with soft X-ray measurements using a pin diode array, ECE measurements, a reflectometer, and an on-axis interferometer digitized to the relevant sampling rate.

For assessing possible pitch-angle scattering of NNB-produced ions by CAEs and GAEs excited in the frequency range $\omega=0.3-1.1 \omega_{BD}$ (similar to MAST and NSTX), several magnetic pick-up coils digitized up to the ion-cyclotron frequency range should be available. A set of three perpendicularly oriented coils at one position is necessary for measuring vertical, radial, and toroidal components of the perturbed magnetic field, and assessing the mode polarization (CAE or GAE). Furthermore, one or two coils are required, separated toroidally, and one or two coils– separated poloidally.

6.4. High priority research items for Initial Research Phase I and II

Here, we describe high priority research items in energetic particle physics. The high priority research items are defined, aiming at efficiently contributing to the achievement of major research goals of the JT-60SA project. The research goals are defined in Chapter 2 as “Headlines”;

Initial Research Phase I (H/He)

H.I.1. Stable operation at high current in large superconducting machine

H.I.2. ITER risk mitigation for non-activated phase

Initial Research Phase II (D)

H.II.1. ITER scenario development

H.II.2. Steady-state high beta scenario development

H.II.3. ITER risk mitigation

(Note: H.I means “Headline I.1”, not indicating hydrogen)

At the beginning, we describe the concept or basic idea of the high priority research items in this research phase. JT-60SA aims to contribute to ITER and DEMO. It is often assumed/hoped that fast ions in ITER and DEMO will behave classically.

However,

A) At least for JT-60SA, there is already strong evidence from simulations by contributors and prior experiments in similar conditions in JT-60U that suggests that we will see many fast-ion-driven MHD fluctuations.

B) It is important to understand these dynamics and quantify their impact on both the bulk plasma and fast ions.

Therefore,

C) We expect that – in the course of developing plasma scenarios to achieve the JT-60SA goals – many experiments, which are both unintended ones as well as dedicated ones,

will be analysed to identify the modes and determine their effect on fast ion confinement, classical and anomalous heating, classical and anomalous current drive, plasma rotation, MHD equilibrium and stability.

- D) For this purpose, an important research item is R&D and V&V of theories and models, which are used to make predictions for ITER and DEMO as well as to reconstruct the plasma profiles and to interpret the experimental observations.
- E) In particular, an urgent task to be performed is the R&D and V&V of models for resonant and nonresonant MHD activity and anomalous heating to be implemented in integrated codes.

Based on the concept, we have built the high priority research items as follows;

For H.I.1 in Initial Research Phase I (H/He):

Stable scenarios at high current in large superconducting machine

- **Further develop and validate numerical tools against initial JT-60SA data**

The tools include synthetic diagnostics. However, most important tools are linear stability codes that can provide boundaries for the onset of benign AEs (for MHD spectroscopy). If possible, models for the onset for diffusive-type EP transport and the transition to strongly non-linear events such as EPMS, ALEs (Abrupt Large amplitude Events) and avalanches should be developed and validated.

- **Develop the ability of time-dependent integrated codes to give us reasonably accurate predictions for MHD equilibria and energetic particle distributions in JT-60SA plasmas, from ramp-up to steady state.**

We should implement in time-dependent integrated codes, e.g. TOPICS, simple empirical/heuristic models for flattening of $q(r)$ and $P(r)$ profiles due to MHD instabilities (double/triple kink-tearing) and energetic-particle-driven modes. Then, the codes should be validated and refined through experimental data for H/He plasmas. Predictions will be made by using the codes for D plasmas of the Initial Research Phase II

- **Identify the most relevant modes and possible avalanche-like phenomena in H/He plasmas and propose mitigation methods**

Codes for energetic-particle-driven modes will be validated against experimental data. Reduced voltage NNBI at low densities in H might drive higher-n AE spectrum, which is more ITER relevant. Using the validated and refined codes, predictions will be made for D plasmas of the Initial Research Phase II and also suggest methods for dealing with/mitigating MHD and energetic-particle-driven modes.

- **Sawtooth period scaling in presence of large energetic-particle pressure**

The prediction of the sawtooth period is important for ITER and DEMO, however quantitative predictions from models are not sufficient. Using both PNB and NNB, JT-60SA has a flexible and controlled energetic ion source in order to investigate this scaling.

For H.I.2 in Initial Research Phase I (H/He):

ITER risk mitigation for non-activated phase

- **Reconfirm NBCD models for MHD-free plasmas**
- **Validate and refine codes in H/He plasma: Once the integrated codes and**

instability codes were successfully validated against JT-60SA data, make predictions for non-activated ITER. (working with Chapter 10)

The important output is to reevaluate likelihood of finding significant MHD activity in ITER. And hopefully, we would like to suggest methods for dealing with/mitigating MHD and energetic-particle-driven modes

For H.II.1 in Initial Research Phase II (D):

ITER scenario development

- **Validate and refine integrated codes against JT-60SA deuterium plasma data for "ITER-relevant" parameters. (working with Chapter 10)**
We can validate and refine integrated codes, using "ITER-relevant" parameters.
- **Using MHD equilibria from integrated codes, validate and refine instability codes against JT-60SA deuterium plasma data for "ITER-relevant" parameters.**
We can contribute to mitigate risks for ITER by providing validated codes.

For H.II.2 in Initial Research Phase II (D):

Steady-state high beta scenario development

- **Validate and refine integrated codes against JT-60SA deuterium plasma data for "DEMO-relevant" parameters. (working with Chapter 10)**
We can validate and refine integrated codes, using "DEMO -relevant" parameters.
- **Using MHD equilibria from integrated codes, validate and refine instability codes against JT-60SA deuterium plasma data "DEMO-relevant" parameters.**
We can contribute to DEMO design activities by providing validated codes.
- **Anomalous heating due to kinetic damping of resonant and nonresonant MHD modes must be studied, modeled, and included into integrated codes.**
This item relates to the so-called alpha channeling, which benefits from modes that heat bulk ions. However, plasma profiles and MHD equilibria should be sufficiently accurate to lowest order, and relevant modes should be reliably predicted. Therefore, this step depends on the success of all preceding modeling and validation activities.

For H.II.3 in Initial Research Phase II (D):

ITER risk mitigation

- **Suggest methods for dealing with/mitigating MHD and energetic-particle-driven modes.**
This step depends on the success of all preceding modeling and validation activities as described above.
- **Heat load evaluation**
Heat load evaluation by "unknown" magnetic perturbation, i.e. magnetic perturbations by ELM-control coils, is important. The perturbations will be calculated by models including the plasma response, in connection with Chapters 4 and 7.
- **Address questions about whether RMPs can be compatible with the ITER and DEMO conditions.**
For instance, aspects to be considered are the wall load on the nearby-stabilizer for high beta, and the effect of fast-ion loss on the operational scenarios, in connection with Chapters 4 and 7.

These are high priority research items in Initial Research Phase I & II. In order to carry out the research items, the availability of following diagnostics and systems is a key:

- Magnetic sensors with high sampling rate, spacing higher-n

- Profile of safety factor, n_e , T_e , T_i (MSE, Thomson scattering, CXRS): crucial for stability evaluation. Toroidal rotation velocity V_t is also used for frequency correction
- Interferometer & ECE for mode structure measurements at a sampling rate of 1 MHz
- Horizontal & vertical line of sights for neutron and gamma profile measurements and FIDA (if available) to measure confined fast ions
- IR cameras to measure large scale loss
- FILD (if available) to measure lost fast ions
- If available, energy and power scans, including modulation, of the NNB source
 NNB is very powerful & controlled energetic particle source for energetic-particle physics research

Reference

- [1] Linear stability codes: TASK/WM, LIGKA, CASTOR-K
- [2] Non-linear codes: MEGA, HMGC, HAGIS/LIGKA
- [3] Transport codes: TOPICS, JINTRAC
- [4] Codes for fast ion distribution computation: OFMC, BAFP, ASCOT, MEGA
- [5] Some of the above mentioned diagnostics are still on the level of proposals due to lack of the installation space. Thus, some of the diagnostics do not appear in APPENDIX D.

7. Pedestal and Edge Physics

7.1. Introduction

JT-60SA is well placed on the position for achieving two main objectives: supporting ITER for burning plasma and complementing ITER for DEMO reactor studies. Although H-mode operation is a robust operating mode in present diverted tokamaks and is beneficial in improving the edge and core confinement, there are some uncertainties in projecting H-mode operation towards ITER and DEMO reactor. Key issues among these uncertainties are the power required to access and maintain stationary high confinement H-mode plasmas, the height and width of the H-mode pedestal affecting the overall confinement and plasma performance and the pedestal control for high β long pulse operation. A better understanding of the L-mode to H-mode transition, the physical mechanisms responsible for the edge transport barrier formation and ELMs would improve prospects for optimal use of the auxiliary heating systems for accessing H-mode, maintaining good confinement, and identifying effective means of controlling ELM behavior consistent with optimal core, SOL and divertor performance. It has to be emphasized that both ITER and DEMO will not be able to tolerate large ELMs. In this regard, the detailed investigation of small or no ELMs (in the case of DEMO) regimes, such as grassy ELMs or QH-mode, and the use of active ELM control methods to mitigate/suppress ELMs is also an important research topic for JT-60SA. Based on this background, the major research items in the pedestal and edge physics area on JT-60SA are described here. Particularly, the high priority research items in the Initial Research Phases I and II have been embodied in line with revised ITER operation schedule and ITER Research Plan as described in Chapter 2.

In JT-60SA, the demonstration of high integrated performance is planned with a metallic wall replacing the carbon walls in the Integrated Research Phase II. The impact of wall material on the pedestal and edge performance is an important research item for both ITER and DEMO. As for a study towards DEMO reactor, control of burning plasma by optimized pedestal condition is one of the most attractive research items. In order to cover the edge pedestal issues in the central research needs for ITER and DEMO, the verification and the validation of the JA and EU integrated edge-pedestal models are also an important issue.

High priority research issues in the Initial Research Phases I and II have been taking shape as described in Chapter 2. Regarding the pedestal and edge physics study, important issues in these phases are summarized in the following sections. Detailed research items, for each experimental phase, up to the Integrated Research Phase are described in section 5.

During the Initial Research Phases I and II, research items that need to be done before the metal wall installation are particularly important because the edge plasma is largely influenced by the wall materials. The dimensionless operation regime is expected to move to relatively high collisionality (ν^*) when the wall material is changed from carbon to metal as JET experimental results have shown. The experiments requiring low ν^* will be a main focus in carbon wall.

7.2. Expected pedestal parameters in JT-60SA

Large ELMs pose a potentially significant threat to the divertor and plasma facing components (PFCs) because of the strong localization of the heat load. This is one of the most crucial issues

in ITER where the maximum energy release during ELMs should be reduced to below 1% of pedestal energy [1]. Fig. 7-1 shows the expected pedestal collisionality for all the typical operational scenarios in JT-60SA in a plot of the normalized ELM energy loss as a function of the pedestal collisionality [2]. Edge collisionality determines the upper bound of type-I ELM energy losses. Under this situation, ELM energy losses in these JT-60SA operation scenarios could be 10-20% of the pedestal energy. Therefore, mitigation methods to reduce the magnitude of large ELMs need to be examined. In JT-60SA, active ELM controls include helically resonant magnetic perturbations (RMPs), using the error field correction coil system, and pellet pace making. In addition, small or no ELM operations, such as grassy ELMs, QH-mode and I-mode, can also be examined within the potential operational area in JT-60SA.

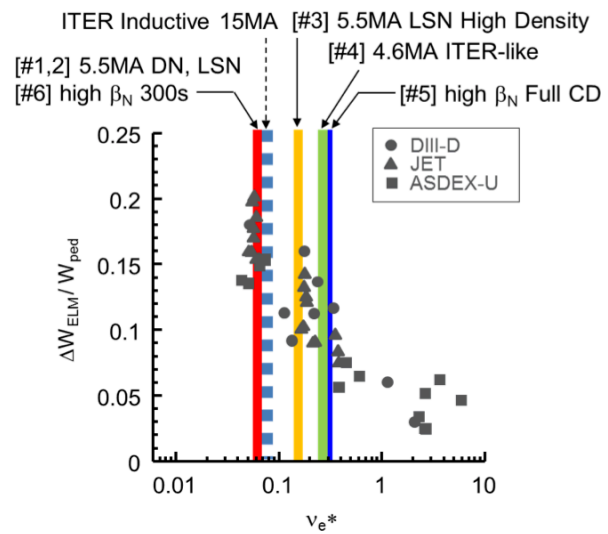


Fig. 7-1. ELM energy loss normalized to the pedestal energy as a function of the edge collisionality. Expected edge collisionalities in JT-60SA are indicated for each operation scenarios. The pedestal collisionality for ITER inductive 15MA operation is also shown for reference.

7.2.1 Pedestal parameters for basic operational scenarios in JT-60SA

Sufficiently heated H-mode plasmas generally show the characteristics of the profile resilience in core temperature that is attributed to a micro-instability driven by temperature gradient. This indicates that the energy confinement and fusion power depend mostly on the pedestal profiles of density, temperature, and pressure in H-mode plasmas. Therefore, it is of crucial importance to appropriately predict the pedestal parameters within the potential operational area.

The EPED model [3] is, to this regard, considered as one of the most reliable models that predict the pedestal width and height of the pressure profile in H-mode plasmas. Table 7-1 shows a set of the pedestal parameters predicted using the EPED model for all the basic operational scenarios in JT-60SA[†]. Provision of an appropriate pedestal prediction would not only give a simple estimate of pedestal pressure and the boundary condition for the core transport simulation but also lead to the research on the optimization of the operational area for the best confinement performance, ELM mitigation or suppression, eventually the study on the optimized fusion power.

In Table 7-1, the suffix ‘EPED1’ indicates the values at the pedestal position defined by the hyperbolic tangent function. The electron pedestal density is assumed to be 90% of the averaged density. The pedestal temperature is evaluated by the pedestal pressure that EPED1 predicted divided by the pedestal density. Note that the pressure is the total one including electron and all ion species. These values can be used for the evaluation of any pedestal relevant studies, such as ELM characterization. However, the values at the pedestal position in the profiles of density, temperature, and pressure tend to systematically be lower as a boundary value for the core

transport simulation, which may in many cases underestimate the confinement performance. On the other hand, the suffix ‘top’ indicates the values at the pedestal top position defined as $\Psi_{\text{top}} = 1 - 1.5\Delta_{\text{EPED1}}$, which can be a suitable boundary for any studies relevant to the core plasma.

Table 7-1. Predicted pedestal pressure and temperature in basic scenarios

No.	#1	#2	#3	#4	#5	#6
Scenario	Full Current, Inductive, DN, 41MW	Full Current, Inductive, LN, 41MW	Full Current, Inductive, LN, 30MW, High density	ITER like, Inductive	High β_N , full-CD	High β_N , 300s
$n_{e\text{-PED}} [10^{19}\text{m}^{-3}]$	5.67	5.67	9.00	8.19	4.50	1.80
β_N	3.1	3.1	2.6	2.8	4.3	3.0
f_{GW}	0.50	0.50	0.80	0.81	0.84	0.39
$P_{\text{EPED1}} [\text{kPa}]$	31.46	32.10	39.09	26.46	14.60	6.86
$\Delta_{\text{EPED1}} [\Psi_N]$	0.0349	0.0342	0.0376	0.0350	0.0529	0.0415
$\beta_{N\text{-EPED1}}$	0.754	0.769	0.937	0.723	1.036	0.679
$P_{\text{top}} [\text{kPa}]$	40.07	40.80	49.24	33.51	19.08	8.85
$\Delta_{\text{top}} [\Psi_N]$	0.0524	0.0513	0.0564	0.0525	0.0793	0.0623
$T_{e\text{-top}} [\text{keV}]$	2.16	2.20	1.68	1.25	1.31	1.49

† The authors would cordially acknowledge the support of EPED calculation by Dr. Phil Snyder of General Atomics, USA [3].

7.3. Main research items on pedestal and edge physics (particularly to contribute to solve ITER urgent issues)

7.3.1 Understanding the operational area of small/no ELM regime for the reduction/mitigation of the divertor heat loads

7.3.1.1 Grassy ELM regime

The high triangularity shape of JT-60SA plasmas (see Fig. 7-2) locates well inside the region suitable for appearance of grassy ELM in the $\delta \sim q_{95}$ space as shown in Fig. 7-3. Grassy ELM can be one of the expected small/no ELMs regime at high δ and high q_{95} required for the ITER steady-state operation. However, recent studies on JT-60U indicate that grassy ELM originates in the peeling-ballooning mode instability at high toroidal mode number due to the reduced elongation [4]. Extension of the grassy ELM regime at highly elongated plasma shape in JT-60SA may be a challenging research item. The flexibility of NBI tangential momentum input in JT-60SA also brings a benefit to study on the appearance of grassy ELM at low torque expected in ITER.

Main objectives are:

- Proof of existence of the grassy ELM regime at low v^* , high q_{95} , high δ and high κ
- Study of the grassy ELM regime at low torque
- Extension of the grassy ELM regime at low q_{95}

- Extension of the grassy ELM regime at high v^* towards operation with the metal wall

Grassy ELMs have been mostly observed at low collisionality. Thus, it is a crucial issue to produce grassy ELM in low collisionality regime close to the ITER condition at high I_p , high δ , and high κ . The grassy ELM regime may be difficult to operate with the metal wall since the edge collisionality becomes higher. Extension of the grassy ELM regime at higher collisionality is therefore an important issue during the carbon wall phase.

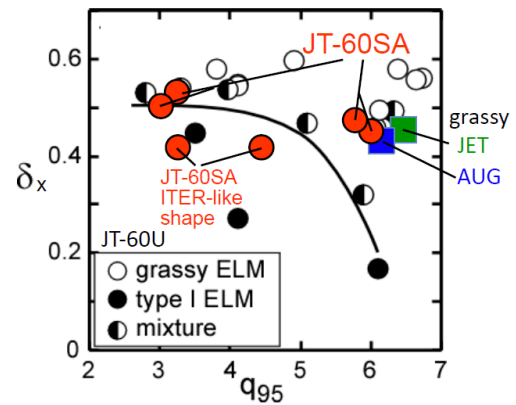
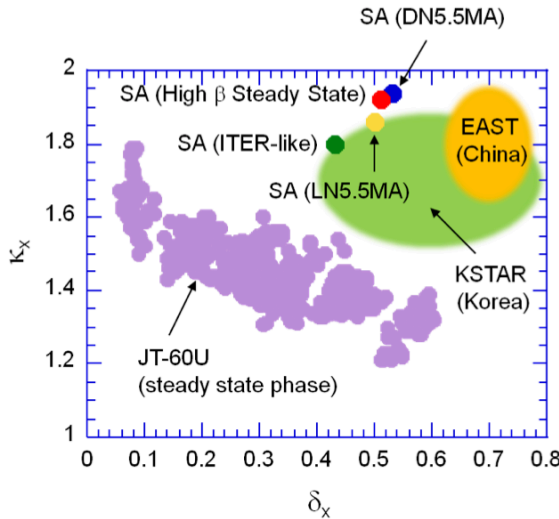


Fig. 7-1. ELM energy loss normalized to the pedestal energy as a function of the edge collisionality. Expected edge collisionalities in JT-60SA are indicated for each operation scenarios. The pedestal collisionality for ITER inductive 15MA operation is also shown for reference.

Fig. 7-3. Operational area of grassy ELMy H-mode in δ - q_{95} space.

7.3.1.2 QH-mode

The QH-mode regime has good confinement, even at low plasma rotation, and no ELMs, and is therefore an ideal candidate operating regime for fusion devices. It was initially discovered only at high q_{95} (≥ 3.7), low density and with counter-NBI. More recently, it was found that counter-NBI was not a requirement and its operating window was enhanced by application of error fields, which introduced a counter-torque in the plasma [5]. High density operation in the QH-mode regime has also been obtained by using highly shaped plasmas to improve the edge stability [5]. At JET a regime similar to the QH-mode with an Edge Harmonic Oscillation (EHO) has been observed, with $q_{95} \sim 3.5$, medium density (up to $0.6 n_{GW}$), co-NBI and co-rotation and small error fields [6]. It would be desirable to extend the operating space of QH-mode regime in JT-60SA and improve the physics basis understanding.

Main objectives are:

- Access to QH-mode regime at low v^* and high q_{95} with counter-NBI
- Study of QH-mode operation regime at low torque
- Extension of QH-mode regime towards low q_{95} at low toroidal rotation, closer to

that of the ITER baseline scenario.

- Extension of QH-mode regime at high v^* (high density) towards operation with the metal wall

JT-60SA could be in an ideal position to study the QH-regime, since devices with metal walls require high gas-puff to prevent impurity penetration and PFC damage, precluding the conventional low density QH-mode. In JT-60SA the low density QH-mode could be reproduced and hopefully strong shaping and available power and pumping might allow expansion of the operating window towards higher densities in view of the transition to a metallic wall device.

7.3.1.3 I-mode

- I-mode, initially found out in Alcator C-mod [7], features a stationary high confinement with steep edge profiles gradients in the ion and electron temperatures but L-mode like particle and impurity transport. This keeps impurities from building up and avoids the triggering of ELMs. Typically the I-mode is obtained when the H-mode power threshold (P_{L-H}) is high, which is usually achieved using the unfavourable ion ∇B drift direction (away from the X-point). During the Initial Research Phase II (Deuterium plasmas) heat load flux limits of $1 \text{ MW/m}^2 \times 100 \text{ s}$ will be allowed for the upper divertor. Hence unfavourable configurations in upper single null (USN) configurations can be envisaged. While it could be argued that the I-mode access window might be rather small at the magnetic fields employed at JT-60SA (2.25 T), I-modes have indeed been obtained on ASDEX Upgrade in a range of $B_T = 1.8 - 3.0 \text{ T}$, suggesting that I-mode studies in JT-60SA can still be very useful to strengthen its physics basis for ITER extrapolation. Turbulence measurements such as Doppler Reflectometer or Beam emission spectroscopy (BES) will be crucial to improve the physics understanding of the decoupling of density and temperature transport in the I-mode regime.

Main objectives are:

- Proof of I-mode existence on a large tokamak (at 2.25 T, with unfavourable configuration in USN plasmas)
- Assess compatibility of divertor heat flux control through impurity seeding.

7.3.1.4 Type II ELM regime

The type II ELM regime is observed only in strongly-shaped plasmas, i.e. with high κ and high δ . Also the plasma density needs to be rather high. The magnitude of the ELM bursts is significantly lower and the frequency is much higher than that of type-I ELM, while the confinement stays almost as good. Type-II ELMs show a similar characteristic to grassy ELMs, but the type-II ELM regime is seen at high density, which fits to the condition of the ITER and burning plasmas. In ASDEX-Upgrade, the type II ELM regime appears at high δ (>0.4) and high q_{95} (>4) in a quasi-double-null (QDN) configuration [8].

Main objectives are:

- Proof of existence of type-II ELMs at high density, high q_{95} , high δ and high κ configuration
- Study of type-II ELM operation regime at low v^* and low torque towards ITER steady state operation.

Previous linear analysis showed that the grassy ELMs on JT-60U occur close to the high- n ballooning boundary [6, 7]. High κ and high δ in JT-60SA can alter the edge stability, moving the edge plasma away from the grassy ELM condition and bring the operational area of a QDN configuration even closer to type-II ELM conditions.

7.3.1.5 Type III ELM regime

The development of highly radiative scenarios with adequate confinement, where extrinsic impurity seeding is used to reduce divertor heat fluxes, is another critical issue for ITER and DEMO. Type III ELMs are typically obtained in those conditions, thus offering the benefit of H-mode operation with small ELMs. The price to pay is a somewhat reduced pedestal confinement in the radiative scenarios compared to the confinement achieved in type I ELMy H-mode plasmas. JT-60SA is well equipped to attempt to compensate the loss in edge confinement with improved core confinement in high β regimes.

Main objectives are:

- Study radiative H-mode scenarios with small ELMs and acceptable divertor heat load reduction at high β

It is worth noticing that, since the impact of seeding on H-mode performance depends on the wall material, results obtained during the C-wall phase might not be transferable to a metallic-wall. In any case, the study of pedestal characteristics during long pulse operation with inter-ELM control mitigation is particularly relevant for JT-60SA. JT-60SA can operate for 60 s with ~ 30 MW of heating power, so that multiple seeding impurities could be used in parallel to create the optimal radiation profile tailored to a reactor device. In particular, the combination of an edge radiator (nitrogen/neon/carbon) and a core radiator (argon/krypton) would be of particular interest. This research topic is mentioned in Chapter 8 (Divertor, SOL and PWI) but also has a direct impact on pedestal studies.

7.3.2 Development of active ELM control methods for ELM mitigation/suppression

ELM control studies in JT-60SA will aim at developing an improved physics basis for the understanding of the applicability of the different ELM control methods planned for ITER, with particular focus on the use of RMPs and pellet pacing. In all cases strategies should be developed to obtain acceptable ELMs (in terms of transient heat loads) or no ELMs while still maintaining good confinement. These studies will necessarily have a strong link with specific aspects of JT-60SA scenario development, such as avoidance of large ELMs in ITBs, integration of ELM control in radiative scenarios or high density operation with pellets/gas. Demonstrating the controllability of RMP coils and pellet pacing in long pulse discharges will also be an important objective during the Integrated Research Phase. In addition to the main ELM control methods, it would also be desirable to test other techniques for ELM pacing available in JT-60SA, such as rapid vertical plasma movements (known as vertical kicks) and ECRH modulation. These experiments would not only contribute to improve our physics understanding of the ELM triggering physics but would also provide additional tools for impurity control, which has been recognized as an important requirement for ELM control systems in ITER.

7.3.2.1 RMP control

In JT-60SA, RMP-based ELM control experiments are possible using the remaining current range of the error field correction coils (EFCCs). Three stack of in-vessel coils (3x6) which are controlled by individual power supplies will be used for ELM suppression/mitigation experiments. Non-linear MHD analysis indicates that two stacks of coils (2x6) are only marginally sufficient to reach the criteria for ELM suppression. The maximum EFCC coil current is 30 kA. Note that RMP control experiment is done using the EFCC coil currents available after the error field correction.

Plasma response to RMP studies such as density pump-out, effect on rotation, ELM suppression or mitigation at different collisionality, dependence of ELM mitigation/suppression efficiency on q_{95} are required for the use of RMP control in ITER. In particular, since the complete ELM suppression in the ITER-relevant low collisionality was observed only at low density (see Fig. 7-4), the extension of the density ranges up to the ITER-relevant region must be considered. In addition, in the ELM suppression and mitigation by the RMP, clear splitting of divertor lobes is observed. Understanding of the plasma response including the dissipative response is a key topic in the long pulse steady state discharge.

- Another important topic to consider is scenario integration with active ELM suppression. JT-60SA's aim is to support high β steady state operation in ITER and DEMO. An attractive scenario is ITB plus ETB, but large ELMs erode the ITB and are not ITER nor DEMO relevant. It is therefore important that scenario development should be linked to passive and active type I ELM mitigation/suppression. Compatibility of ELM mitigation/suppression with high divertor radiation should also be addressed from a scenario development viewpoint.

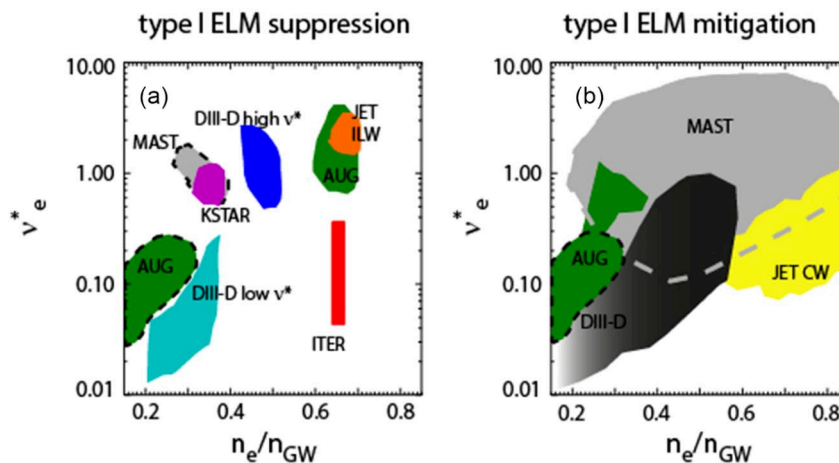


Fig. 7-4. Experimentally determined access condition in terms of pedestal collisionality (v_e^*) versus pedestal density as a fraction of the Greenwald density (n_e/n_{GW}) for (left) suppression of type I ELMs and (right) type I ELM mitigation [9].

ELM suppression at low plasmas rotation is also an important research topic for ITER and DEMO. JT-60SA has the capability to create low torque, high performance plasmas using balanced beams. Experiments exploiting this capability are therefore an attractive research area in JT-60SA.

Main objectives on this topic are:

- Demonstration of ELM mitigation/suppression in the ITER-like scenario (4.6 MA/2.28 T, $q_{95}=3.2$) by $n=3$ RMP field in low collisionality plasmas
- Identify operational window for ELM suppression, in terms of q_{95} , collisionality, Greenwald density fraction, plasma shape and plasma rotation, to provide guidance for physics validation of theory and numerical modeling
- Optimization of the RMP configuration, including the minimum set of coils for ELM mitigation/suppression, in the integrated scenario

In JT-60SA, the installation of metal coated wall materials is planned during the Integrated Research Phase. RMP experiments were carried out in JET with both the C-wall and the ITER-Like Wall (ILW). Some observations were similar but others were different. For example, strong mitigation of type I ELMs was observed with the application of an $n=2$ field in high collisionality H-mode plasmas in JET with the ILW, while almost no effect on the ELMs was observed in similar conditions in C-wall experiments [10]. The reasons behind this different behaviour have not yet been identified. From this point of view, the RMPs experiments during the Initial Research Phase will be addressed as a comprehensive task in view also of the changeover to the metal wall, so that the effects of the wall materials on the plasma response to RMPs can be assessed, in view to provide useful information to better understand this ELM control approach in ITER.

7.3.2.2 Pellet ELM pacing

Pellet ELM pacing is one of the key techniques for ELM mitigation in ITER. The JT-60SA pellet injection system includes an injector for ELM pace making, with a typical pellet size of $\sim 1.4 \text{ mm}^3$, which is similar in size to that used in JET for ELM pacing. A real-time frequency control is also planned. The pellet frequency is planned to be increased up to 60 Hz. Both fuelling and ELM pacing studies will be possible. Key issues to be studied concerning the ELM pacing aspect include penetration/mass required for small pellets to trigger ELMs, dependence of ELM pacing efficiency (including maximum frequency) on pedestal characteristics and the net effect on energy and particle confinement. Another important aspect for ITER is the analysis of the ELM energy deposition profile (radial-toroidal distribution) at the divertor for pellet-triggered ELMs, notably its dependence of the ELM size (for increased ELM frequency), plasma current and q_{95} . A further key goal for the Initial Research Phase II would be to demonstrate the compatibility of high density operation with pellet injection and ELM mitigation/suppression using RMP coils.

Here the main objectives are to:

- Demonstrate ELM pacing with pellets and mitigation of the transient heat loads due to ELMs in low collisionality plasmas.
- Identify critical parameters affecting the ELM triggering physics for further validation of theory and numerical modeling
- Assess the compatibility of high density operation with pellet injection and ELM mitigation/suppression using RMP coils

7.3.2.3 Vertical kicks

Triggering of ELMs via vertical plasma position oscillations is now routinely applied

for ELM control. These vertical plasma oscillations, often called vertical kicks, have been included as a backup ELM control system in ITER during the initial operation at low I_p (<10 MA) [11], with particular focus on the impurity control aspect during the access to and exit from H-mode.

Experiments in JT-60SA could contribute to a better understanding of the ELM triggering mechanism in low collisionality plasmas such as those predicted for JT-60SA during the initial carbon-wall phase, improving the prospects for more optimal use of this method in ITER. In addition, experiments in JT-60SA will provide a useful technical demonstration, since JT-60SA is a super-conducting tokamak like ITER. More R&D is required to establish the maximum vertical displacement amplitude and frequency that can be produced in JT-60SA.

7.3.2.4 ECRH modulation

The use of ECRH modulation for ELM pacing could also be tested in JT-60SA using the power modulation with the frequency of >5 kHz prepared for the NTM control. A better understanding of how the ELM dynamics might be affected by the edge power deposition and/or current drive will allow detailed physics investigations on ELM physics that could be used to develop other methods to triggering small ELMs. These type of experiments will greatly benefit from the high $T_{e,ped}$ plasmas expected in JT-60SA ($T_{e,ped} \sim 1-2$ keV) since power absorption/current drive efficiency increases with T_e .

7.3.3 L to H-mode transition studies

7.3.3.1 General L-H transition studies

JT-60SA is in a unique position to carry out L-H transition studies towards ITER at small ρ^* , low v^* , high density (with $n_e = 0.5 - 1 \times 10^{20} / m^3$) and low torque conditions, together with a large fraction of electron heating using ECH and NNB. Based on the ITPA 2008 scaling for the L-H threshold power P_{L-H} [12], in JT-60SA P_{L-H} is expected to be ~ 9.5 MW at 5.5 MA (2.25 T) and $n_e/n_{GW} \sim 50\%$ (see Fig. 7-5), and $P_{L-H} \sim 5.9$ MW in steady state scenario. In JT-60SA, the predicted L-H threshold power for hydrogen, helium and deuterium plasmas is well within the expected heating capabilities available during the Initial Research Phase, allowing the isotope scaling of the H-mode power threshold to be explored. Given the uncertainties in the L-H-mode threshold scaling when applied to ITER, these studies can be particularly useful in view of the initial, low-activation phase of ITER operations in hydrogen or helium.

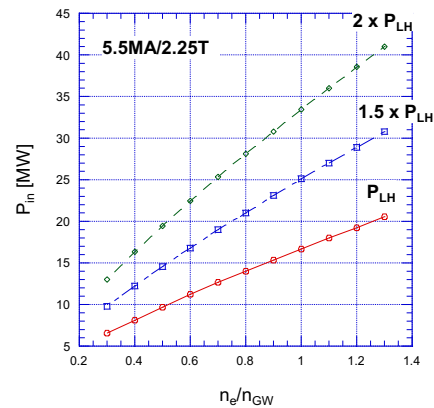


Fig. 7-5. LH threshold power at 5.5MA/2.25T in JT-60SA based on the scaling [12].

L-H transition studies will also include exploration of several parameters that are known to affect P_{L-H} , such as influence of q_{95} (scan in I_p) and density/magnetic field dependence of P_{L-H} , electron vs. ion heating methods, impact of rotation and changes in divertor geometry (X-point

height, X-point to target distance). Experiments in JET [13] and AUG [14] have found a significant decrease of P_{L-H} after the changeover to a metallic wall. The impact of Z_{eff} of P_{L-H} should therefore be included in the JT-60SA L-H transition studies during the C-wall in preparation for the installation of the metal wall. Moreover, the density dependence of the P_{L-H} has been found to be non-monotonic in many devices, with the existence of a minimum density (n_e^{min}) value below which P_{L-H} increases with decreasing density. In JT-60SA, operation with the carbon wall will allow studies on the low-density branch of the L-H transition to be performed.

Recent JET experiments [15] have shown that the addition 10-15% of He allows access to H-mode operation in H plasmas at lower input power. The confirmation of this result in JT-60SA would give more confidence in the usefulness of this approach for the initial non-active operational phase in ITER.

7.3.3.2 L-H transition studies related to ITER scenario development

The exploration of the L-H transition physics will also assess several aspects that are relevant for particular aspects of ITER scenarios. ITER may have to access H-mode during the current ramp-up. Since large ELMs must be mitigated in ITER, this implies that ELM mitigation methods should be turned on before or just after the L-H transition and this can have an impact on the P_{L-H} . For example, in most devices the application of RMPs causes an increase in P_{L-H} [16]. It is therefore important to examine the influence of ELM mitigation techniques on P_{L-H} during the I_p ramp-up, including their influence on the first type I ELM. Not only the L-H transition but also the H-L transition is important for ITER. The existence of hysteresis as well as the dependence of P_{H-L} on plasma current should also be studied.

7.3.4 Impact of pedestal on H-mode performance

The capability of high current access, balanced beam operation and the tuneable ratio of electron/ion heating place JT-60SA in an excellent position to carry out ITER relevant studies. The pedestal structure as well as ELM behaviour will be explored over a wide range of I_p , pedestal collisionalities and densities, in particular with the ITER-like scenario up to $I_p = 5.5$ MA and $n_e = 1 \times 10^{20} / \text{m}^3$ in order to establish a more robust prediction for the $Q=10$ baseline scenario in ITER. Developing of robust H-mode scenarios at high I_p will be a priority during the Initial Research Phase in JT-60SA. The available heating power will determine the quality of the H-mode plasma that can be achieved. This is a critical issue in ITER that will operate at relatively low input power above the L-H transition. It is known from existing experiments that operation close to the H-mode power threshold has intrinsic difficulties associated to long ELM free phases, causing large oscillations in the main plasma parameters and increased radiation, followed by H-L transitions. Experiments in JET have shown that ELM control (via vertical kicks in this case) can be effective to reduce the required heating power to access stationary H-mode plasmas with $H_{98} \sim 1$ [17]. Understanding the H-mode plasma performance at power levels marginally above the H-mode power threshold and the impact of ELM control in those conditions are important areas of research in JT-60SA, aimed at reducing the uncertainties regarding the power level required for reliable H-mode operation in ITER.

Although the focus of Initial Research Phase I (Hydrogen and Helium) in JT-60SA is preparation for the subsequent phase in deuterium, it would be desirable to allocate some dedicated experimental time to investigate the dependence of plasma transport and confinement

on the main hydrogenic ion isotope mass, which is of fundamental importance for understanding turbulent transport and, therefore, for accurate extrapolations of confinement from present tokamak experiments, which typically use a single hydrogen isotope, to burning plasmas such as ITER, which will operate in deuterium–tritium mixtures. The favourable scaling of global energy confinement time with isotope mass, which has been observed in many tokamak experiments, remains largely unexplained theoretically. Moreover, the mass scaling observed in experiments varies depending on the plasma edge conditions. JT-60SA can contribute to these studies, in particular connecting its findings with those obtained in H and D plasmas in JT-60U [18], in H, D, T and D-T plasmas in JET with C-wall [19] and in the isotope studies carried out in JET-ILW [20]. In addition, JT-60SA offers the possibility to explore the isotope effect in regimes where electron and ion temperatures can be decoupled (high T_i/T_e at low density or high T_e/T_i in dominated electron heating plasma), thus providing a wide range of plasma conditions for detailed comparisons with theory.

In terms of objectives for this topic, four main aspects are highlighted here:

- Determine H-mode operational boundaries: (a) H-mode quality at low input power above P_{L-H} , (b) assess the necessary power above P_{L-H} to achieve stationary H-mode (regular type I ELMs) with good confinement and (c) establish type I/III ELMs boundary (high density limit).
- Assess the impact of active ELM control methods (RMPs, pellets) on the power requirements to access good H-mode confinement.
- Examine the characteristics of the H-mode pedestal, ELM characteristics and H-mode confinement in JT-60SA when approaching ITER conditions (high triangularity, high I_p , low rotation, main electron heating, low collisionality).
- Isotope effect studies: (a) isotope effect on plasma confinement and edge plasma performance (pedestal structure, ELM losses); (b) isotope dependence of the power requirements to access good H-mode confinement and (c) isotope identity experiments in H and D

7.3.5 Establishment of physics basis on the edge pedestal characteristics

In H-mode, the height and width of the pedestal impact both core and edge physics. The pedestal structure, the width and the height, and inter-ELM transport will be investigated over a wide range of I_p and density in order to improve our confidence in the prediction of $Q=10$ plasmas performance in ITER. Extended configuration flexibility towards high δ and high κ is beneficial in sustaining high pedestal pressure or accessing type-II ELM/grassy ELM regime with high β plasma.

7.3.5.1 Pedestal scaling studies

Dimensionless parameter scans in triangularity, collisionality and Larmor radius (ρ^*) close to ITER-like values in JT-60SA to examine their influence (or lack thereof) on pedestal structure. Also, scan from identity points with current machines (JET, AUG, DIII-D) towards lower ρ^* could be done.

Influence of aspect ratio on pedestal stability (through its impact on the bootstrap

current): differences between JET and JT-60SA will be small but sufficient to justify some studies on this topic. This could be particularly relevant for advanced scenarios in steady-state conditions (aspect ratio changes significantly in the extrapolation to ITER).

Pedestal width scaling experiments with β_p are hampered by the fact that most diagnostic measurements are carried out in the outboard midplane. In this case two cancelling effects exist: the widening of the barrier in flux space (as one of the ruling models dictate) and the flux compression because of increase in global β_N . For this reason it is important to carry out high field side measurements by means of Thomson scattering or ECE in JT-60SA. At the high field side the two effects discussed above are amplified; as β_p increases the pedestal widens and the flux surface expand.

In particular for high density operation, variations on the fuelling mechanisms (gas vs. pellet fuelling) and detailed studies of their impact on the pedestal structure and SOL characteristics are issues that need to be addressed for ITER and DEMO.

7.3.5.2 Test of edge stability models

In order to test edge stability models (such as ELITE and MISHKA) a very high degree of accuracy of experimental pedestal profiles in T_e , n_e , T_i , J_{ped} , Z_{eff} , V_t , V_p , E_r as well as the neutral density profile is required. In addition the diagnostic time resolution needs to be sufficiently high to study the profile dynamics towards and through the ELM event. Moreover relative alignment of the measured profiles and an accurate magnetic equilibrium are important for comparison with models.

7.3.5.3 Test of pedestal turbulence simulations

Similar to the stability model testing, the turbulence simulations using gyrokinetic codes require accurate measurement of profiles and well constructed equilibria. Furthermore in order to compare the non-linear fluxes of the simulations high degree power accounting (ELMs, radiation, inter-ELM transport) is needed. Finally, to compare characteristics of the turbulence (frequency, mode structure, electromagnetic vs. electrostatic character) pedestal fluctuation measurements (BES, Doppler reflectometer, magnetics, ECE) are essential.

7.3.5.4 Ripple / TBM studies

The installation of test blanket modules (TBMs) increases the localized toroidal field (TF) ripple in ITER. The effects of these local TF ripple on the alpha particle loss, pedestal performance, edge rotation, ELM characteristics and so on are important to understand for suitable evaluation of acceptable amount of ferromagnetic materials and to enable extrapolation of results from present tokamaks to ITER. To investigate these effects in JT-60SA, ferromagnetic materials are installed into the horizontal port plug temporary. The TF ripple amplitude inside the plasma region of JT-60SA reaches 0.9% at the outer midplane under the TFC. The TF ripple amplitude is modified around the midplane by the ferritic inserts (FIs) and the normalized toroidal field is reduced to <0.5%. In ITER, the TF ripple amplitude is expected to be ~1.3%, ~0.7%, and 0.3% for 1.8 T, 2.65 T, and 5.3 T, respectively. The TBMs enables us to examine the effects of TF ripple towards ITER operation.

7.4. New research items due to the operation of JT-60SA

A list of new research items that will be possible in JT-60SA is presented below. Operations with high beta, long pulse, and electron dominant heating are attractive research areas for ITER and DEMO reactor.

- Control of high pedestal performance with moderate ELMs in high beta long pulse operation
- Relation between recycling and pedestal characteristics in the long pulse operation with forced water cooled divertor
- Edge and pedestal characteristics in advanced tokamak plasmas (compatibility of favorable confinement with internal transport barrier and reduction of ELM heat load)
- H-mode pedestal structure and ELM characteristics with main electron heating using 10 MW negative ion based neutral beam and 7 MW electron cyclotron heating system
- Pedestal and ELM characteristics at high plasma current (~ 5 MA)
- H-mode study with high density close to H-mode operation in ITER
- Edge pedestal characteristics in the variation of wall materials
- Improve understanding on edge density behaviour and plasma fuelling (gas vs. pellets). Dependence of fuelling efficiency by gas and pellets on plasma parameters
- Explore different ways of controlling inter-ELM heat loads in long pulses (multiple seeding impurities to optimize the radiation profile, development of real time control tools).

In JT-60SA, dominant electron heating is possible by the installation of 10 MW negative ion based neutral beam and 7 MW electron cyclotron heating system. Besides, RMP control using error field correction coil system, long pulse operation for 100 s with 20MW NBs (or 60 s with 30 MW NBs), high plasma current up to ~ 5 MA are possible under the forced water cooled divertor system. Based on these specifications of JT-60SA device, we propose the following objectives on the pedestal and edge physics research.

- Establishment of physics basis and control methods on the pedestal and edge plasmas which can be extrapolated to ITER and DEMO reactor.
- In particular, reduction/mitigation of ELM heat load which is one of the most crucial issues in ITER, pedestal and ELM characteristics under dominant electron heating, and the compatibility of high pedestal confinement and wall saturation in high beta long pulse discharge for DEMO reactor are focused.
- Control of burning plasma by optimized pedestal condition

7.4.1 Effects of metal wall on edge pedestal and ELM characteristics

In preparation of ITER and DEMO, plasma facing components in JT-60SA will be converted from carbon to full tungsten (W) after the Integrated Research Phase I is completed. Experiments in the previous experimental phases will be carried out with Carbon as a wall material, which is less restrictive on the achievable operational space and allowed wall power loads, thus allowing testing high performance and high temperature edge conditions.

Experiments in existing metallic wall devices have shown that the H-mode pedestal confinement can be strongly affected by the choice of first wall materials through plasma impurity composition and the operational measures required to prevent first wall damage (e.g.

gas fuelling). The ASDEX Upgrade carbon wall was replaced by a DEMO-relevant full W-wall and divertor [21], whereas in JET the carbon wall was fully replaced by an ITER-like Be main chamber first wall and W divertor (ILW) [22].

In devices that use W as a plasma facing component, a common pattern has been found, that the pedestal and global confinement are affected by the requirement for increased gas fuelling (to screen high-Z impurities influxes) as well as a change in pedestal stability due to a decrease of the low-Z impurity concentration in the pedestal region. Basically, the requirement for strong gas puff leads to the conventional confinement degradation that has generally been seen at high densities. The use of enhanced particle control through divertor pumping has allowed recovering good H-mode performance ($H_{98} \sim 1$ and $\beta_N \sim 1.8-2$) in the JET-ILW baseline scenario at 2-3 MA. The beneficial effect of divertor pumping on confinement has been observed at both low [23] and high triangularity [24], but only at the lower gas fuelling level compatible with stationary conditions. Operation at high density ($n_e/n_{GW} \geq 0.8$) while keeping a sufficient H-mode confinement ($H_{98}=1$) is key requirement to achieve $Q=10$ in ITER and a similar comment can be applied to DEMO (with $n_e/n_{GW}=1.1-1.3$). JT-60SA offers a unique opportunity to investigate the impact of wall materials in the H-mode performance at high density (and at high triangularity) in a large scale device, thus contributing to reduce the uncertainties in the extrapolability of such regimes to ITER and DEMO.

The reduction in the pedestal pressure at high density in high triangularity H-mode plasmas can be partially overcome by nitrogen seeding in JET-ILW [25] and AUG [26]. The changes in H-mode performance associated with the change in JET wall composition from C to Be/W point to D neutrals and low-Z impurities playing a role in pedestal stability, elements which are not currently included in pedestal models. The role of low-Z impurity on pedestal stability and confinement has not yet been understood and thus should be an important topic of investigation in JT-60SA.

In both JET for the high density branch of P_{L-H} [13] and AUG [14], the L to H-mode threshold power was reduced by 20-30% after the full transition to a metal wall environment. The significant reduction of the carbon concentration may be a key factor in the observed reduction of P_{L-H} with a metallic wall, and thus studying the influence of low-Z impurity concentration on the L to H-mode physics can also be an important issue in JT-60SA.

7.4.2 Predictions and modeling of the edge pedestal plasmas in JT-60SA

In advance to the operation of JT-60SA, the predictions of the edge pressure gradient and the spatial width of H-mode pedestal based on the edge stability analysis are important issues for ITER and DEMO reactor. An example of the linear MHD stability calculation for Scenario 2 (5.5 MA, $n_e/n_{GW}=0.75$), with plasma profiles taken from scenario simulations reported in [27], is shown in Fig. 7-6. At this high density, the ballooning component of the PBM becomes unstable in the pedestal region ($\psi=0.8-1.0$). The integrated edge-pedestal model of TOPICS-IB will be improved

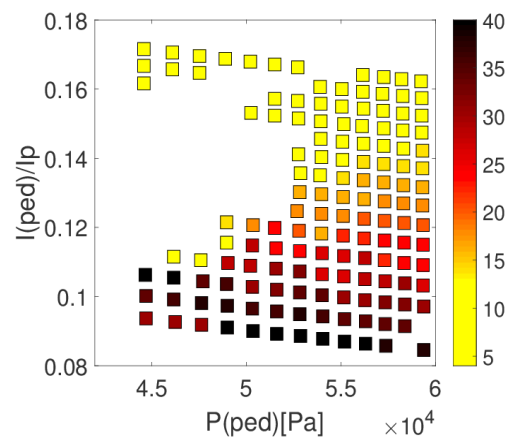


Fig. 7-6. Edge stability diagram based on linear calculation for scenario 2 (5.5MA, $n_e/n_{GW}=0.75$).

further by the sophisticated modeling of edge pedestal structure based on the theory and experimental database. In the strategy for application and improvement of theoretical models and simulation codes, these codes should cover issues in the central research needs for ITER and DEMO. Therefore, the verification (code-to-code benchmark tests) and the validation (code-to-experiment comparison) among the JA and EU integrated edge-pedestal models, such as TOPICS, JOREK, JINTRAC, MISHKA and RMP non-linear MHD modeling, are very important. They can be used for the prediction of the JT-60SA experiments and the extrapolation to ITER and DEMO plasma. After verifying the gyrokinetic code results (see 3.5.3), these codes will be used to predict the critical gradients in pedestal that can be sustained in the inter-ELM period and in combination with the MHD stability codes, will be used to predict the pedestal structure (width and height) prior to an ELM crash.

7.5. Research items in each phase

It is not considered likely that there will be sufficient operational time available during the Initial Research Phase I to carry out dedicated physics studies with the required diagnostic information. Thus, all research topics in this chapter are assumed to start in the Initial Research Phase II, this includes the request for an additional Hydrogen campaign to complete the proposed isotope studies.

(1) Initial Research Phase, Phase II (Deuterium, up to 33MW):

H1. ITER scenario development

- First assessment of type-I ELMy H-modes with parameter scans of power, gas, heating method, etc. in D-plasma
- Characterize the pedestal and ELMs in reactor relevant low v^* regime and at high triangularity
- Initial exploration of I-mode
- Isotope study by comparison between H and D in phase II.

H2. Steady-state high beta scenario development

- Access to small ELM regime (QH-mode, grassy ELMs) in which low density and/or v^* are required

H3. ITER risk mitigation

- Determine power threshold for L-H transition in hydrogen plasmas: (a) validate/extend existing scalings; (b) identify hidden parameters affecting the L-H transition: rotation, divertor geometry, etc; (c) validate/extend L- to H- transition models
- Determine the operational boundaries for type I ELMy H-mode in hydrogen plasmas: power requirements for $H_{98}=1$ operation and Type I /Type III ELMs boundary at high density
- Establish effectiveness of ELM mitigation with RMPs and low v^* and physics model validation
- Characterize H-mode plasma performance with marginal input power above P_{L-H}
- Determine impact of RMPs on the L-H power threshold

Others:

- Commissioning/validation of edge/pedestal diagnostics (diagnostic information

essential for comparison with deuterium operation)

- Establishment of physics basis on H-mode pedestal and L-H transition
- If possible, explore L-H transition and H-mode performance with mixed isotopes. During the deuterium phase, there will be hydrogen phases for the purpose of out-gassing that could be used in conjunction with deuterium beam injection.
- Understanding of pedestal characteristics under the dominant electron heating
- ELM mitigation/suppression experiments using RMPs (+ active ELM control using pellet pace making)
- Investigation of the pedestal characteristics accompanied by the compatibility of high beta and reduction/mitigation of ELM heat load
- Physics studies for extension towards the Integrated Research Phase
- Extension of grassy ELM, type-II ELM, QH-mode regime at high v^* towards the metal wall
- Access to type-II ELM regime at high density and QDN configuration

(2) Integrated Research Phase, Phase I, II (Deuterium, up to 37 MW):

Operational scenario study on long sustainment of high performance pedestal in high beta operation.

- Sustainment of high pedestal performance in long pulse discharges for 100 s under the forced water cooled divertor
- High density H-mode experiment (comparison gas/pellet fuelling)
- H-mode experiment under the dominant electron heating in long pulse duration
- Sustainment of high pedestal performance in H-mode operation with small/no ELMs and under the RMP control
- Control of burning plasma by optimized pedestal condition
- Impurity seeding effect under the metal wall condition
- Develop robust scenario with good pedestal conditions and inter-ELM heat load reduction by combining various impurities (N/Ne/C and K/Ar)

(3) Extended Research Phase (Deuterium, up to 41 MW):

- Pedestal and ELM characteristics in double null plasma configuration
- Sustainment of high pedestal performance in high beta long pulse operation
- Scan of operational conditions expected during metal-wall operation (gas puffing rates, central heating, ELM pacing for impurity control)
- Explore the effects of modulated edge ECRH/ECCD for ELM frequency control

References

- [1] A. Zhitlukhin et al, Nucl. Mater. 363-365 (2007) 301
- [2] A. Loarte et al, Nucl. Mater. 313-316 (2003) 962
- [3] P. B. Snyder et al., Phys. Plasmas 16 (2009) 056118
- [4] H. Urano, et al., Proc. 26th IAEA Fusion Energy Conference (Kyoto, Japan, 2016), IAEA-CN-234/EX/3-4
- [5] A. Garofalo et al., Physics of Plasmas 22, 056116 (2015)
- [6] E. R. Solano et al. Phys. Rev. Lett. 104, 185003 (2010)
- [7] A.E. Hubbard et al. Nucl. Fusion 57 (2017) 26039
- [8] J. Stober et al. Nucl. Fusion 41 (2001) 1123
- [9] A. Kirk, et al., Nucl. Fusion **55** (2015) 043011.

- [10] Y. Liang, et al., Nucl. Fusion **53** (2013) 073036.
- [11] A. Loarte et al., Nuclear Fusion 54 (2014) 033007
- [12] Y. R. Martin et al, J. Phys: Conf. Series 123 (2008) 012033
- [13] C. Maggi et al., Nuclear Fusion 54 (2014) 023007
- [14] F. Ryter et al., Nuclear Fusion 53 (2013) 11303
- [15] J. Hillesheim et al., Proc. 26th IAEA Fusion Energy Conference (Kyoto, Japan, 2016), IAEA-CN-234/EX/5-2
- [16] M.E. Fenstermacher et al., Proc. 23rd IAEA Fusion Energy Conference (Daejeon, Rep. of Korea, 2010), IAEA-CN-180/ITR/1-30
- [17] E. de la Luna et al., Proc. 24th IAEA Fusion Energy Conference (San Diego, USA, 2012), IAEA-CN-197/EX/6-1
- [18] H. Urano et al., 2008 Nucl. Fusion 48 045008. H. Urano et al., 2012 Phys. Rev. Lett. 109 125001. H. Urano et al., 2013 Nuclear Fusion 53 083003
- [19] Cordey J G et al 1999 Nucl. Fusion 39 301
- [20] Maggi CF et al., Plasma Phys. Control. Fusion 60 (2018) 014045
- [21] R. Neu et al., Phys. Scr. (2009) 014038
- [22] G. Matthews et al, Physica Scripta, T128 (2007) 137
- [23] E. Joffrin et al, Nuclear Fusion 57 (2017) 086025
- [24] E. de la Luna, et al., Proc. 26th IAEA Fusion Energy Conference (Kyoto, Japan, 2016), IAEA-CN-234/EX/P6-11
- [25] C. Giroud et al., Nuclear Fusion 53 (2013) 113025
- [26] J. Schewinzer et al., Nuclear Fusion 51 (2011) 11303
- [27] J. Garcia, et al., Nucl. Fusion 54 (2014) 093010

8. Divertor, SOL and PWI

With JT-60SA's objectives being sustaining high-confinement and high-density plasmas for up to 100 s at high heating power the primary aim of divertor, scrape-off layer (SOL) and plasma wall interaction (PWI) research is the safeguarding of the plasma facing components of JT-60SA. Furthermore, JT-60SA shall serve as an experiment to provide a solid scientific basis for power and particle exhaust for supporting the operation of ITER and extrapolating to DEMO, for which integrated scenarios in a metallic wall are a key. Therefore, JT-60SA will undergo two distinct operational phases in view of PWI and power exhaust studies. These two phases consist of PFCs being either C or W. The first phase will consist of C as a plasma facing component. Commissioning of the device will start in upper single null operation with inertially cooled protection tiles located at the top of the device and serving as an upper divertor. With further completion of the device, a lower divertor with water-cooled CFC tiles will have been installed that handles 10 MW/m^2 for up to 5 s followed by a water-cooled CFC mono-block divertor designed for 15 MW/m^2 for up to 100 s. During this first phase the main activity in this chapter is the protection of the machine with SOL upstream conditions being particularly challenging in scenarios #2 and #5, as the density at the separatrix, n_e^{sep} , is expected to be low. Despite the intrinsic C impurity additional seeding of impurities such as Ar may be required to mitigate the power load to the target (be it by reducing the pedestal pressure and thus ELM size and/or the inter ELM power loads, as observed on JET with C PFCs).

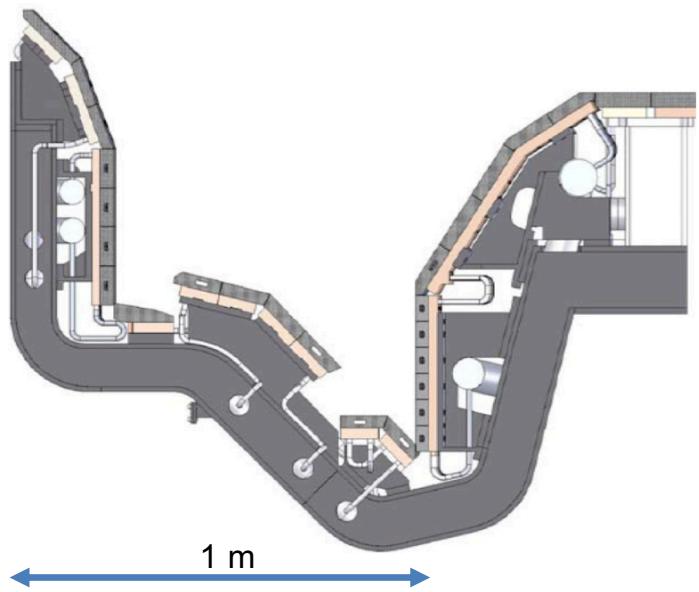


Fig. 8-1 Cross-section of the divertor cassette with a V-shaped corner.

In order to prepare for the second phase of operation some impurity transport studies for heavy impurities will be required. These will serve to develop strategies that will be needed to prevent the accumulation of heavy impurities in the core plasma. The means to do these studies might be limited by operative and technical restrictions of diagnostics or heating schemes.

The second phase will consist of a full metal wall, meaning that all PFCs will be covered by either W coated CFC or potentially even solid W, with the latter most likely limited to the outer divertor region. In this phase protecting the PFCs at low Greenwald density and low gas throughput will be particularly challenging as the experience from the devices ASDEX Upgrade and JET have demonstrated. However, ultimately it will be tried to aim to reconcile current drive scenarios with the protection of a metal wall. In the frame of this chapter, the 2nd phase will focus on achieving integrated power and particle exhaust scenarios as well as providing well diagnosed discharges that allow for an ultimate validation of relevant numerical codes. ITER and DEMO relevant exhaust scenarios using extrinsic impurity seeding species such as N_2 , Ne and Ar will be studied. JT-60SA will gain a particular DEMO relevance as the entire wall will be covered by a high Z metal such as W, similar to ASDEX Upgrade, but on a larger major radius device.

Among the research in the area of Divertor, SOL and PWI, the highest priorities have been given to the following research items in the Initial Research Phase I and II as described in Chapter 2:

Headline-I-1. Stable operation at high current in large superconducting machine:

- EC wall conditioning

Headline-II-1. ITER scenario development:

- Detachment physics and code validation

Headline-II-2. Steady-state high beta scenario development:

- Fuelling and pumping for density control
- Protecting target plates by detached divertor

Headline-II-3. ITER risk mitigation:

- SOL width scaling
- H/D ratio control by gas-puffing and pellet
- He pumping

These research items are recognized to contribute significantly to the JT-60SA project. Hereafter, details of these research items are described in view of practical experiments in JT-60SA with objectives, significance, and expected results in accordance with the research phases, where available hardware capability is defined.

8-1. Initial Research Phase I

In the latter part of this research phase, hydrogen or helium plasmas with an auxiliary heating power of 19 MW together with the lower divertor equipped with water-cooled CFC tiles are available. Only one prioritized research item, Electron Cyclotron Wall Conditioning (ECWC), is assigned in Chapter 8. In devices with a carbon wall, which is a major hydrogen reservoir, particles retained in the wall are required to be removed in order to obtain a reproducible discharge conditions. This is especially needed to recover from a disruption for example. In superconducting tokamaks, wall conditioning techniques commonly used in normal conducting tokamaks are difficult to employ. This is not only an issue for JT-60SA but also in other superconducting devices such as ITER. Hence developing another wall conditioning technique, as for example an RF discharge cleaning method with He gas, such as ECWC, is required. The parameters with the highest wall cleaning efficiency determined in JT-60SA will contribute to determine operational parameters in larger devices such as ITER along with some scaling, as for example the injection of EC power over the wall surface area.

EC wall conditioning:

As electron cyclotron waves with frequencies of 82 GHz, 110 GHz and 138 GHz are

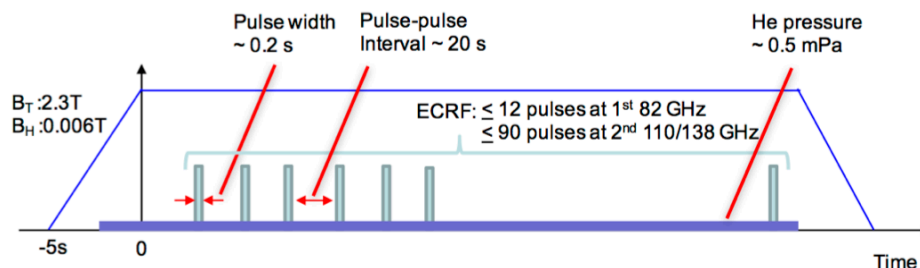


Fig.8-2 A scenario of electron cyclotron wall cleaning (ECWC).

available in JT-60SA, ECWC with a fundamental EC wave at 82 GHz is considered to be the best option. However, only a limited number of pulses (< 12 pulses) with a pulse width of 0.2 s at 82 GHz are available while more pulses (< 90 pulses) are available with second harmonics at 110 GHz and 138 GHz. Hence, the development of ECWC with the second harmonic waves as well as with the fundamental one is an urgent issue. The goal of this research is to determine the operational parameters of ECWC to maximize the outgassing efficiency. For this purpose, systematic scan of parameters will be performed with matched toroidal magnetic field with an EC-pulse width around 0.2 s, an EC-pulse interval around 20 s (\sim a ratio of vacuum vessel volume to a pumping speed), and He pressure of ~ 5 mPa based on the present knowledge as shown in Fig. 8-2. Table 8-1 shows priorities of the parameter scans. In addition, several poloidal magnetic field patterns at about 0.006 T ($\sim 0.3\%$ of the toroidal magnetic field) will be tested to improve the outgassing efficiency. Further, a trapped particle configuration (TPC) will be considered as one of the poloidal field patterns to enhance the outgassing efficiency. Because the EC stray radiation may damage vacuum components significantly, this parameter-scan should be performed carefully, for example, by starting with low injection power.

Table 8-1. Priority of ECWC parameter scans for (upper) the pulse-interval scan and (lower) the He pressure scan over the EC pulse width.

EC pulse width Pulse-interval	0.1 s	0.2 s	0.5 s	1.0 s
10 s	2	1	2	
20	1	1	1	2
40	2	1	2	

EC pulse width He Pressure	0.1 s	0.2 s	0.5 s	1.0 s
1 mPa	2	1	2	
5	1	1	1	2
10	2	1	2	
100		3		

8-2. Initial Research Phase II

In this research phase, deuterium plasmas with a deuterium neutral beam heating power up to 30 MW together with an ECRF power of 3 MW are available. However, the water-cooled mono-block divertor will not be yet ready. Hence although long-pulse experiments with a flat top duration of 100 s are not yet possible, physics studies within a limited pulse length, i.e., a peak heat load on the target plates of $10 \text{ MW/m}^2 \times 5 \text{ s}$, can be initiated.

The enhanced heating system can deliver sufficient power to the divertor plasma (> 20

MW/m²), allowing to address a key research issue in this chapter, i.e., radiative plasma cooling study for protecting target plates. Given that Scenario 2 and 5 require low separatrix densities (30-40% of the line-averaged density, $2.2 \times 10^{19} \text{ m}^{-3}$ and $1.7 \times 10^{19} \text{ m}^{-3}$, respectively), it is a real challenge to reduce the heat load onto the divertor target down to 10 MW/m² with such low upstream density. Thus, in this research phase, within the available cooling capability, basic characteristics of the divertor plasma such as roll-over density, neutral and impurity compression, impurity transport/radiation, and so on will be investigated, in view of preparing the long-pulse experiment planned in the next research phase. In addition, accumulation of the basic data on detachment physics experiments will be used as input for code validation.

In this research phase, ITER-risk-mitigation related studies are also addressed. In experiments at a plasma current of 5.5 MA such as Scenario 2, a high poloidal magnetic field at the separatrix (B_p^{sep}) can contribute to the validation of the SOL width scaling (SOL width $\lambda_q \sim B_p^{\text{sep} 1.19}$) [1], by extending the experimental data set beyond the basis of the current scaling for B_p^{sep} towards ITER and DEMO relevant values. This is one of the issues to be addressed in high-current and large devices such as JT-60SA before ITER. He-pumping study can also be initiated in this research phase by using He neutral beam as a mimic of He ash produced by DT reaction in the plasma core. It is expected from results in JT-60U He-pumping experiment that the He-pumping efficiency depends on the divertor geometry. Thus, comparing the He-pumping efficiency between JT-60U and JT-60SA can provide significant knowledge, which contributes to the determination of the divertor geometry for DEMO. Another important hardware enhancement in this research phase is a pellet injector, which plays an essential role for density control along with gas-puffing, neutral beam fueling, and the cryo-panel divertor pumping. The pellet injector contributes to core fueling while the gas-puffing mainly contributes to peripheral fueling. Hence the combination of the pellet and the gas-puffing is a suitable tool for controlling the HD ratio, which is a mimic of the DT ratio control in ITER and DEMO.

Protecting target plates by detached divertor:

This research is basically associated with impurity seeding. It is predicted that radiative cooling by intrinsic carbon alone is not sufficient to reduce the heat load down to 10 MW/m², except for high density operation such as Scenario 3. Thus, impurity seeding is mandatory. Given that the absolute separatrix density in Scenario 2 is the highest except for Scenario 3, it is better to initiate first the radiative cooling experiment for Scenario 2. Figure 8-3 shows the operational space for Scenario 2 in terms of deuterium and argon puffing rates, predicted by the

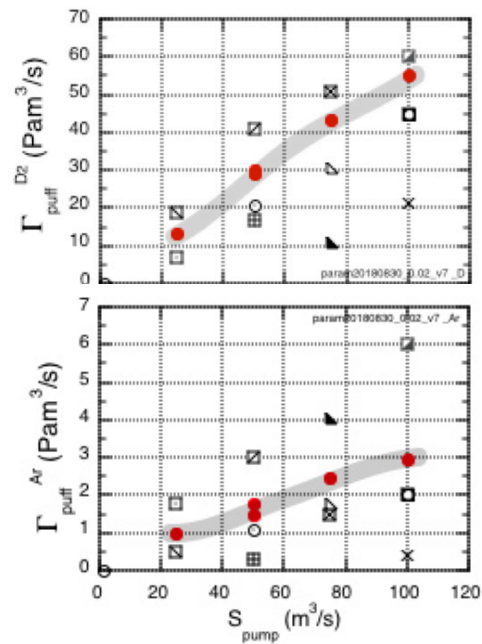


Fig.8-3 (upper) deuterium and (lower) argon puffing rate as a function of divertor pumping speed. Closed symbols show operational space, where low separatrix density ($< 2.5 \times 10^{19} \text{ m}^{-3}$) and low peak heat load on the target plate ($< 10 \text{ MW/m}^2$) are satisfied simultaneously, predicted by SONIC [2].

SONIC code [2]. With increasing divertor pumping speed, both the deuterium and the argon puffing rates increase in order to simultaneously satisfy the following two conditions: low separatrix density ($< 2.5 \times 10^{19} \text{ m}^{-3}$) and low peak heat load on the target plate ($< 10 \text{ MW/m}^2$). The operational space indicates that required Ar puffing rate is $\sim 5\%$ of the D_2 puffing rate. In terms of low core contamination, the experiment around the lower limit is preferred. Hence after confirmation of the operational space, the Ar injection rate will be tried to reduce below the operational space at fixed D_2 puffing rate. Also, replacement of part of Ar puffing by N_2 or Ne puffing is planned because of lower core contamination and higher radiative characteristics of these species in the divertor. For this purpose, N_2 or Ne is puffed into the divertor plasma through the pumping slots while Ar is puffed into the SOL plasma through the upper or the low vertical port.

In order to simulate impurity seeded plasmas, a transport code with capability to simulate several impurity species including an intrinsic impurity, as for example carbon, at the same time is required. It is already possible for the SONIC code to simulate C and Ar transport with a Monte-Carlo technique. Further improvement to simulate three impurity species is planned for analysis of a mixture seeding experiments, for example, Ne and Ar, in addition to C. The SOLPS-ITER as well as the EDGE2D-EIRENE codes and COREDIV will also be used on JT-60SA data and in preparation of its operation.

In this research phase, as preparation for the long-pulse operation, radiation feed-back control experiment will be initiated. One of the issues in the radiation feed-back control is an overshoot/undershoot of the radiation power over/below the reference value due to the time delay from the injection to the radiation increase. In order to avoid the overshoot, a time-dependent simulation code, instead of a steady-state simulation code, is required. Development of the time-dependent SONIC code is planned to be ready in this research phase.

Detachment physics and code validation:

This research item consists of several fundamental studies. Detachment onset significantly depends on the heating power and the neutral pressure at the divertor, with the latter being determined by the ratio of the particle fueling rate to the divertor pumping speed in steady-state plasmas, which is influenced by the conductance between the main and the divertor chamber. In JT-60SA, the V-shaped corner contributes to enhancing the neutral pressure, leading to divertor detachment at low fueling rate, or low mid-plane density. The density for the onset of detachment, or “roll-over” of the particle flux to the divertor target plate is measured in order to establish a database, which is used as an input for validation of simulation codes. For simplicity, L-mode plasmas with low heating power without seeding impurity is preferred for this experiment as well as experiments with higher power and low ELM frequency or with high density and small ELMs.

At high neutral density, absorption of neutral hydrogen emissions in the divertor plasma, particularly Ly_α , is considered to increase the ionization rate. In order to simulate the Ly_α absorption, transport simulation of Ly_α emission is required, resulting in a big computational cost as for example by the EIRENE code. Hence approximation with an escaping factor is one of the methods and is planned to be implemented in the SONIC code.

Impurity transport is also one of the essential studies in terms of detachment physics. In order to analyze the impurity transport to determine for example a radial diffusion coefficient of an impurity, both the source distribution and the transported ion distribution, respectively represented by neutral impurity emission and highly ionized impurity ion emission, are needed. In addition, the impurity compression ratio, defined as a ratio of the impurity density in the divertor to that in the core plasma, is of significance in terms of impurity transport. Therefore, quantitative spectroscopy in the divertor and the core plasmas are key diagnostics. Two-

dimensional visible spectroscopy, which covers the whole area of the divertor with a spatial resolution of 1 cm is available along with core VUV and CXRS spectroscopy. For the intrinsic impurity, carbon, it is also important to measure the source flux by physical and chemical sputtering in order to validate the sputtering models, implemented in the simulation codes.

Fueling and pumping for density control:

Another hardware enhancement in this research phase is a pellet injector. The pellet injector can contribute to enhancing the core fueling rate significantly as shown in Fig. B-2. At an injection rate of 10 Hz with a pellet size of 2.4 mm ϕ x 2.4mm l , it is expected to reach the required line-averaged electron density, i.e., 50% of Greenwald density, in Scenario 2 on the assumption that the confinement time of the pellet fueled particles is equal to that of the NB fueled particles. Because the injection frequency can be increased up to 20 Hz, some room for density control will be available, allowing for real-time feed-back control of the core electron density by pellet injection.

Impurity injection will be performed through the inner and the outer divertor pumping slots, and the lower and the upper ports. Because the injection rate is independently controlled, the residual time of impurities puffed from different ports in plasma, i.e., the time from the injection to the pumping out can be characterized.

SOL width scaling:

The heat flux decay length in the SOL in ITER is predicted by a well-established scaling, $\lambda_q \sim B_p^{-1.19}$ [1]. In order to validate the SOL width scaling over the present B_p range, a high poloidal magnetic field operation by a maximum plasma current of 5.5 MA will be initiated. As shown in Fig. 8-4, the poloidal magnetic field of Scenario 2 lies beyond the present B_p range, contributing to validation of the SOL width scaling, but further high poloidal magnetic operation would be preferable. Although the SOL width scaling is for inter ELM with the divertor attached, the scaling for detached plasmas is more relevant to ITER and DEMO. This is a very important mission to be addressed in a large device with a high plasma current such as JT-60SA.

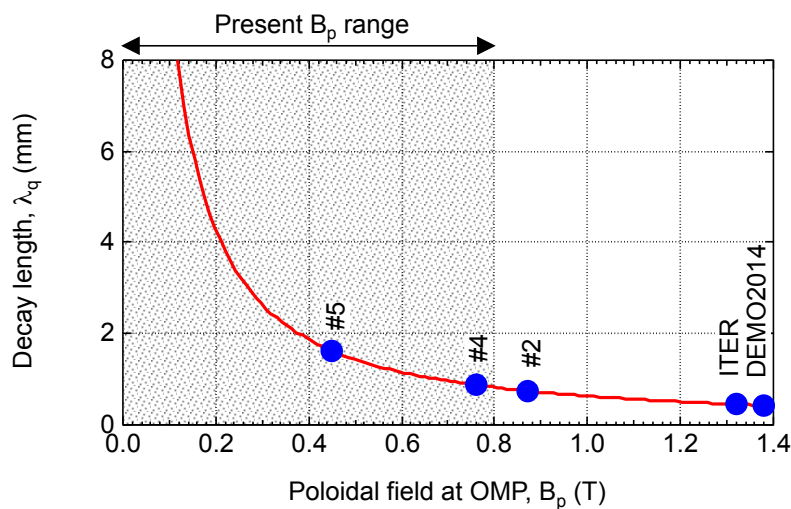


Fig.8-4 Scaled heat flux width as a function of the poloidal magnetic field at mid-plane [1] together with several data predicted in JT-60SA, ITER and DEMO.

H/D ratio control by gas-puffing and pellet:

As a mimic of deuterium-to-tritium (DT) ratio control in ITER and DEMO, hydrogen-to-deuterium (HD) ratio control experiment will be initiated. One of the experimental scenarios is to inject hydrogen by the pellet injector while deuterium is injected by neutral beams and gas puffing. Another scenario is to use two independent extruders, one for injecting hydrogen pellets and the other one for deuterium pellets. In both cases, a measured HD ratio is used for a real-time control of the injection rate of hydrogen and deuterium. For the analysis with simulation code, a bit tricky improvement is required: two species of fuel particles are simulated simultaneously. This is because the HD ratio is controlled around a ratio of 1:1 although the minor fuel particle can be treated as an impurity if the ratio is very high or low. This implementation in the SONIC code is also planned in time for this experiment.

He pumping:

He exhaust is one of the most important issues in DT fusion devices. In JT-60U, H-mode operation without He accumulation was established but with the divertor plasma attached. In JT-60SA, He-pumping experiments in an H-mode plasma with the divertor in the detached regime will be initiated in this research phase with the He neutral beam injection mimicking the He ash produced by DT reaction. In this experiment, He neutral beam injectors with up to 8 beam lines can be used to mimic the He production while the other deuterium beams are used for heating. From a ratio of core He density to He injection flux, an effective He confinement time is evaluated together with a He compression ratio from a divertor He density by the two dimensional visible spectroscopy. In JT-60U, it was found that momentum transfer from D^+ to He via elastic collision is a key process to enhance the He exhaust rate. From an asymmetric Doppler profile of the spectral line shape of the He I line, the effect of the elastic collision will be evaluated as performed in JT-60U. Because the elastic collision depends on the divertor geometry, a comparison between JT-60U and JT-60SA contributes to the design of the divertor in DEMO. Due to specific processes with He, significant improvement may be needed for analysing He transport with simulation codes. He atoms at a metastable level, due to the long life time, may need to be treated as independent similarly to ground level He atom. In addition, absorption of He I line increases He atom ionization rates, similarly to the Ly_α absorption. Implementation of these effects in the SONIC code is planned for the time for the experiment.

Preparation of a metallic wall:

Different methods of injecting high Z materials as trace impurities into the plasma during the C-wall phase in anticipation of the transition to a high Z, i.e. W-wall, are considered. Laser blow off of Mo or W appear not to be possible due to technical constraints. It is unlikely that a planned removable probe can be used as a source of the trace impurities. Therefore, a remaining option may be the injection of gaseous high Z impurities, such as Kr and WF_6 into the plasmas of the different operating scenarios in order to attempt to study the migration and particularly the core accumulation and re-distribution physics. This will be important in order to support or even to confirm numerical studies made in preparation related to the transport of high Z impurities in the core plasma and determine the risk of core accumulation in view of the core and pedestal plasma profiles and the available heating systems for on and off-axis heating. Mimicking the expected source distribution of high Z impurities will be nearly impossible in the C-wall phase of the device, but these experiments should shed light onto the potential requirement for heating upgrades that may become necessary when transitioning to a high Z wall over the operational time of the device. The impurity transport will be interpreted using state of the art numerical tools available through the Japanese and European scientific

communities at the time of the experiments.

PWI studies:

A material test by plasma exposure is of significance for studies on erosion, melting, blistering, deposition and hydrogen retention in the materials, in particular, metals, for future fusion devices. In order to investigate the temperature dependence of the above described characteristics, the installation of several material probe systems with heaters is under consideration at the inner and the outer divertor, and on the louver, for instance. In particular, a bulk tungsten probe, with controlled temperature (above ductile-brittle transition temperature and below recrystallization temperature) would be important from an engineering aspect for developing plasma-facing components for future fusion devices such as DEMO.

A metal probe pre-irradiated by neutrons is one of the methods to investigate effects of neutron irradiation on deuterium retention from comparison with non-irradiated metal probe. It would be useful if the probe can be inserted and retrieved between pulses. This probe can also be used for a thickness monitor of boron layer produced by boronization.

Because of significantly high heat and particle flux, it is expected that the outer divertor target plate is eroded. On the other hand, thick deposition is expected on the inner divertor target plate and on the louver above the divertor cryo-panels. The mass balance between these locations is useful for material migration studies. After the Initial Research Phase II and the Integrated Research Phase I, respectively some divertor bolted tiles and mono-blocks together with armor tiles on the stabilization plates and those on the inner wall are exchanged. Some of these tiles will be available for post-mortem analysis and also for observation of arcing signatures. In addition to the mass balance analysis, from the erosion depth, the lifetime of the plasma-facing components, in particular, the outer divertor plates can be estimated. This information is important toward the Integrated Research Phase, where significant erosion is expected by repetition of long-pulse discharges with high heating power. Hence this estimation should be obtained before the Integrated Research Phase.

Dusts and co-deposit on various locations are collected after the Initial Research Phase II. In order to continue the dust and co-deposit collection after the Integrated Research Phase I, development of remote handling methods should be established. This will also contribute to dust and co-deposit removal in ITER.

Estimation of particle inventory inside the vessel is one of the most important PWI issues. Because of lower safety factor and lower toroidal ripple in JT-60SA compared to JT-60U, the particle retention distribution in the main chamber is expected to be different. Understanding of retention mechanism by comparing results in JT-60U and JT-60SA may be helpful for design of future devices even with non-carbon plasma-facing components. This study will continue after the changeover to a full tungsten PFCs.

8-3. Integrated Research Phase onwards

JT-60SA will explore compatibility of long-pulse high- β plasmas and metal plasma-facing components in support of ITER and DEMO after the primary mission of JT-60SA, i.e., long-pulse high- β plasmas, is achieved with carbon plasma-facing components; carbon has advantages as shown in Table 8-2, and satisfies the requirements in the present fusion experimental researches. Hence the original project agreement between JA and EU concluded that carbon plasma-facing components are the most reliable for achievement of the long-pulse high- β plasmas in JT-60SA. However, the disadvantage of high fuel retention and short lifetime is not acceptable in ITER and DEMO. Here ‘metal’ does not indicate only tungsten but other advanced metal materials.

Table 8-2 Comparison of advantages and disadvantages between carbon and metal (tungsten)

	Advantage	Disadvantage
Carbon (CFC)	<ul style="list-style-type: none"> Rich operational experience Highly radiative in divertor Low radiative efficiency in core plasma High thermal shock resistance Wide operational temperature window High heat flux resistance High thermal conductivity 	<ul style="list-style-type: none"> Lifetime (high sputtering yield) No active control in divertor Flakes/dust leading to disruption High retention leading to high outgassing Neutron-induced damage
Tungsten (coating)	<ul style="list-style-type: none"> Long lifetime (low sputtering yield) Possibility to access high density Low retention High thermal conductivity Less dust production Larger headroom for use of radiative cooling Less/easier conditioning 	<ul style="list-style-type: none"> Highly radiative in core plasma Potential accumulation in core Narrow operational temperature window Possible melting and recrystallization Delamination of coatings Activation by neutron irradiation Lower plasma Te in divertor required to limit sputtering (ELMs important)

Metal plasma-facing components have the advantage of low fuel retention, long lifetime and low radiative power in the peripheral plasmas. The advantage of low fuel retention results in low outgassing, alleviating difficulties of steady-state particle control. The advantage of low radiative power contributes to access to high-density regime over the density regime limited by carbon radiation in the peripheral plasmas. However, once the metal ions penetrate into the core plasma, they tend to accumulate and radiate significantly, lowering the core plasma temperature. Hence issues with metal plasma-facing components are suppressing sputtering of the metal plasma-facing components, shielding generated metal ions by peripheral plasmas, avoiding metal accumulation in the core plasma, and expelling accumulated metal ions from the core plasma. A larger operational window between the onset of divertor detachment and the H- to L-mode transition has been found in the metal devices JET and ASDEX- Upgrade and is thus expected for the metal phase of JT-60SA. Nevertheless, operation with a metallic wall will require the use of seed impurities for mitigating the power flux and dropping the divertor target temperatures to acceptable levels. Such impurities will most likely be Ne, N₂ and Ar. Experience also indicates that operation with a metallic wall may in this context also require higher fuel throughput levels than what will have been used in the C-wall phase. Thus, the overall throughput of fueling gas and impurities will be considerably higher in the metal phase compared to the C-wall phase. JT-60SA will be the first larger device with an entire wall covered by a high Z material thus bridging the gap between ASDEX-Upgrade and JET to DEMO as ITER will operate with a fully metallic wall with low Z main chamber walls, while DEMO will likely operate with high Z materials on all PFCs. JT-60SA will in its metal phase therefore provide an important corner stone for numerical predictions to DEMO and operational support to ITER. Due to the possible achievement of a low enough density operation at the given heating power combined with its high achievable current, JT-60SA may well be in the position to study if the predictions for ITER with respect to impurity screening for high Z

impurities due to steep pedestal gradients hold, providing an important intermediate data point for the existing predictions for ITER.

Table 1-5 shows changeover plans from the carbon plasma-facing components to metal ones. The present plan proposes that the changeover to full metal plasma-facing components is scheduled after the Integrated Research Phase I. Because nearly full heating power and carbon mono-block divertor plates are available in the Integrated Research Phase I, it is possible that the long-pulse high- β plasma up to 60 s is achieved. In addition, after this phase and before the Integrated Research Phase II, if manned access inside the vacuum vessel is still possible, this leads to minimum time consumption for the changeover and has been therefore selected as the desired timing for the change-over.

Reference

- [1] Th. Eich *et al.*, *Nucl. Fusion* **53** 093031 (2013).
- [2] H. Kawashima *et al.*, *submitted to Plasma Fusion Res.* (2018)

9. Fusion Engineering

The mission of the JT-60SA project includes to support ITER and research towards DEMO by addressing key physics and engineering issues. Fusion engineering aspects are fundamental to machine physics operation and hence, many engineering issues have already been addressed in the previous chapters. Therefore, the present chapter focusses on some complementary areas in which JT-60SA can provide essential understanding of fusion engineering and design in view of ITER and DEMO, especially in the fields of component development for blanket technology, plasma facing material and plasma-wall-interaction research and return of experience from the operation of various technology systems at JT-60SA. At the end of this chapter, an overview table is summarizing along which timeline the results from JT-60SA feed the target machines ITER and DEMO.

9.1 Component Development for Blanket Technology

Considering the existing designs of the JT-60SA in-vessel components, of the planned Test Blanket Modules (TBMs) to be tested in ITER and of the DEMO breeding blankets, the following main areas for relevant tests to be performed in JT-60SA in support of ITER and DEMO are seen: (i) Test of Instrumentation Equipment, (ii) Ferro-magnetic Influence Test, and (iii) Blanket Mockup Neutronics Measurement. The recently established alignment of the ITER TBM programme with the EU Blanket programme ensures a particularly high impact of such tests. JT-60SA provides two potential test configurations, namely the diagnostic port size mock-up and the full port size mock-up (see Figs. 9-1 and 9-2).

The detailed description of each test area of component development is summarized as follows:

(1) Test of Instrumentation Equipment

In the development of fusion engineering components, component mockup tests in fusion machines are the most important evaluation step. The functionality of the measurement equipment in the fusion machine environment needs to be qualified and its reliability demonstrated. Such tests should essentially aim at providing information to the ITER TBM programme by testing relevant instrumentation. This set of tests is to certify the performance of various instruments and their measurement equipment for component development. Particularly relevant could be the tests of fiber optic sensors (based on regenerated FBG technology) to measure temperature and strain in the TBM structure (for example EM forces and induced deformations at the TBM attachments due to plasma transients or disruptions). For this test, small mockups in diagnostic ports can be used (Fig. 9-1). This test will give valuable qualification data of ITER Test Blanket instrumentation as well as for DEMO. The test has to take place in time to be considered in the TBM final design.

(2) Ferro-magnetic Influence Test

Breeding blankets of DEMO utilize reduced activation ferritic martensitic steels so that they have enough durability to high temperature usage and high dose irradiation. In the blanket development program, ITER TBM testing is one of the most important missions. ITER is basically made of austenitic steels, therefore, existence of ferritic TBMs in ITER induces TF ripples all the more as they are distributed toroidally asymmetric. Prior to the ITER TBM testing, the ferro-magnetic effect of the test blanket modules on ITER plasma needs to be carefully evaluated to reduce the risk in achieving the ITER mission of $Q=10$.

JT-60SA provides the most valuable test environment to quantify the expected effect of the TBM structures in ITER. Once JT-60SA has achieved stable and repeatable plasma operation, mock-ups of different sizes could be variably positioned and tested using the diagnostic port and the full size port. The tests of ferromagnetic samples could be coupled with the tests on relevant instrumentation (see above) to measure the strain on the tested structures. The time duration is expected to be several years before start of DD phase of ITER (Fusion Power Operation Phase), when the decision of TBM structure manufacturing will be made, c.f. Fig. 9-3. The ferro-magnetic effect can be flexibly simulated by electromagnets in the port (this would be in the same way as done in the study at DIII-D). This method shall be considered to start the ferro-magnetic influence test earlier.

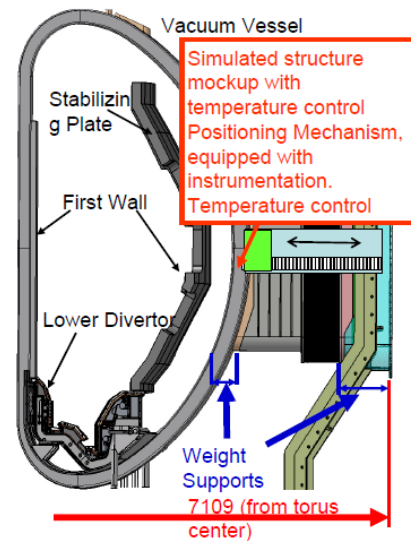


Fig. 9-1 Configuration Image of Diagnostic Port Size Mockup

(3) Blanket Mockup Neutronics Measurement

This test is targeted to support the final design of the ITER Test Blanket. It is to obtain neutronics performance data on simulated blanket module mockups by DD neutrons in the Initial Research Phase II of JT-60SA (to be re-confirmed in the Integrated Research Phase) and validate blanket module neutronics performance. Small mockups of diagnostic port size to large full port size mockup can be considered. JT-60SA can also provide the ideal environment to test the neutronic instrumentation. Local neutron measurement in the mockup shall be required to confirm neutronics performance in the blanket. A wide range on n-instrumentation is being designed and should be assessed against the possibility of an early validation in JT-60SA environment (for example miniaturized sensors to measure local neutron field parameters in the Breeder Units (Self Powered Neutron Detectors, Fission Chambers, Single-Crystal Diamond). Reliable neutron measurement equipment shall be developed in the test of measurement equipments described above.

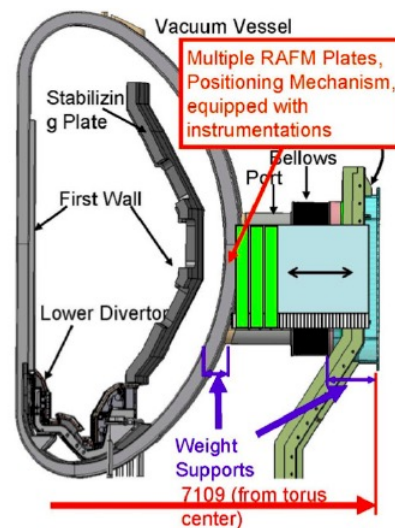


Fig. 9-2 Configuration Image of Full Port Size Mockup

9.2 Plasma Facing Material and Plasma-Wall-Interaction Research

In next generation fusion devices, such as DEMO, plasma facing material will be metal because tritium retention and erosion is expected to be much smaller in an all-metal wall device than that in a carbon wall device. Therefore the major research issues of plasma-material interactions for engineering should be focused on metal. They are categorized into (1) hydrogen isotope retention, (2) erosion and embrittlement of metallic plasma facing components, (3) safety and maintenance issues, and (4) development of new materials. In order to demonstrate high beta plasma sustainment as a primary mission, JT-60SA will start as a full carbon wall tokamak, and then be modified towards an all-metal device after achievements of all primary

missions. Researches of basic mechanisms of interactions between plasma and metal should be conducted in cooperation with laboratory experiments.

The detailed description of each issue of plasma facing material and plasma interaction research is summarized as follows:

(1) Hydrogen Isotope Retention

The tritium retention in the vacuum vessel should be minimized in a future fusion reactor from the viewpoints of tritium self-sufficiency and safety. In comparison with carbon devices, hydrogen isotope retention is expected to be much smaller in all-metal devices. However, even then, the vacuum vessel tritium inventory is still a major contribution to the overall inventory in DEMO. Although JT-60SA will not use tritium, it is a perfect test bed to investigate retention mechanisms. Measurements in C will be essential as reference to demonstrate the change in retention when moving to W wall (Integrated Research Phase II). JT-60SA will contribute towards answering some of ITER and DEMO questions on retention by extending the work done on other devices and exploiting the unique capabilities of the new machine. Two exemplary topics are explained in the following:

- (i) JT-60SA long-pulses will allow to study steady-state conditions for fuel retention in a large diverted tokamak and in H-mode (in C complementary to Tore Supra / in full W in addition to WEST).
- (ii) Fuel removal techniques (isotope exchange, baking etc.) can be studied if global gas balance is available and sensitive enough (relevant in full-W).

Particle balance analysis during plasma experiment and postmortem analysis of plasma facing components in JT-60SA before and after installing the all-metal divertor and first wall should be conducted to understand the hydrogen isotope retentions and their distribution in vacuum vessel, respectively. In order to measure fuel retention in JT-60SA one will need a good and reliable way of measuring a global gas balance. This means quantification (PVT analysis) and assessing composition of the pumped gas. In the full-W machine, the retention fraction will likely be in the order of 0.05% determined by implantation. With boronisation it will be in the order of 0.5% due to moderate co-deposition. In the full-C device it is approximately 15% at the expected low wall temperature. JT-60SA will then need a system which is capable of measuring this wide range of retention fractions. The system will need also to be able to analyze seeding gases: N₂, Ar, Kr etc. Development of *in-situ* monitoring of retained hydrogen isotopes and helium is important to investigate the retention properties during long pulse discharges.

It is also necessary to investigate the effects of neutron irradiation damages on hydrogen isotopes retention. To use neutron-irradiated material samples is the best way for the investigation, but using heavy ion-irradiated material samples can simulate that to a degree. Before the use of ion-irradiated samples, difference and consistency of hydrogen isotope retention between neutron-irradiated materials and ion-irradiated materials should be studied.

Additionally in DD plasma operation, it can be very relevant to measure the H isotopes permeation through samples of ferromagnetic material and test if applicable the instrumentation developed in the TBM program for the development of sensors to measure local tritium concentration. The impact of such tests is considered to be very high and useful to validate the predictive tools developed for the tritium transport through interfaces.

(2) Erosion and embrittlement of metallic plasma facing components

To estimate the lifetime of plasma facing components in DEMO, a good understanding of mechanisms of erosion and embrittlement are necessary. For the case of refractory metals, physical sputtering rates are smaller than that of carbon and there is no chemical sputtering.

However, refractory metals can melt at the high heat fluxes typically appearing during ELMs or disruptions. The surface of the metal is being deformed by the melt layer, and such surface can melt easier than a smooth surface. Other erosion processes caused by blistering and embrittlement have to be investigated as well.

Neutron and helium irradiation induced damages modify the physical properties of metals. Tritium retention properties are also affected by the irradiation. The effects of the irradiation on metals have to be also investigated.

A mock-up coated with different thickness and/or different coating technologies of W functional gradient material could be tested in diagnostic ports to measure and qualify their behaviour (melt layer, embrittlement etc.). When not perturbing JT-60SA test campaign, artificial defects of different sizes could be created on W-coated mock-up to quantify the resistance to cracks, the predicted crack development patterns etc.

(3) Safety and maintenance issues

For a DT machine, it has to be avoided that activated dusts and dusts retaining tritium are released from the inside of vacuum vessel to atmosphere when the vacuum vessel is accidentally opened. Hot dust can be oxidized when cooling water is being accidentally released in vacuum vessel, and the reaction produces hydrogen. That means dusts have potential hazard in DEMO and ITER. Therefore, dust amounts should be minimized in DEMO and ITER.

To understand the mechanisms of metal dust generation, laboratory experiments and modeling activities are important. In JT-60SA with all metal wall, dust transport and deposition profiles should be investigated. *In-situ* dust monitor and dust removal methods should be developed.

(4) Development of new plasma facing materials

Tungsten is a candidate plasma facing material in ITER and DEMO. However, tungsten has some brittleness. Development of advanced tungsten alloys, such as ultra-fine grained W-TiC is important toward DEMO. In JT-60SA, such new material can be tested in fusion environment for example by using a movable material probe system.

9.3 Return of experience from JT-60SA technology

Development and improvement of remote handling (RH) maintenance systems are essential for reliable machine operation of JT-60SA. The RH system for JT-60SA will be implemented in two steps. Special tools for cutting and welding of pipe connection will be developed and used from the first installation of lower divertor cassettes. The experience of using these tools in JT-60SA will be useful to develop similar tools for RH of the ITER TBM. Main RH systems such as vehicles and manipulators will be developed and used in RH maintenance of in-vessel components before the Integrated Research Phase II. Design of these systems can be improved based on the initial experience of the ITER RH system and the ongoing DEMO programmes. Modification to full metal wall plasma facing components and installation of upper divertor cassette shall be accomplished by the RH system. Therefore, the RH system shall be completely developed and tested before the Integrated Research Phase II. Design of full metal PFC and upper divertor cassette shall be compatible with the RH system. Modification and improvement of supports and coolant pipes in the VV may be required to adopt the fully RH compatible PFC before prohibition of in-vessel human work. Huge effort shall be required to develop and test the RH system sufficiently in advance before the Integrated Research Phase II. JT-60SA can also be used for testing of RH and in-vessel inspection tools for ITER and DEMO. It is expected that the great experience on RH in JET will make large

contribution on this area.

Reliable operation and improvement of technical systems at JT-60SA is essential to ensure the success of the experiment. Moreover, it can provide return of experience (RoX) with these systems, if the technology used at JT-60SA is similar or related to the one foreseen at ITER and DEMO. Relevant systems of interest are (1) pumping, (2) fuelling, (3) cryogenic, (4) magnets, (5) power supply, (6) NBI heating systems, and (7) ECRH heating systems. The detailed description of the relevancy of these systems is summarized as follows:

(1) Pumping systems

The most central vacuum pumping system of any fusion device is the torus vacuum pumping system which takes the exhaust gas via the divertor and feeds it to stack or – in case of DT experiments – to the tritium plant for further clean-up and recovery.

JT-60SA: JT-60SA is utilizing in-vessel cryopumps located underneath the divertor cassettes, supplied with 3.7 K. The capacity of the cryopumping system is designed such that regeneration can be performed off-shot, usually over night. For fast vessel pump-down there are turbopumps backed by roots pumps connected (catalogue items). The vacuum systems are similar (partly identical) to those already utilized in JT-60U times.

ITER: ITER is using 6 customized, fully tritium-compatible cryosorption pumps as primary (= high-vacuum) pumps, supplied with 4.5 K. The pumps are located in dedicated pumping ports at the lower level of the machine. In order to provide the requested pumping speed over the longer pulse durations foreseen in ITER, the pumps have to undergo intra-shot regeneration, i.e. at any time, always 4 of the 6 are pumping whereas the other 2 are under regeneration. For this purpose, the cryopumps are equipped with an integral inlet valve. For regeneration and for pump-out of the torus vessel, roughing pumps are needed. ITER will use again cryopumps, but located in the tritium building (thus exploiting higher allowed tritium inventories there) which are regenerating to higher pressures than the primary cryopumps to allow for cross-over to mechanical pumps. Depending on the tritium content, different pump technologies will be used for the final stage that compresses to ambient pressure.

DEMO: For reasons of efficient inventory limitation within the quasi steady-state operation scenario envisaged (with pulse durations in the order of 2 h), DEMO has to utilize continuous pumping technologies both for primary and for rough pumping. They are based on mercury as working fluid and currently under development (first-of-its-kind). Cryopumps are only seen as a fallback solution. As further means to minimize inventories a direct internal recycle loop is foreseen, which is utilizing metal foil pumps that are also not used in other machines so far.

The pump technologies at ITER and JT-60SA are somehow similar, but different when it comes to detailed design (supply temperature, location). This makes it impossible to draw lessons in terms of cryogenic consumption, which normally is one of the key issues. The JT-60SA cryopump is not toroidally continuous but consists of 9 segments that are individually cooled so that they can be switched on and off. This allows to vary the pumping speed (in a similar way as done at ITER by using individual inlet valves) and to study the influence on plasma stability, in particular for high density scenarios. Due to the position of the JT-60SA cryopumps, the response time should be very short. Indeed, this is an unknown area for the ITER pumps.

RoX aspects: It is recommended to study the impact of varied (spatially and absolutely)

pumping speed in a parametric manner by varying the number of pumps. This would allow to study the impact of changing (integral) pumping speed (from 100% to 0%) on plasma exhaust (divertor recycle flux pattern) and stability, as well as the impact of symmetry of the provided pumping speed (by representing the same number of active pumps in symmetric or asymmetric arrangement). The experimental results would represent valuable information that can be used as benchmark case for collisional neutral gas exhaust modelling. The same, then validated codes could then be applied for modelling ITER (scaling for the ITER cryopump size), and (as it holds independent of the chosen pump technology) also for DEMO.

(2) Fuelling systems

On all large scale machines, fuelling is done with pellet injection. The pellet launching system (PLS) has to cover two tasks, one is to provide sufficient D_2 , or H_2 particle flux for particle fuelling and the other is to provide a sufficient pellet rate for ELM control and possible ELM mitigation. Any PLS is composed of three main sub-systems: pellet source, pellet accelerator and pellet guiding system

JT-60SA: Pellets of adequate sizes and rates for fuelling or pacing purposed are produced by cooling, liquefying and freezing a compressed flow of D_2 or H_2 in the according pellet sources. Punched from the extruded ice rod, pellets are accelerated by a stop cylinder double arm centrifuge to a pre-set speed. The transfer system, guiding tubes installed inside the torus vessel in case needed equipped with a funneling entrance section guarantee pellet delivery to the torus inboard launch site in order to enable for efficient fueling and pacing actuation.

ITER: The ITER pellet injection system (PIS) has the mission of supplying DT fuel pellets for maintaining density and controlling the isotopic mixture and also must provide smaller D_2 pellets to trigger rapid ELMs to prevent large natural infrequent ELMs from occurring. The PLS will be able to inject from the high field side for fueling and low or high field side for ELM triggering through guide tubes inside the vacuum vessel and each injector is to be able to accomplish both missions through the use of a guide tube selector to choose which injection location the pellets are transferred to the plasma. Pellet formation is to be accomplished in a continuous screw extruder cooled by supercritical helium with the pellets cut from the extrusion and loaded into a gas gun on demand at rates up to 16Hz for ELM mitigation and 4 Hz for fueling per injector, with up to 6 injectors to be eventually installed. The PLS will recirculate internally both excess extrusion fuel and propellant gas in order to minimize the gas processing done by the tritium plant.

DEMO: The DEMO systems are not yet fully defined, but will follow a similar line, using continuous screw extruders, and probably a centrifuge for acceleration via a suitably chosen guiding tube.

All three machines are going to apply similar pellet technology to cover the same tasks of fuelling and ELM control. In order to achieve optimized performance, pellet launch from the technically more intricate vessel inboard side is envisaged, requiring pellet transfer through a guiding system. Optimised performance for all tokamaks and both the fuelling and pacing actuation will be achieved when accomplishing the goal with a minimum applied particle flux.

RoX aspects: The JT-60SA PLS will sound out technology limits and foster development of possible advanced solutions for ITER and DEMO, e.g. with respect to the optimization of the launch scheme found to form a considerable bottleneck in ITER. Development of control tools

and strategies will allow to master pellet specific features like the discrete nature of the fuelling and the resulting impact on plasma diagnosing. Finally, JT-60SA can explore also the feasibility of the pellet tool to serve for tasks like the efficient delivery of plasma enhancement or radiative exhaust gases by admixing them into the fuel.

(3) Cryoplant systems

The aim of the cryoplant is to provide the helium (gaseous and supercritical) at cryogenic temperature for all the users (e.g. magnets, current leads, cryopumps, thermal shields).

JT-60SA: The cryogenic system of JT-60SA is composed by the helium refrigerator, containing the warm compressors and a refrigerator cold box (RCB). The RCB supplies 80 K helium for the thermal shields, 50 K for the current leads, and supercritical helium for the magnet system (4.4 K; 5 bar) from connections to the Auxiliary Cold Box (ACB). The ACB supplies the TF and PF coils at ~4.5 K and the cryopump at 3.7 K.

ITER: The ITER cryogenic system is composed of three cold process boxes of the magnet plant, and one dedicated cold process box of the cryopumps plant. It further contains 1.8 MPa warm (300 K nominal) and 80 K tanks for storing the gaseous He, and two identical 80 K He cold boxes together with two identical liquid nitrogen (LN2) auxiliary cold boxes for final cooling of the He flow to 80 K.

DEMO: The DEMO configuration has not been elaborated so far.

The JT-60SA cryogenic system foresees two LHe baths inside the ACB, one for 3.7 K users (cryopumps) and one for 4.5 K users (magnets), whereas the ITER cryogenic system foresees 5 LHe baths (one for cryopumps, one for central solenoid, one for toroidal field coils, one for poloidal field and correction coils, one for structures). One of the key role of the cryogenic system of ITER is to provide load smoothing to the refrigerator with active control systems.

RoX aspects: As the two systems differ substantially in terms of number of LHe baths, the major relevancy lies in the impact of this difference on the transient evolution of the heat load to the refrigerator. Several control options to smooth the peak load to the refrigerator may be experimentally studied; these results could then be used to validate existing codes. In addition, the effect of different lengths of the dwell time may be experimentally assessed, both considering the effect on the smoothing strategy and also studying the time needed to bring the cryoplant back to the initial state after different operation scenarios.

(4) Magnet systems

The aim of the magnet system is to generate the magnetic field for the plasma confinement. Different magnets are operated according to specific (different) current scenarios (drivers) and subjected to different thermal and mechanical loads. During the reactor lifetime, the magnets will experience several normal operation transients (cool-down, pulsed operation, warm-up) and possibly some off-normal ones (fast discharge, quench).

JT-60SA: The fully superconducting (SC) magnet system of the JT-60SA is composed by 18 toroidal field (TF) NbTi coils, 4 identical central solenoid (CS) Nb₃Sn coils, and 6 equilibrium field (EF) NbTi coils. The TF coils winding pack (WP) is composed by double-pancake wound, square-in-square cable-in-conduit conductors (CICCs) without low-impedance cooling channel. All pancakes are cooled in parallel. No radial plates are present. The WP is encapsulated in a

steel casing guaranteeing mechanical support to the coils and cooled by a cryogenic loop separated from the WP one. The TF structures also support the CS and EF coils. The CS WP is composed by double-pancake wound circle-in-square CICC with low impedance central channel. All double-pancakes are cooled in parallel. The strands are equal to the ones of the ITER TF conductor. The mechanical (Lorentz) forces acting on the CS are withstood by 9 pre-compression structures, independently cooled. The EF coils WP is composed by square-in-square CICC with low-impedance cooling channel. All the SC coils and structures are cooled by supercritical He (SHe) at $T \sim 4.5$ K and $p > 4$ bar.

ITER: The fully superconducting magnet system of ITER is composed by 18 TF Nb₃Sn coils, 3 CS Nb₃Sn coils, 6 poloidal field (PF) NbTi coils, and 18 NbTi correction coils (CC). The TF coils WP is composed by double-pancake wound, circle-in-circle CICC with low-impedance cooling channel. All pancakes are cooled in parallel. The CICC is encapsulated in SS radial plates to compose the WP. The latter is encapsulated in a steel casing guaranteeing mechanical support to the coils and cooled by a cryogenic loop separated from the WP one. The TF structures also support the PF coils and partially the CS. The CS WP is composed by double-pancake wound circle-in-square CICC with low impedance central channel. All pancakes are cooled in parallel. The mechanical (Lorentz) forces acting on the CS are withstood by 9 pre-compression structures, independently cooled. The PF coils WP is composed by circle-in-square NbTi CICC with low-impedance cooling channel. The WP is two-in-hand wound. All CCs are NbTi CICC double-pancake wound. The 6 upper and 6 lower CCs are circle-in-circle conductors without low-impedance channels, while the 6 side CCs are circle-in-square CCs are circle-in-square conductors with low-impedance channel. All the SC coils and structures are cooled by SHe at $T \sim 4.5$ K and $p \sim 6$ bar.

DEMO: The fully superconducting magnet system of DEMO is currently in its pre-conceptual design phase. The current design foresees 18 TF Nb₃Sn coils, 5 CS Nb₃Sn coils, 6 poloidal field (PF) NbTi coils. The TF coils WP is to be identified among three different proposals, including two layer-wound options (with graded SC, Cu and jacket cross sections to minimize the WP dimensions and follow the mechanical load and magnetic field radial gradients) and a pancake-wound option. All layers or pancakes are cooled in parallel. The pancake-wound option features an ITER-like CICC with a low-impedance channel, while the two layer wound options feature two or three low-impedance channels and a different manufacturing strategy (react&wind vs wind&react). The TF structures, supporting the PF coils and partially the CS, and their cooling is still under design. The CS WP is to be selected between two proposals, featuring in one case a layer-wound rectangular CICC with two or three low-impedance channels and in the other case a pancake-wound ITER-like CICC with one low-impedance channel. The use of HTS for the innermost layers is under consideration for the layer-wound option. The design options for the PF coils WP are still under definition. Both layer and pancake winding are under consideration, as well as two-in-hand winding.

All the considered tokamaks are fully superconducting and cooled by SHe. Concerning the differences, the JT-60SA TF coils adopt NbTi SC, as opposed to both ITER and DEMO.

RoX aspects: Very valuable lessons can be drawn from tests to be performed during the commissioning or operation phases:

- (i) Concerning the warm-up/cool-down, some ad-hoc developed optimization strategies could be tested in order to assess the possibilities to reduce the unavailability of the machine. The measurements could show if the optimization strategies are successful.

Different scenarios with different He mass flow rates in the structures and in the CICC can be tested.

- (ii) Concerning the pulsed operation, it could be useful to check the heat loads (by means of outlet He temperature measurements) acting on the TF coil system, assessing the capabilities of the Monte Carlo codes used for the estimation of the same loads in ITER, possibly in similar scenarios.
- (iii) As far as fast or slow discharges are concerned, it could be possible to test different ramps / time constants for the dump of the different magnet systems to investigate the heat deposited in the structures and consequently the required recooling time before the subsequent shot is started.
- (iv) The efficacy of the CS cooling by means of double-pancakes parallel paths should be assessed and compared with the single-pancake parallel cooling path of the TF WP, in order to add information to and help in the choice between pancake/layer cooling of the DEMO coils.
- (v) Experimental data should be collected for the validation of existing thermal-hydraulic, mechanical and electro-magnetic codes currently used in the analysis of ITER and design of DEMO magnets. As layout of the cooling paths of the different magnets in the three machines is often different, together with the mass to be cooled (because of the different dimensions), the impact of these differences on the cooling efficiency should be assessed e.g. by dedicated simulations, to allow for transfer to other tokamak designs.

(5) Power supply systems

The electrical system of present fusion experiments is generally divided in the pulsed power system providing power to the magnets and to the additional heatings and the steady state system feeding all the auxiliaries.

JT-60SA: Regarding the magnet protection, the solutions adopted in all the fusion experiments including ITER are based on mechanical devices, which is an approach that leaves significant room for improvements in terms of RAMI. On the contrary, the technology developed for the JT-60SA Quench Protection Circuits (QPC) is based on a new mechanical-static hybrid circuit breaker, using power semiconductors called Integrated Gated Commutated Thyristors. The backup protection is presently based on explosive actuated breakers, called pyrobreakers, developed in the Efremov laboratory for ITER. The technology for the high power magnet PS is based on four quadrant thyristor converters. For the low power fast PS for RWM control, a solution based on new silicon-siliconcarbide semiconductors has been developed. The switching networks circuit breakers are based on the same technology of the QPCs. The 500 keV negative NBI PS are those ones of the JT-60U, suitably upgraded for the long pulse operation, from 10 to 100s. High voltage (HV) technologies have been developed to handle the HV section of the acceleration grid PS; the low voltage one is based on IEGT (injection-enhanced gate transistor) inverters. Gyrotrons are adopted for ECRH and PS based on Pulse Step Modulator technology to supply them.

ITER: The circuit breakers of the ITER Fast Discharge Units are different, based on mechanical-vacuum hybrid technology. The backup protection uses pyrobreakers. The technology for the magnet PS is the same as of JT-60SA. The circuit breakers for the ITER switching networks are different: based on mechanical plus thyristor switches and associated counterpulse network. The negative NBI PS is similar to the JT-60SA one, but rated for 1MV and the ion source is radiofrequency based instead of filament based, with associated differences in the PS systems. The technologies for RF heating are similar, thus useful

feedbacks will be produced as well

DEMO: In general, the approach for the design of the plant electrical system for DEMO should be addressed on the one hand to solve some still open issues and on the other hand to achieve strong improvements in terms of RAMI.

RoX aspects: The use of the JT-60SA QPC is expected to prove the benefits of the static technology in terms of reduction of the maintenance needs and RAMI in general; this aspect is surely DEMO relevant. The operation of the pyrobreakers will give useful indications for ITER. The use of the magnet PS at JT-60SA will produce many useful inputs for ITER, in particular as far as the control optimization is concerned. As regards DEMO, it is expected that the technology for the DEMO magnet PS shall be different from the present one, mainly to solve the issues related to the high power steps and derivatives and the huge amount of reactive power demand associated with the solution based on thyristor converters. The importance of the negative NBI PS for ITER is extremely high. The operation of the negative NBI PS will surely produce useful indication for DEMO too, but significant improvements in terms of efficiency need to be studied for DEMO.

(6) NBI Heating systems

NBI is the most important technology to heat the plasma by momentum transfer of the injected highly energized neutral particles. NBI also provides the function of current drive, an essential feature for long pulse operation of burning plasmas.

JT-60SA: The NBI system is the most powerful heating device at JT-60SA (30 MW → 34 MW in the Extended Research Phase). The whole system consists of twelve positive-ion-based NBI (P-NBI) units and two negative-ion-based NBI (N-NBI) units (see Appendix A). The dominant role of the P-NBI beamlines is heating (mainly ions) and torque input control with some contributions to current drive in a very versatile arrangement: 8 units for perpendicular injection, 2 units for co-tangential injection and 2 units for counter-tangential injection. In total 20 MW are installed and are planned to be upgraded to 24 MW. The N-NBI beamline with 10 MW at 500 keV beam energy has co-tangential injection for heating (mainly electrons) and off-axis current drive with small torque. The combination of the systems allows high flexibility for customized usage. Pulse duration to 60 s is partially available with extensions to 100 s. The beams operate in deuterium. For operation in hydrogen the power decreases roughly by a factor of two for the P-NBI system; a specification for N-NBI is not given. The ions (positive and negative) are generated in arc sources which require regular maintenance. For production of negative ions, caesium is used. The beamlines are equipped with cryopumps.

ITER: ITER is using only N-NBI systems consisting of two beamlines with the option to add a third one. The power of one beamline is 16.7 MW at the beam energy of 1 MeV. The beams will operate in hydrogen and in deuterium. Pulse duration up to 1000 s (hydrogen) and 3600 s (deuterium) is foreseen. Higher current densities have to be achieved in hydrogen to compensate for the reduction in the beam energy to 870 keV. The ions are generated in an RF-driven ion source (basically maintenance free). For production of negative ions, caesium is used. The beamlines are equipped with cryopumps.

DEMO: For heating and current drive N-NBI systems are under discussion. The power and the pulse length depend on the DEMO case. For a pulsed tokamak the dominant role is heating and minor contributions to current drive, meaning that about 50 MW is considered to be sufficient.

In a steady state tokamak current drive is mandatory, i.e. power levels in the order of 150 MW are discussed. In this advanced scenario the presently used neutralization technique, the gas neutralizer, will be most likely replaced by advanced technologies (laser neutralizer). As RAMI plays a dominant role, caesium is regarded as one of the foremost reliability and availability risks. Another demanding requirement is the energy efficiency and the overall wall-plug efficiency. Deuterium operation is mandatory.

The N-NBI system is the common feature of all three devices. The system of JT-60SA is/will be the most relevant N-NBI system in operation in terms of acceleration voltage (500 keV), pulse length (100 s) and ion species (D). Thus, operation experience, availability and reliability of the system are of uttermost significance for ITER and DEMO. As addressed in APPENDIX A voltage holding, achievement of the targeted currents, stability in long pulses and caesium recycling are still open issues which will be addressed by JT-60SA. Beam homogeneity is also a key but might strongly depend on the source and the Cs dynamics. As ITER (and also DEMO) will use RF-driven sources the results from arc sources will be of limited significance.

RoX aspects: It is therefore recommended to study the voltage holding and focus on the achievement of the acceleration of the large beams. Availability and reliability of the system are also key. Estimates can be made on the Cs consumption and principle studies on the beam homogeneity, extraction and beam optics could be carried out. The comparison of deuterium operation to hydrogen operation is also a crucial issue. Although the results can be not directly transferred to the ITER and DEMO system which use RF sources instead of arc sources, a better insight is gained and a comparison with results from the NBTF would be extremely supportive. Experience on the influence of the gas from the torus into the beam line can be gained. Regeneration of cryopumps and consequences on ion source performance can be addressed as well.

(7) ECRH Heating systems.

JT-60SA: The ECRF system in JT-60SA is used for the stabilization of NTMs as described in Section 2 of Chapter 4, the study of heat transport, ITB physics, plasma initiation and etc. Furthermore, a wall cleaning by EC wave is planned. The system consists of a gyrotron, waveguide transmission line and a launcher having both poloidal and toroidal steering function. In the Initial Research Phase, four gyrotrons capable of 1 MW output, four transmission lines and two launchers are to be installed and the injection power of about 3 MW is expected. In the Integrated Research Phase, the total number of the gyrotrons and transmission lines will be increased to 9, and the number of the launcher will totally be four. The required pulse duration of the gyrotrons is 100 s and the total injection power of 7 MW is foreseen. The dual frequency of gyrotron oscillation (110 GHz and 138 GHz) is required. The development of the dual frequency gyrotron has been developed since 2012 and 1 MW output for 100 s both at 110 GHz and 138 GHz was achieved in 2014. It is also able to oscillate 82 GHz to be used for plasma start-up and wall cleaning. Output of 1 MW for 1 s was successfully achieved in 2015. The EC power is injected from four upper outboard ports, P-1, P-4, P-8 and P-11 with both poloidal ($-15 \leq \Theta_p \leq 35$) and toroidal ($-15 \leq \Theta_t \leq 15$) steering function. The RF power modulation from 0.5 Hz \sim >5 kHz is also planned to be implemented based on the requirements of the experiments.

ITER: In ITER, a 170 GHz, 24 MW Electron Cyclotron Heating and Current Drive (EC H&CD) system is to be installed for central heating and current drive of plasma as well as off-axis control of magnetohydrodynamic (MHD) instabilities. The system consists of 24 gyrotrons, 12

high voltage power supplies, 24 waveguide transmission lines connected to both one equatorial (EL) and four upper (UL) launchers. Eight gyrotrons procured by Japan and Russia will be used for the ITER first plasma schedule in 2025 and the rest of them will be installed by 2028. The transmission line (TL), which is to be provided by US, namely has the function of transmitting the generated RF power and the waveguide type TL has been selected. Both EL and UL are required to steer the injection beam in poloidal direction, in order to perform central H&CD and off-axis CD to control MHD activities such as sawteeth and neo-classical tearing modes.

DEMO: An EC H&CD system configuration for a DEMO reactor would be similar with that of ITER. The expected toroidal magnetic field of DEMO reactors is 5.5~6 T, which is only several percent higher than that of ITER. This means that the required oscillation frequency of the next generation gyrotron would be an order of ~200 GHz. Higher frequency oscillation, 220~250 GHz would be required to enhance ECCD efficiency and an oscillation mode selection could be an extension of the ITER gyrotron. Regarding to an output power and electrical efficiency, ~2 MW and 60~70% would be required, respectively. The definite path to develop such a gyrotron is clear, but some advanced technology will be required to satisfy all requirements. A steering mirror of a launcher placed near plasma in ITER or JT-60SA will have to be removed since it will be exposed by high energy neutrons and easily damaged. One is to introduce a multi-frequency gyrotron and no steering mirror is necessary in this case. Another is to introduce a remote steering antenna consisting of an oversized rectangle waveguide and a steering mirror installed at the waveguide inlet, where is far from plasma. The former can discretely change the deposition location of RF power and the latter could continuously change it.

RoX aspects: Together with W7-X, it will be the first long pulse (>10s) and high power (9 MW) EC H&CD system at 100 GHz range consisting of multi-number of the sub-systems such as a gyrotron, transmission line, launcher and so on. Two gyrotrons will be operated by one HVMPs and two sets of APS/BPS at JT-60A, which are the similar sets of ITER power supply system. The gyrotron can oscillate at 82 GHz, 110 GHz and 138 GHz and a steering RF beam without using the rotating mirror can also be tested. The system operation results/experience would definitely be useful for both ITER and DEMO EC H&CD system.

9.4 Summarized schedule

Fig. 9-3 is illustrating how the different fusion engineering contributions of JT-60SA detailed above are linked with the schedules of ITER, the aligned TBM blanket schedule and DEMO.

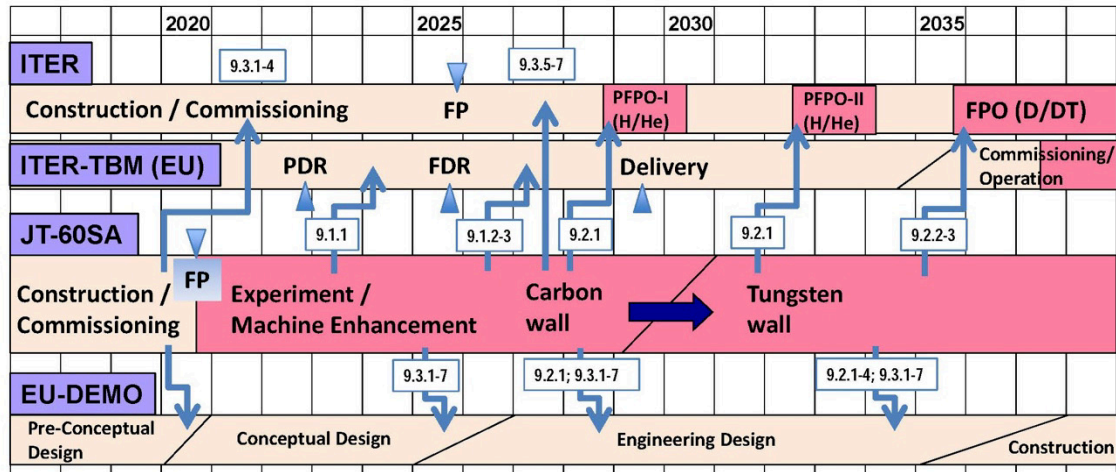


Fig. 9-3 Expected Schedule of Fusion Engineering Research using JT-60SA. The numbers in the boxes refer to the sections in this chapter.

This timeline is reflecting the latest versions of the time plans of ITER and DEMO:

- (i) The ITER Research Plan (as of 2017) foresees the first plasma (FP) in December 2025, followed by three operational phases (always separated by assembly phases), namely two pre-fusion power operation phases (PFPO-I and –II) and the fusion power operation phase (FPO) to start in December 2035. The aligned programme of the European TBM and Breeding Blanket and reorganization of the TBM project (as of 2018) provides the two EU TBM concepts (water-cooled lithium-lead and helium-cooled pebble bed) via conceptual, preliminary (PDR) and final (FDR) design reviews with final delivery to ITER in July 2029 (the auxiliary systems will be delivered earlier).
- (ii) The European Fusion Roadmap v2.0 (as of 2018) sets out a phased development plan with the decision for DEMO construction in the late 2030s, and construction accomplishment and operation of the DEMO plant beyond 2040.

As illustrated in Fig. 9-3, the research plan of JT-60SA is in many aspects very well linked to the other projects and is able to provide essential input in time to all phases of ITER and DEMO.

10. Theoretical Models and Simulation Codes

10.1. Introduction

The theoretical models and simulation codes play an indispensable role to understand various linked phenomena expected to appear in burning plasmas with high-beta and high-bootstrap-fraction, and to predict the behavior of such plasmas in ITER and DEMO. The theoretical models and simulation codes can predict plasma behaviors which are not yet found in the experiment and thus play a key role to plan the experiment in order to confirm the prediction. The prediction confirmation by the JT-60SA experiment leads to the validation of theoretical models and simulation codes in high-beta high-bootstrap-fraction plasmas. The validated theoretical models and simulation codes will be applicable to the prediction of burning plasmas in ITER and they will be validated again with the experimental observations of burning plasmas in the ITER experiment. The validation of the theoretical models and simulation codes by both the JT-60SA and ITER experiments is required to reliably predict the behavior of burning plasmas in DEMO. Figure 10-1 shows a strategy for application and improvement of theoretical models and simulation codes.

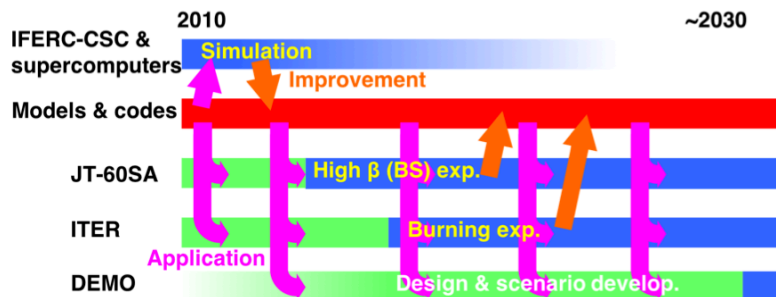


Fig. 10-1 Strategy for application and improvement of theoretical models and simulation codes

The JT-60SA tokamak has specific properties that can be exploited for the validation of models and codes in some well defined areas. A non exhaustive list of specific JT-60SA properties and the corresponding models that could be validated is presented in Table 10-1.

The development and improvement of theoretical models and simulation codes, both before and during the JT-60SA operation, require substantial manpower and computational means. At least a part of this programme is being carried out on several high-performance supercomputers, such as in the computer simulation center initiated by the Broader Approach project (IFERC-CSC, see http://www.iferc.org/CSC_Scope.html). These petaflop-class computers represent a large improvement on present day processing power available for fusion applications.

Table 10-1: JT-60SA specific properties and related possibilities of model validation

JT-60SA specificity	Model validation
Flexible magnetic configuration, covering ITER shape to strongly shaped plasmas	Models of effect of shaping on plasma confinement and MHD stability
Flexible wall and divertor configuration, planned evolution from C to W	Divertor models. Pedestal models. Migration models for different PFC materials.
Non-dimensional parameter (v^* , ρ^* , β) ranges of ITER and DEMO relevant plasmas	Models for the effect of non-dimensional parameters on confinement, ELMs, etc.
Extensive set of in-vessel coils for MHD control	Models for the impact of magnetic perturbations on plasma confinement, ELMs, MHD instabilities
Powerful and flexible NBI system; ECCD system for mode control	Models connecting safety factor and rotation profiles with plasma transport. Models for NTM stabilisation
Plans for a rather extensive diagnostic system	Turbulence theories, MHD theories, fast particle kinetic models, etc.
High beta, high bootstrap and advanced scenario capability	Integrated scenario models. ITB theories. Bootstrap current theories.
Long pulse capability, beyond the global resistive time	Integrated scenario models. Real-time control models.

10.2. Research issues in theoretical models and simulation codes

The theoretical models and simulation codes should cover issues in the central research needs for ITER and DEMO (see Table 1-2 Central research needs for ITER and DEMO and required device capabilities) and include not only physics issues but also engineering issues shown below.

- Physics issues :

- heat / particle / momentum transport and confinement (ITB, ETB, L-H / H-L transition, model validation at low injected torque, low ratio T_i/T_e and dimensionless parameter regimes of ITER and DEMO relevant plasmas)
- neoclassical physics (e.g., electrical conductivity and bootstrap theories, neoclassical toroidal viscosity (w/ RMP cases), impurity transport)
- turbulence (validation of gyrokinetic codes with advanced turbulence diagnostics)
- MHD instabilities (NTM onset and stabilization by profile control and ECCD, ELM suppression and mitigation, RWM stabilization by rotation and active magnetic control, disruptions)
- pedestal physics (model validation at collisionality of ITER and DEMO relevant plasmas)
- fast particle physics (AEs, AEs effect on fast particle transport, fast-particle exciting global MHD instability, development and validation of kinetic codes for ions)
- fueling / heating / current and rotation drive (gas, pellet, NB, EC)
- SOL / divertor, plasma-wall interactions (detachment, MARFE, SOL flow, wall erosion, redeposition)
- operation scenario (startup, optimization, shutdown, cyclic scenarios, modeling of burn simulation experiments)

- Engineering issues :

- external coil current/voltage (TF, PF, RMP)

- diagnostic modeling
- model based controls for specific real time applications (e.g., current profile control, sawteeth / NTM control, ELM control etc.)
- development of integrated control systems (combined control of plasma position & shape, particle, energy, current, MHD, etc.)

First, codes which can describe each of the above issues need to be developed and improved in order to understand the mechanisms and predict them. Several codes already exist both in Japan and in the EU (see subsection 10.3), which constitute a good basis for this effort. We should make the strategy to develop codes/models towards DEMO by knowing existing/developing code/models and then finding missing codes/models to be developed in future. Then, an integrated code including the modules which describe the above issues is necessary for understanding the physics mechanisms linked with each other and predicting complicated behavior of self-regulating plasmas. It is also indispensable for developing operation scenarios and establishing the integrated control system. By using the integrated code, researchers are able to examine operation scenarios before actual experiments in JT-60SA, ITER and DEMO. Critical control issues in ITER and DEMO, such as the ELM mitigation by pellet and RMP, should be studied. In addition, owing to the limitation of available measurements in DEMO, it is necessary to develop a tokamak simulator which provides reliable and precise prediction of the dynamic behavior of burning plasmas. The integrated code covering all key physical and engineering issues becomes the tokamak simulator. Such a tokamak simulator coupled with diagnostic measurements and active control through coil system and other actuators will contribute in constructing a robust real-time control system for DEMO. Especially for this real-time control, the calculation time of codes should be reduced by using exclusive computers or by developing simplified models/codes which reasonably reproduce results obtained from time-consuming codes. In fact, what is needed is a hierarchy of tokamak simulators, from 0-D system codes, to 0.5-D codes (current diffusion codes with simplified treatment of equilibrium and profiles), up to 1.5-D integrated modeling codes (including 2-D free boundary equilibrium and sophisticated modules for the sources). Modeling and simulation studies based on the JT-60SA experiments should aim to develop this kind of burning plasma simulator applicable to ITER and DEMO.

In order to efficiently carry out the verification (including code-to-code benchmark tests) and the validation (code-to-experiment comparison) of available codes, it is required to establish a common framework which defines the interface for data exchange among the codes and comparison with experimental data. This framework is helpful not only for direct comparison between the codes and the experiments, but also for smooth integration of various codes. Each code is modular on the basis of the framework so that the researcher can integrate necessary codes according to the purpose of his/her research. Such a framework is now being developed in several activities in Japan and EU. In Japan, BPSI (Burning Plasma Simulation Initiative) has developed a framework based on the data interface named BPSD, which defines the standard dataset applicable to the data exchange between various codes. In Europe, the ITM (Integrated Tokamak Modelling) EFDA Task Force (later WPCD within EUROfusion) has developed a framework including a data structure (covering both experimental and simulation data), an integrated modeling simulation platform and a machine independent modular transport solver (ETS). Basing on the existing frameworks developed by its member countries, ITER Organization has developed an integrated modeling framework IMAS (Integrated Modelling and Analysis Suite) [1]. This framework has been already released and installed in several institutes, and includes now first physics application codes such as 1.5D transport simulators, equilibrium codes, as well as practical methods to enable remote data access to experimental

data. Experimental and simulated data are presented with the same device-generic structures, which makes straightforward the comparison between simulations and experiments of potentially multiple tokamaks, as is foreseen both before the start and during the exploitation of JT-60SA (see Sec. 10.4 and 10.5). The European modelling activities are now moving to the IMAS framework, and the Japanese ones are making functions to use IMAS in their codes. These represent a clear opportunity for joint modelling activities on JT-60SA as well as a way to actively contribute to the preparation of ITER exploitation.

With the cooperation on these activities, the framework to be developed in JT-60SA research should aim to be extended as a standard framework for DEMO. In the process of verification and validation, the model uncertainty should be identified and quantified. We shall utilize the measured data in experiments in order to minimize the model uncertainty and thus to improve the prediction reliability of the codes.

10.3. Codes and models

Non-exhaustive lists are given in Tables 10-2 and 10-3 (at the end of this chapter) of the main JA and EU codes/models that have been or will be used for JT-60SA modelling and prediction, and that could profit from validation by JT-60SA experiments. The main purpose of these lists is to make the strategy to develop codes/models towards DEMO by knowing existing/developing codes/models and then finding missing codes/models to be developed and/or included in future. In the present list, missing codes/models are for disruption, L-H/H-L transition, density limit and so on. The strategy to develop codes/models towards DEMO should be elaborated and will be shown in this chapter. Additionally, the framework of codes/models should be prepared for the efficient validation with JT-60SA experiments and also for integrating codes. The list also helps to accelerate research works in the JT-60SA Research Plan by using codes/models in the list. Owing to the JT-60SA specific properties (non-exhaustive list shown in Table 10-1), each code/model in the list has its own research items which can be validated only in JT-60SA experiments, e.g. turbulence character in the dimensionless parameter regime of ITER and DEMO relevant plasmas. Results of JT-60SA modeling and prediction will be shown in subsection 10.6 and lead to new research proposals in other chapters.

10.4. Research activity before the start of JT-60SA experiment

Before the start of JT-60SA experiment, theoretical models and simulation codes are developed, improved and validated by using the experimental data in various tokamaks. In particular, an integrated modelling set of prescriptions should be prepared and validated in order to have a sound basis for the JT-60SA simulations. These include transport, pedestal, rotation and source models. It appears that simulations of JT-60SA scenarios should be based at least on experimental results of the two machines that are the most similar, for size and configuration: JT-60U and JET. Therefore, a validation exercise is being undertaken, based on the following steps:

- a limited number of reference JT-60U and JET shots is chosen, representing the main scenarios (H-mode, hybrid, and advanced). These shots are mainly based on NBI H&CD
- a simulation data exchange method is established
- Models of transport, pedestal, rotation and so on are selected and tested
- actuator computations are benchmarked (a part of this work has already been carried out in the framework of ITPA)
- predictive simulations of the reference shots are performed with both Japanese and EU codes and models, with the aim of finding a unified modelling framework that works for both

- machines: this should give the maximum confidence for prediction of JT-60SA
- use this modelling framework to run predictive simulations for JT-60SA with both Japanese and EU codes
 - for the predicted scenarios, perform linear MHD analysis; for the most interesting cases, try non-linear MHD analysis

Such program has been and will be carried out for the typical scenarios of both machines including L-mode and H-mode plasmas. After completing this validation exercise, any of the validated codes will be used for the plasma design, for clarifying the operation boundary, defining target plasmas and planning operation scenarios to realize the target plasma and so on. Major part of the code development and the plasma design is being carried out using the high-performance computers such as in IFERC-CSC. Computation resources for JT-60SA, ITER and DEMO research should be established considering their operation schedules. The verification of the codes and the validation with experimental data will be carried out in cooperation with the ITPA activity.

10.5. Research activity during the JT-60SA experiment

After the start of JT-60SA experiment, validation of the theoretical models and simulation codes using the experimental data becomes available. Emphasis should be made on the model validation for the phenomena specific to high-beta and high-bootstrap-current physics such as RWM, NTM, ITB in the JT-60SA experiment. In the Initial Research Phase of JT-60SA, simulation codes will be validated and improved individually. This will require an effort of coherence between code development and validation on one side, and implementation of adequate diagnostics on the other side. The direct comparison between the experiment and the first principle simulation such as the turbulence and nonlinear phenomena, will be also carried out. In the Integrated Research Phase and the Extended Research Phase, the integrated code will be developed and validated. The validated theoretical models and simulation codes will be used for the prediction of ITER plasmas and the development of standard, hybrid and steady-state operation scenarios proposed for the ITER experiment. The validation will be also carried out for ITER experiments, especially on burning plasma physics such as the alpha particle transport and its related instabilities. The theoretical models and simulation codes validated by both JT-60SA and ITER experiments help to reliably predict the behavior of burning high-beta high-bootstrap-fraction plasmas and to develop operation scenarios in DEMO. All these efforts will contribute to the development of comprehensive tokamak simulators available for ITER and DEMO.

10.6. Research results on theoretical models and simulation codes

Computer simulations are used throughout this report to determine and illustrate the capabilities of JT-60SA to carry out its scientific programme. This Section presents a more systematic description of the simulation characteristics and results, including the procedure of model verification and validation, hypotheses and general simulation results.

10.6.1. Comparison and modeling of JT-60U and JET plasmas in typical operational domains in L-mode and H-mode

In preparation for experiments in future devices such as JT-60SA and ITER, development of proper operation scenarios for each research item is indispensable. For more detailed and accurate prediction of the plasmas in those operational domains, it is important to build appropriate physics models and codes for predictive modeling. For development of those codes

and physics models, benchmark against experimental data is valuable. In both JT-60U and JET, plasmas in important domains that are foreseen in JT-60SA have been developed. As those plasmas are closer to those in JT-60SA in important parameters, benchmark of the codes and models against these JT-60U and JET plasmas serves to improve the predictive modeling towards scenario development for JT-60SA. This validation exercise, once completed, will lay the foundations of a systematic predictive simulation programme for JT-60SA, with the aim of preparing the experiments and providing a reference for their future interpretation.

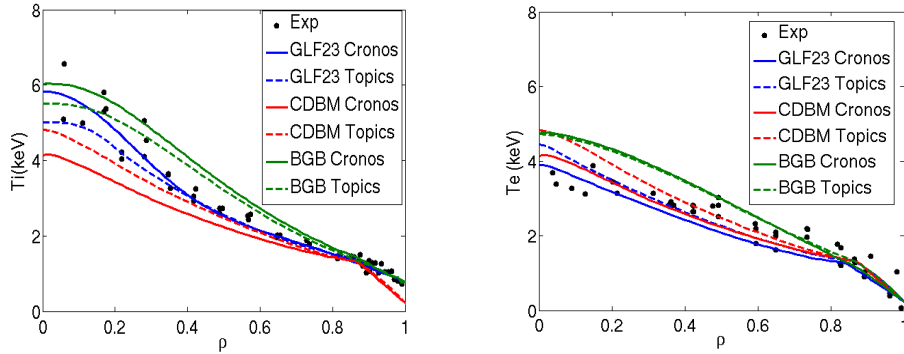


Fig. 10-2: Comparison between the ion (left) and electron (right) temperatures profiles with those obtained with CRONOS (solid) and TOPICS (dashed) with GLF23, CDBM and Bohm-gyro-Bohm transport models, for JT-60U discharge 33655 (H-mode).

Predictive simulations for electron and ion temperature profiles have been carried out for JT-60U and JET plasmas with three transport models, CDBM, GLF23 and Bohm-gyro-Bohm, and by adjusting, as a first step, the pedestal, rotation and density to experimental values whenever available. To carry out this programme, the integrated modelling codes TOPICS and CRONOS are used. NB power depositions and driven currents are calculated by OFMC for JT-60U discharges and by NEMO/SPOT for JET ones, and are fixed in the simulations. The two NB codes have been confirmed to give very similar results for a reference JT-60SA H-mode plasma (Scenario 2). For both JT-60U and JET H-mode typical discharges, both TOPICS and CRONOS give very similar results, as shown in Figure 10-2 for the JT-60U shot 33655. Moreover, all three transport models give a general good agreement with experiments; CDBM slightly underestimates temperatures, BgB slightly overestimates temperatures, and GLF23 gets closer to the experimental data. As a result, CDBM or BgB can be used for rough estimation and GLF23 for more precise estimation in the JT-60SA H-mode simulation [2].

However, the analysis of hybrid and advanced scenarios has shown that the agreement of models and experimental data is more difficult due to the overestimation or underestimation of the impact on turbulence of important effects such as rotation or fast ions population. For hybrid plasmas, GLF23 gives too high ion temperatures when rotation is taken into account and too low when it is not taken. On the other hand, CDBM tends to give the correct ion temperature but slightly underestimates electron temperature, whereas BgB always overestimates temperatures. Therefore in this regime it is found that the CDBM transport model is more reliable than GLF23 [2].

For ITB plasmas with full current drive condition as an advanced scenario, CDBM underestimates ion and electron temperatures in some experiments, but gives correct temperatures in other experiments. On the other hand, BgB gives correct temperatures in some experiments, but overestimates or underestimates temperatures in other experiments. GLF23 always underestimates temperatures. As a result, it is found that CDBM can be used for a conservative prediction [3].

Regarding density transport, GLF23 gives reasonable results both for H-modes and hybrid

regimes and it is able to reproduce the increase of density peaking experimentally found in hybrid scenarios compared to standard H-mode ones. Therefore, self-consistent simulations including current diffusion, temperatures and density have been carried out for inductive H-modes, using only GLF23, and hybrid scenarios using GLF23 for particle transport, and GLF23 or CDBM for temperatures. The simulations give a margin of confidence for the experimental profiles [2].

Regarding the pedestal, it has been checked that using the so-called Cordey empirical scaling gives on average a fair estimate of the pedestal pressure. Checks with MHD computations could improve this estimate. However, the simulations require separate values of the pedestal density and temperatures. To this end, pedestal density has been estimated by assuming that in the pedestal region the particle diffusion coefficient has the same value as the neoclassical ion heat diffusivity [2].

Plasmas in L-mode have been analysed by performing simulations with the transport models CDBM, GLF23 and TGLF for selected cases from JET in the ramp-up. This is done in order to perform predictive simulations for JT-60SA with the CRONOS code. In general, CDBM has been found to reproduce such plasmas with reasonable accuracy.¥

Additionally, such L-mode plasmas have been used as a basis to calibrate the code METIS for fast JT-60SA ramp-up simulations and in general fast scenario analyses. Whereas it is difficult to find a universal set-up of the code which is able to reproduce any L-mode plasma during the ramp-up, it is found that the reproducibility of general plasmas quantities such as I_i or beta can be simulated with enough confidence.

This methodology, i.e., the combination of the above prescriptions for heat transport, particle transport, pedestal and computation of NBI heating source, will then be applied for simulating JT-60SA scenarios, with a reasonable margin of confidence.

10.6.2. Simulations of JT-60SA scenarios

The global parameters or working points of the main JT-60SA scenarios have been determined by the ACCOME code and presented in Sec. 1 and 3 (0-D values in Tables 1-3 and 3-1). These values have to be re-evaluated by full space and time-dependent simulations with integrated modelling tools, such as 1.5-D codes. The 0-D values can also be checked and improved by an intermediate simulation level, such as 0.5-D codes and equilibrium codes. This has been done systematically by means of the METIS code, which combines full solution of the current diffusion equation, simplified heat and current sources and simplified 2-D equilibrium. The results of these simulations in the stationary phase are in very good agreement with the previously quoted 0-D values [4]. An example of the main time and space dependent quantities obtained by METIS for hybrid scenario (Scenario 4-2) is shown in Fig. 10-3. The equilibria and profiles obtained by this type of codes can then be used for various purposes, e.g., benchmark of H&CD calculations done with different codes, and MHD stability calculations. The model validation procedure described in Sec. 10.6.1 will enhance the reliability of results.

Following the analysis performed in Sec. 10.6.1, JT-60SA scenarios have been also simulated using the CRONOS suite of codes [2]. For that purpose, the GLF23 transport model has been used for simulating particle and heat transport for both inductive H-mode scenario (Scenario 2) and hybrid scenario (Scenario 4-2) whereas a combination of CDBM for heat transport and GLF23 for particle transport has been also considered for the hybrid regime. The pedestal pressure has been calculated following the same procedure applied in Sec. 10.6.1. In these simulations, current diffusion equation has been also solved, however, especially for the inductive H-mode scenario, a continuous sawtooth model has been applied in order to calculate the $q=1$ region. In general, the typical characteristics of each scenario have been recovered with

the present design of machine subsystems on JT-60SA. In Fig. 10-4, the predicted density and temperature profiles obtained for the inductive H-mode scenario are shown. Due to the uncertainty of the density at the top of the pedestal, two boundary conditions at that location have been considered, one which leads to a $f_{GW}=0.5$, in agreement with the 0-D value, and another one which leads to higher density ($f_{GW}=0.75$). For any conditions, the results are similar in each scenario. A large sawtooth radius, $\rho \sim 0.45$, with $q_{95} \sim 3$, moderate density peaking and thermal improved confinement $H_{98(y,2)} \sim 1$ has been found at the inductive H-mode scenario with $I_p = 5.5$ MA when 41 MW of input power is added. The pedestal pressure is $P_{ped} \sim 50$ kPa located at of $\rho = 0.94$. For the hybrid scenario, at lower total current, $I_p = 3.5$ MA, and input power, 37 MW, $q_{95} \sim 4.5$ with $q < 1$ only for $\rho < 0.2$ and $H_{98(y,2)} \sim 1.2$ is obtained. The pedestal pressure is $P_{ped} \sim 30$ kPa located at $\rho = 0.95$. This confirms, on the basis of the analysis of present-day experiments, that the power and magnetic systems available on JT-60SA are adequate for the operation of these plasma scenarios.

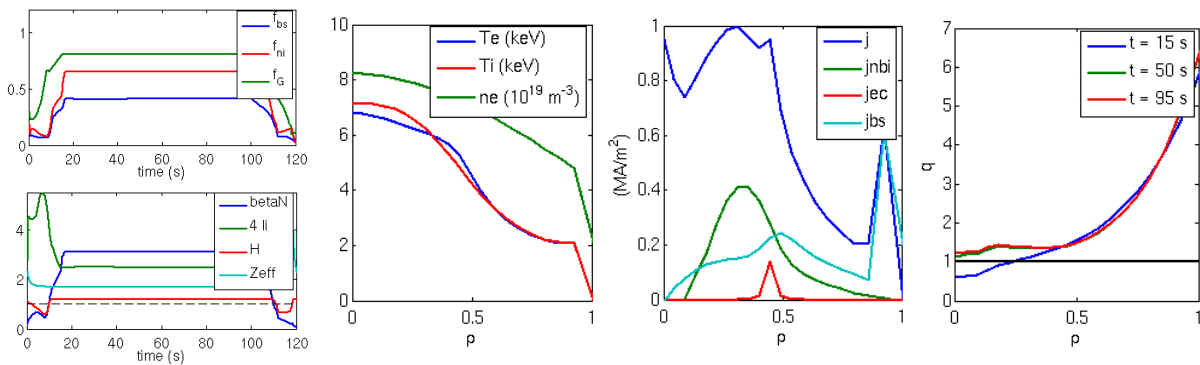


Fig. 10-3: METIS simulations of hybrid scenario (Scenario 4-2). From left to right: time evolution of bootstrap, non-inductive and Greenwald fractions (top); time evolution of β_N , $4I_i$, H factor and Z_{eff} (bottom); temperature and density profiles at $t = 95$ s; current density and current sources profiles (NBI, ECCD, bootstrap) at $t = 95$ s; safety factor profile evolution.

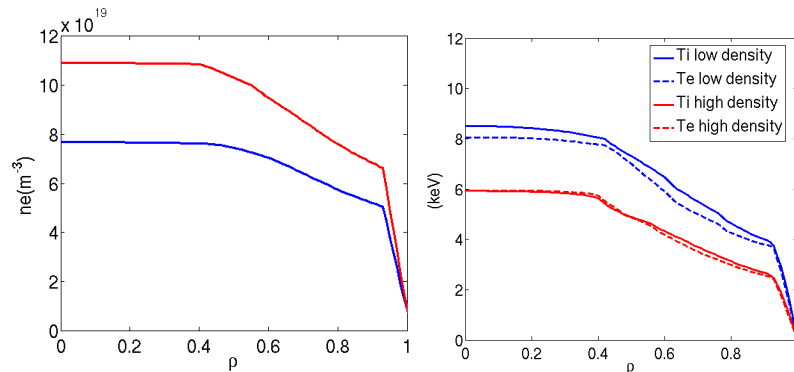


Fig. 10-4: JT-60SA inductive H-mode simulation densities (left) Electron and ion temperatures (right) for two cases with $f_{GW}=0.5$ (in agreement with the reference 0-D value) and higher density ($f_{GW}=0.75$)

Since CDBM can be used for the conservative prediction of thermal transport in ITB plasmas with full current drive (CD) condition as described in Sec. 10.6.1, JT-60SA high-beta steady state plasmas (Scenario 5-1, $I_p = 2.3$ MA) has been conservatively predicted within the machine capability by using TOPICS [3]. In the prediction, the density profile was prescribed the same as in the ACCOME analysis for the 0-D values in Tables 2-3 and 3-1, in which the

separatrix electron density is kept at one third of line averaged density ($\sim 1.7 \times 10^{19} \text{ m}^{-3}$), and pedestal profiles were determined on the basis of EPED1 pedestal width scaling and a stability check by the linear MHD code MARG2D. Various states with the high- β_N (>3.5) and nearly full CD condition could be obtained by using various sets of actuators in JT-60SA. One example was a plasma using 17 MW NB and 7 MW EC powers, resulting in $H_{98(y,2)} = 1.5$, $\beta_N = 3.9$, $f_{BS} = 0.72$, which are close to the previously quoted 0-D values. The predicted parameters were verified by the CRONOS simulation with CDBM, although a slight discrepancy exists within the reasonable range considering the different models used, except for the CDBM model. The normalized beta value is a little lower than the previously quoted 0-d value of $\beta_N = 4.3$. This is mainly due to better confinement enhancement factor of $H_{98(y,2)} = 1.5$ than the assumed value of $H_{98(y,2)} = 1.3$ for the previously quoted 0-D value made with the full power of actuators, resulting in that the full CD condition can be achieved with lower power and the beam pressure becomes lower. For the scenario, the core accumulation of impurity seeded to reduce the divertor heat load below 10 MW/m^2 has been predicted by the divertor code SONIC and TOPICS with settings chosen to maximize the accumulation. It was found that Ar seeding reduces the divertor heat load and its accumulation in the core is so moderate that the core plasma performance can be recovered by additional heating within the machine capability to compensate for Ar radiation [5]. These conservative predictions indicate that the present design of JT-60SA has enough power to explore high-beta steady-state plasmas and their controllability. The predicted plasma will be further studied in several aspects of physics, such as the MHD stability, toroidal rotation and bulk-particle transport.

Two high-beta steady state scenarios with 7 MW EC and 30 or 17 MW NB were simulated with the integrated suite of core/SOL/divertor codes JINTRAC [6]. Various fuelling rates/locations were investigated and it was found that high values of beta, and acceptable levels of power load on the divertor outer-target, can be achieved without impurity seeding for separatrix densities above $2 \times 10^{19} \text{ m}^{-3}$ and in conditions of partial divertor detachment. Several simulations of the JT-60SA scenarios have been performed with other integrated codes ASTRA and JINTRAC, and transport models BgB, CDBM and GLF23 [7]. The results from the different codes are in broad agreement and the main plasma parameters generally agree well with the previously quoted 0-D value. The sensitivity of the results to different transport models and, in some cases, to the ELM/pedestal model has been investigated.

10.7. Summary

The validation of theoretical models and simulation codes with the aim of establishing a solid basis for the design of ITER and DEMO scenarios is one of the main objectives of the JT-60SA scientific programme. At the same time, preparation of the JT-60SA operation requires extensive modelling work with existing codes, new code development and an efficient data exchange platform. These activities are being carried out through a JA-EU cooperation, which makes use of the IFERC-CSC and other supercomputers. Results have been shown in the validation of the most appropriate set of models for integrated modeling against JT-60U and JET discharges, and then the prediction of JT-60SA scenarios using the validated models.

[1] F. Imbeaux et al, Nucl. Fusion **55** (2015) 123006

[2] J. Garcia et al., Nucl. Fusion **54** (2014) 093010

[3] N. Hayashi et al., Nucl. Fusion **57** (2017) 126037

[4] G. Giruzzi et al., 39th EPS Plasma Physics Conference - 16th Int. Congress on Plasma Physics, P5.018 (2012)

[5] N. Hayashi et al., Nucl. Fusion **58** (2018) 066001

- [6] M. Romanelli et al., Nucl. Fusion **57** (2017) 116010
[7] L. Garzotti et al., Nucl. Fusion **58** (2018) 026029

Table 10-2: JA codes and models

Equilibrium	
TOSCA	2D free-boundary equilibrium code suitable for designs of tokamak experiments. It can calculate the best current of poloidal coils given to achieve reference plasma parameters. <i>K. Shinya, J. Plasma Fusion Res. 76, 479 (2000).</i>
ACCOMME	2D free-boundary equilibrium code consistent with steady-state NB driven, EC driven, ohmic and bootstrap currents calculated in code. <i>K. Tani, M. Azumi and R.S. Devoto, J. Comp. Phys. 98, 332 (1992)</i>
HINT2	3D equilibrium code applicable to helicals and tokamaks. It can take account of an equilibrium response to the perturbed field by RMP. <i>Y. Suzuki, et al., Nucl. Fusion 46, L19 (2006)</i>
MECS	MHD Equilibrium Control Simulator developed to study control techniques with the power supply capability of PF coils and the reconstructed plasma boundary by Cauchy condition surface (CCS) method. <i>Y. Miyata et al. Plasma Fusion Res. 9, 3403045 (2014)</i>
Transport and turbulence	
GT5D	Global gyrokinetic toroidal 5D full-f Eulerian code has capabilities of simulating ion temperature gradient driven - trapped electron mode turbulence with self-consistent evolutions of turbulent transport and plasma profiles. <i>Y. Idomura et al., Nucl. Fusion 49, 065029 (2009)</i>
GKV/GKV-X	Linear and nonlinear gyrokinetic solver based on the local flux tube model, applicable to both axisymmetric and non-axisymmetric configurations. <i>M. Nunami et al., Plasma Fusion Res. 6, 1403001 (2011)</i>
FORTEC-3D	Solves the drift-kinetic equation using the df Monte Carlo method and can be applied to evaluate neoclassical transport (radial flux and bootstrap current) in tokamaks and stellarators. It can also evaluate neoclassical toroidal viscosity in tokamaks with RMPs. <i>S. Satake et al., Phys. Rev. Lett. 107, 055001 (2011)</i>
KEATS	Solves the drift kinetic equation using the δf Monte-Carlo method without the assumption of nested flux surfaces, and can be applied to a toroidal plasma having an ergodic region caused by resonant magnetic perturbations (RMPs). <i>R. Kanno et al., Plasma Phys. Control. Fusion 52, 115004 (2010)</i>
MHD	
MARG2D	Linear, ideal, incompressible MHD stability analysis for axisymmetric tokamak equilibria. This code can identify the stability even when an equilibrium is stable. Toroidal mode numbers from $n=1$ up to $n=500$ can be calculated. <i>S. Tokuda and T. Watanabe, Phys. Plasmas 6, 3012 (1999)</i>
MINERVA	Linear, ideal MHD stability analysis code for axisymmetric tokamak equilibria with plasma rotation. Toroidal mode numbers from $n=1$ up to $n=500$ can be calculated. <i>N. Aiba et al., Comput. Phys. Commun. 180, 1282 (2009)</i>
RWMaC	Studies stability of resistive wall modes in tokamak geometry and calculates growth rates and real frequencies of RWMs. <i>N. Aiba, J. Shiraishi, and S. Tokuda, Phys. Plasmas 18, 022503 (2011)</i>
High-energy particles	
TASK/WM	Three-dimensional full wave code in toroidal configuration is used for Alfvén eigen mode analysis by searching eigen modes in a complex wave frequency plane or by calculating damping rate of waves excited by antenna. <i>A. Fukuyama, T. Akutsu, Proc. of 19th IAEA FEC IAEA-CN-94/TH/P3-14 (2002)</i>
MEGA	Hybrid simulation code to study nonlinear dynamics of energetic particles and MHD in realistic geometry. The time evolution of energetic particles and MHD fluid is computed self-consistently. <i>Y. Todo, and T. Sato, Phys. Plasmas 5, 1321 (1998)</i>
BB-solver	Solves long time nonlinear behaviours of energetic particle driven modes based on 1D Berk-Breizman model and reproduces quasi-periodic bursts of chirping AEs by taking account of collisional processes between energetic particles and a bulk plasma. <i>M. Lesur et al., Phys. Plasmas 16, 092305 (2009)</i>
OFMC	Guiding-centre orbit following Monte Carlo code for charged particle behaviour in realistic 3-D tokamak geometry. It can calculate the $j \times B$ torque as well as the collisional one produced by energetic particles. <i>K. Tani et al., J. Phys. Soc. Jpn. 50, 1726 (1981)</i>
AWECS	1D linear gyrokinetic δf particle-in-cell code to study the kinetic excitation of Alfvén instabilities in high- β plasma. It is capable of simulating kinetic ballooning modes, Alfvénic ITG modes and drift-Alfvén instabilities in low- β regime. <i>A. Bierwage and L. Chen, Commun. Comput. Phys. 4, 457 (2008)</i>

Divertor, SOL and PMI	
SONIC	A suite of integrated divertor codes for 2D SOL/divertor characteristics. The code consists of a plasma fluid code SOLDOR, a neutral Monte-Carlo code NEUT2D, and an impurity Monte-Carlo code IMPMC. <i>H. Kawashima, et al., Plasma Fusion Res. 1, 031 (2006)</i>
EDDY	Combines ion reflection and sputtering of plasma-facing materials with transport of released atoms/molecules with gyromotion and diffusion. <i>K. Ohya, Physica Scripta T124, 70 (2006)</i>
IMPGYRO	Monte-Carlo code for high-Z impurity transport. The code directly solves the 3D motion of equation, including the Larmor gyration. It is coupled with EDDY for appropriate treatment of plasma-surface interactions, such as sputtering, reflection. <i>M. Toma, et al., J. Nucl. Mater. 390-391, 207 (2009)</i>
Integrated operation scenarios	
TOPICS	Integrated modeling code based on the 1.5D transport code. It integrates MARG2D, EC-Hamamatsu, TASK/WM, SONIC, the linear version of GT5D and so on. <i>N. Hayashi et al., Plasma Fusion Res. 6, 2403065 (2011)</i>
TASK	Integrated tokamak transport modelling code including equilibrium, diffusive transport, ray tracing, full wave analysis, and velocity distribution function analysis. The data exchange interface BPSD is partly implemented. <i>A. Fukuyama, et al., Proc. of 20th IAEA FEC IAEA-CSP-25/CD/TH/P2-3 (2004)</i>
TASK/TX	1D multi-fluid transport code solves transport equations for electrons and ions coupled with Maxwell's equations in cylindrical coordinate. It gives a consistent solution among the radial electric field and poloidal/toroidal flows as well as other transport variables. <i>M. Honda and A. Fukuyama, J. Comput. Phys. 227, 2808 (2008)</i>
TOTAL	Toroidal Transport Analysis Linkage code is utilized for tokamak and helical burning plasma prediction and experimental analysis. Especially, tungsten impurity effects and NTM effects on core transport can be evaluated in tokamak plasmas. <i>K. Yamazaki and T. Amano, Nucl. Fusion 32, 633(1992).</i>
Heating and CD	
EC-Hamamatsu	Ray-tracing coupled to a relativistic Fokker-Planck code to calculate the EC heating and CD in a general tokamak equilibrium. <i>K. Hamamatsu and A. Fukuyama, Fusion Eng. Des. 53, 53 (2001)</i>
TASK/WR	Ray tracing and beam tracing analysis of electron cyclotron and lower hybrid wave propagation and absorption in tokamaks. The current drive efficiency is calculated by the Fokker-Planck analysis of momentum distribution function, TASK/FP. <i>A. Fukuyama, Fusion Eng. Des. 53, 71 (2001)</i>

Table 10-3: EU codes and models

Equilibrium	
HELENA	2D equilibrium code with given plasma boundary of arbitrary shape. Also calculated are the infinite-n ballooning stability and the ideal and resistive Mercier criterium. <i>G.T.A. Huysmans et al., CP90 Conf. on Comp. Physics, Word Sci. 1991, p.371.</i>
CHEASE	Accurate fixed boundary 2-D magnetic reconstruction code for MHD studies. It solves Grad-Shafranov equation in axi-symmetric toroidal geometry for thermal (one-temperature) plasma. Computes bootstrap fraction, ballooning stability, ideal interchange (Mercier) and resistive interchange stability. <i>H. Lütjens et al., Comput. Phys. Commun. 97, 219 (1996)</i>
Transport and turbulence	
QUALIKIZ	Quasilinear model based on the linear gyrokinetic code KINEZERO, which calculates the linear growth rates of unstable modes to characterise the microturbulence. It accounts for all unstable modes and sums up the contributions over a wave-number spectrum. <i>C. Bourdelle et al., Phys. Plasmas 14, 112501 (2007)</i>
GEM	Gyrofluid electromagnetic turbulence code, which describes the fluctuation free-energy conservation in a gyrofluid model by means of the polarization equation. This relates the ExB flow and eddy energy to the combinations of the potential, the density, and the perpendicular temperature. <i>B Scott, Phys Plasmas 12, 102307 (2005)</i>
GYSELA	Non-linear, 5-D, full-f gyrokinetic code. It uses a fixed grid with a Semi-Lagrangian scheme for an accurate description of fine spatial scales. <i>V. Grandgirard et al., Plasma Phys. Contr. Fusion 49, B173 (2007)</i>
CENTORI	Fully toroidal (arbitrary aspect ratio, arbitrary beta) two-fluid, electromagnetic turbulence simulation code. It allows the computation of turbulence in realistic tokamak geometries and at high beta. <i>A. Thyagaraja and P.J. Knight, Progress in Industrial Mathematics at ECMI 2008 (Berlin: Springer) p 1047 (2010)</i>
GENE	Gyrokinetic Vlasov code. It solves the nonlinear gyrokinetic equations on a fixed grid in five-dimensional phase space (plus time). <i>T. Görler et al., J. Comp. Phys. 230, 7053 (2011)</i>
NEMORB	Global gyrokinetic Lagrangian Particle-In-Cell code, including electromagnetic effects. <i>A. Bottino et al., Plasma Phys. Contr. Fusion 53, 124027 (2011)</i>
TRINITY /GS2	Direct coupling between a transport solver and local nonlinear gyrokinetic calculations. This code enables first-principles simulations of the full fusion device volume over the confinement time feasible on current computing resources. <i>M. Barnes et al., Phys. Plasmas 17, 056109 (2010)</i>
MHD	
MISHKA	Ideal, incompressible MHD stability analysis of axisymmetric tokamak equilibria. The full spectrum of MHD waves (TAE modes etc.) can also be calculated, including modes driven by an external antenna. Toroidal mode numbers n=1-50 can be calculated. <i>A.B. Mikhailovskii et al., Plasma Phys. Rep. 23, 844 (1997)</i>
CASTOR	Linear, resistive MHD stability analysis of axisymmetric tokamak equilibria. The full spectrum of MHD waves (TAE modes etc.) can also be calculated, including modes driven by an external antenna. Toroidal mode numbers n=1-20 can be calculated. <i>W. Kerner et al., J. Comp. Phys., 142, 271 (1998)</i>
XTOR	3D nonlinear MHD code. Includes resistive MHD effects, anisotropic thermal transport, some neoclassical effects. <i>H. Lütjens, J.F. Luciani, J. Comp. Phys. 227, 6944 (2008)</i>
CARMA	Studies RWM by self-consistent coupling between MARS-F (single fluid MHD code, including the effects of plasma rotation and using various damping models to approximate the ion Landau damping) and CARIDDI (a 3D time-domain eddy currents code). <i>F. Villone et al., in 34th EPS Conf. on Control. Fusion and Plasma Phys., ECA Vol. 31F, P5.125 (2007).</i>
STARWALL	Three-dimensional stability code to compute the growth rates of RWMs in the presence of nonaxisymmetric, multiply connected wall structures and to model the active feedback stabilization of these modes. <i>E. Strumberger et al., Phys. Plasmas 15, 056110 (2008)</i>
GRAF	Solution of the generalized Rutherford equation for tearing mode evolution, including island rotation and asymmetry effects. <i>E. Lazzaro, S. Nowak, Plasma Phys. Contr. Fusion 51, 035005 (2009).</i>
JOREK	Non-linear extended MHD code JOREK resolves realistic toroidal X-point geometries including main plasma, scrape-off layer and divertor region. It includes divertor boundary conditions, 3D resistive wall effects, two-fluid effects and neoclassical flows. <i>GTA Huysmans and O. Czarny Nuclear Fusion 47, 659 (2007)</i>

High-energy particles	
HAGIS	Kinetic δf code, computing the nonlinear resonant interaction of fast particle distributions with linear MHD eigenmodes in toroidal geometry. Full orbit effects and nonlinear mode perturbations are retained. The model nonlinearly evolves the spectrum of linear modes, resolving the linear and nonlinearly-saturated phases of wave growth and reactive frequency shifts. <i>S.D. Pinches et al., Comp. Phys. Comm. 111, 133 (1998)</i>
HYMAGYK	Hybrid MHD Gyrokinetic code, built by interfacing an equilibrium module, a MHD module adapted for the computation of the perturbed scalar and vector potentials, and a gyrokinetic particle-in-cell module (yielding the energetic ion pressure tensor returned to the MHD solver). <i>G. Vlad et al., 11th IAEA TM on Energetic Particles in Magnetic Confinement Systems, P-25, 2009</i>
LIGKA	Linear MHD gyro-kinetic code in realistic tokamak geometry, self-consistently treating general energetic particle distribution functions. It can be used to calculate stability boundaries of Alfvénic modes. <i>Ph. Lauber et al., J. Comp. Phys. 2268, 447 (2007)</i>
ASCOT	Guiding-centre orbit following Monte Carlo code for studies of charged particle behaviour in realistic 3-D tokamak geometry. <i>J. Heikkinen et al., Comp. Phys. Comm. 76, 215 (1993)</i>
SPOT	Monte Carlo code that follows fast particle guiding centre orbits in an arbitrary axi-symmetric geometry. <i>M. Schneider et al., Plasma Phys. Contr. Fusion 47, 2087 (2005)</i>
Divertor, SOL and PMI	
EDGE2D/ EIRENE	Solves a set of fluid equations describing the edge plasma, coupled to a kinetic (Monte Carlo) description of the neutrals on a 2D grid for the divertor, SOL and a small annulus of the main plasma (on closed flux surfaces). <i>D. Reiter, J. Nucl. Mat. 196, 241 (1992)</i>
SOLPS	This solves a set of fluid equations describing the edge plasma, coupled to either a fluid or kinetic (Monte Carlo) description of neutrals on a 2D grid for the divertor, SOL and a small annulus of the main plasma (on closed flux surfaces). <i>R. Schneider et al., Contrib. Plasma Phys. 46, 3 (2006)</i>
BIT1	Particle-in-cell Monte Carlo code. Multiple-ion, multiple-neutral scrape-off layer transport code, taking account of plasma-wall interactions. Includes some elements of plasma-surface interactions: secondary electron collisions, and neutral recycling. <i>D. Tskhakaya and S. Kuhn, J. Nucl. Mat. 313-316, 1119 (2003)</i>
DIVGAS	Describes the neutral dynamics in the upper divertor and sub divertor region with the Direct Simulation Monte Carlo method to solve the Boltzmann equation. <i>S. Varoutis et al., Fus. Eng. Des. 121, 13 (2017)</i>
Integrated operation scenarios	
ASTRA	Solution of a set of transport equations consistent with models for sources, together with the Grad-Shafranov equation in general toroidal geometry (tokamak or stellarator). <i>G.V. Pereverzev and P.N. Yushmanov, IPP-Report, IPP 5/98, February, 2002</i>
JETTO	Solution of a set of transport equations consistent with models for sources, together with the Grad-Shafranov equation in general tokamak-related toroidal geometry. Set of 6 transport equations: poloidal flux, electron and ion temperature, ion density and toroidal rotation. It's linked with 1D core impurity transport code SANCO. <i>G. Cenacchi and A. Taroni, ENEA, ISSN/0393-6633, 1988</i>
JINTRAC	A system of 25 interfaced tokamak-physics codes for the integrated simulation of all phases of a tokamak scenario including transients. Amongst the other features, JINTRAC allows for integrated transport simulations of core/edge/SOL/divertor. <i>M. Romanelli et al. Plasma Fusion Res. 9, 3403023 (2014)</i>
CRONOS	Suite of numerical codes for the predictive/interpretative simulation of a full tokamak discharge. It integrates, in a modular structure, a 1D transport solver with general 2D magnetic equilibria, several heat, particle and impurities transport models, as well as heat, particle and momentum sources. <i>J.F. Artaud et al., Nucl. Fusion 50, 043001 (2010)</i>
ETS	'European Transport Simulator' (ETS) is the new modular package for 1D discharge evolution developed within the EFDA Integrated Tokamak Modelling (ITM) Task Force. It consists of precompiled physics modules combined into a workflow through standardized input/output data structures. <i>D. Kalupin et al., Nucl. Fusion 53, 123007 (2013)</i>

METIS	0.5 D code, computing the time evolution of global plasma quantities for given waveforms of control parameters in a discharge with short CPU time. It solves current diffusion equation with an approximate equilibrium evolution, simplified treatment of sources and of spatial dependences. Stationary transport equations are solved on discrete time slices. <i>J.F. Artaud et al., Nucl. Fusion 58, 105001 (2018)</i>
RAPTOR	RAPTOR (RAPid Plasma Transport Simulator) is a 1D tokamak transport code specially designed for rapid execution compatible with needs for real-time execution or for use in nonlinear optimization schemes. <i>F. Felici et al. Plasma Physics and Controlled Fusion 54 (2012) 025002</i>
Heating and CD	
NEMO	Modular code for simulating ionization during NBI in tokamak plasmas. It uses the narrow beam model and includes different types of cross-sections for the beam attenuation. <i>M. Schneider et al., Nucl. Fusion 51, 063019 (2011)</i>
GRAY	Quasi-optical propagation of a Gaussian beam of electron cyclotron waves in a general tokamak equilibrium, taking account of diffraction effects. It includes the full relativistic dielectric tensor and linear CD calculation. <i>D. Farina et al., Fus. Sci. Techn. 52, 154 (2007)</i>
LUKE/C3PO	Versatile ray tracing for radio-frequency waves and 3-D relativistic bounce-averaged electron Fokker-Planck solver <i>J. Decker, Y. Peysson, et al., Phys. Plasmas 17, 112513 (2010)</i>

Appendix

Appendix A: Heating and Current Drive Systems

1. Neutral Beam System

One of the characteristic features of JT-60SA is three types of NBI systems with variety of the injection geometries. The JT-60U NBI system will be upgraded to extend the injection duration from 30 s (JT-60U) to 100 s (JT-60SA). The long pulse injection from each injector can be achieved with the upgrades of power supplies, magnetic shield, a part of the beamline components and control systems. Totally, the JT-60SA NBI system injects D⁰ beams of 20 MW and 30 MW for 100 s and 60 s respectively in the initial and the integrated research phases, and 34 MW for 100 s in the extended research phase. In order to realize 34 MW for 100s, magnetic shield in the perpendicular positive-ion-based NB injectors should be entirely modified.

The NBI system consists of twelve positive-ion-based NBI (P-NBI) units and two negative-ion-based NBI (N-NBI) units as summarized in Table A-1-1. This P-NBI system includes eight perpendicular injection, two co-tangential injection, and two counter-tangential injection units with the beam energy of 85 keV and the beam power of 1.7MW/unit (Initial & Integrated Research Phases) and 2 MW/unit (Extended Research Phase). In case of H⁰ injection, the power is decreased to 0.8MW/unit. The N-NBI system includes two units (upper and lower) with the beam energy of 500keV and the beam power of 5MW/unit. The layout of the NBI system is shown in Fig. A-1-1. The location of the NBI injectors is the same as that of the JT-60U. The beam trajectories are shown in Fig.A-1-2. The beam line of the N-NBI unit is shifted downward from the equatorial plane by ~0.6 m in order to drive off-axis plasma current for flat or reversed magnetic shear operations. The deposition profiles with P/N-NBI in the scenario #2 and #3 are shown in Fig. A-1-3 and A-1-4, respectively.

Table A-1-1 Neutral Beam System in JT-60SA

D ⁰ Beam	No. of unit	Energy (keV)	Power /unit (MW)	Total Power (MW)	duration (s)
Positive Ion Source NB : for heating (ion heating dominant), torque input control, some current drive					
Perpendicular – upper (#2,4,6,14)	4	85	1.7 -> 2 (initial & integrated research phases: 1.7MW/unit, extended research phase: 2MW/unit)	6.8 -> 8	100
Perpendicular – lower (#1,3,5,13)	4			6.8 -> 8	
CO-tangential – upper (#10)	1			1.7 -> 2	
CO-tangential – lower (#9)	1			1.7 -> 2	
CTR-tangential-upper (#8)	1			1.7 -> 2	
CTR-tangential-lower (#7)	1			1.7 -> 2	
Negative Ion Source NB: for heating (electron heating dominant), current drive, small torque & particle input					
CO-tangential – upper (NNB-U)	1	500	5	5	100
CO-tangential – lower (NNB-L)	1			5	
Total	(*) Initial & Integrated Research Phases: 30MW x 60s, 20MW x 100s, Extended Research Phase: 34MW x 100s			30.4 ->34	100 (*)

The P-NBIs are used for heating (ion heating dominant), torque input control (CO-tangential, CTR-tangential and Perpendicular injections), and some contribution to current

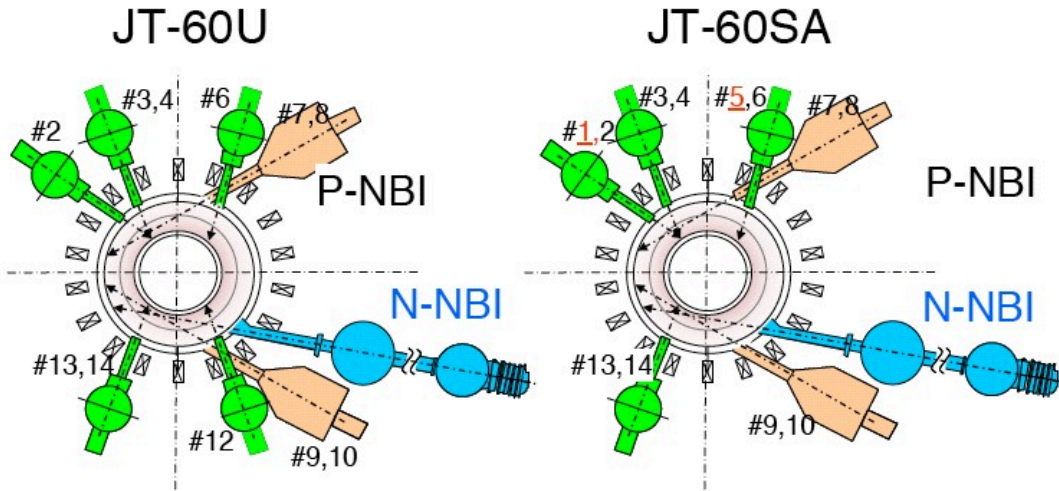


Fig. A-1-1 Layout of the NBI Systems in JT-60U and JT-60SA

drive (CO-tangential, CTR-tangential). The N-NBIs are used for heating (electron heating dominant), and current drive with small torque and particle input. We can select any combinations of these NBs, and control the heating profile, the current profile and rotation profile separately. For example, we can change the NB current drive power, the torque input, the ratio of the electron heating to the total heating power with the total heating power kept constant. In addition, we can simulate the α -particle heating by, for example, using a real time power control of some unit of the P-NBs as the α -heating power while a current profile is control with N-NBs. By combining with ECH, the above capabilities are more expanded in terms of the ITER and DEMO relevant heating conditions; such as dominant electron heating and low central fueling enabled by N-NB and ECH, and low external torque input enabled by N-NB, ECH, perpendicular P-NBs and balanced injection of CO and CTR tangential P-NBs. Technically, the P-NBI system will be modified to ensure the capability of modulated injection. After the upgrade of the control system and optimization of the operation, the modulated injection within $<10\sim 20\text{Hz}$ will be expected. Modulation of N-NBI is under consideration.

The key issues for the realization of N-NBI for JT-60SA are voltage holding capability of the negative ion source and a long pulse production of the large-area negative ion beam.

As for the voltage holding capability, by optimizing gap lengths between the acceleration grids, QST has achieved stable sustainment of 500 kV of rated acceleration voltage for JT-60SA (Fig.A-1-3) [1]. The influence of the beam acceleration on breakdown at the higher current will be examined in the future.

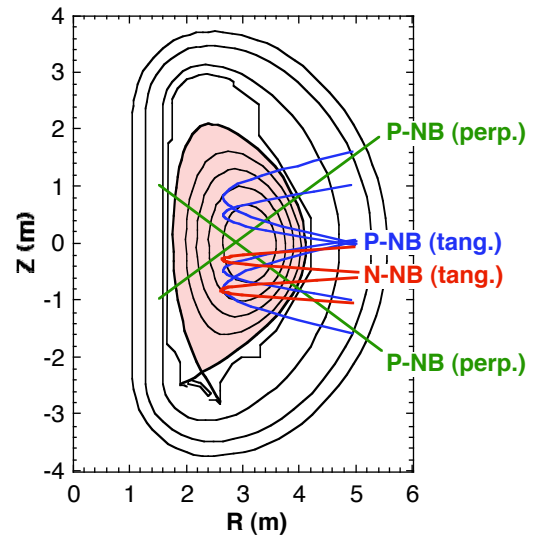


Fig. A-1-2 Beam trajectories of P-NBs and N-NBs with a plasma equilibrium for $I_p=5.5\text{ MA}$ Lower single Null operation.

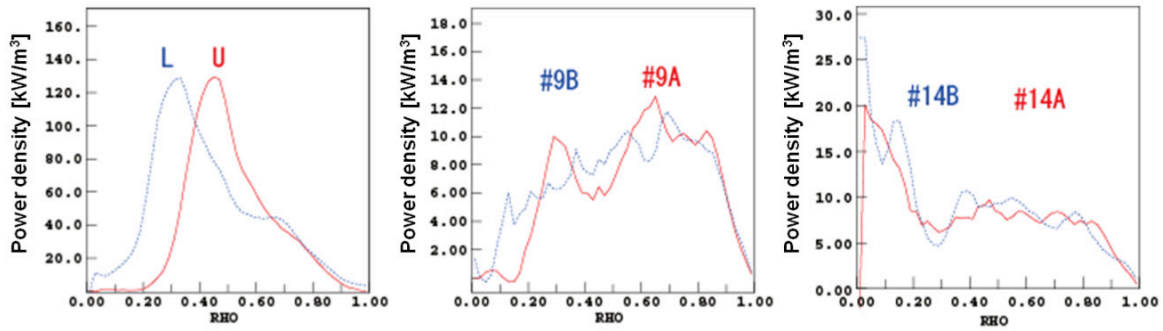


Fig. A-1-3 Deposition profiles of the P/N-NBI with the beam power of 2 MW and 5 MW per unit on the scenario 2. #9 and #14 injectors are co-tangential-lower and perpendicular-upper units, respectively. Each unit of the P-NBI has two ion sources (A and B).

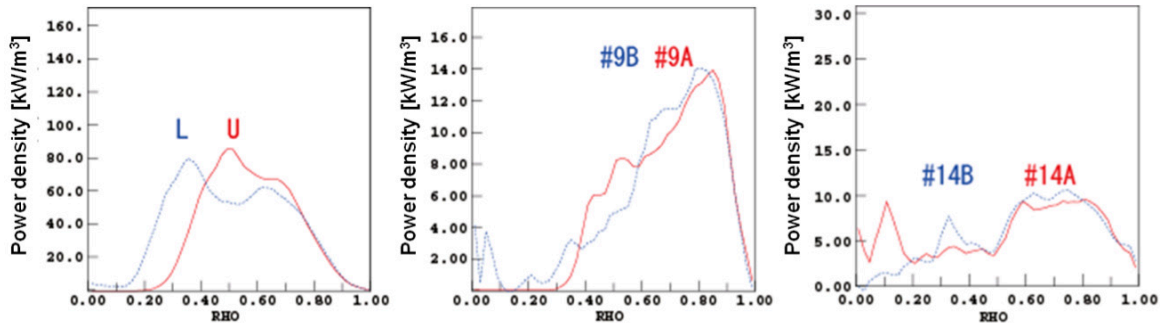


Fig. A-1-4 Deposition profiles of the P/N-NBI with the beam power of 2 MW and 5 MW per unit on the scenario 3 (high density case).

As for the large-area extraction of negative ions, the uniform production of the source plasma is essential, which results in the uniform negative ion profile. Based on the results previously obtained in a small ion source in QST, the magnetic filter field configuration in the JT-60SA ion source has been modified. The original transverse filter field produced by a current flowing in the plasma grid (PG) has been changed into the so-called tent-shaped filter. In the tent-shaped filter, the direction of the magnetic field line is adjusted to suppress the localization of the primary electrons due to $B \times \text{grad } B$ drift. After the optimization of this filter field to expand the uniform plasma production, the uniform production area increased from 68% in the original PG filter to 83%. Also the achieved total negative ion current was increased from 17 A in JT-60U to 32 A by this modification in 2014 [2]. This negative ion current has satisfied the requirement of JT-60SA of 22 A, for the pulse duration of 1 s.

As for the long pulse beam production, a temperature of the PG, where a cesium layer is formed to enhance surface production of negative ions, should be controlled at 200-250C during long pulse duration. In ITER, high-temperature and high-pressure water is designed. In JT-60SA, high-temperature fluorinated (i.e. Galden®) fluid having boiling point of 270C, which is widely used in semiconductor products for easy handling, is designed to flow through cooling channels in the PG. This PG temperature control system was developed and tested in the test stand with the JT-60SA negative ion source. In 2012-2013, the proof of principle system was applied for 1/10 extraction area and the long pulse capability of the PG temperature control system was demonstrated. Achieved current density for 100 s has reached to 120-130A/m² which is about 90% of the rated value for JT-60SA negative ion source [3]. Based on this result, the PG temperature control system for whole extraction area was developed and tested in 2014.

The available negative ion current for 100 s increased to 15 A, which is about 70% of the rated current (Fig.A-1-6) in 2014 [4]. The arcing of the arc discharge and the breakdown of the extraction voltage on high current extraction should be reduced to increase the sustainable current for long pulse operation. Although the PG temperature was sustained for 100s, negative ion current was gradually degraded on the long time scale due to the temperature increase of the arc chamber. This temperature increase causes the recycling of cesium on the wall. The cooling capability of the arc chamber will be modified in future after the investigation of the

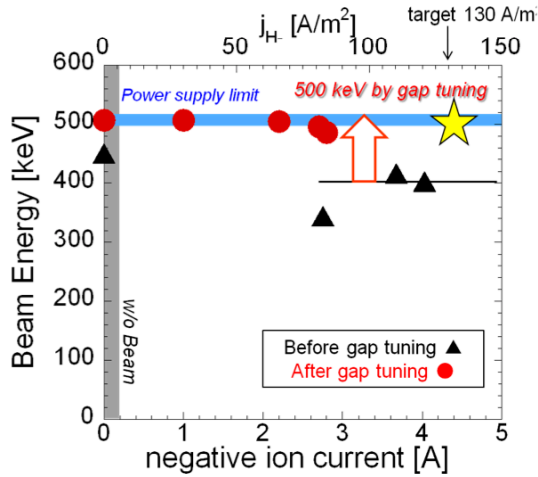


Fig.A-1-5 Achieved beam energy by JT-60SA negative ion source (after gap tuning) and original ion source (before gap tuning). Cs recycling effect.

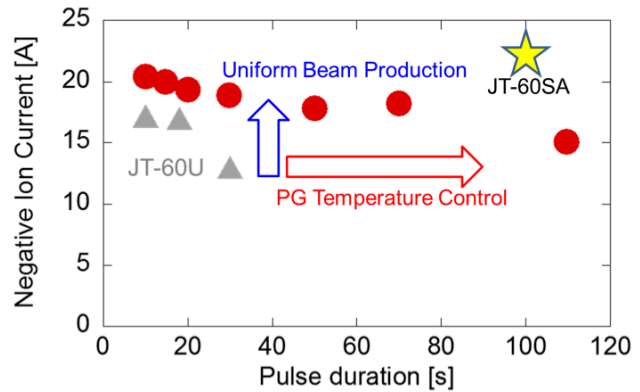


Fig. A-1-6 Progress of long pulse operation of the JT-60SA negative ion source at the teststand (w/o acceleration) The PG temperature is actively controlled to keep the negative ion production.

In 2015, long pulse acceleration of positive and negative ion beams have significantly progressed by developing long pulse acceleration techniques.

As for the positive ion beam, 2MW hydrogen ion beam with 80 keV, 25 A was successfully accelerated for 100 s by using the ion source for P-NBI as shown in Fig. A-1-7 [5]. In this experiment, the new control technique to stabilize a beam current has been developed by regulating the gas input for plasma production according to a time constant of pumping capability of the system including the ion source. Since the obtained beam power and pulse length satisfied the JT-60SA design values in the initial and integrated research phases of 1.9 MW 100 s per ion source, 20 MW injection from P-NBI can be expected for 100 s in JT-60SA operation.

As for the negative ion beam, 185 MW/m² high power density H⁻ beam was accelerated for 60 s for the first time by using 5-stage electrostatic accelerators having same design concept as that for JT-60SA negative ion source. Achieved energy density has reached to 11 GJ/m² which has much exceeded the target value of that for JT-60SA of 6.5 GJ/m². This long pulse acceleration was obtained by developing a

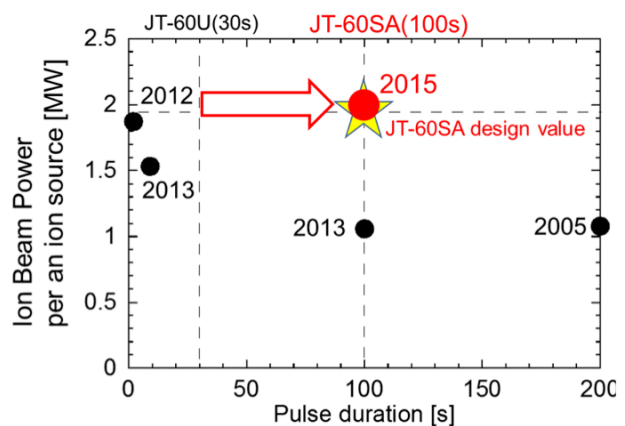


Fig. A-1-7 Progress of long pulse acceleration of the JT-60SA positive ion source.

design technique of voltage holding capability of the accelerator and a control technique of the high-power-density negative ion beam. The voltage holding capability of the multi-stage accelerator was designed by taking the area effect into account and optimizing the nested structure of multiple stages of the grid supports. In addition, each beamlet was controlled precisely by updating extractor, and aperture configuration on acceleration grids was modified to reduce secondary electron emission. By applying these developed techniques to the JT-60SA negative ion source, a long pulse acceleration of 500 keV, 130A/m² for 100s has been tested in 2016-2018.

Reference

- [1] Kojima A. Hanada M. Tanaka Y. *et al* 2011 *Nucl. Fusion* **51** 083049
- [2] Yoshida M. Hanada M. Kojima A. *et al* 2015 *Fusion Eng. Des.* **96-97** 616
- [3] Kojima A. Hanada M. Yoshida M. *et al* 2014 *Rev. Sci. Instrum.* **85**, 02B312
- [4] Kojima A. Umeda N. Hanada M. *et al* 2015 *Nucl. Fusion* **55** 063006
- [5] Kojima A. Hanada M. Jeong S.H. *et al* 2016 *Fusion Eng. Des.* **102** 81

2. ECRF system

The ECRF system in JT-60SA plays important roles in many phases of JT-60SA discharges. One of the major roles of the ECRF system is to stabilize NTMs as described in Section 2 of Chapter 4. Capability of localized electron heating and current drive is advantageous for the study of heat transport, ITB physics and rotation physics and so on, as described in Section 5. In addition to heating and current drive, the EC wave is to be used to assist plasma initiation because available one-turn voltage is much lower than that in JT-60U due to the limitation of the superconducting poloidal field coils. Furthermore, EC wave is planned to be used for between-shot wall cleaning. In this case, the usage of the ECRF system should be optimized so that the ECRF system is available for both the plasma experiments and the discharge cleaning in the experiment sequences within the limitation of the facility.

In the Initial Research Phase, 4 gyrotrons with the output power of 1 MW are to be installed. Pulse duration of the 2 gyrotrons is 5 s and that of the other 2 gyrotrons is 100 s. By taking into consideration the transmission loss of about 25%, injection power of about 3 MW will be possible. In the Integrated Research Phase, the total number of the gyrotrons will be increased to 9, and the pulse duration of all the gyrotrons will be 100 s, by which about 7 MW injection will be possible. Main specifications are listed in Table A-2. The EC wave is injected from the upper outboard ports at the P-1, P-4, P-8 and P-11 sections as shown in Fig. A-6. The injection angle of the EC wave is changed both poloidally and toroidally by using a linear-motion launcher shown in Fig. A-7. Range of the injection angles is under investigation. Note that the range of the poloidal injection angle is related to the beam width [1]: Narrow beam width at the deposition location corresponds to wider beam width at the mirror 2, resulting in narrower range of the poloidal injection angle. As for the toroidal injection angle, the range is typically 30°, e.g. -15° to +15°. Design analysis indicates that the toroidal injection angle of $\sim \pm 25^\circ$ is possible by installing the mirror 2 with a slight tilt in the toroidal direction. It was agreed in RCM-3 that the toroidal angle range is designed so as to maximize the toroidal injection angle in the co-direction.

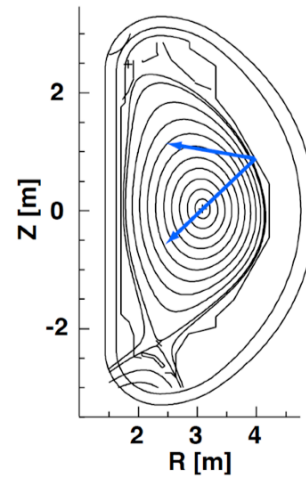


Fig. A-6 Plasma cross section and the direction of EC waves.

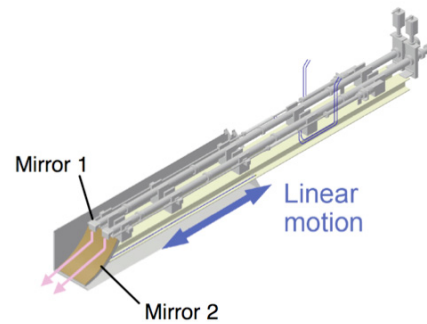


Fig. A-7 Schematic view of a linear-motion launcher. Poloidal injection angle is changed by moving the mirror 1 back and forth. Toroidal injection angle is changed by rotating the mirror 1.

Table A-2: Specifications of ECRF system

Research phase	Number of gyrotrons	Injection power & pulse duration	Injection port	ECRF frequency
Initial Research Phase	4	1.5 MW × 5 s 1.5 MW × 100 s	P-1, P-4, P-8, P-11 (Upper outboard port)	110 GHz, 138 GHz
Integrated Research Phase	9	7 MW × 100 s		
Extended Research Phase				

In addition to single-pulse injection with a fixed power, power modulation will be required in some experiments. For transport and ITB studies, power modulation from ~ 0.5 Hz (i.e. 1 s on and 1 s off) to several tens of Hz will be needed. For NTM control, power modulation with the frequency of >5 kHz is required. The mode frequency of an $n = 1$ mode was about 5 kHz in JT-60U, and it became twofold for an $n = 2$ mode. The mode frequency may be higher in JT-60SA due to larger torque input by NNB. Thus, the ECRF system should be designed with enough margin for the modulation frequency. In addition, modulation frequency should be able to be changed according to the temporal change in the NTM frequency. Diagnostic signals such as magnetic probe and ECE can be used to synchronize the modulated EC wave with the NTM rotation, as was demonstrated in JT-60U. Applicability of a fast directional switch in the transmission line will be investigated in parallel.

EC wave will be fully absorbed by the JT-60SA plasma if the optical thickness of the plasma is high enough, which is the case in most of the tokamak discharges of JT-60SA (See Fig. A-8 for ECH/ECCD properties of 110 GHz EC wave in Scenario 5). However, when the EC wave is used for plasma initiation and wall cleaning, single-path absorption may be low. In this case, high-power EC wave will be reflected inside the vacuum vessel. The strategy to prevent any damage of in-vessel components and diagnostics by stray RF is under investigations (e.g. monitoring by sniffer probes and/or hardening of the relevant components).

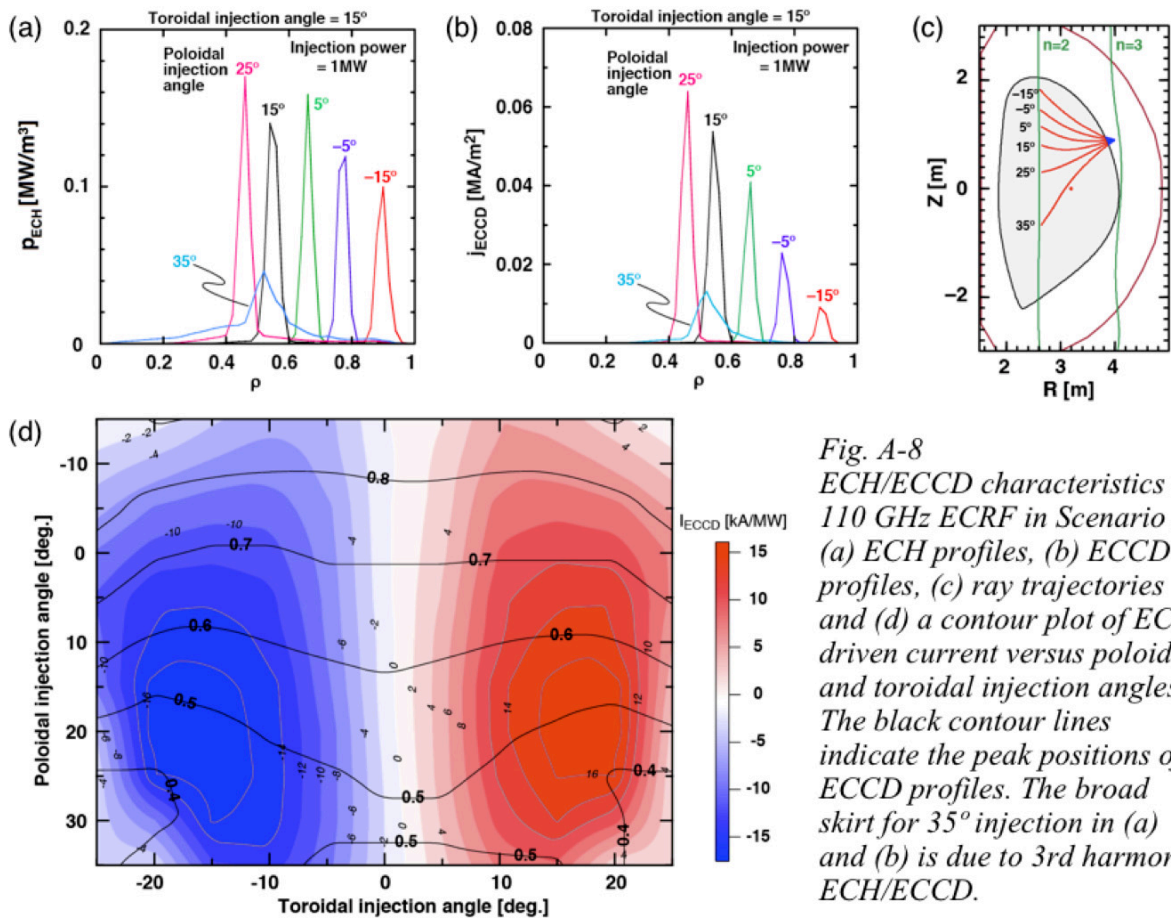


Fig. A-8
ECH/ECCD characteristics of 110 GHz ECRF in Scenario 5. (a) ECH profiles, (b) ECCD profiles, (c) ray trajectories and (d) a contour plot of EC-driven current versus poloidal and toroidal injection angles. The black contour lines indicate the peak positions of ECCD profiles. The broad skirt for 35° injection in (a) and (b) is due to 3rd harmonic ECH/ECCD.

The original frequency of design for the gyrotron is 110 GHz. However, the cold resonance surface of the second harmonic EC is located at $R = 3.38$ m for ECRF operations at

$B_t = 2.25$ T with 110 GHz waves. This is fairly off-axis region. Furthermore, the EC wave at this frequency will be fully absorbed before reaching the resonant surface due to the Doppler shift effect. At this high field operation, EC waves can only penetrate up to $\rho \sim 0.7$ and have therefore limited applicability (See Fig. A-9.) On the other hand, this implies that 110 GHz ECRF is useful for edge ECH/ECCD for e.g. ELM control. ECH/ECCD calculations show that frequency in the range of 130-140 GHz is suitable for central ECH/ECCD at high toroidal field.

The gyrotron engineering criteria indicate that a suitable solution for the second frequency is 138 GHz ($TE_{22,8}$ for 110 GHz and $TE_{27,10}$ for 138 GHz). By this frequency, ECH/ECCD at $\rho \sim 0.3-0.8$ becomes possible in Scenario 2 as shown in Fig. A-10.

The results shown in Figs. A-8 to A-10 do not consider the tilt of mirror 2 and the astigmatism of injected beams. Calculations including these effects have also been carried out for typical scenarios [2] (Note that the values of the mirror curvatures and tilt angle in this reference are not the finalized ones.).

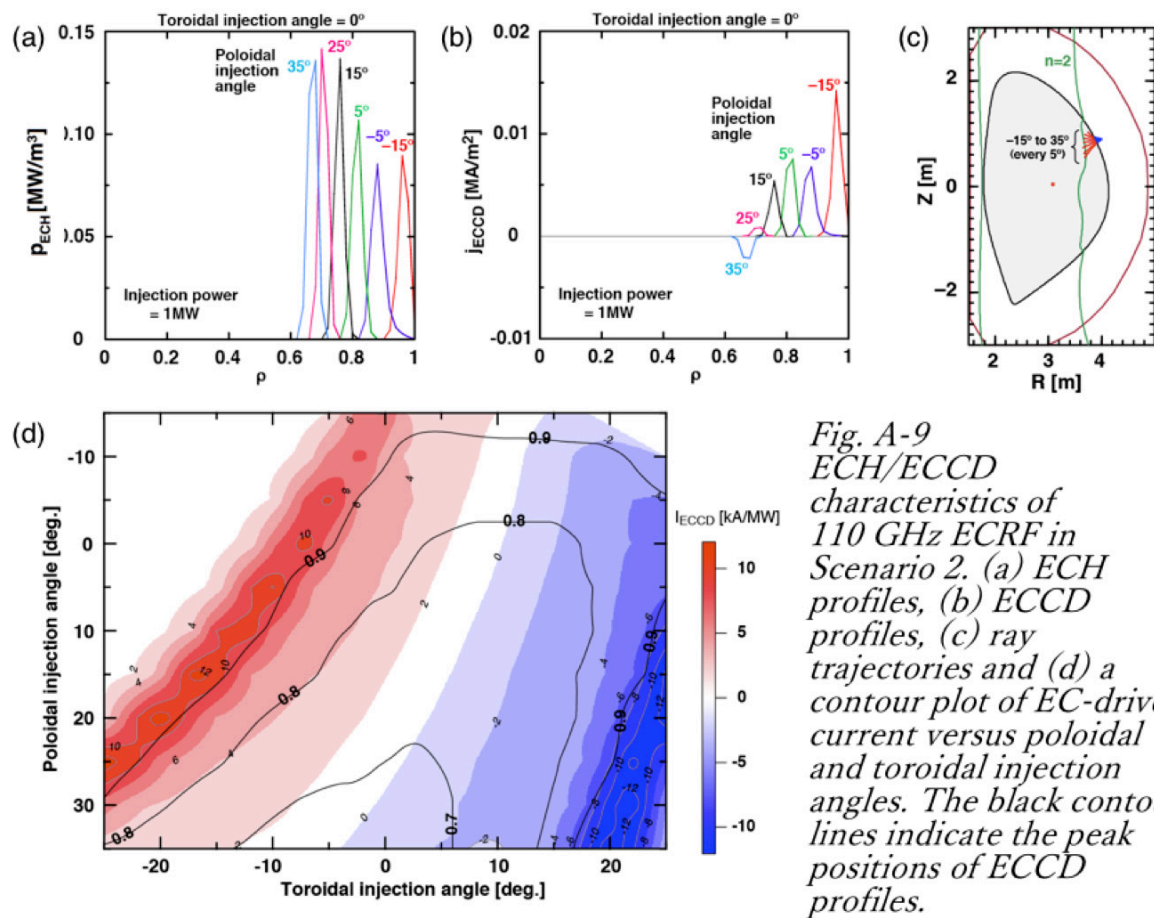


*Fig. A-9
ECH/ECCD
characteristics of
110 GHz ECRF in
Scenario 2. (a) ECH
profiles, (b) ECCD
profiles, (c) ray
trajectories and (d) a
contour plot of EC-driven
current versus poloidal
and toroidal injection
angles. The black contour
lines indicate the peak
positions of ECCD
profiles.*

In order to extend the operation domain of JT-60SA, the development of a dual-frequency gyrotron was started in JAEA. It is planned that all the gyrotrons will be able to operate at those two frequencies in the Integrated Research Phase. Some of the transmission line components, such as polarizers and diamond windows, need to be designed so that they allow transmission of both the EC wave frequencies. The operation of the dual-frequency gyrotron was started in 2012, and 1 MW output for 100 s both at 110 GHz and 138 GHz was achieved in 2014 [3]. A wide-band polarizer, which allows polarization control both at 110 GHz and 138 GHz, has been developed in collaboration with Ibaraki University. High-power

transmission tests at 0.9 MW for 20 s were successful [4].

In addition to these two frequencies, development aiming at oscillations at 82 GHz as a third frequency was continued (oscillation mode: $TE_{17,6}$), and 1 MW output for 1 s was successfully achieved in 2015 [5]. The result is promising for wall cleaning and/or plasma initiation using fundamental harmonic EC waves (The cold resonance layer is located at $R = 2.30$ m for $B_t = 2.25$ T).

Dedicated experiments on wall cleaning using 2nd harmonic X-mode EC waves were carried out in TCV. An optimized combination of horizontal and vertical magnetic field, whose magnitude of 0.1-0.6% of that of the toroidal field, was found to lead to shorter breakdown time, wider wall coverage and enhanced fuel removal. A standard ohmic plasma was successfully sustained after EC wall cleaning. [6]

Stray radiation study using JT-60SA 3D CAD data has been carried out. The expected wall loads and diffuse EC stray radiation amount was estimated. The feasibility of installing sniffer probes at upper vertical ports was also investigated. [7].

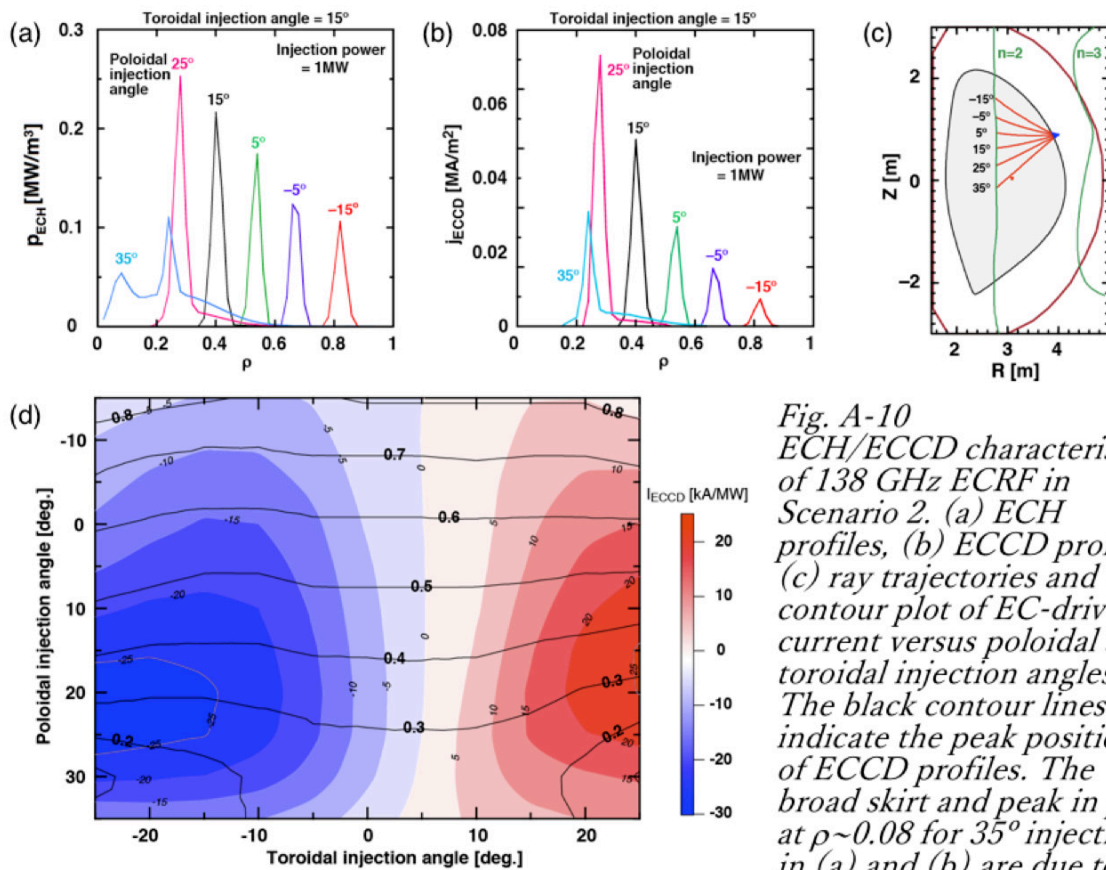


*Fig. A-10
ECH/ECCD characteristics
of 138 GHz ECRF in
Scenario 2. (a) ECH
profiles, (b) ECCD profiles,
(c) ray trajectories and (d) a
contour plot of EC-driven
current versus poloidal and
toroidal injection angles.
The black contour lines
indicate the peak positions
of ECCD profiles. The
broad skirt and peak in p_{ECH}
at $\rho \sim 0.08$ for 35° injection
in (a) and (b) are due to 3rd
harmonic ECH/ECCD.*

- [1] T. Kobayashi et al, Fusion Eng. Design **84** (2009) 1063.
- [2] C Sozzi et al., Proc. 44th EPS Conference on Plasma Physics, P1.143 (2017)
- [3] T. Kobayashi et al., Nucl. Fusion **55** (2015) 063008.
- [4] N. Horie et al., Fusion Eng. Design **122** (2017) 218.
- [5] T. Kobayashi et al., Proc. IRMMW-THz 2015.
- [6] D. Douai et al, Nucl. Fusion **58** (2018) 026018.
- [7] A. Moro et al., Fusion Eng. Design **123** (2017) 435.

Appendix B: Divertor Power Handling and Particle Control Systems

1. Divertor Power Handling

Figure B-1 shows the configuration of lower divertor. All plasma facing components (PFCs) for the lower divertor shall be water-cooled for high power and long pulse heating. Carbon armor tiles bolted on water-cooled copper alloy heatsinks are applied to remove $0.3\text{-}2\text{ MW/m}^2 \times 100\text{s}$ and $10\text{ MW/m}^2 \times <10\text{s}$ of heat load. Inner and outer vertical targets with bolted CFC (carbon fiber composite) tiles (Fig. B-2(a)) will be replaced with monoblock targets which can remove $10\text{-}15\text{ MW/m}^2$ of steady heat load (Fig. B-2(b)) after the Initial Research Phase II. Divertor cassette with integrated coolant pipe connection for PFCs is introduced. Each cassette has 10 degree of toroidal width and can be installed and replaced through large horizontal port of vacuum vessel (VV) by remote handling system similar to those for ITER blanket. PFCs on the divertor cassette are designed as replaceable modules. Each PFC can be replaced and upgraded independently by human work in hot cell after removal of the cassette from VV. Specifications of plasma facing components are summarized in table B-1.

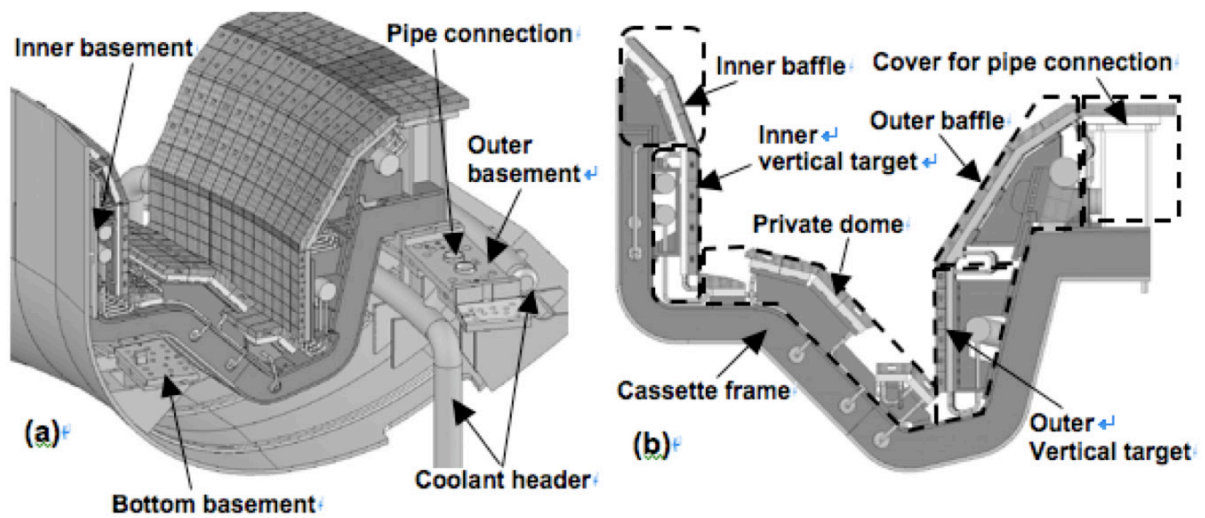


Fig. B-1 Configuration of plasma facing components for lower divertor.

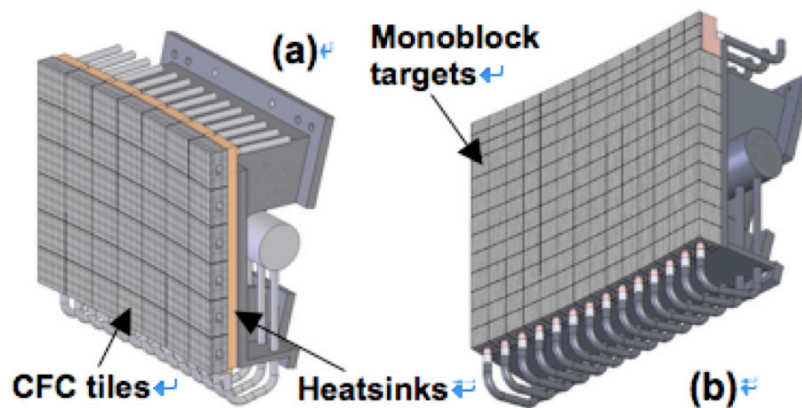


Fig. B-2 Outer vertical targets with bolted CFC tiles (a) and monoblock targets (b).

Table B-1 Specifications of PFCs for the lower divertor

Plasma facing components	Heat flux (MW/m ²)	Duration (sec)	Heat cycles
Inner and outer vertical targets with bolted CFC armor tiles	1	100	5000
	3	20	1500
	10	5	1500
Outer vertical target with monoblock targets	10	100	10000
	15	100	3000
Inner vertical target with monoblock targets	7	100	10000
	10	100	3000
Private dome	1	100	10000
	2	100	3000
	10	5	3000
Inner and outer baffles	0.3-1	100	13000
Cover for pipe connection	0.3	100	13000

2. Particle Control Systems

Particle control in JT-60SA will be performed by gas puff, pellet injection, neutral beam injection and pumps. Here, achievable density by the gas puff and by the pellet injection is estimated, and specifications of the fueling devices for the main plasma are determined.

Figure B-3 shows achievable density by additional fueling (gas puff or pellet injection) at a heating power of 40 MW and an NB fueling rate of $2.5 \times 10^{21} \text{ s}^{-1}$, estimated from a steady-state particle balance analysis. In the case the particle confinement time of the particles fueled by the additional fueling is equal to that of the NB fueled particles, *i.e.*, $\tau_p^{\text{add}} = \tau_p^{\text{NB}}$, which may be possible by ideal pellet injection, the required additional fueling rates for Scenario #2 and #3 are estimated to be $4.9 \times 10^{21} \text{ s}^{-1}$ and $6.4 \times 10^{21} \text{ s}^{-1}$, respectively. These fueling rates can be achieved by 10 Hz and 13 Hz of $2.4 \text{ mm}\phi \times 2.4 \text{ mm/l}$ -pellet injection, respectively. In the case that the particle confinement time of the additional fueling is half of that of the NB fueled particles, *i.e.*, $\tau_p^{\text{add}} = 0.5 \tau_p^{\text{NB}}$, the required additional fueling rates for Scenario #2 and #3 increase up to $9.1 \times 10^{21} \text{ s}^{-1}$ and $1.2 \times 10^{22} \text{ s}^{-1}$, respectively. Because these fueling rates are around the limit of a particle injection rate of one pellet source with 20 Hz ($= S_{\text{pellet}}$), another pellet source may be required in particular for

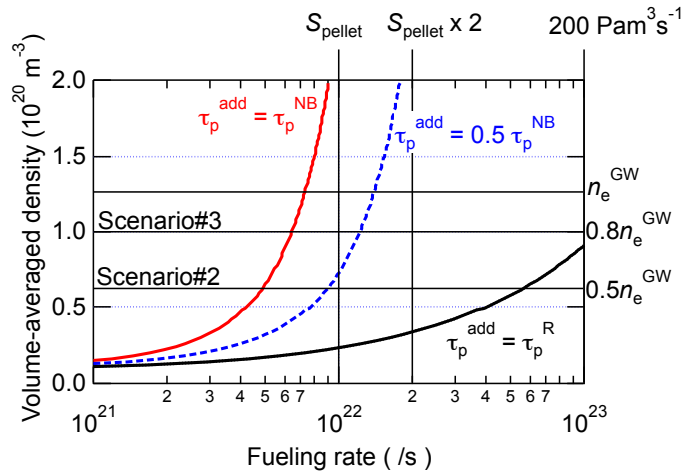


Fig. B-3 Estimated electron density as a function of the fueling rate of an additional fueling system (the gas puff or the pellet injection) under an NB heating power of 40 MW. The particle confinement time of particles fueled by the additional fueling system is indicated by τ_p^{add} , that of NB fueled particles by τ_p^{NB} , and that of recycled particles by τ_p^{R} . S_{pellet} indicates the particle injection rate of the pellet system with a size of $2.4 \text{ mm}\phi \times 2.4 \text{ mm/l}$ at an injection frequency of 20 Hz, and n_e^{GW} the Greenwald density.

Scenario #3. In the case the particle confinement time of the additional fueling is equal to that of the recycled particles, *i.e.*, $\tau_p^{\text{add}} = \tau_p^{\text{R}}$, for example gas puffing, a very high fueling rate is required to achieve the density of Scenario #2 and #3. In these cases, an X-point MARFE may occur, leading to lower confinement compared to the required level for Scenario #2 and #3. Hence the fueling for the main plasma should be performed by another method with high particle confinement time such as pellet injection. Based on the above estimation, specifications described below are determined.

Gas puff: as described above, gas puffing is not expected as a main fueling method for the main plasma. However, in case that pellet injectors do not work as required, a maximum capability of $300 \text{ Pam}^3\text{s}^{-1}$ ($1.8 \times 10^{23} \text{ s}^{-1}$) will be prepared. As a future upgrade option, another $90 \text{ Pam}^3\text{s}^{-1}$ is under consideration. As shown in Fig. B-4(a), ten gas supply lines in total will be prepared. For the main chamber, three lines are connected to the upper ports and two lines to the lower ports as shown in Fig. B-4(b). For the divertor chamber, except for P-6 section, where one line is connected directly, one line is shared by three nozzles located at different toroidal port sections at P-2, P-5 and P-17, and the other line at P8, P11 and P14. In addition, gas lines connected to the inner and the outer divertor are independent in order to control the gas-puffing rate independently for the inner and the outer divertor plasma. Hence 5 lines in total will be prepared for the divertor chamber. In addition to hydrogen and deuterium, N_2 , Ne, Ar, Kr, Xe, CD_4 , CH_4 , C_2H_4 and C_2H_6 , will be prepared. The puffing rate will be able to be controlled by a real-time feedback control system.

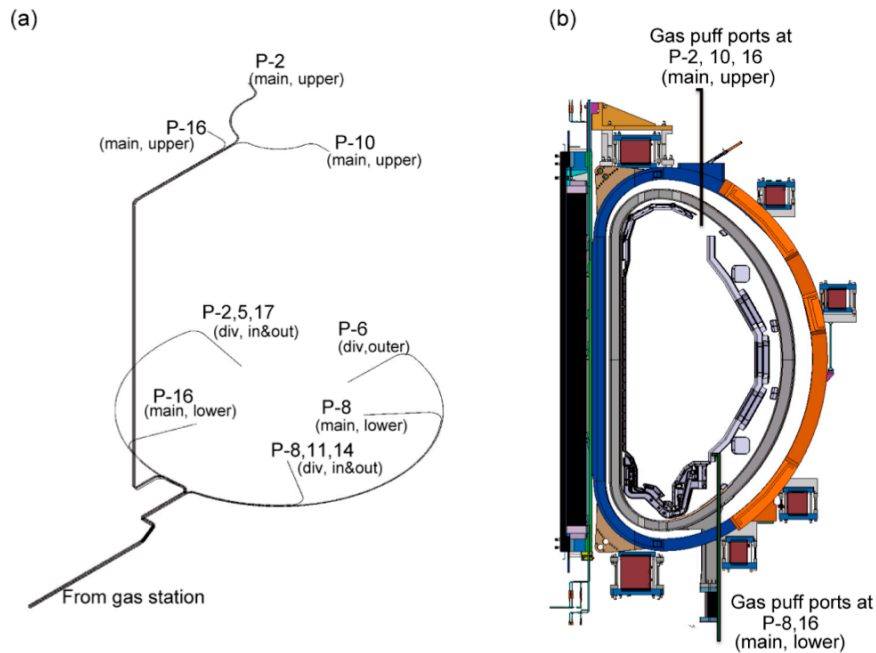


Fig. B-4 (a) Layout of gas supply lines and (b) locations of gas puff ports on the poloidal cross-section of JT-60SA.

Pellet injection: as described above, pellet injection is expected as a main fueling method for the main plasma. One pellet injector, at least, with a typical pellet-size of $\sim 2.4 \text{ mm}\phi \times 2.4 \text{ mm/l}$ and a maximum injection frequency of $\sim 20 \text{ Hz}$ with a real-time frequency control for the plasma density feedback control is planned. For future upgrade, three pellet injectors are planned for ELM-pacing experiments at up to 60 Hz . For disruption mitigation studies, Ne pellet will be prepared as a killer pellet. Fast TV monitor systems will observe the ablation position of the pellet in two directions, and the plasma parameters of the ablation cloud of the pellet will be determined from visible spectroscopy.

Pumping: The JT-60SA cryopump will be prepared below the divertor cassette as shown in Fig B-5. The maximum pumping speed of the cryopump is $100 \text{ m}^3\text{s}^{-1}$ at steady-state and $300 \text{ m}^3\text{s}^{-1}$ at peak. The total pumping capability is $10000 \text{ Pam}^3 / \text{shot}$ and $100000 \text{ Pam}^3 / \text{day}$. The cryopump consists of nine 40° cryopanel, each of which is individually connected to an independent cryoline. Hence 10 steps of the pumping speed between 0 and $100 \text{ m}^3\text{s}^{-1}$ are available. For He-exhaust experiments, Ar frost can be produced on the cryopanel. Regeneration of the cryopump, followed by glow discharge cleaning will be performed at night. In addition to the cryopump, two pumping lines with 16 turbo-molecular pumps in total will be prepared.

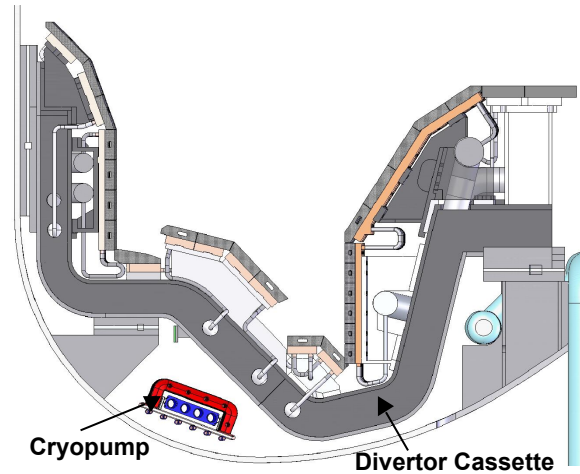


Fig. B-5 locations of the cryopanel on the poloidal cross-section of the divertor.

Table B-2 Specifications of particle fueling and pumping systems and results of SONIC simulation

System	JT-60U (D/s)	JT-60SA (D/s)	SONIC Simulation	
			Scenario #2	Scenario #5-1
Gas puff	1.8×10^{23} ($300 \text{ Pa m}^3/\text{s}$)	1.8×10^{23} ($300 \text{ Pa m}^3/\text{s}$) Future upgrade: $+ 0.5 \times 10^{23}$ ($90 \text{ Pa m}^3/\text{s}$)	1.5×10^{22}	2.5×10^{21}
pellet	1.0×10^{22}	3.0×10^{22} (3 sources)		
NB	2.0×10^{21}	2.0×10^{21}	2.6×10^{21}	2.6×10^{21}
N-NB	5.0×10^{20}	5.0×10^{20}		
Gas jet	Used	No request		
Divertor pumping	$28 \text{ m}^3/\text{s}$ (effective)	$0-100 \text{ m}^3/\text{s}$	1.6×10^{22} at $50 \text{ m}^3/\text{s}$	4.4×10^{21} at $30 \text{ m}^3/\text{s}$

Appendix C: Stability Control Systems

In-vessel components

Three types of active coils with copper conductor will be installed in the vacuum vessel on JT-60SA as shown in Fig. C-1. Fast Plasma position control and stabilization of vertical instability will be performed with a pair of fast plasma position control coils (FPCCs) and the stabilizing plate. Six pairs of error field correction coils (EFCCs) in the toroidal direction are for error field correction and ELM mitigation by resonant magnetic perturbation. The resistive wall mode control coils (RWMC) consist of three coils in the poloidal direction and six coils in the toroidal direction. RWM will be stabilized with RWMC and the stabilizing plate.

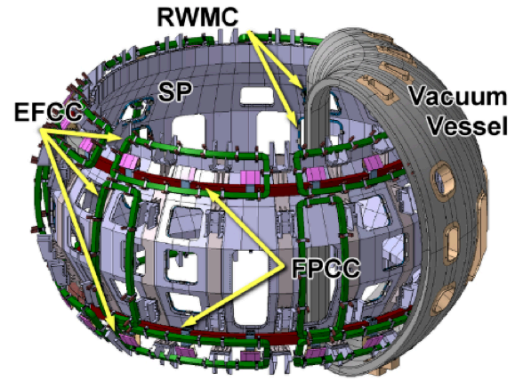


Fig.C-1 In-vessel components in JT-60SA.

Table C-1. Specifications of In-vessel coils & Stabilizing plates

Name	Purpose	Specification	Figure
FPPC Fast Plasma Position control Coil	fast position (vertical & horizontal) control	Number: 2 (Upper & Lower) Max current: 120 kAT Location: Behind SPs	
EFCC Error Field Correction Coil	error fields ($n \neq 0$) correction and resonant magnetic field perturbation	Number: 18 (Tor 6 x Pol 3) Max current: 45 kAT Location: Behind SPs	
RWMC Resistive Wall Mode control Coil	RWM feedback control	Number: 18 (Tor 6 x Pol 3) Max current: 2.2 kAT Location: In front of SPs	
SP Stabilizing Plate	passive stabilization of VDE and RWM	Wall time constant: ~40ms	

C-1. Fast position control coil (FPPC)

JT-60SA is a full superconductor machine. Therefore, a pair of FPCC with copper conductor will be installed for fast plasma position control and stabilization of vertical instability. Each coil has 23 turns conductor and maximum current is 120kAT. Independent power supplies

will be connected to each coil block to control vertical and horizontal field at the same time.

C-2. Error field correction coil (EFCC)

On JT-60SA error fields of several gauss are predicted due to errors of manufacturing and assembly of TFC and PFC (CS and EF coils), and NB correction coils that can reduce magnetic fields at NB injectors. These error fields should be reduced in order to keep null region at plasma initiation and to avoid $m/n=2/1$ lock mode in the I_p ramp phase. For this purposes, EFCCs are planned to be installed in the vacuum vessel. The EFCCs are also useful to apply resonant magnetic perturbations (RMPs) for MHD study such as RMP effects on RWM and NTM, and ELM control. Figure C-2 shows poloidal mode spectra with $n=3$ odd and even pattern in 5.5MA single null configuration (Scenario #2). These indicate that even parity is efficient to resonance at rational surface in the peripheral region.

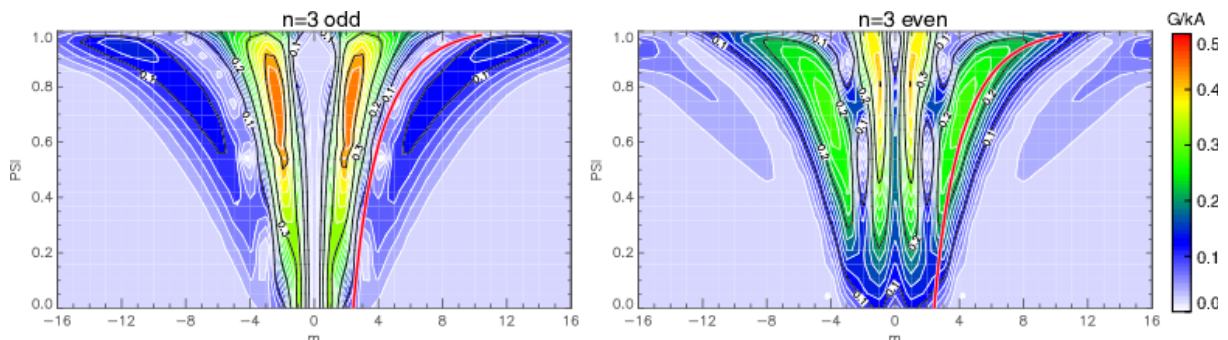


Fig.C-2 Poloidal mode spectra with $n=3$ odd and even pattern in 5.5MA single null configuration (Scenario #2). Red line indicates magnetic field line of equilibrium. Vertical axis is poloidal flux as magnetic surface indexes.

C-3. Resistive wall mode control coil (RWMC)

Stabilization of resistive wall mode is necessary to achieve the high beta value exceeding no wall beta limit. RWM can be stabilized by plasma rotation, however it can be destabilized by other MHD events, for example ELM, fishbone EWM and so on with sufficient plasma rotation. Therefore we prepare the active coils RWMCs for RWM control. Each RWMC has two-turn conductor and is installed on the plasma side of the stabilizing plate in order to minimize the shielding effect of the stabilizing plate on high frequency magnetic field for RWM control. Each coil finally has an independent amplifier and the so-called “mode control” feedback control scheme will be applied in order to control $n=1, 2$ and 3 RWM simultaneously.

C-4. Stabilizing plate (SP)

The primary function of the stabilizing plates (SPs) is to increase the ideal beta limit and to improve plasma positional stability. The SPs should be connected electrically in toroidal and poloidal directions for stabilizing effects. The total electromagnetic force due to eddy current can reach ~ 1 MN for each toroidal sector during disruptions. Therefore, the SPs have been designed as a double-wall structure made of SUS316L to have enough stiffness. The thickness of each shell is 10mm and distance of them is 70mm. The SPs are supported by 18 support frames and their legs from VV just behind the TFC position. The plasma side surface is covered with bolted carbon armour tiles on cooled copper alloy heat sinks that are water cooled as a first wall.

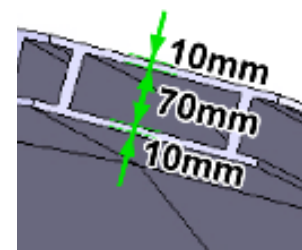


Fig. C-3 Cross section of the stabilizing plates

Appendix D: Plasma Diagnostics Systems

1. Plasma Diagnostics Systems

Measurement requirements from the JT-60SA Research Plan are compiled in Tables D-1 for the machine protection, D-2 for the core plasma measurements, D-3 for the Edge, SOL, Divertor measurements and D-4 for the fluctuation measurements, respectively. The plasma diagnostics, referred in these tables, are planned in JT-60SA and allocations to the port are shown in Table D-6. While some specifications are not met in the present design of the diagnostics systems, these specifications are recognized as the target parameters for upgrading in the later research phase of JT-60SA.

Table D-1: Measurements for machine protection in JT-60SA

Measurement	Diagnostic	Range or Coverage	Time resolution	Spatial resolution or Wave No.	Accuracy	Target
First wall and plasma visible image	Visible TV	~100% coverage of first wall	0.1-10 ms			
First wall visible image and wall temperature	Infrared TV camera (first wall)	Wall temp.=0~1200 degree ~100% coverage of first wall	0.025 ms	<10 mm	10%	$<f_{ELM} \sim 10-1000$ Hz
Heat loading profile in the divertor	Infrared TV camera (divertor)	Wall temp.=0~1200 degree ~100% coverage of divertor	0.025 ms	<10 mm	10%	$<f_{ELM} \sim 10-1000$ Hz
Neutron flux	Neutron monitor	1.0E+0-1.0E+7 c/s	1 ms	Integral	~10%	
Divertor leg position	Divertor Langmuir probe	Divertor	1 ms			

Table D-2: Core measurements in JT-60SA

Measurement	Diagnostic	Range or Coverage	Time resolution	Spatial resolution or Wave No.	Accuracy	Target
Current profile	Motional Stark effect polarimeter	pich angle~0-15 degree $0 < r/a < 1$	~ 10 ms	~87 mm or $dr/a \sim 0.07$	~0.2 degree in pich angle	j_r control $< 1/100 \tau_R$
Line-averaged electron density	CO2 laser interferometer / polarimeter	tangential & vertica	~ ms	Integral		$< 1/100 \tau_S$
Electron density profile	YAG laser Thomson scattering system	$n_e = 0.1 - 30E+19 \text{ m}^{-3}$ $0 < r/a < 1$	~ ms - 20 ms	20-30 mm or $dr/a \sim 0.05 - 0.1$	~5%	$< 1/10 \tau_{\text{local}}$ $< 1/10 L_{n_e}$
Electron temperature profile	YAG laser Thomson scattering system	$T_e = 0.1 - 30 \text{ keV}$ $0 < r/a < 1$	~ ms - 20 ms	20-30 mm or $dr/a \sim 0.05 - 0.1$	~5%	$< 1/10 \tau_{\text{local}}$ $< 1/10 L_{T_e}$
Electron temperature profile (fast)	Electron cyclotron emission diagnostics	$T_e = 0.1 - 20 \text{ keV}$ $0 < r/a < 1$	~0.001-0.01 ms	~10-20 mm or $dr/a < 0.02$	~5%	$< 1/10 L_{T_e}$
Ion temperature profile	Charge exchange recombination spectroscopy	0.1-50 keV $0 < r/a < 1$	~1 ms	~10-20 mm or $dr/a \sim 0.05$	~5%	$< 1/10 \tau_{\text{local}}$ $< 1/10 L_{T_i}$ ITB behavior
Toroidal rotation profile	Charge exchange recombination spectroscopy	-500 - +500 km/s $0 < r/a < 1$	~1 ms	~10-20 mm or $dr/a \sim 0.05$	~5 km/s	$< 1/10 \tau_{\text{local}}$ $< 1/10 L_{v_t}$ ITB behavior
Poloidal rotation profile	Charge exchange recombination spectroscopy	-500 - +500 km/s $0 < r/a < 1$	~1 ms	~10-20 mm or $dr/a \sim 0.05$		
Radiation profile (main)	Bolometer (main)		~ 1 ms	~50-100 mm	~10%	$< 1/100 \tau_S$ $< 1/10 L_{n_e}$ at ITB
Z_{eff} profile	Z_{eff} monitor (visible bremsstrahlung emission)	$0 < r/a < 1$	0.1 ms	50-100 mm or $dr/a \sim 0.2$	10%	$< 1/100 \tau_S$ $< 1/10 L_{n_e}$ at ITB
Impurity density profile Ion temperature profile (core)	Crystal spectrometer (core)	$0 < r/a < 1$	~2-3 ms	~10-20 mm		$< 1/100 \tau_S$ $< 1/10 L_{n_e}$ $< 1/10 L_{T_i}$ at ITB
Impurity species monitoring	VUV spectrometer (core)		~100 ms	Integral	10%	
pellet monitor	Fast Visible TV		0.02 ms	~100 mm		
Energy spectrum of fast neutron	Neutral particle analyzer (Diamond detector)	0- ~ MeV $dE \sim 15-20 \text{ keV}$	~ 1ms	1 line for vertical, 1 line for horisontal		
Fast ion Da light	Fast ion Da		< ~ ms	$dr/a \sim 0.1$		

Table D-3: Edge, SOL, Divertor measurements in JT-60SA

Measurement	Diagnostic	Range or Coverage	Time resolution	Spatial resolution or Wave No.	Accuracy	Target
Electron density profile (pedestal / SOL)	YAG laser Thomson scattering system (pedestal)	$0.7 < r/a < 1.1$	~ ms	~5 mm	~5%	Type I ELM ($f_{ELM} \sim 10-100$ Hz) <1/10 dped
Electron density profile (pedestal)	Li-beam probe	$0.8 < r/a < 1.1$	0.01 ms	~1-5 mm	<15%	Type I & grassy ELM ($f_{ELM} \sim 10-500$ Hz) <1/10 dped
Electron temperature profile (pedestal / SOL)	YAG laser Thomson scattering system (pedestal)	$0.7 < r/a < 1.1$	~ ms	~5 mm	~5%	Type I ELM ($f_{ELM} \sim 10-100$ Hz) <1/10 dped
Electron temperature profile (pedestal / SOL)	Electron cyclotron emission diagnostics (pedestal)	$0.7 < r/a < 1.1$	~0.01-0.02 ms	~10 mm	~5%	Type I & grassy ELM ($f_{ELM} \sim 10-1000$ Hz) <1/10 dped
Ion temperature profile (pedestal / SOL)	Charge exchange recombination spectroscopy (pedestal)	$0.7 < r/a < 1.1$	~0.1-1 ms	~5 mm	~5%	Type I ELM ($f_{ELM} \sim 10-100$ Hz) <1/10 dped
Toroidal rotation profile (pedestal / SOL)	Charge exchange recombination spectroscopy (pedestal)	$0.7 < r/a < 1.1$	~0.1-1 ms	~5 mm	~5 km/s	Type I ELM ($f_{ELM} \sim 10-100$ Hz) <1/10 dped
Poloidal rotation profile (pedestal / SOL)	Charge exchange recombination spectroscopy (pedestal)	$0.7 < r/a < 1.1$	~0.1-1 ms	~5 mm		Type I ELM ($f_{ELM} \sim 10-100$ Hz) <1/10 dped
Carbon ion density profile (pedestal / SOL)	Charge exchange recombination spectroscopy (pedestal)	$0.7 < r/a < 1.1$	~0.1-1 ms	~5 mm		Type I ELM ($f_{ELM} \sim 10-100$ Hz) <1/10 dped
Radiation profile (divertor)	Bolometer (divertor)	divertor	~ 1 ms	~20-30 mm	~10%	<1/100 τ_s < P_{rad}
ELMs and L-H transition Recycling	D_α emission monitor	divertor first wall	<0.01 ms	~100 mm		Type I & grassy ELM ($f_{ELM} \sim 10-1000$ Hz) <1/10 dped
Divertor electron density	Divertor Thomson (SOL, Divertor)	divertor	10 ms	10 mm along leg		
Divertor electron density (low power)	Divertor Langmuir probe (SOL, Divertor)	divertor	1 ms	10 mm along leg		
Divertor electron temperature	Divertor Thomson (SOL, Divertor)	divertor	10 ms	10 mm along leg		
Divertor electron density (low power)	Divertor Langmuir probe (SOL, Divertor)	divertor	1 ms	10 mm along leg		
SOL plasma flow	Reciprocating Mach probe (SOL, Divertor)	divertor	0.002 ms	~1 mm along leg		< $f_{ELM} \sim 10-1000$ Hz
Density fluctuation Blob	Fast Visible TV	$0.7 < r/a < 1.1$	0.005 ms	1 mm		< $f_{ELM} \sim 10-1000$ Hz < Blob size

Table D-3: Edge, SOL, Divertor measurements in JT-60SA (cont'd)

Measurement	Diagnostic	Range or Coverage	Time resolution	Spatial resolution or Wave No.	Accuracy	Target
Divertor/SOL Impurity spectrum, flux, flow	Visible spectrometer (SOL, divertor)	Te:0.1-100eV ne:1e18-1e21 /m3 at divertor	0.01-0.1 ms	~5-10 mm	10%	$<f_{ELM} \sim 10-1000$ Hz <mean free path of neutral
Radiation power of each species	VUV spectrometer for the divertor	Te:0.1-100eV ne:1e18-1e21 /m3 at divertor	1 ms	2 lines for inner and outer divertor 1 line for X-point	10-30%	$<f_{ELM} \sim 10-1000$ Hz < L_{Prad}
Gas pressure and composition	Neutral gas pressure gauge (Pelling gauge, Fast response ionization gauge)	0.01-1 Pa	100 ms	TBD	10%	

Table D-4: Fluctuation measurements in JT-60SA

Measurement	Diagnostic	Range or Coverage	Time resolution	Spatial resolution or Wave No.	Accuracy	Target
Soft X-ray fluctuation	Soft X-ray detector array	Te=0-20keV	~500 kHz	~50-100mm or dr/a~0.1	~5-10%	m>5 AE Sawtooth
Electron temperature fluctuation	Electron cyclotron emission diagnostics	Te=0.1-20 keV 0<r/a<1	~0.001-0.01 ms	~10-20 mm or dr/a<0.02	~5%	Sawtooth, NTM MHD mode EHO <Island width
Density fluctuation	Reflectometer Doppler reflectometer	ne=1.4- 8x10E19 m^-3	0.001 ms			ITG, TEM
Density fluctuation	Motional Stark effect polarimeter (BES)	Core	>100 kHz	dr/a~0.05-0.1		AE NTM <Island width
Density fluctuation	CO2 laser interferometer / polarimeter		0.001 ms	Integral		MHD mode ITG
Density fluctuation (pedestal)	Li-beam probe	0.8<r/a<1.1	~0.001 ms	~1-5mm	<15%	ELM with RMP and pellet < $f_{ELM} \sim 10-1000$ Hz
Density fluctuation Blob	Fast Visible TV	0.7<r/a<1.1	0.005 ms	1 mm		< $f_{ELM} \sim 10-1000$ Hz <Blob size

2. Magnetic sensors

Table D-5: Magnetic sensors

Sensors	physical quantity	temporal resolution	number of sensors & spatial resolution	note
Magnetic probe	equilibrium	DC~20kHz	46 Btheta	Toroidally 2 Poloidally 23
	RWM	DC~20kHz	108 Br & Btheta	Toroidally 6 Poloidally 18
	MHD fluctuations	DC~500kHz	41 Btheta	Poloidally 32 for poloidal mode toroidally 9 for toroidal mode
Saddle loop	RWM and MHD fluctuations	DC~20kHz	18 on stabilizing plate 18 on outboard vacuum vessel	Toroidally 6 Poloidally 3
Flux loop	one-turn voltages	TBD	7 on stabilizing plate 27 on vacuum vessel	
Diamagnetic loop	stored energy	TBD	3 sets	
Rogowski coil	plasma current	TBD	4 sets	
Halo current probe	halo current	TBD	20	Maximum 48
Eddy current probe	eddy current	TBD	TBD	

*TBD : to be determined

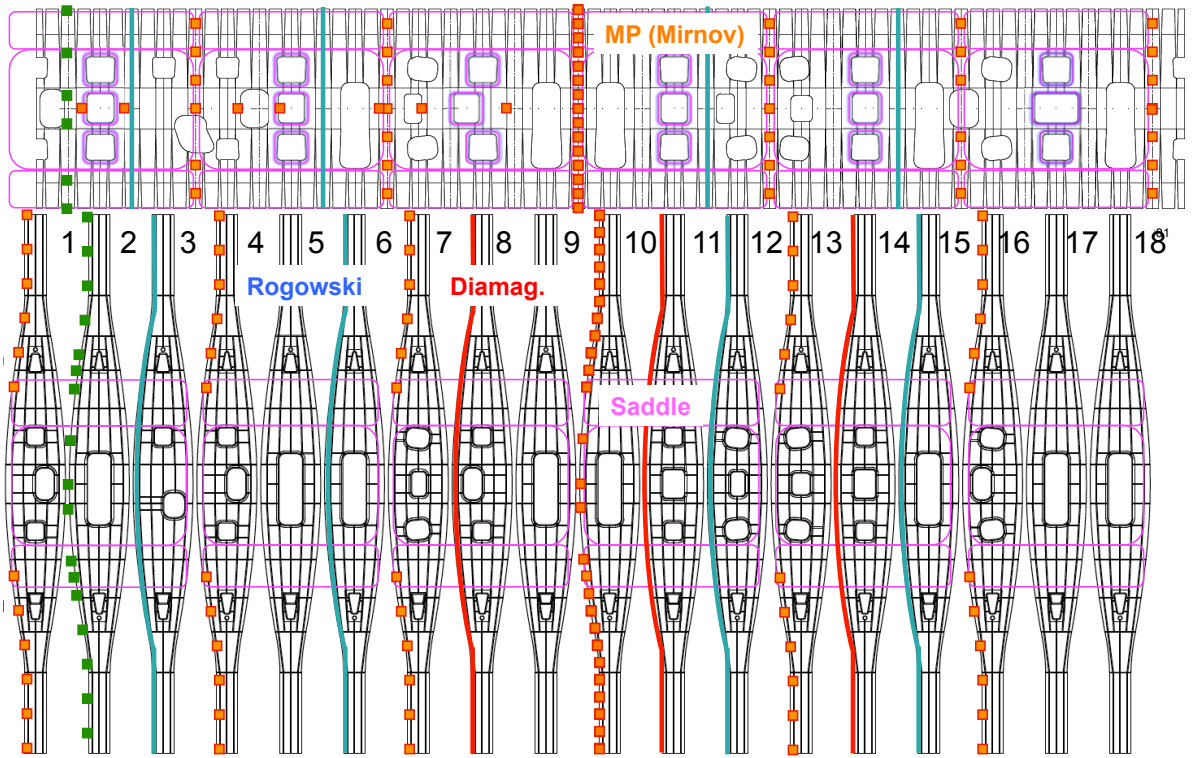


Fig. D-1 Position of magnetic sensors

3. Halo current measurement

In order to measure halo currents at divertor regions, Rogowski coil type probes are planned to be distributed in each divertor cassette. Figure D-2 shows schematic setup of halo probes in poloidal cross section of a divertor cassette. Poloidally, five probes are possible to be installed for halo width measurement. These can measure halo currents flowing in inner-baffle, inner-target, outer-baffle, outer-target and dome regions. Toroidally, some of these probes are planned to be distributed to measure toroidal peaking factor of halo currents.

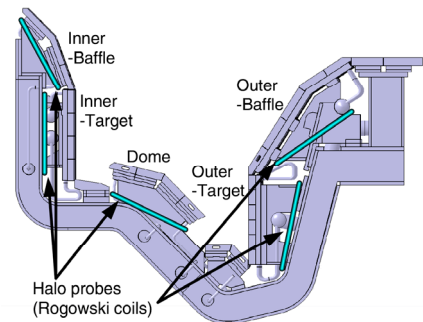


Fig. D-2 Schematic setup of halo probes in poloidal cross section of a divertor cassette,

4. Port allocation

Allocation of Neutron Monitors (fission chambers) and active beam spectroscopy (CXRS and MSE) is strongly restricted by arrangement of the NBI system around the JT-60SA. As for the YAG Thomson scattering, a tangential laser path is adopted in order to cover from the edge plasma to the plasma center. In addition, CO₂ laser for interferometer shares the common tangential port in order to ensure the cross calibration accuracy of density measurement. The tangential ports are prepared in P1 and P8 sections to avoid spatial interference with the NBI tanks (see Fig. D-3). In accordance with this laser path, P1 lower oblique, P2 horizontal and P5 horizontal ports are assigned for collecting Thomson scattering light from the outer edge (high field side), core, and inner edge (low field side) of plasmas, respectively (see Fig. D-4).

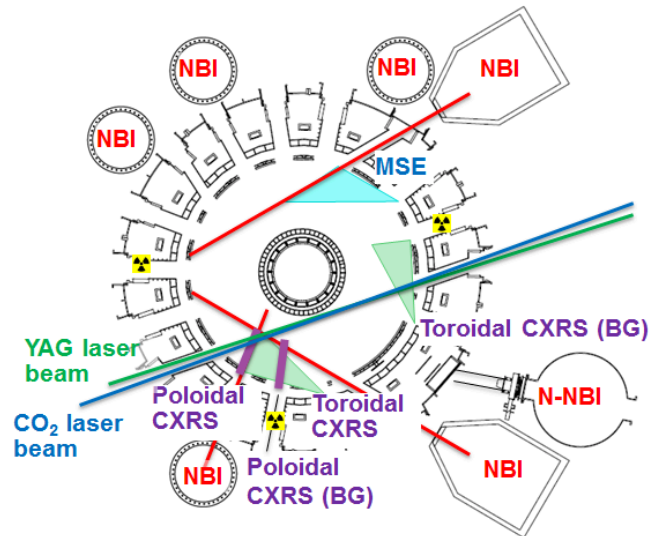


Figure D-3 Allocation of Neutron Monitors (fission chambers) and active beam spectroscopy (CXRS and MSE) and laser beam chords are viewed from the top.

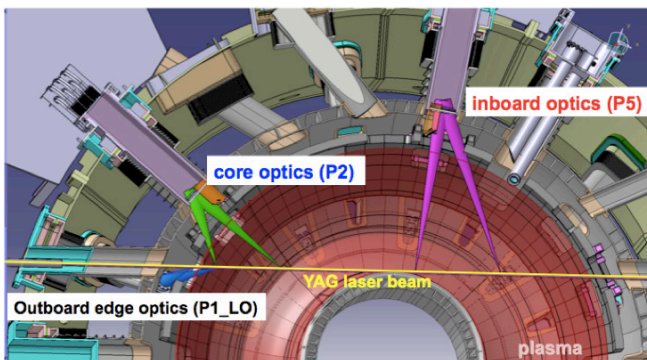


Figure D-4 Collection of optics of Thomson scattering along YAG laser path

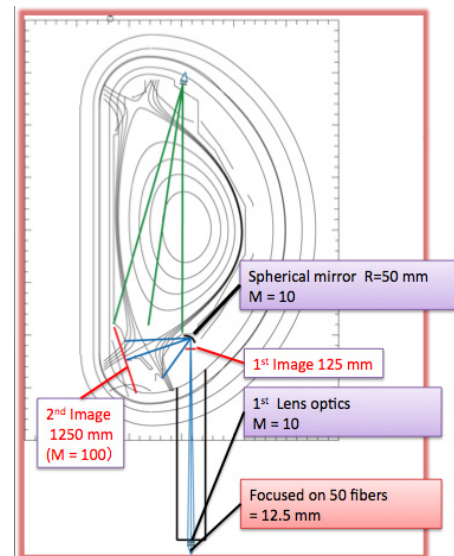


Figure D-5 Design of viewing chords for visible divertor spectroscopy.

In order to measure the divertor plasma parameters in details, viewing slits are prepared between the divertor cassette at P2, P6, P10 and P16 sections. Those slits will be assigned for the essential divertor diagnostics, such as bolometer, visible divertor spectrometer, retractable

material probe and divertor Thomson scatterings. For example, visible divertor spectroscopy measures the divertor plasma with vertical chords and horizontal chords through the divertor cassette, enabling tomographic reconstruction of emissivity of light (see Fig. D-5).

Allocation of the vacuum vessel port to the plasma diagnostics are shown in Table D-5. Feedthroughs for the magnetic sensor coils and thermo couples and Langmuir probes are distributed all around the torus and they are allocated to small branches in most of the upper oblique, horizontal and lower oblique ports.

Table D-6 Vacuum Vessel Port and Allocation

Sec.	Port	Use	Port User
P1	Upper	Cooling water	In-vessel
	Upper Oblique	ECRF	ECRF
	Horizontal	CO ₂ Laser interferometer/polarimeter (tangential), YAG laser Thomson scattering, Zeff monitor, Neutral gas pressure gauge	Diagnostics
	Lower Oblique	YAG laser Thomson scattering (edge)	Diagnostics
	Lower	Cooling water, Liquid He for cryopanel	In-vessel
P2	Upper	Glow electrode (TBD), Gas fueling	Vacuum Vessel
	Horizontal	YAG laser Thomson scattering (central), Charge exchange recombination spectroscopy (toroidal, BG), In-vessel coil feeder	Diagnostics In-vessel
	Lower	Divertor Thomson scattering (TBD) Gas fueling to divertor Cooling water	Diagnostics Vacuum Vessel In-vessel
P3	Upper	Cooling water	In-vessel
	Horizontal	N-NBI	NBI
	Lower	Cooling water, Liquid He for cryopanel	In-vessel
P4	Upper	Neutron emission profile monitor, Neutral particle analyser	Diagnostics
	Upper Oblique	ECRF	ECRF
	Horizontal	T-NBI(#9,10)	NBI
	Lower Oblique	D _α emission monitor	Diagnostics
	Lower	Boron gas introduction Cooling water	Vacuum Vessel In-vessel
P5	Upper	Cooling water	In-vessel
	Horizontal	Charge exchange recombination spectroscopy (toroidal), YAG laser Thomson scattering (high field side) Glow electrode, In-vessel coil feeder	Diagnostics In-vessel
	Lower	Cooling water, Liquid He for cryopanel	In-vessel
P6	Upper	Visible spectrometer for divertor	Diagnostics
	Horizontal	Remote Handling Neutron monitor, Infrared TV camera (main), Infrared TV camera (divertor) (TBD), Charge exchange recombination spectroscopy (poloidal, BG), Visible TV camera Glow electrode	Remote Handling Diagnostics Vacuum Vessel
	Lower	Visible spectrometer for divertor Gas fueling to divertor Cooling water	Diagnostics Vacuum Vessel In-vessel

P7	Upper	Cooling water	In-vessel
	Upper Oblique	P-NBI(#14)	NBI
	Horizontal	Charge exchange recombination spectroscopy (poloidal) Pellet	Diagnostics Vacuum Vessel
	Lower Oblique	P-NBI(#13)	NBI
	Lower	Cooling water, Liquid He for cryopanel	In-vessel
P8	Upper	CO2 Laser interferometer/polarimeter (vertical), Neutral gas pressure gauge	Diagnostics
	Upper Oblique	ECRF	ECRF
	Horizontal	CO2 Laser interferometer/polarimeter (tangential), YAG laser Thomson scattering, Zeff monitor, Neutral particle analyser	Diagnostics
	Lower Oblique	In-vessel coil feeder	In-Vessel
	Lower	CO2 Laser interferometer/polarimeter (vertical), Neutral gas pressure gauge Cooling water	Diagnostics In-vessel
P9	Upper	Cooling water	In-vessel
	Horizontal	Remote Handling VV inspection Electron cyclotron emission diagnostics, Fast visible TV for pellet	Remote Handling Vacuum Vessel Diagnostics
	Lower	Cooling water, Liquid He for cryopanel	In-vessel
P10	Upper	Gas fueling	Vacuum Vessel
	Horizontal	Neutron monitor, VUV Spectrometer, Neutron emission profile monitor, Crystal spectrometer	Diagnostics
	Lower	Boron gas introduction Reciprocating material probes (TBD) Gas fueling, Cooling water	Vacuum Vessel Diagnostics Vacuum Vessel In-vessel
P11	Upper	Cooling water	In-vessel
	Upper Oblique	ECRF	ECRF
	Horizontal	Electron cyclotron emission diagnostics In-vessel coil feeder	Diagnostics In-vessel
	Lower Oblique	Glow electrode	Vacuum Vessel
	Lower	Cooling water, Liquid He for cryopanel	In-vessel
P12	Upper	VUV spectrometer for divertor	Diagnostics
	Upper Oblique	P-NBI(#2)	NBI
	Horizontal	Pellet Pellet spectroscopy (TBD)	Vacuum Vessel Diagnostics
	Lower Oblique	P-NBI(#1)	NBI
	Lower	Gas fueling to divertor Cooling water	Vacuum Vessel In-vessel
P13	Upper	Cooling water	In-vessel
	Upper Oblique	P-NBI(#4)	NBI
	Horizontal	In-vessel coil feeder (FPPC)	In-vessel
	Lower Oblique	P-NBI(#3)	NBI
	Lower	Cooling water, Liquid He for cryopanel	In-vessel
P14	Upper	Soft X-ray detector array	Diagnostics
	Upper Oblique	Exhaust Soft X-ray detector array	Vacuum Vessel Diagnostics
	Horizontal	Soft X-ray detector array In-vessel coil feeder	Diagnostics In-vessel

	Lower Oblique	Exhaust Soft X-ray detector array	Vacuum Vessel Diagnostics
	Lower	Boron gas introduction Soft X-ray detector array Cooling water	Vacuum Vessel Diagnostics In-vessel
P15	Upper	Cooling water	In-vessel
	Horizontal	Remote Handling Infrared TV camera (divertor), Visible TV camera Glow electrode	Remote Handling Diagnostics Vacuum Vessel
	Lower	Cooling water, Liquid He for cryopanel	In-vessel
P16	Upper	Glow electrode (TBD), Gas fuelling	Vacuum Vessel
	Upper Oblique	P-NBI(#6)	NBI
	Horizontal	T-NBI(#7,8)	NBI
	Lower Oblique	P-NBI(#5)	NBI
	Lower	Bolometer Gas fueling Cooling water	Diagnostics Vacuum Vessel In-vessel
P17	Upper	Cooling water	In-vessel
	Horizontal	Motional Stark effect polarimeter In-vessel coil feeder	Diagnostics In-vessel
	Lower	Cooling water, Liquid He for cryopanel	In-vessel
P18	Upper	Bolometer	Diagnostics
	Horizontal	Remote Handling Neutron monitor, Infrared TV camera (divertor) (TBD), Visible TV camera, Bolometer, Li-beam probe (TBD), Reflectometer (TBD), EDICAM	Remote Handling Diagnostics
	Lower	Boron gas introduction Cooling water	Vacuum Vessel In-vessel

Appendix E: Fast ion confinement in ripple field

The effect of the TF ripple on the fast ion confinement was investigated. A limited area is available to install the ferritic inserts (FI) in JT-60SA. A reference design of the installation of the FI has been developed in order to investigate the effect of the reduced ripple on the fast ion confinement, though the compatibility of the FI with other components has not yet been checked in the design. Here, the calculation results of the fast ion confinement are described for the TF coils (TFC) alone case and for the FI case.

Figure E -1 shows the ripple contour between 0.4% to 1% for TFC alone. It can be said that the ripple amplitude inside the plasma region is less than 0.9%. The reference design of the installation of the FI has been developed under the following limitations;

- 18-fold symmetric installation
- Region of the installation in the toroidal direction: less than $\pm 2.0^\circ$ from just below TFC
- Region of the installation in the poloidal direction: less than $\pm 1\text{m}$ from the mid plane
- Clearance from the vacuum vessel: larger than 70mm
- Thickness of one plate is about 30 mm
- Saturation magnetization: 1.4T (corresponds to the saturation magnetization of SUS430 at the room temperature of 24°C)

The resultant geometrical information of the FI is as follows;

Region in the toroidal direction: $\pm 1.8^\circ$

Region in the poloidal direction: $\pm 10.5^\circ$ ($\sim \pm 0.609\text{ m}$)

Clearance from the vacuum vessel: 70 mm

Thickness: 60 mm (two plates).

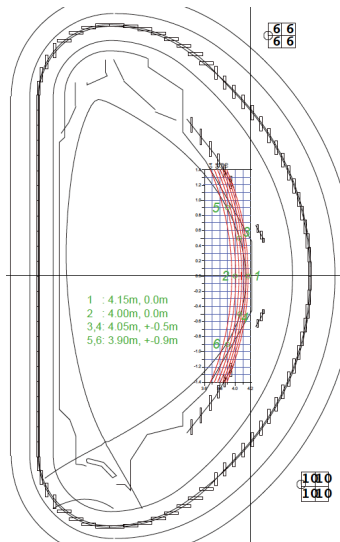


Fig. E-1(a): Ripple contour is shown from 0.4 to 1.0% by at intervals of 0.1%.

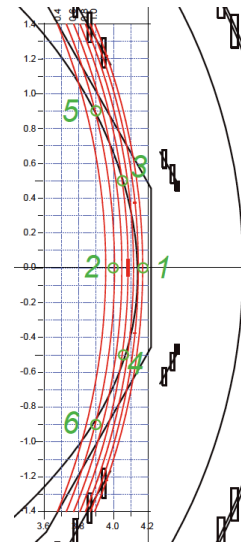


Fig. E-1(b) Six evaluation points are defined. Point 1: (R4.15m, Z0.0m), Point 2 (R4.00m, Z0.0m), Point 3 (R4.05m, Z0.5m), Point 4 (R4.05m, Z-0.5m), Point 5 (R3.90m, Z0.9m), Point 6 (R3.90m, Z-0.9m).

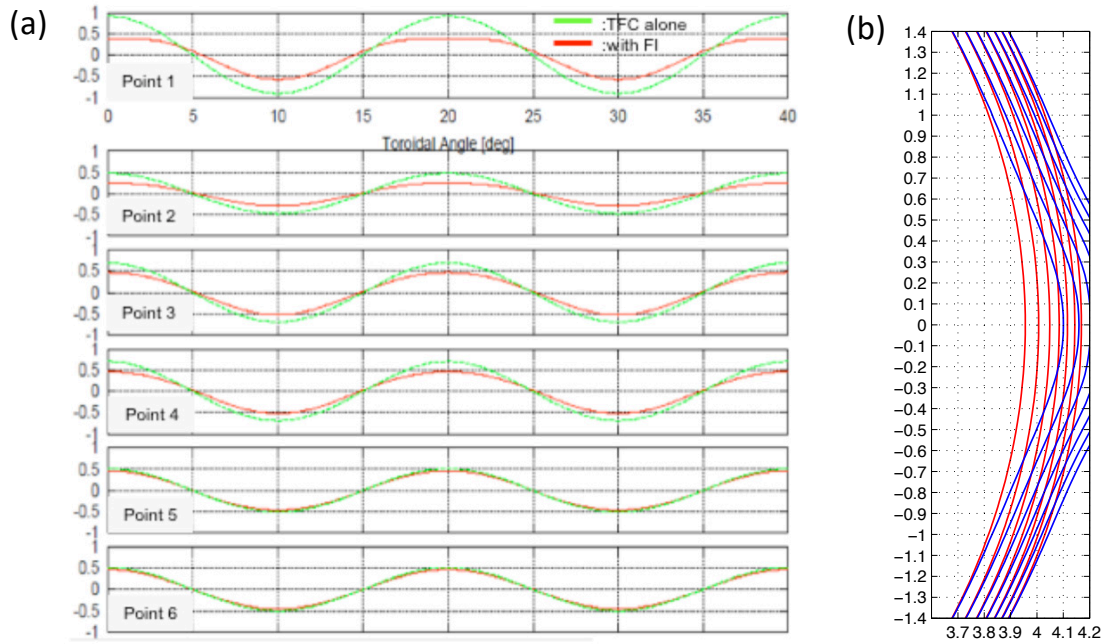


Fig. E-2: (a) Toroidal variation of the normalized toroidal field in the toroidal angle of 0 to 40 degrees at the six evaluation points shown in Fig. 1(b). Green curve is for TFC alone. Red curve is with FI. (b) Ripple contours for TFC alone (red) and with FI (blue).

In Fig. E-2(a), the toroidal variation of the normalized toroidal field, $(B_t - \langle B_t \rangle) / \langle B_t \rangle * 100$ [%]), is shown at the six evaluation points. The evaluation points are shown in Fig. E-1(b). The peak value of the normalized toroidal field corresponds to the ripple amplitude for TFC alone. Figure E-2(b) depicts the contour of the peak value of the normalized toroidal field, which corresponds to the ripple contour. The ripple contour is modified around the mid-plane due to the installation of the FI around the mid-plane. The normalized toroidal field is less than 0.5% for all of the six evaluation points and for the area inside the stabilizing plate.

Table E-1: OFMC calculation result for the confinement of the fast ions produced by the positive-ion-source NBs for five operation scenarios. The definition of the improved power is the difference between the third line (TFC alone) and the second line (with FI).

	Senario #1	Senario #2	Senario #3	Senario #4	Senario #5
Absorbed power for TFC alone [%]	89	88	86	89	87
Absorbed power with FI [%]	91	91	89	92	90
Absorbed power fraction for TFC alone [MW]	21.27	21.08	20.53	21.42	20.82
Absorbed power fraction with FI [MW]	21.77	21.72	21.38	22.06	21.51
Improved power [MW]	0.50	0.64	0.85	0.64	0.68

Using the OFMC code, the absorbed power of the fast ions produced by NB has been calculated. Table E-1 is the results for the full injection of the positive-ion-source NBs for Senario #1-#5. The difference of the fast ion confinement is small. The absorbed power fraction is plotted for each ion sources for Scenario #3, in which the improved power is largest, in Fig. E-4. The confinement of beam ions produced by co-tangential injectors is good even in the case of TFC alone because the ripple amplitude is small in most of the whole area inside the stabilizing plate as shown in Fig. E-1. The difference of the fast ion confinement comes from the fast ions due to the perpendicular injectors.

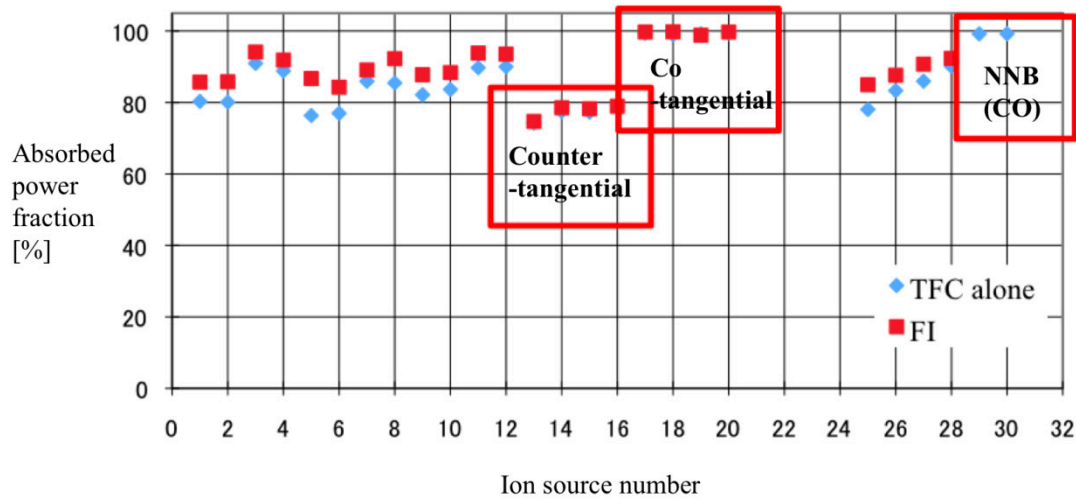


Fig. E-4: OFMC calculation result for NB ion confinement for Scenario #3. The horizontal axis is the number of the beam sources. Number 13-16 are injected in the counter direction to the plasma current tangentially. Number 17-20, 29, and 30 are injected in the co direction to the plasma current tangentially. Number 1-28 are positive ion sources. Number 29 and 39 are negative ion sources.

Appendix F: Operational scenarios

In order to satisfy the missions of the JT-60SA project, several design scenarios are identified. In the identification, the scenarios are determined so as the target parameters to be achieved. Then the machine should be capable of investigating these scenarios, in terms of the capabilities of the magnets, the power supply, the cryogenics, the force tolerance and so on. These scenarios are, therefore engineering scenarios. How to reach the parameters is not considered, but the machine should accommodate the plasmas. These typical scenarios are listed in Table 3-1.

The procedure to identify a scenario is as follows. Identify typical parameters to be achieved. For example, in the steady state high β_N case, they were β_N , $H_{H(98,y2)}$, f_{GW} and $V_{\ell} = 0$ V.

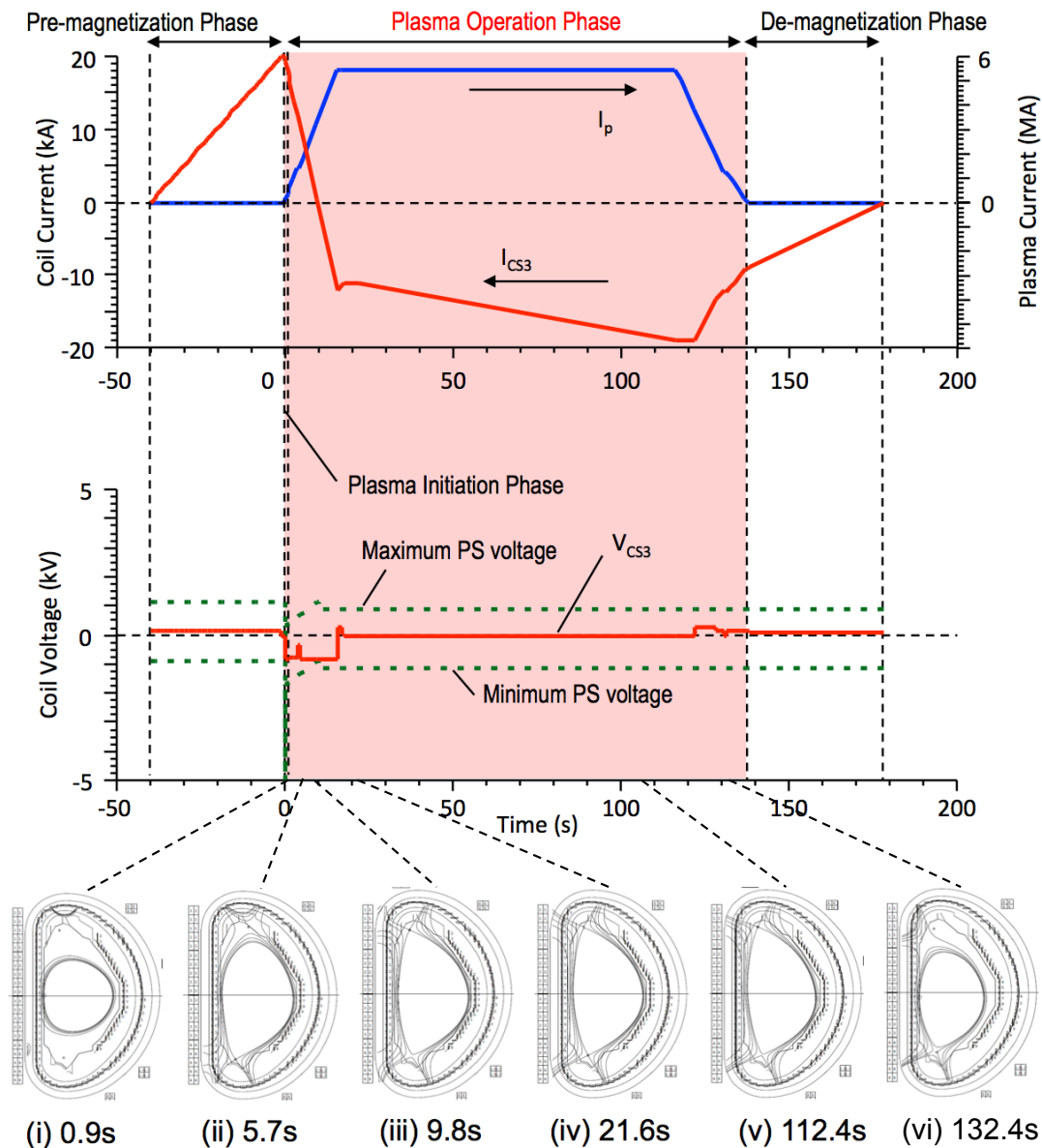


Fig. F-1: Schematic waveform of the central solenoid (CS3) current, the plasma current, the coil voltage. Bottom: the plasma cross sections at several times.

Then a target plasma satisfying these parameters was evaluated with the ACCOME code. Using the same or similar values of β_p and ℓ_i obtained by the code, temporal evolutions of the coil

current and voltage is evaluated by TOSCA. An example of the scenario is shown in Fig. F-1. This corresponds to Scenario 1 in Table 3-1. In this case, the objective is to sustain a 5.5 MA double null plasma for 100 s with available power at $f_{GW} = 0.5$. In a case of inductive scenario, the poloidal flux available at the current flat top defines the pulse length. The flux state at the pre-magnetization is identified mainly by the central solenoid (CS) current. Then the flux supplied by the CS is used to increase the plasma current and to compensate the loss by resistivity. The resistive part is evaluated using the Ejima coefficient, 0.45 in these cases. Until one of the CS or the poloidal field (PF) coils reaches the maximum, the current in the CS can be increased after reaching the flat top, and thus the available flux at the flat top can be evaluated. As the flat top length is assumed to be 100 s in this case, the plasma resistivity, in other words the electron temperature, should match the available flux. As the density is prescribed, this identifies the total stored energy and then the $H_{H(98,y2)}$ factor.

Evolution of the plasma cross section is prescribed as shown in the Figure F-1. The most important is to limit the coil voltages within the power supply capacities. This brings limitation in, for example, the current ramp-up speed, changing speed of the plasma cross section, heating/ β_p waveform and so on. The eddy currents induced at the passive structures, the vacuum vessel and the stabilization plate, have a certain contribution to the equilibrium, thus the coil current distribution, especially at the ramp-up and down phases. A coil voltage can be evaluated by summing time derivative of the fluxes produced by all coils, passive structures and the plasma at each coil. In the case of fully non-inductive scenarios, the available flux at the flat top does not matter in principle, since zero loop voltage is assumed.

In a plasma operation, divertor formation timing is a key for tailoring a target plasma towards the main performance. Capability of earlier formation of a divertor configuration is preferable. In the scenarios identified, the divertor formation timing is intended to be as early as possible. However, as the controllability of the divertor formation depends on the stray field due mainly to the CS current, the timing is affected by the CS current, which largely swings from the positive to the negative value. As initial magnetization is set lower for the lower current cases, such as the full non-inductive case, than that in higher current inductive cases, the divertor formation timing is earlier in the non-inductive case.

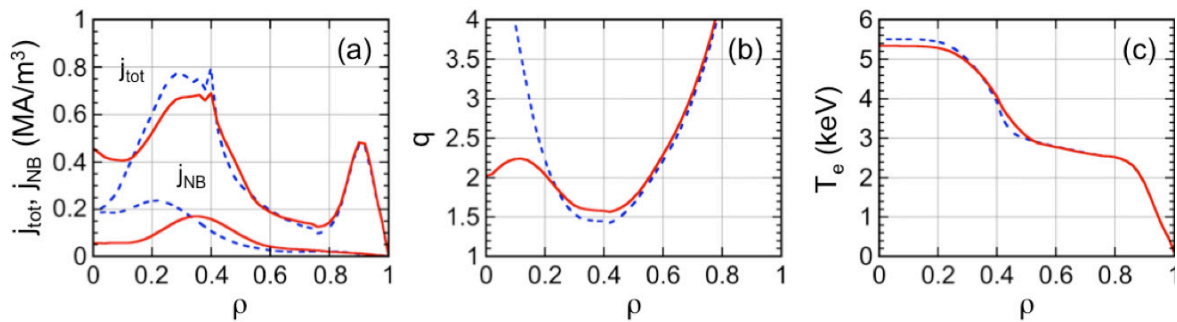


Fig. F-2: (a) The total and NB driven current profiles just before the N-NB beam line switch over (dashed lines) and 10 s after the switch over (solid lines). The q profile (b) and the electron temperature profile (c) just before (dashed line) and 10 s after (solid line) the switch over.

Detailed analysis of the plasma characteristics is in progress. For the control of the transport and the MHD stability, control of the current profile ($j(\rho)$) is a key issue. In JT-60SA, the N-NB is the most powerful external current driver and has two beam lines. By using these two beam lines independently, the N-NB driven current profile can be controlled. Though the fraction of the N-NB driven current is relatively small in a high β_N scenario, it is expected to play an effective role. Change in the safety factor profile ($q(\rho)$) due to the change in the driven

current profile and its impact on the temperature profile was investigated using TOPICS and the CDBM transport model (see Section 10). The target of the evaluation is a 2.3 MA high β_N plasma. The injected N-NB beam line was switched over from the inner beam line to the outer beam line, the former drives current at $\rho \sim 0.2$, while the latter does at $\rho \sim 0.4$ as shown in Figure F-2 (a). The change in the driven current changed the total current (F-2 (a)) thus $q(\rho)$ (F-2 (b)). This change in $q(\rho)$ causes the change in the transport and therefore in the temperature profile (F-2 (c)).

Among physics quantities, the toroidal rotation velocity profile ($V_t(\rho)$) plays important roles not only in the transport but also in the MHD stability. Since JT-60SA is equipped with co tangential N-NB and both co and ctr tangential P-NBs, $V_t(\rho)$ can be changed considerably. It has been evaluated how widely $V_t(\rho)$ can be changed in a 2.3 MA high β_N plasma. TOPICS and OFMC (see Section 10) are used in the evaluation. Evaluated $V_t(\rho)$ is shown in Figure F-2. As shown in the figure $V_t(\rho)$ can be changed widely. In JT-60U and DIII-D, it is reported that even with low $V_t(\rho)$ the resistive wall mode (RWM) can be suppressed, even slower than 0.3% of the Alfvén velocity in JT-60U. A profile corresponding to 0.3% of the Alfvén velocity is also shown in the figure for comparison. In the outer region, $\rho > 0.5$ where the eigenfunction of RMW will grow largely, $V_t(\rho)$ can be smaller or larger than 0.3% of the Alfvén velocity. Therefore, it would be expected that $V_t(\rho)$ can be changed widely enough to study the RMW

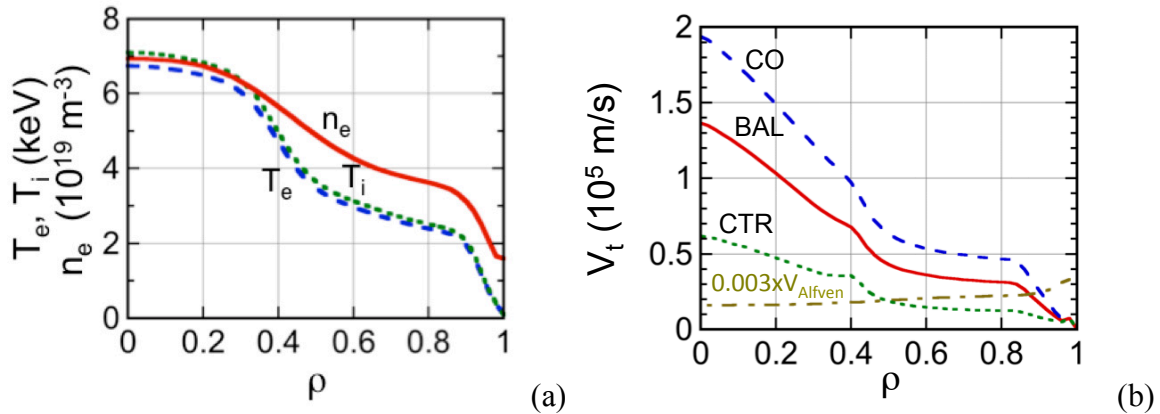


Fig. F-3: (a) Prescribed density and temperature profiles for the evaluation. (b) The V_t profiles for combinations of tangential NBs, BAL: N-NB + co- and ctr-P-NB, CO: N-NB + co-P-NB, CTR: N-NB + ctr-P-NB. 3% of the Alfvén velocity is also plotted for comparison.

suppression by the toroidal rotation.

Appendix G: Design guide lines for additional components

1. Basic magnetic configuration

The reference directionality of the toroidal current and field shall be as follows: plasma current in the clockwise direction looking from above with the same direction for the toroidal field, giving a downward ion grad-B drift direction. The directionality of the TF and Plasma current (and PF) shall be reversible simultaneously by reconfiguring the connections at the Power Supplies.

The PF system should provide plasma initiation with a toroidal electric field of 0.5 V/m and EC assist power (0.8MW). The value of magnetic stray field at breakdown should be less than 1 mT in a region with centre located at $R = 2.7$ m, $Z = 0$ m and minor radius 0.8 m. Inductive plasma current ramp-up is assumed to take place in an expanding-aperture limiter configuration located on the inboard first wall. The flux swing capability of the poloidal field system shall satisfy the plasma operation scenarios.

Device systems shall be designed to be compatible with the maximum envelope Poloidal Field map, as shown in Fig. G-1.

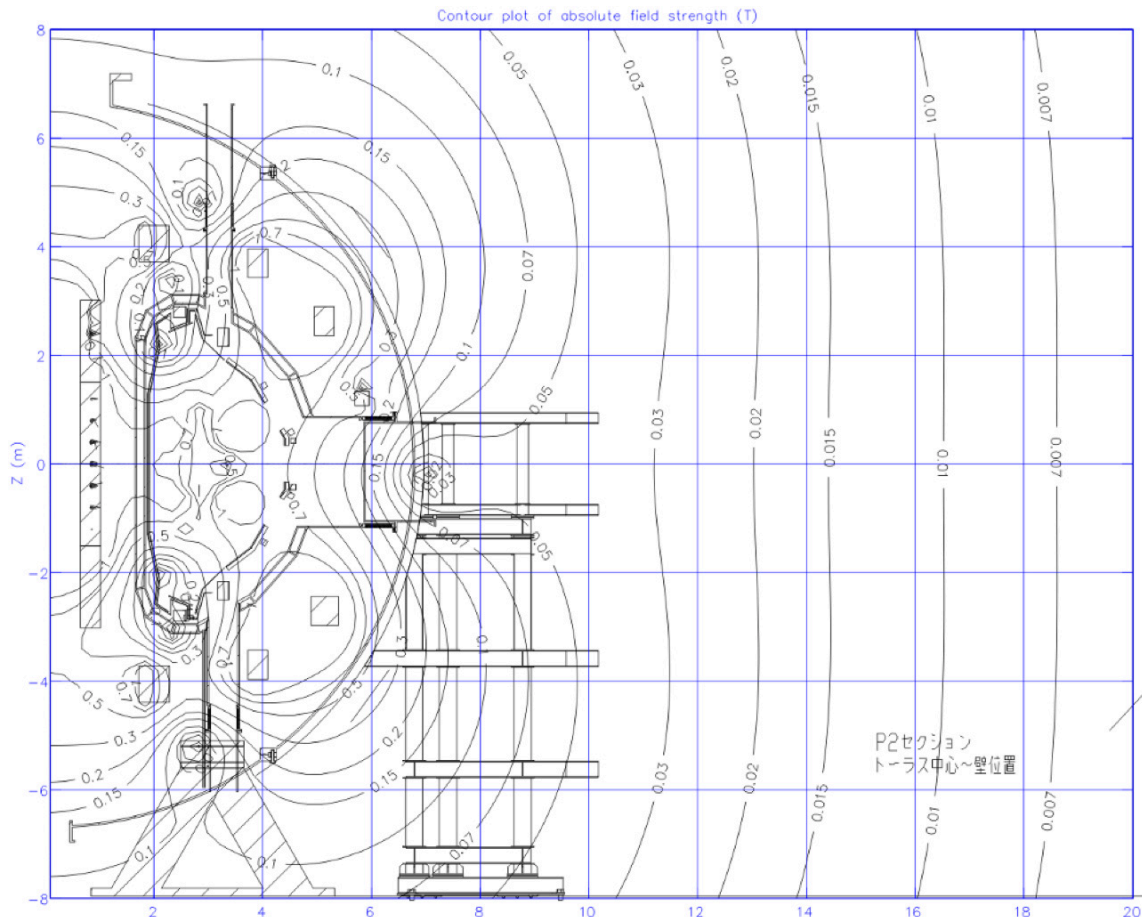


Fig. G-1 Maximum field levels in the torus hall

2. Daily and annual operation scenario

The JT-60SA experimental time shall be 10 hours per day. The experiment shall be conducted by an operation team in two shifts, including one hour for both pre- or post-experimental inspection. Regeneration of cryo-panels for fuel pumping, wall conditioning by glow discharge cleaning, and cooling of cryo-panels for the next day experiment, shall be carried out overnight

by an operation team for the cryogenic system operating on three shifts. The nominal repetition time is determined mainly by the duty cycle of 1/30 for NBI, such as 1800s for 60s flattop of NBI and 3000s for 100s flattop. The repetition rate can be increased to 4000s in case of a discharge that is terminated by a plasma disruption. 100s discharges with full NBI power shall be possible only every 3000s due to the duty cycle capability of the injectors.

Annual operation shall consist of an experimental period and a maintenance period. Prior to shut down for maintenance, exhaust of tritium gas for less than one month and warming up of the superconducting coils for about one month are planned. The annual maintenance period is foreseen to last about 5 months, including warming up and cooling down periods. During the maintenance period, annual inspections of JT-60SA facilities are planned according to safety regulations for electricity, high pressure gas, cranes etc. Maintenance and adjustment of heating systems and diagnostic systems and installations of new facilities or diagnostic systems will also be done. Between the warming up period and the cooling down period, for about 2.5 months, inspection or repair of in-vessel components is planned using the remote handling systems. Work in the cryostat shall also be possible in the initial experimental phase before the radiation dose increases. After the in-vessel maintenance period, cooling down of superconducting coils including preparation of the cryogenic system takes about 1.5 months. After the completion of the cooling down of the superconducting coils, the JT-60SA operation restarts for commissioning and experiments. The operation cost for this scenario has to be assessed with the understanding that parts and maintenances will come from both Parties and the operation plans have to be adjusted to match the financial resources.

3. Ports

Figure G-2 shows shape and size of large horizontal port. Large horizontal ports in P-6, 9, 15 and 18 for remote handling maintenance are recommended to install large additional components, because there is enough space for installation work at the outside of cryostat. Allowable mechanical momentum on the port stub of cryostat for large horizontal port is 40 kNm around vertical and toroidal axis.

Size of other typical ports is summarized in table G-1.

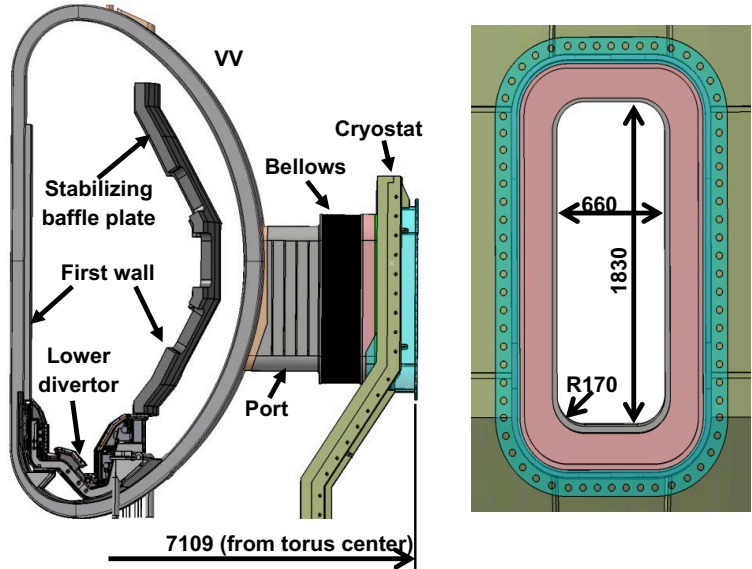


Fig. G-2 Large horizontal port

Table G-1 Size of typical ports

	Type	Port section	Size
Oblique	upper and lower	P1, 4, 8, 11, 14	W480 mm x H480 mm, R80 mm
	upper	P3	W650 mm x H546 mm, R80 mm
Horizontal	normal	P8, 11, 14	W600 mm x H800 mm, R100 mm
	normal	P13	W500 mm x H600 mm, R100 mm
	tangential	P1, P8	W520 mm x H890 mm, R200 mm
	tangential	P7, P12	W400 mm x H680 mm, R100 mm

4. Mechanical loads and transients

JT-60SA systems shall be designed to withstand all foreseen loading conditions, normal and off-normal. Acceptable damage levels will be commensurate with the probability of the loading condition. For the vacuum vessel and ex-vessel components, off-normal events (with an estimated frequency $< 1/\text{year}$) damage levels B (for example per ASME Sec III Appendix N-Dynamic Analysis Methods) may be used. For the In-vessel components, acceptable damage levels shall be established and documented on a case-by-case basis, depending on the experimental uncertainties.

The following mechanical loads shall be taken into account in the design of systems:

- electromagnetic loads both due to the standard tokamak operation as well as during transients such as plasma disruptions and coil fast discharges,
- pressure loadings, due to normal conditions (e.g. during commissioning) and transients due to off-normal events such as coolant or vacuum leaks,
- thermal loads, for example due to plasma, magnet cooldown, other transients,
- mechanical loads at interfaces due to neighbouring components (incl. thermal expansion/shrinkage),
- seismic loads,
- others, as evaluated by the system designer,
- any applicable foreseeable combination of the above.

4.1 Load transitions

The fatigue life of components and systems shall be evaluated according to Table G-2.

Table G-2 Design Number of Loading Transitions

Nominal # of operation shots	18,000
TF Coil energisation	3,000
Magnet cooldown/warmup from RT	100
Vessel/In-vessel baking transient	200
Vessel pumpdown from atmospheric	100
Cryostat pumpdown from atmospheric	100
Full current major plasma disruptions	2000
Full current VDEs	300
TF coil fast discharges	200

Shortest current decay time of major plasma disruption and VDEs are 4 ms and 10 ms, respectively.

4.2 Seismic Events

The ground motion Design Response Spectra (DRS) to be used for seismic analyses are specified in Table G-3, for horizontal seismic events, for different damping coefficients, and in terms of pseudo-acceleration.

**Table G-3 Seismic Design Response Spectra –
Pseudo-acceleration versus Frequency and Damping – Horizontal Seismic Event**

Frequency (Hz)	Pseudo acceleration (m/s ²) for each damping rate		
	1%	2%	5%
0.1	0.272	0.23	0.17
1.4	4	3.38	2.5
3.3	9.6	8.10	6
7	9.6	8.10	6
20	2.1	2	1.9
100	2.1	2	1.9

The vertical component ground DRS is linearly scaled from the horizontal spectra with a factor of 2/3.

Seismic response analysis of the structure shall be performed taking into account:

- the criteria defined in ASME III Appendix N- Dynamic Analysis Methods,
- soil structure interaction between the Tokamak Building and the underlying soil,
- an integrated model of the entire tokamak to take into account the interaction between components.

For multi-degree-of-freedom (DOF) systems, the concept of response spectrum can also be used in most cases by extracting the normal vibration modes and combining them with a modal superposition method. This consists in transforming the system of differential equations of motion for the multiple-DOF system into a set of independent differential equations and superimposing the results to obtain the solution of the original system. Thus, the modal superposition method reduces the problem of finding the response of a multi-degree-of-freedom system to the determination of the response of single-degree-of-freedom systems. An upper limit for the maximum response may be obtained by adding the absolute values of the maximum modal contribution. Generally the results obtained by this method will overestimate the maximum response. Another estimate of the maximum response, which is widely accepted and which gives usually reasonable results, is the Square Root of the Sum of the Squared values of the modal contribution (SRSS method). However when some of the modes are closely spaced, the use of the SRSS method can be optimistic. Following the NRC Recommendation 1 the absolute value summation has been considered only for closely spaced modes, which are those with frequencies differing by 10% or less. In damping, the energy of the vibrating system is dissipated by various mechanisms. In materials, these include plasticity, thermal effects of repeated elastic straining, and internal friction. In structures other effects can even more contribute to energy absorption such as friction at mechanical connections. For analysis convenience damping is generally assumed to be viscous in nature. The damping values in Table G-4, expressed as a percentage of the critical damping coefficient, are the ones

recommended by the NRC. The values given for each item are generally considered to be nearly lower bounds and hence conservative.

Table G-4 Damping factors for seismic analysis

Type of Structure	Damping
Welded steel	2%
Bolted steel	4%
Reinforced concrete	4%
Large diameter piping D>12in	2%
Small diameter pipes D≤12in	1%

4.3 Machine displacement and accelerations

The table G-5 indicates the design displacements at key location in the machine.

Table G-5 Machine design displacements and accelerations

TF Magnet	
Vertical displacement of top of TF magnet due to energization	- 8 mm
Toroidal max displacement of TF magnet at top OIS region	< ± 20mm
Radial Contraction of Magnet due to Cooldown	~16 mm
Horizontal displacement during seismic event	~13mm
Vertical downward displacement of top of magnet due to cooldown	~28mm
Max acceleration at top of magnet during seismic event	~ 10m/s ²
Vacuum Vessel	
Radial displacement at baking	18 mm
Vertical displacement at baking	25 mm
Radial displacement by seismic motion at baking	9 mm
Vertical displacement by seismic motion at baking	3 mm
Horizontal acceleration by seismic motion at baking	
-5.0 m < Z < -1.5 m (VV-leg to lower oblique port)	9.0 m/s ²
-1.5 m < Z < +0.8m (Horizontal port)	10.6 m/s ²
+0.8 m < Z < +2.2 m (Upper oblique port)	11.1 m/s ²
+2.2 m < Z < +4.3 m (Upper vertical port)	12.1 m/s ²

5. Operation conditions of VV

Plasma operation temperature: 50°C

Baking temperature: 200°C

Vacuum pressure: ~10⁻⁶ Pa

Allowable He leak rate of additional components: 1x10⁻⁸ Pam³/s